

Investigating the palynostratigraphy and palaeoenvironments of the southern Palaeotethyan Carboniferous-Permian succession of the Salt Range, Pakistan

Thesis submitted for the degree of
Doctor of Philosophy
at the University of Leicester

by

Irfan U. Jan

BSc Hon (University of Peshawar, Pakistan)

MSc (University of Peshawar, Pakistan)

Department of Geology



**University of
Leicester**

2011

Abstract

Palynological investigation of the Carboniferous-Permian Nilawahan Group of the Salt Range, consisting of the Tobra, Dandot, Warchha, and Sardhai formations, led to age determination and palynostratigraphic correlation. The sedimentological analyses of these units resulted in the palaeoenvironmental syntheses.

The palynological assemblages from the Late Pennsylvanian Tobra Formation correlate with the Oman, and Saudi Arabia Palynological Zone 2 (OSPZ2), the South Oman 2165B Biozone, the eastern Australian *Microbaculispora tentula* Opper-zone and western Australian Stage 2 (*sensu* Backhouse 1991). The Tobra Formation represents deposition via glacio-fluvial processes associated with the final stages of the Gondwana glaciation.

The overlying Dandot and Warchha formations are found to be barren of palynomorphs during the present study. The Dandot Formation occurs between the Upper Pennsylvanian Tobra Formation, and the Artinskian Stage Warchha Formation and it therefore ranges from the Late Pennsylvanian to Artinskian. The Dandot Formation represents deposition in an intertidal to shallow marine settings that developed as sea level rose following waning of the Carboniferous-Permian glaciation.

The Warchha Formation is dated as Artinskian Stage, based on the presence of plant megafossils. The Warchha Formation represents deposition in a fluvial system.

The Sardhai Formation at the top of the Nilawahan Group is dated as Middle Permian, Wordian Stage, based on the presence of stratigraphically diagnostic *Florinites? balmei*, and is correlated with the Oman and Saudi Arabia Palynological Zone 6 (OSPZ6). This correlation shows that *Florinites? balmei* is endemic to the southern neo-Tethys area.

The Sardhai Formation was deposited in a shallow marine setting, associated with neo-Tethys opening and sea floor spreading during the Wordian.

Acknowledgments

I would like to extend great thanks to my supervisors, Dr. Sarah J. Davies, and Dr. Jan A. Zalasiewicz (University of Leicester, UK) and Prof. Michael H. Stephenson (British Geological Survey, UK), for their invaluable scientific discussions, support and keen interest during the course of this project. I truly appreciate their enthusiasms, supervisory skills and expertise in the field that led to the successful completion of this thesis. Dr. Mark Williams at the Department of Geology, University of Leicester is thanked for helping with scientific as well as routine issues, during the time of my PhD stay here at the department. He has always been a very helpful and motivating staff member of the department. The geology department staff members at the University of Leicester generally proved very nice and always provided with some feedback and help at the departmental seminars that resulted in improvement of this manuscript. David Riley, Chris Willcox, Stephen Grebby and other PhD colleagues; seniors and juniors in the department proved good mates and extended support whenever needed. The clerical, technical, experimental and research staff always proved helpful and facilitating during this time. Prof. Asif Khan (Director National Centre of Excellence in Geology, University of Peshawar, Pakistan), Mr. Muhammad Haneef (Chairman Department of Geology, University of Peshawar, Pakistan) are thanked for the organisational support during fieldworks in Pakistan. Prof. Michael G. Petterson (University of Leicester) is cordially thanked for helping with arranging the collaboration among the University of Leicester, UK, the British Geological Survey, UK and the National Centre of Excellence in Geology, University of Peshawar, Pakistan that ended up in a successful completion of this work. In terms of financial assistance, the Higher Education Commission of Pakistan, the National Centre of Excellence in Geology, University of Peshawar, the British Geological Survey, UK and the University of Leicester, UK, are

thanked for supporting this research. The additional financial assistance from different organisations/professional societies/institutes and individuals included, the sponsorship from the British Geological Survey, UK to attend the Milos 2009 Greece workshop. The sponsorship from the UK-IODP, to attend the Urbino Summer School on palaeoclimatology, 2009 Italy. The financial support from the International Federation of Palynological Societies, for poster presentation at the 3rd Palaeontological Congress, 2010, London. The financial support from Dr. Sarah J. Davies, to attend the palynology master class 2010 at the Netherlands (jointly organised by the American Association of Stratigraphic Palynologists and TNO, Utrecht) and to support a trip to Poland for attendance and oral presentation at the CIMP Poland 2010 General Meeting, Warsaw. Prof. Michael H. Stephenson helped in funding processing samples for palynology. The Commission Internationale de Microflore du Paléozoïque (CIMP) sponsorship to the student presenter at the CIMP Poland 2010 General Meeting. The Geological Society of London's Edmund Johnson Garwood Fund for travelling to and from BGS to undertake research work.

I feel very fortunate to have had the opportunity of studying for a doctor degree at the University of Leicester, UK, to meet with friendly and knowledgeable researchers in and outside the UK and my great supervisory group. In my endeavours my parents, brothers, sisters and my family members, especially my wife, always supported me and encouraged my work.

I hope that this work proves a helpful guide to the wider geological community, and also strengthens future research and collaborative links between the University of Leicester, the British Geological Survey, UK and the National Centre of Excellence in Geology, University of Peshawar, Pakistan.

Table of contents

Abstract	<i>i</i>
Acknowledgments	<i>ii</i>
Table of contents	<i>iv</i>
Table of figures	<i>x</i>
List of tables	<i>xv</i>
List of plates	<i>xvi</i>
1 Chapter 1: Introduction	1
1.1 Scientific rationale	1
1.2 Project aims and objectives	4
1.3 Structure of this thesis	5
1.4 Materials and methods	6
1.4.1 Fieldwork	6
1.4.1.1 Fieldwork details	8
1.4.2 Laboratory processing and analyses	11
1.4.2.1 Processing of the samples	11
1.4.2.2 Laboratory analyses	21
1.4.3 Data representation	22
1.4.3.1 Palynology data representation	22
1.4.3.2 Sedimentology data representation	22
2 Chapter 2: The Carboniferous-Permian world and review of Gondwana palynostratigraphy	23
2.1 Carboniferous-Permian time scales	23

2.1.1	Carboniferous time scale	23
2.1.1.1	The North American system	23
2.1.1.2	The Upper Carboniferous in Russia	25
2.1.2	Permian time scale	26
2.1.2.1	The Cisuralian Series, Lower Permian	26
2.1.2.2	The Guadalupian Series, Middle Permian	28
2.1.2.3	The Lopingian Series, Upper Permian	30
2.2	The Carboniferous-Permian palaeocontinental configuration	30
2.2.1	Gondwana	31
2.2.2	Euramerica	31
2.2.3	Angara	32
2.3	Review of Carboniferous-Permian Gondwana palynostratigraphy	33
2.3.1	Arabian palynostratigraphy	33
2.3.1.1	Saudi Arabian palynostratigraphic trends	33
2.3.1.2	Yemen	35
2.3.1.3	Oman	36
2.3.2	Australian palynostratigraphy	41
2.3.2.1	Western Australian palynostratigraphy	42
2.3.2.2	Eastern Australian palynostratigraphy	43
2.3.3	South African palynostratigraphy	44
2.3.4	South American palynostratigraphy	46
2.3.4.1	Brazil	46
2.3.4.2	Argentina	51
2.3.5	Peninsula Indian palynostratigraphy	54
3	Chapter 3: Sedimentological analyses of the Carboniferous-Permian succession of the Salt Range	58
3.1	Abstract	58

3.2	Previous sedimentological work	60
3.3	Present sedimentological analysis	63
3.3.1	Facies analysis	64
3.3.1.1	Conglomeratic facies	67
3.3.1.1.1	Gmc: Clast-supported massive conglomerate	67
3.3.1.1.2	Gmm: Matrix-supported massive conglomerate	68
3.3.1.2	Sandstone-dominated facies	70
3.3.1.2.1	Sf: Fining upwards pebbly sandstone	70
3.3.1.2.2	Sm: Massive sandstone	70
3.3.1.2.3	Fss: Fine-grained sandstone and siltstone	73
3.3.1.2.4	St: Trough cross-bedded sandstone	74
3.3.1.2.5	Sp: Planar cross-bedded sandstone	76
3.3.1.2.6	Sr: Ripple-laminated sandstone and interlaminated mudstone	76
3.3.1.2.7	Sh: Hummocky cross-stratified sandstone	80
3.3.1.3	Mud-dominated facies	80
3.3.1.3.1	Fm: Massive mudstone	80
3.3.1.3.2	Fl: Laminated mudstone	82
3.3.1.4	Limestone-dominated facies	82
3.3.1.4.1	Lsf: Thin-bedded sandy limestone	82
3.4	Tobra Formation facies association	83
3.4.1	DFFA: Debris flow-dominated alluvial plain facies association	83
3.4.2	SFFA: Stream flow dominated alluvial plain facies association	84
3.4.3	OFA: Overbank facies association	84
3.5	Grain size analyses and provenance of the Tobra Formation	86
3.6	Tobra Formation depositional environment	90
3.7	Dandot Formation facies association	97
3.7.1	ISFA: Intertidal to shallow marine facies association	97

3.8	Dandot Formation depositional environment	99
3.9	Warchha Formation facies association	100
3.9.1	ECS: Erosive-based cross-bedded sandy bedform element	100
3.9.2	LCS: Lenticular cross-bedded sandstone bodies with erosional bases	102
3.9.3	RSFA: Red mudstone interbedded with thin sandstone and calcretes	102
3.9.4	PSFA: Pebbly sandstone	104
3.9.5	ACF: Abandoned channel fill deposits	104
3.10	Grain size analyses and provenance of the Warchha Formation	104
3.11	Warchha Formation depositional environment	107
3.12	Sardhai Formation facies association	108
3.12.1	DLSFA: Deep lacustrine to shallow marine facies association	108
3.13	Sardhai Formation depositional environment	108
3.14	Sedimentological synthesis	110
4	<i>Chapter 4: Systematic palynology</i>	114
4.1	Introduction	114
4.2	Pollen/Spore classification	114
4.3	Descriptive terminologies	115
4.4	Pollen	115
4.5	Spores	116
4.6	Systematic description	124
4.7	Plates explanation	152
5	<i>Chapter 5: Palynology and palynostratigraphy of the Upper Pennsylvanian</i>	
	<i>Tobra Formation</i>	162

5.1	Abstract	162
5.2	Previous palynological work on the Carboniferous-Permian succession of the Salt Range, Pakistan	163
5.3	Present palynological investigation	166
5.3.1	Palynology of the Tobra Formation at Zaluch Nala section, western Salt Range	167
5.3.2	Palynology of the Tobra Formation at Khewra-Choa section, eastern Salt Range	170
5.4	Correlation of the Tobra Formation	176
5.4.1	Correlation with Arabia	176
5.4.1.1	Correlation with Oman	176
5.4.1.2	Correlation with Saudi Arabia	180
5.4.1.3	Correlation with Yemen	182
5.4.2	Correlation with Australia	183
5.4.3	Correlation with South American	184
5.4.3.1	Correlation with Chacoparana Basin, Argentina	184
5.4.3.2	Correlation with central-western Argentina	185
5.4.3.3	Correlation with Amazonas Basin, Brazil	186
5.4.4	Correlation with India	187
5.5	Age of the Tobra Formation Assemblages	187
5.6	Conclusions	189
6	<i>Chapter 6: Palynology and palynostratigraphy of the Middle Permian Sardhai Formation</i>	191
6.1	Abstract	191
6.2	Description of the Sardhai Formation assemblages	191
6.3	Correlation of the Sardhai Formation with other Permian Tethys successions	195
6.3.1	Correlation with Arabia	195

6.3.2	Tethyan correlation	204
6.4	Palaeogeographic distribution of <i>Florinites? balmei</i>	206
6.5	Conclusions	207
7	Chapter 7: Palynological synthesis	209
7.1	The palynomorphs of the Tobra Formation	209
7.2	The palynomorphs of the Sardhai Formation	211
8	Chapter 8: Conclusions and recommendations for future work	212
9	Appendices	216
9.1	Appendix 1 Showing the processed samples for palynology and their population. MPA stands for the BGS in-house palynological laboratory processing code (See Appendix 2 for the exact stratigraphic positions of the palynology samples prefixed with MPA).	216
9.2	Appendix 2 Stratigraphic positions of palynology and sedimentology samples in the Nilawahan Group, Salt Range, Pakistan. (For locations of these sections, see Fig. 1.3, chapter 1).	218
9.3	Appendix 3 Paper published in the (journal) " <i>Palynology</i> ".	219
9.4	Appendix 4 Paper published in the (journal) " <i>Review of Palaeobotany and Palynology</i> ".	233
9.5	Appendix 5 Stratigraphic ranges of the palynomorphs in the Nilawahan Group at the Saiyiduwali section (Khisor Range). The arrows represent ?continuity of the taxa up section.	244
9.6	Appendix 6 Stratigraphic ranges of the palynomorphs in the Nilawahan Group at the Zaluch Nala section (western Salt Range). The arrows represent ?continuity of the taxa up section.	245

9.7 Appendix 7 Stratigraphic ranges of the palynomorphs in the Nilawahan Group at the Khewra-Choa section (eastern Salt Range). The arrows represent ?continuity of the taxa up section.	246
---	------------

References	247
-------------------	------------

Table of figures

<i>Fig. 1.1 Chief Carboniferous-Permian basins of Gondwana. 1-9. South American basins, 10-15. South African basins, 16. Yemen, 17. Oman, 18. Himalayan zone, 19-20. Indian basins, 21- 32. Australian basins, 33- 34. Antarctic basins (From Stephenson 2008a).</i>	3
<i>Fig. 1.2 Geographical location map of Pakistan. The study area can be seen highlighted</i>	4
<i>Fig. 1.3 Geological sites studied, 1. Khewra-Choa section, 2. Pail section, 3. Warchha gorge section, 4. Zaluch Nala section (Salt Range),</i>	7
<i>Fig. 1.4 Simplified Carboniferous-Permian stratigraphy of the Salt Range and central part of the Khisor Range. The present study deals with the Nilawahan Group (Modified after Gee 1989; Wahid et al. 2004).</i>	9
<i>Fig. 1.5 Outcrop of the sections in the eastern Salt Range, a. Khewra gorge section, b. Tobra Formation in the Khewra gorge section, c. Khewra-Choa section (eastern Salt Range). View looking northeast.</i>	12
<i>Fig. 1.6 Outcrop of the Pail section, a, b & c show a conformable contact between the Tobra Formation and overlying Dandot Formation in the central Salt Range. Westwards, the Warchha Formation unconformably overlies the Tobra Formation (see Fig. 1.9). View looking southwest.</i>	13
<i>Fig. 1.7 Outcrop of the Warchha gorge section in the central Salt Range. Top and bottom photos show, the Sardhai Formation (i.e. Gondwanan succession) overlain by the Tethyan Zaluch Group (represented by carbonates of the Amb, Wargal and Chiddru formations). View looking northwest.</i>	14
<i>Fig. 1.8 Outcrop of the Zaluch Nala section in the western Salt Range, a. Sardhai Formation overlain by the Zaluch Group (i.e. Amb, Wargal and Chiddru formations), b. Warchha Formation in the Zaluch Nala section, c. Tobra Formation in the Zaluch Nala section. View looking northeast.</i>	15
<i>Fig. 1.9 Photomosaic of the Khisor Range showing Tobra, Warchha and Sardhai formations. The Dandot Formation is missing. The cliff is approximately 400 metres. View looking northeast.</i>	16
<i>Fig. 1.10 Brief overview of research undertaken in the Salt Range.</i>	17

Fig. 1.11 Palynological processing summary chart (Modified after Wood et al. 1996).	20
Fig. 2.1 Geological time scale of the Late Carboniferous to Permian (Modified after Gradstein et al. 2004).	24
Fig. 2.2 The Late Carboniferous palaeocontinental reconstruction	31
Fig. 2.3 The Late Permian palaeocontinental reconstruction (Source: http://www.scotese.com) .	32
Fig. 2.4 Oman and Saudi Arabia Late Carboniferous to Early Permian palynological schemes (From Stephenson et al. 2003).	34
Fig. 2.5 Correlation of Oman and Arabian Peninsula biozones and a portion of the Khulan Formation of Yemen (From Stephenson & Al-Mashaikie 2010).	36
Fig. 2.6 The biozonation of the Al Khlata Formation of South Oman (From Penney et al. 2008).	38
Fig. 2.7 Al Khlata Formation palynostratigraphic scheme proposed in the Mukhaizna Field in south Oman (From Stephenson et al. 2008).	40
Fig. 2.8 Correlation of palynozonations for Australia (From Stephenson 2008a).	41
Fig. 2.9 Correlation of palynozonations for the two main Carboniferous-Permian basins of South Africa (Modified after Stephenson 2008a).	45
Fig. 2.10 Correlation of palynozonations for the main basins of South America	47
Fig. 2.11 Brazilian Late Carboniferous to Early Permian palynological scheme	48
Fig. 2.12 Argentinian Late Carboniferous to Early Permian palynological schemes	52
Fig. 2.13 Correlation of the Carboniferous-Permian (and Triassic) formations and palynology events of India, eastern Australia and Pakistan. The shaded portion represents the Carboniferous to Permian time interval (Modified after Veevers & Tewari 1995).	56
Fig. 2.14 Comparison of the main Carboniferous-Permian palynozones of the Gondwana regions	57
Fig. 3.1 Geological map of the Salt Range and Khisor Range, showing the locations selected for sedimentological investigations. 1. Khewra-Choa section (eastern Salt Range), 2. Pail section (central Salt Range), 3. Warchha gorge section (central Salt Range), 4. Zaluch Nala section (western Salt Range) and 5. Saiyiduwali section (Khisor Range; modified after Jan & Stephenson 2011).	59
Fig. 3.2 Key for the lithologies and sedimentary structures documented in the study.	60

<i>Fig. 3.3 Stratigraphy and correlation of the Nilawahan Group, the Tobra, Dandot, Warchha and Sardhai formations. For locations and horizontal distance of these sections, refer to Fig. 3.1. For key refer to Fig. 3.2 (Modified after Jan & Stephenson 2011).</i>	61
<i>Fig. 3.4 Percentage cumulative frequency curves of the Nilawahan Group samples. See Appendix 2 for sample locations and Fig. 3.2 for sample codes.</i>	64
<i>Fig. 3.5 Log ES-The distribution of lithofacies types and facies associations in the Carboniferous-Permian succession of the Khewra-Choa section (eastern Salt Range). For detailed stratigraphic location of the units (formations), refer to Fig. 3.3. For key, refer to Fig. 3.2.</i>	66
<i>Fig. 3.6 Characteristic examples of lithofacies present in the Carboniferous-Permian succession of the Salt Range. Stratigraphic location given on Figs. 3.5, 3.7 and 3.8.</i>	69
<i>Fig. 3.7 Log WS1-The distribution of lithofacies types and facies associations in the Tobra Formation (Zaluch Nala section, western Salt Range). For detailed stratigraphic location of the unit (formation), refer to Fig. 3.3. For key refer to Fig. 3.2.</i>	72
<i>Fig. 3.8 Log WS2-The distribution of lithofacies types and facies associations in the Warchha Formation (Zaluch Nala section, western Salt Range). For detailed stratigraphic location of the unit (formation), refer to Fig. 3.3. For key refer to Fig. 3.2.</i>	75
<i>Fig. 3.9 Characteristic examples of lithofacies present in the Carboniferous-Permian succession of the Salt Range and Khisor Range. Stratigraphic location given on Figs. 3.5, 3.8 and 3.11.</i>	77
<i>Fig. 3.10 Burrows in facies Sr (Ripple-laminated sandstone and interlaminated mudstone).</i>	78
<i>Fig. 3.11 Log CS-The distribution of lithofacies types and facies associations in the Carboniferous-Permian succession of the Pail section (central Salt Range). For detailed stratigraphic location of the units (formations), refer to Fig. 3.3. For key refer to Fig. 3.2.</i>	79
<i>Fig. 3.12 The facies and facies associations variations in the Tobra Formation from the Saiyiduwali section (Khisor Range), through the Zaluch Nala section (western Salt Range) Pail, and Warchha gorge sections (central Salt Range) and into the Khewra-Choa section (eastern Salt Range). The histograms of the sedimentology samples are also shown. For sedimentology sample locations refer to Appendix 2. Refer to Fig. 3.1 for locations of these units and Fig. 3.2 for key.</i>	85
<i>Fig. 3.13 Photomicrographs of some of the lithofacies in the Tobra Formation. For facies codes and mineral symbols refer to Fig. 3.2.</i>	87

<i>Fig. 3.14 Variation in the grain roundness (histograms) from the Saiyiduwali section (Khisor Range), through the Zaluch Nala section (western Salt Range), Warchha gorge sections (central Salt Range) and into the Khewra-Choa section (eastern Salt Range). Sedimentology sample locations refer to Appendix 2. Refer to Fig. 3.1 for locations of these units and to Fig. 3.2 for key.</i>	89
<i>Fig. 3.15 The QFL diagram for the Tobra Formation and interpretation of provenance (c.f. Dickinson 1985). See Fig. 3.2 for key to samples.</i>	90
<i>Fig. 3.16 Depositional model 1 of the Tobra Formation in an alluvial fan setting showing the distribution of the major facies associations. See Fig. 3.2 for key. The figure is not to scale.</i>	93
<i>Fig. 3.17 Block diagram of the idealised depositional model 1 of the Tobra Formation. See Fig. 3.2 for facies codes.</i>	94
<i>Fig. 3.18 Depositional model 2 of the Tobra Formation in a tectonically active region showing the distribution of the major facies associations. See Fig. 3.2 for key. The figure is not to scale.</i>	96
<i>Fig. 3.19 The facies and facies association variation in the Dandot Formation from the Pail section (central Salt Range) to the Khewra-Choa section (eastern Salt Range). Refer to Fig. 3.1 for locations of these units and Fig. 3.2 for key.</i>	98
<i>Fig. 3.20 Idealised depositional model of the Dandot Formation. See Fig. 3.2 for facies codes.</i>	99
<i>Fig. 3.21 The facies and facies association variation in the Warchha Formation from the Saiyiduwali section (Khisor Range), through the Zaluch Nala section (western Salt Range) and into the Khewra-Choa section (eastern Salt Range). Refer to Fig. 3.1 for locations of these units and Fig. 3.2 for key.</i>	101
<i>Fig. 3.22 Characteristic examples of facies associations in the Warchha Formation.</i>	102
<i>Fig. 3.23 Variation in the grain roundness (histograms) of the Warchha Formation at the western Salt Range, Zaluch Nala section. Refer to Fig. 3.1 for location of this unit and Fig. 3.2 for key.</i>	103
<i>Fig. 3.24 The QFL diagram for the Warchha Formation samples and interpretation of provenance. See Fig. 3.2 for key to samples.</i>	105
<i>Fig. 3.25 Photomicrographs of some of the lithofacies of the Warchha Formation. For facies codes and mineral symbols refer to Fig. 3.2.</i>	106
<i>Fig. 3.26 Idealised depositional model for the Warchha Formation sedimentation. The palaeocurrent directions of the river system are after Ghazi & Mountney (2009). See Fig. 3.2 for facies associations.</i>	107

<i>Fig. 3.27 The facies and facies association variation in the Sardhai Formation from the Khisor Range, through the western Salt Range and into the central Salt Range. Refer to Fig. 3.1 for locations of these units and Fig. 3.2 for key.</i>	109
<i>Fig. 3.28 Idealised depositional model for sedimentation of the Sardhai Formation. See Fig. 3.2 for facies codes.</i>	110
<i>Fig. 4.1 Orientation and dimensional attributes of trilete spore (From Modie 2007).</i>	117
<i>Fig. 4.2 Orientation and dimensional attributes of monolete spore (From Modie 2007).</i>	118
<i>Fig. 4.3 Orientation and dimensional attributes of monosaccate pollen (From Modie 2007).</i>	119
<i>Fig. 4.4 Orientation and dimensional attributes of bisaccate pollen (From Modie 2007).</i>	120
<i>Fig. 4.5 Orientation and dimensional attributes of monocolpate pollen (From Modie 2007).</i>	121
<i>Fig. 4.6 Spore classification scheme (From Neves & Owens 1966).</i>	122
<i>Fig. 4.7 a. Shows a dipoloxylonoid outline for bisaccate pollen, b. Shows a hapoloxylonoid outline for bisaccate pollen (From Punt et al. 2007).</i>	123
<i>Fig. 5.1 Location map of the, 1. Khewra-Choa section (eastern Salt Range) and 2. Zaluch Nala section (western Salt Range)</i>	164
<i>Fig. 5.2 Carboniferous-Permian stratigraphy of the Salt Range, Pakistan, showing the measured section of the Tobra Formation at Khewra-Choa section (eastern Salt Range) and Zaluch Nala section (western Salt Range; modified after Jan & Stephenson 2011).</i>	165
<i>Fig. 5.3 Tobra Formation near the entrance to the Zaluch Nala section (From Jan & Stephenson 2011).</i>	168
<i>Fig. 5.4 The Tobra Formation in the Khewra-Choa section (eastern Salt Range).</i>	169
<i>Fig. 5.5 Abundance chart for the Tobra Formation, Zaluch Nala section (western Salt Range; from Jan & Stephenson 2011).</i>	171
<i>Fig. 5.6 Abundance chart for the Tobra Formation, Khewra-Choa section (eastern Salt Range).</i>	177
<i>Fig. 5.7 The biozonation of the Al Khlata Formation of South Oman, showing stratigraphically important groups and main accessory taxa (Modified after Penney et al. 2008).</i>	178
<i>Fig. 5.8 The Mukhaizna Field, south Oman biozonation, showing stratigraphically important taxa (Modified after Stephenson et al. 2008).</i>	180
<i>Fig. 5.9 Oman and Saudi Arabia Palynological Zone schemes</i>	181

<i>Fig. 5.10 Correlation of the Tobra Formation Zaluch Nala palynological assemblages with Arabian, Australian, South American and Indian biozones</i>	188
<i>Fig. 6.1 Location map of the, 1. Zaluch Nala section (western Salt Range) and 2. Syidiuwali section (Khisor Range; modified after Gee 1989; Ghazi & Mountney 2009; Jan et al. 2009; Jan & Stephenson 2011).</i>	192
<i>Fig. 6.2 Carboniferous-Permian stratigraphy of the Salt Range, showing the measured section of the Sardhai Formation at Zaluch Nala section (western Salt Range) and Saiyiduwali section (Khisor Range; modified after Jan & Stephenson 2011).</i>	193
<i>Fig. 6.3 Vertical beds of the Sardhai Formation underlain by red beds of the Warchha Formation (to the right in the photo). Rock outcrop to the left (represented by arrow) is 5 m high (Modified after Jan et al. 2009).</i>	194
<i>Fig. 6.4 Measured section of the Sardhai Formation at the Saiyiduwali section (Khisor Range; modified after Jan et al. 2009).</i>	195
<i>Fig. 6.5 Measured section of the Sardhai Formation within the Zaluch Nala section (western Salt Range).</i>	196
<i>Fig. 6.6 Abundance chart for the Sardhai Formation, at the Saiyiduwali section (Khisor Range). The arrowed bars represent the continuity of the taxa.</i>	198
<i>Fig. 6.7 Abundance chart for the Sardhai Formation, Zaluch Nala section (western Salt Range).</i>	199
<i>Fig. 6.8 Correlation of the OSPZ6 biozone between Southeast Turkey, northern Iraq, central Saudi Arabia, Oman and Pakistan</i>	205
<i>Fig. 6.9 The mid-Permian (Roadian-Wordian) continental configuration. Solid circles indicate the location of <i>Florinites? balmei</i> across, 1- Oman, 2- Salt Range, 3- UAE, 4- Kuwait, 5- Saudi Arab, 6- Qatar and 7- southeast Turkey (From Jan et al. 2009).</i>	208
<i>Fig. 7.1 Palynomorph list of the Nilawahan Group. Taxa are concentrated in the Tobra and Sardhai formations.</i>	210

List of tables

<i>Table 3.1 Graphic measures from the grain size analyses of some of the Nilawahan Group samples. See Appendix 2 for the sample details and Fig. 3.2 for sample and facies codes.</i>	65
--	----

Table 3.2 Summary of lithofacies types present in each stratigraphic unit (formation) in the Carboniferous-Permian succession of the Salt Range. A positive sign indicates that the lithofacies is present. See Fig. 3.2 for key to lithofacies. _____ 83

List of plates

<i>Plate 1</i> _____	153
<i>Plate 2</i> _____	155
<i>Plate 3</i> _____	157
<i>Plate 4</i> _____	159
<i>Plate 5</i> _____	161
<i>Plate 6</i> _____	172
<i>Plate 7</i> _____	174
<i>Plate 8</i> _____	200
<i>Plate 9</i> _____	202

1 Chapter 1: Introduction

1.1 Scientific rationale

The late Palaeozoic marks a significant epoch in the Earth's palaeoclimatic history, with prolonged cold-climatic conditions, known as late Palaeozoic ice house (Fielding *et al.* 2008a). The important feature of the late Palaeozoic ice house is that, it represents the last time preceding the Cenozoic icehouse and the only time since the beginning of terrestrial vegetation that Earth entered and exited from a long-lived icehouse condition (Fielding *et al.* 2008a; Gastaldo *et al.* 1996). The resultant widespread glacial and deglacial deposits of the late Palaeozoic, particularly Carboniferous-Permian, occur in the scattered continental fragments of Gondwana (Fig. 1.1), e.g. South America, Africa, Falkland Islands, Antarctica, India, Pakistan (Frakes *et al.* 1975) and Australia (Visser 1997). With a few exceptions (e.g. particularly Salt Range, Pakistan), the palaeoclimate and palaeoenvironments of these glacial and subsequent deglacial deposits, which have been corroborated by palynology, sedimentology and stable isotopic ($\delta^{18}\text{O}$ and $\delta^{13}\text{C}$) trends, have been studied in much detail in the last few years (e.g. Caputo *et al.* 2008; Isbell *et al.* 2008; Isbell *et al.* 2003a, 2003b; Jones & Fielding 2004; Martin *et al.* 2008; Mory *et al.* 2008; Stephenson 2008a and references therein; Fielding *et al.* 2008b, c and references therein).

The events of glaciation and deglaciation in these deposits have been correlated using a range of available information, including pollen and spores (e.g. Kyle & Schopf 1982; Foster & Waterhouse 1988; Lindström 1995), invertebrate fauna (e.g. Amos & López-Gamundi 1981; Archbold 1999), marine flooding surfaces (e.g. López-Gamundi 1989; Isbell *et al.* 1997) and radiometric dating of zircons contained in volcanic tuffs (e.g. Roberts *et al.* 1996; Bangert *et al.* 1999).

However, it has been observed that with a few exceptions (e.g. Australia), most of the Late Carboniferous and Early Permian cold climate nonmarine glacial deposits of Gondwana are devoid of marine microfauna, e.g. foraminifera, corals and conodonts (Archbold & Dickins 1997), which form the basis for the standard chronostratigraphic stages (Jin *et al.* 1997) and thus palynology has been developed as an important tool for correlation (Stephenson 2008a). In addition to use for inter- and intra-basinal correlation, the palynology of these deposits also show palaeoclimate-based palynostratigraphic trends, e.g. the appearance and diversification of monosaccate pollen, cheilocardioid spores, monocolpate pollen and bisaccate pollen (Stephenson 2008a). These palaeoclimate-controlled palynological trends of the Gondwana basins are used in the correlation of these successions across Gondwana.

Challenges in using palynology, however, arise in correlating the Gondwana palynological assemblages precisely to the International/Russian stages. These challenges can be attributed to two major reasons.

Firstly, marine intervals in Gondwanan deposits that could help to devise a firm and a reliable framework for the palaeontological and geochemical data, across this regionally wide area and which, in turn, could be correlated with the International/Russian stages are rare.

The second challenge is the endemism in the palynological assemblages of the Gondwanan successions, which demonstrated different taxa to the International stages (Stephenson 2008a). Nonetheless the importance of palynology has always been appreciated as one of the successful tools in correlating these strata across Gondwana and with the International stages. The palynological work in Gondwana is primarily driven by oil and gas exploration e.g. in the Middle East, South America and Australia and coal exploration in India and Australia (Stephenson 2008a).

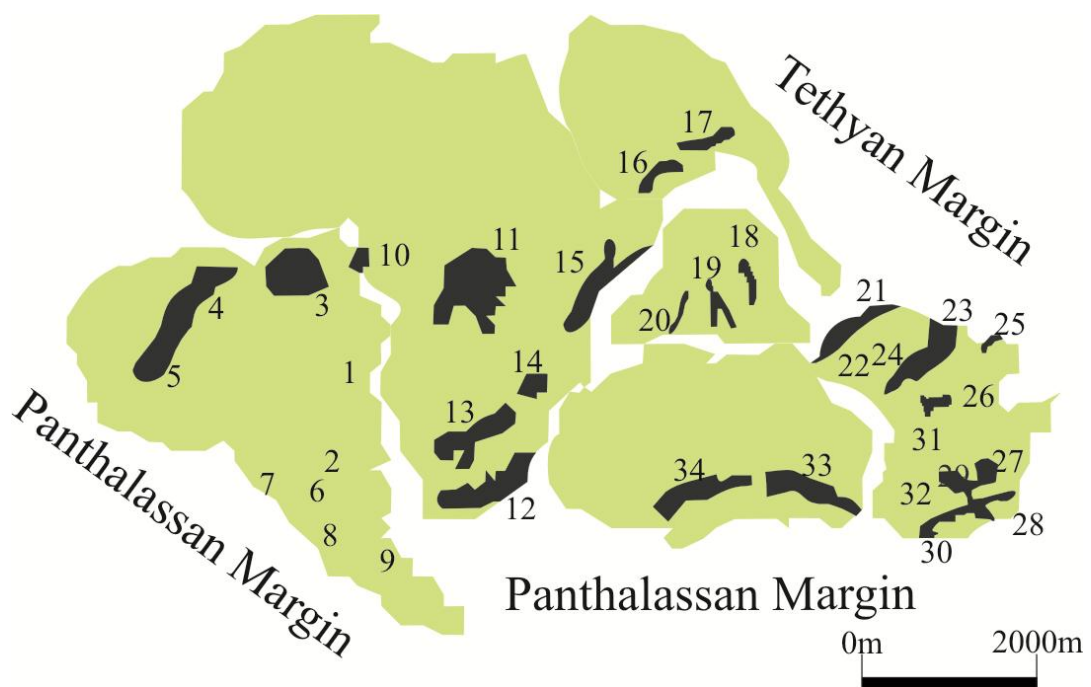


Fig. 1.1 Chief Carboniferous-Permian basins of Gondwana. 1-9. South American basins, 10-15. South African basins, 16. Yemen, 17. Oman, 18. Himalayan zone, 19-20. Indian basins, 21- 32. Australian basins, 33- 34. Antarctic basins (From Stephenson 2008a).

The Carboniferous-Permian succession of the Salt and Khisor ranges of Pakistan (Fig. 1.2) is relatively little-studied and the palaeogeography and palaeoclimatology of this southern Palaeotethys area is poorly constrained. This research combines palynological (fossil plant spore and pollen) and sedimentological analysis to place the successions in their regional stratigraphic context and understand vegetation changes and the evolution of depositional environments in this area during the Carboniferous-Permian glacial and deglacial time.

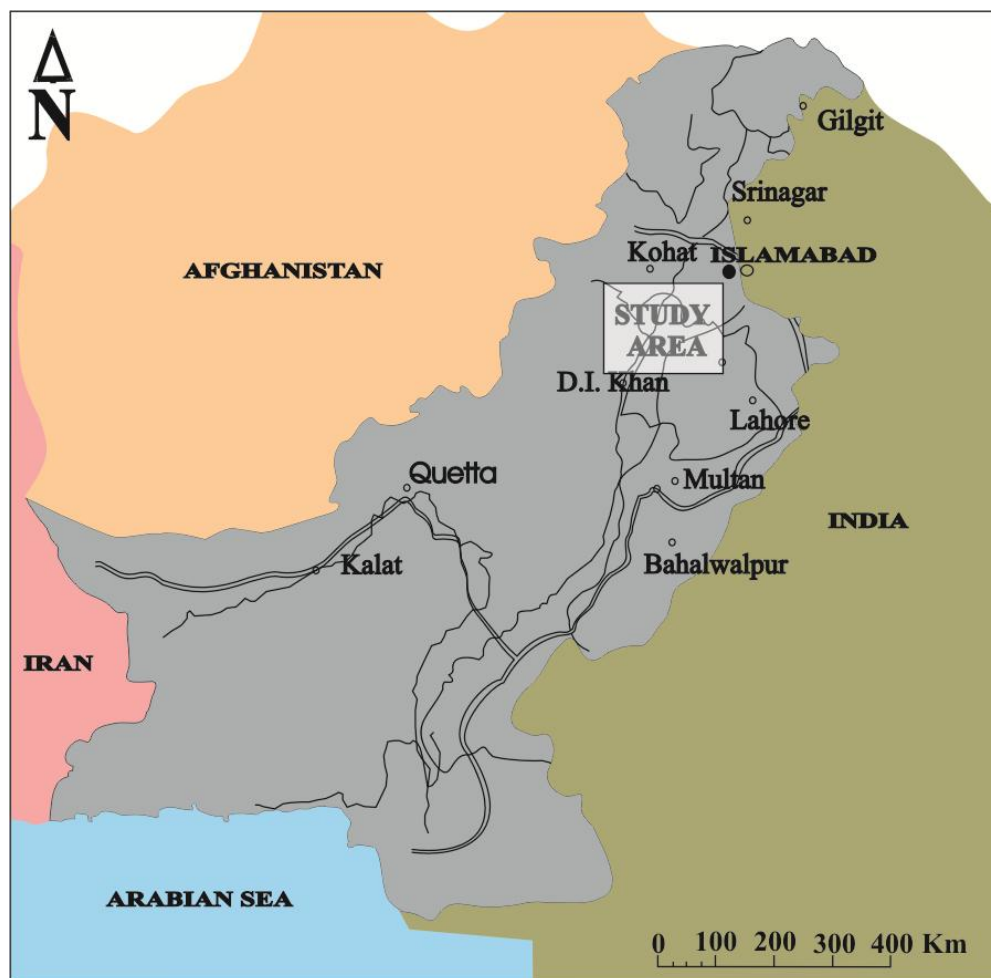


Fig. 1.2 Geographical location map of Pakistan. The study area can be seen highlighted
(Modified after Baker *et al.* 1988).

1.2 Project aims and objectives

The broad research aims to:

- 1 Record the palynology (plant microfossils) and sedimentology of the terrestrial Carboniferous-Permian Gondwanan succession of the area.
- 2 Correlate the successions with the regional stratigraphy.
- 3 Integrate palynological, sedimentological and published palaeontological data to correlate across the Salt and Khisor Ranges and describe the palaeoenvironment.

The Carboniferous-Permian palynostratigraphy of Pakistan will help correlate the succession with the biostratigraphically best-resolved sedimentary successions of Gondwana (especially the Middle East), and understand the chronological position of these deposits in the context of late Palaeozoic Gondwanan glaciations. The sedimentological analysis of these successions will help to develop depositional models and their evolution for the palaeoenvironments during the late Palaeozoic ice house.

1.3 Structure of this thesis

This thesis is comprised of 8 chapters.

Chapter 1 deals with the introduction to the work, the scientific rationale and objectives.

The later part of this chapter highlights information about the Carboniferous-Permian succession of the area (i.e. the Salt Range and Khisor Range, Pakistan), discusses the field methodology, laboratory techniques and data representation methods, used during the study. Chapter 2 gives a brief background to the Carboniferous-Permian world, time scale development and palaeocontinental configuration. The later part of chapter 2 gives a review of the selected Carboniferous-Permian Gondwanan palynostratigraphy.

Chapter 3 underlines the sedimentological investigations of the Carboniferous-Permian, Nilawahan Group of the Salt Range and the results of the palaeoenvironment analysis.

Chapter 4 describes the systematic palynology of the stratigraphically diagnostic taxa.

Chapter 5 discusses the palynostratigraphy of the Upper Pennsylvanian Tobra Formation. This chapter is modified from the paper that is published in the (journal)

“*Palynology*”. The paper is included in the appendices. Chapter 6 discusses the palynostratigraphy of the Middle Permian, Sardhai Formation. This chapter is modified from the paper that is published in the (journal) “*Review of Palaeobotany and Palynology*”. The paper is also included in the appendices. Chapter 7 is based on palynological synthesis. Chapter 8 describes conclusions and recommendations.

1.4 Materials and methods

The methodology of this study included the fieldwork, palynology, and sedimentology samples collection, and laboratory processing and analyses.

1.4.1 Fieldwork

The Cretaceous under thrusting of the Indian Plate beneath the Eurasian Plate gave rise to many conspicuous tectonic features around the northern and northwestern peripheries of the Indian Plate. As a result of this under thrusting, spectacular mountain ranges of the Himalaya and a succession of foreland fold-and-thrust belts were created, when a thick sheet of the sedimentary rocks overrode the Indian Craton (Alam 2008). The Salt Range represents the active frontal thrust zone of the Himalaya in Pakistan and with its Trans-Indus ranges (i.e. Khisor, Shinghar, Surghar, Marwat ranges and Khisor ranges), it represents a complex summit between the outer ranges of the northwestern Himalayas and the Sulaiman Mountain Arc (Baker *et al.* 1988; Gee 1989). The area that covers the southern slopes of the Potwar Plateau as well as that of the Surghar Range, extending from Jogi Tilla to Makarwal has been referred to as the Salt Range (Fig. 1.3). This constitutes a distance of more than 250 km. The area is divided into the Cis-Indus Salt Range (areas to the east of the river Indus) and Trans-Indus Salt Range (areas to the west of the river Indus). Locally the Salt Range is further divided into eastern, central and western parts (Shah 1980). The Carboniferous-Permian succession of Pakistan comprises approximately 610 m of sedimentary strata and crops out in the Salt Range and Trans-Indus Khisor (Fig. 1.3). The succession is also exposed in the Marwat and Surghar ranges, which have not formed part of this study (Kummel & Teichert 1970). The succession represents the southern side of a rift flank basin along the northern Gondwanan coastal margin (Wardlaw & Pogue 1995; Jan *et al.* 2009).

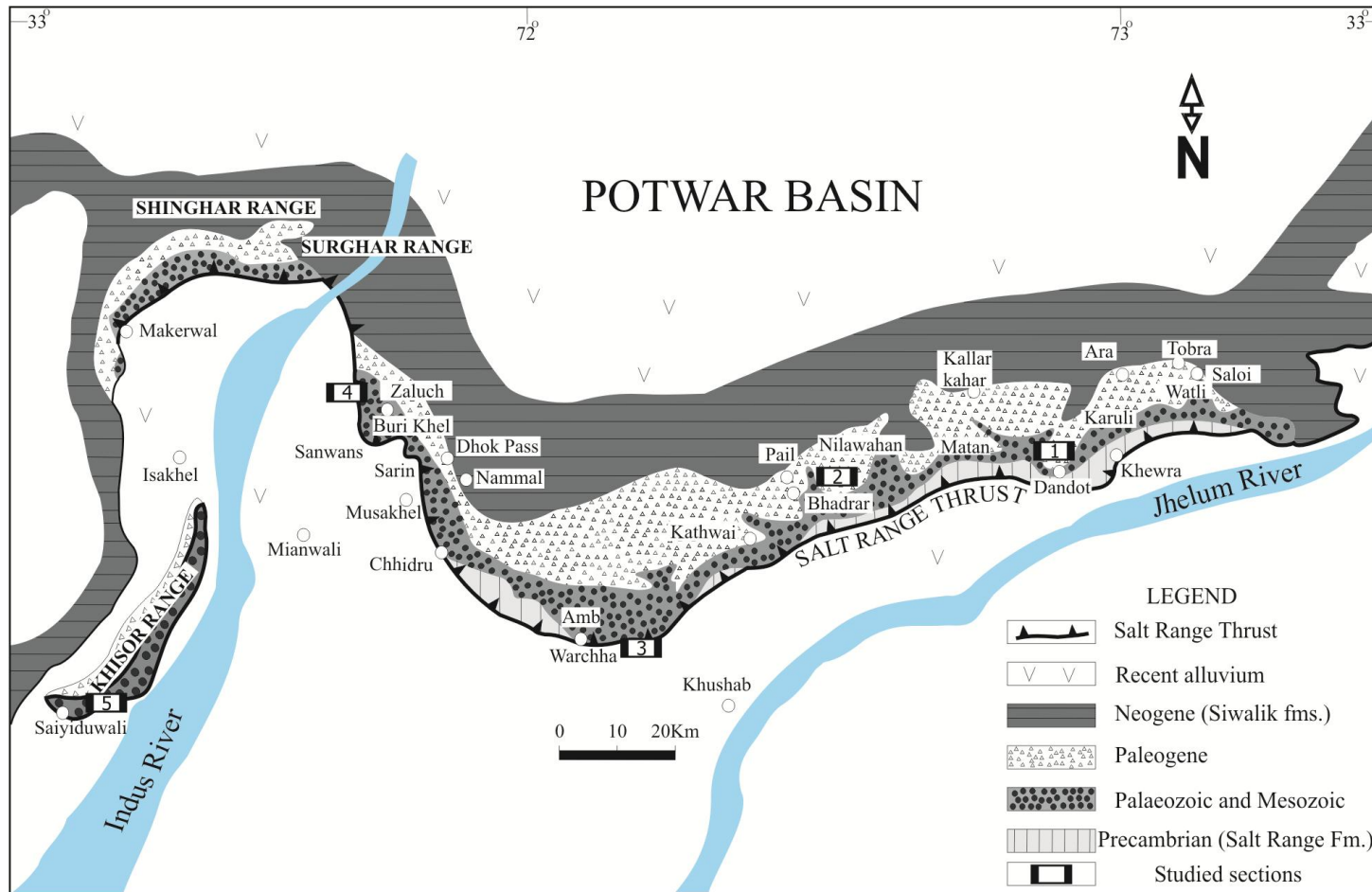


Fig. 1.3 Geological sites studied, 1. Khewra-Choa section, 2. Pail section, 3. Warchha gorge section, 4. Zaluch Nala section (Salt Range), 5. Saiyiduwali section, Khisor Range (Modified after Ghazi & Mountney 2009).

The succession in the Salt Range and Khisor Range is divided into two groups (Fig. 1.4), the terrestrial Gondwana succession, represented by the Nilawahan Group, and the shallow marine Tethyan succession, represented by the overlying Zaluch Group (Wardlaw & Pogue 1995; Jan *et al.* 2009). The Nilawahan Group comprises of the Tobra, Dandot, Warchha and Sardhai formations and the Zaluch Group comprises of the carbonate dominated Amb, Wargal and Chidru formations (Wardlaw & Pogue 1995; Jan *et al.* 2009).

1.4.1.1 Fieldwork details

During the first geological field season in the Salt Range and the Trans-Indus, Khisor Range (Fig. 1.3), conducted in March 2008, the focus was on collecting samples for palynology from the constituent stratigraphic units in the Nilawahan Group.

Sampling was undertaken in the following key sections,

1. Khewra-Choa section, eastern Salt Range, N 32° 39' 58.5" and E 72° 59' 12.2" (Fig. 1.5c).
2. Zaluch Nala section, western Salt Range, N 32° 46' 56.1" and E 71° 38' 35.4" (Fig. 1.8).
3. Saiyiduwali section, Khisor Range, N 32° 11' 45.2" and E 70° 59' 22.1" (Fig. 1.9).

Apart from the sections mentioned above, some considerations were also given to exposures of possible Nilawahan Group in the Khewra gorge (Fig. 1.5a & b) and Tobra village sections in the eastern Salt Range (N 32° 40' 29.5" and E 73° 99' 15.3").

However, due to the poor exposure, no sampling was undertaken in these sections. The samples collected during the first field work were taken to the laboratories of the British Geological Survey for palynological processing.

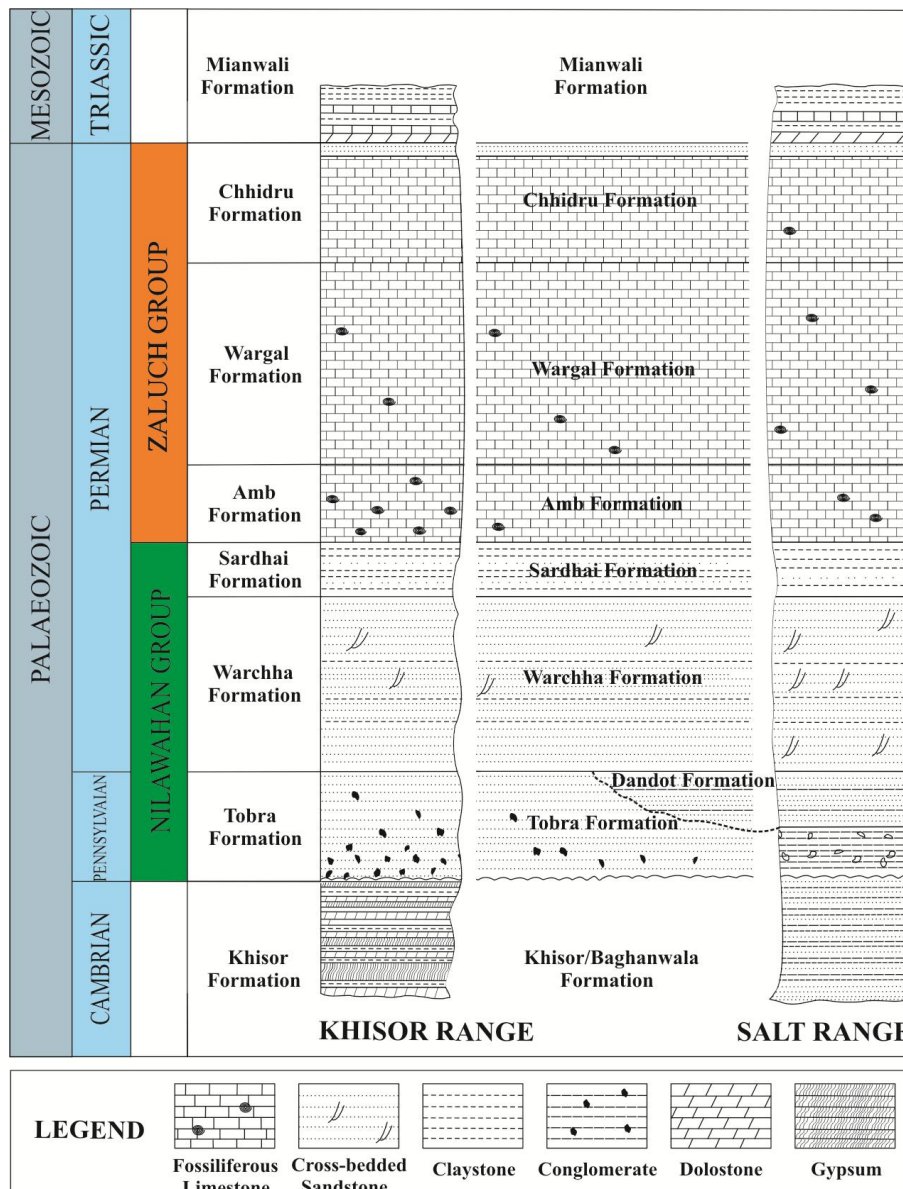


Fig. 1.4 Simplified Carboniferous-Permian stratigraphy of the Salt Range and central part of the Khisor Range. The present study deals with the Nilawahan Group (Modified after Gee 1989; Wahid *et al.* 2004).

During the second field season that was conducted in March 2009; the focus was on sedimentological investigation of the previously visited sections. Some new sections were also studied. The following are the studied locations visited during the second field season,

1. Khewra-Choa section, eastern Salt Range, N 32° 39' 58.5" and E 72° 59' 12.2"

(Fig. 1.5c).

2. Pail section, central Salt Range, N 32° 35′ 49.42″ and E 72° 27′ 15.7″ (Fig. 1.6).
3. Warchha gorge section, central Salt Range N 32° 25′ 41.92″ and E 72° 01′ 40.19″ (Fig. 1.7).
4. Zaluch Nala section, western Salt Range, N 32° 46′ 56.1″ and E 71° 38′ 35.4″ (Fig. 1.8).
5. Saiyiduwali section, Khisor Range N 32° 11′ 45.2″ E 70° 59′ 22.1″ (Fig. 1.9).

Field work methodology

The following methodology was employed during fieldwork for selecting and sampling sections.

Selection of Carboniferous-Permian sections

A reconnaissance investigation of the area was undertaken, which included identifying and locating potential sites for measuring, logging and sampling the formations.

The available literature pertaining to the Carboniferous-Permian succession studies of the Salt Range is sparse, and most of the literature dates back to the mid twentieth century (Fig. 1.10). Nonetheless the work of Teichert (1967) and Balme (1970) provided a basis for establishing potential sites for sampling and investigation of the formations. Local literature, e.g. Ghauri *et al.* (1977) also helped in selecting sections in the field work, where the Carboniferous-Permian successions have been reported and where it can be studied with comparative ease.

Data collection

Palynology sampling

The palynological sampling was adopted in line with the following criteria,

1. Samples were collected from potential intervals in the Carboniferous-Permian formations; represented by claystone lithologies. A few samples were also collected from the siltstone and sandstone intervals.

2. The samples were achieved by digging for a minimum of 300 mm into the rock, to avoid any unwanted oxidation effects on the palynomorphs to maximise pollen and spore yields. Samples have been collected along the north-face of the exposures to reduce the effects of weathering from direct sunlight.
3. Varied resolution for palynological sampling, between 0.5 m to 1 m has been adopted during the field work.

The palynology sample population in each stratigraphic unit is given in Appendix 1 (see appendices) and the stratigraphic positions of these samples are shown in Appendix 2.

Sedimentary logging and sampling

The formations have been logged carefully in as much detail as possible, supported by numbered photos and sketches. The sites where the samples for palynology and sedimentology have been collected from the formations have been located on logs (see Appendix 2).

1.4.2 Laboratory processing and analyses

1.4.2.1 Processing of the samples

Palynology sample processing

The miospores produced by their parent plants, are taken up by various agencies mostly water, and wind currents and dispersed. These are ultimately deposited in sedimentary rocks. A process known as maceration is used to retrieve these miospores from the host rock material.

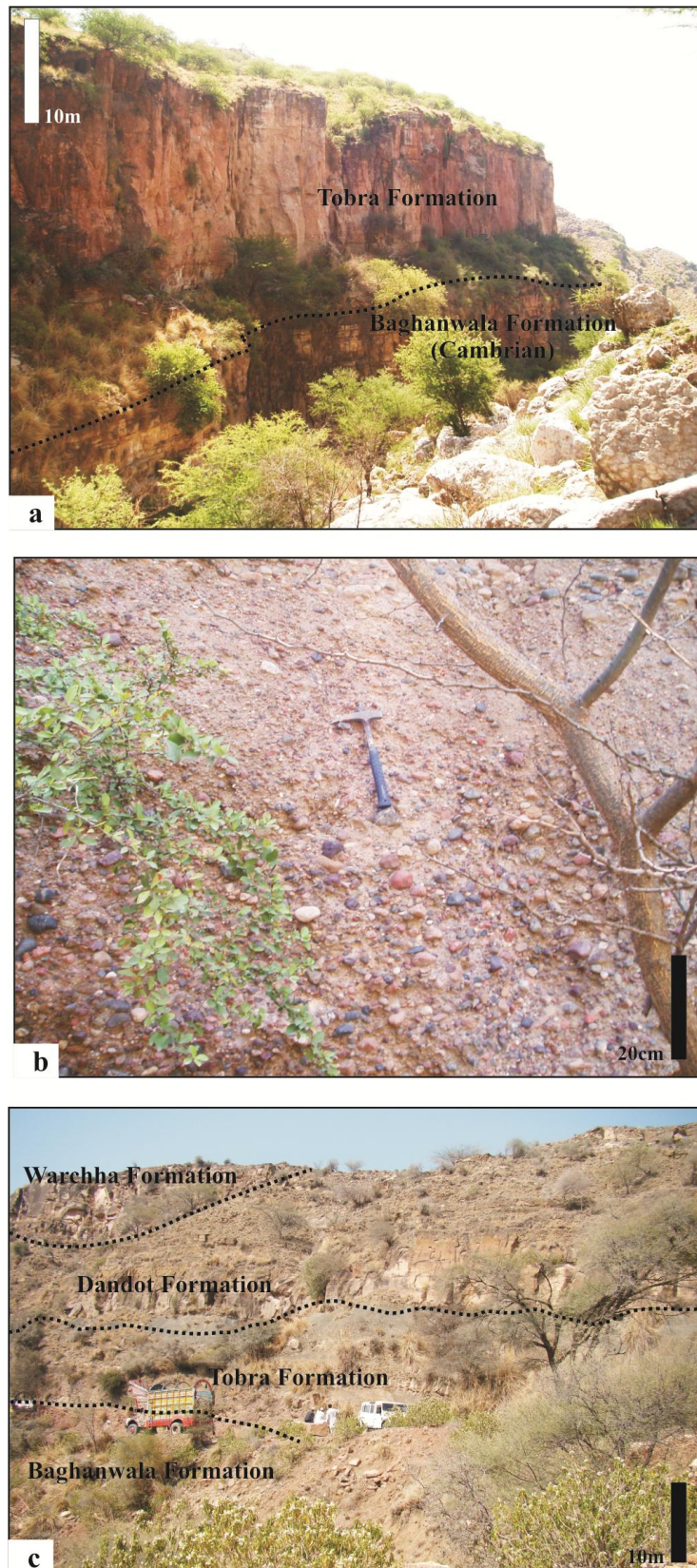


Fig. 1.5 Outcrop of the sections in the eastern Salt Range, a. Khewra gorge section, b. Tobra Formation in the Khewra gorge section, c. Khewra-Choa section (eastern Salt Range). View looking northeast.

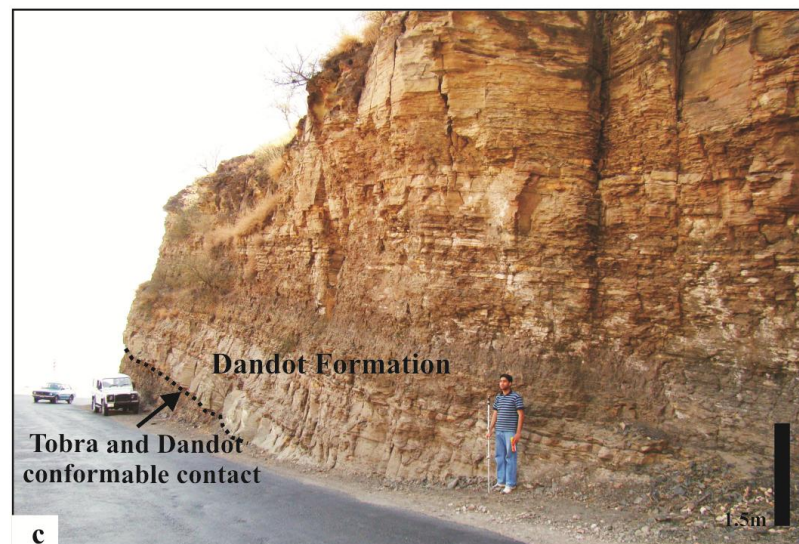
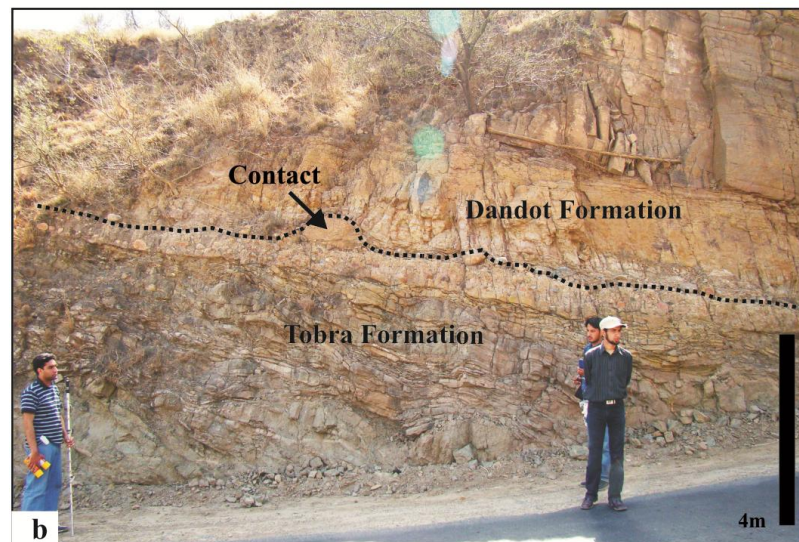


Fig. 1.6 Outcrop of the Pail section, a, b & c show a conformable contact between the Tobra Formation and overlying Dandot Formation in the central Salt Range. Westwards, the Warchha Formation unconformably overlies the Tobra Formation (see Fig. 1.9). View looking southwest.

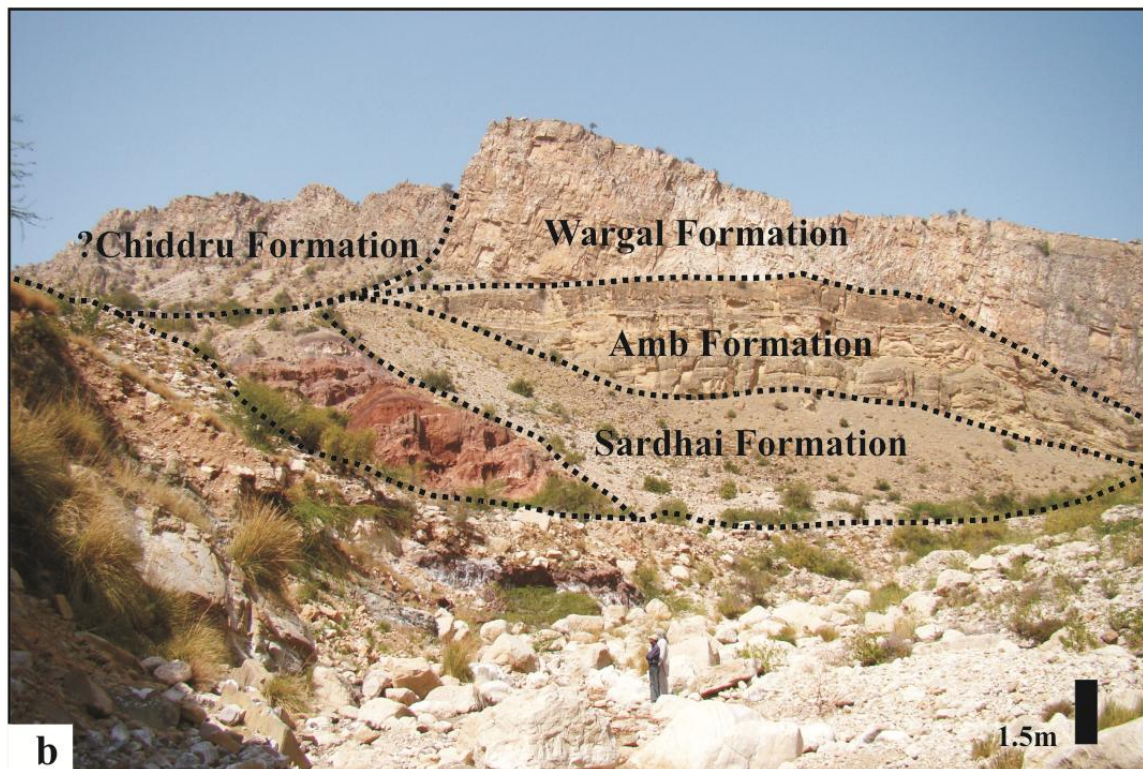
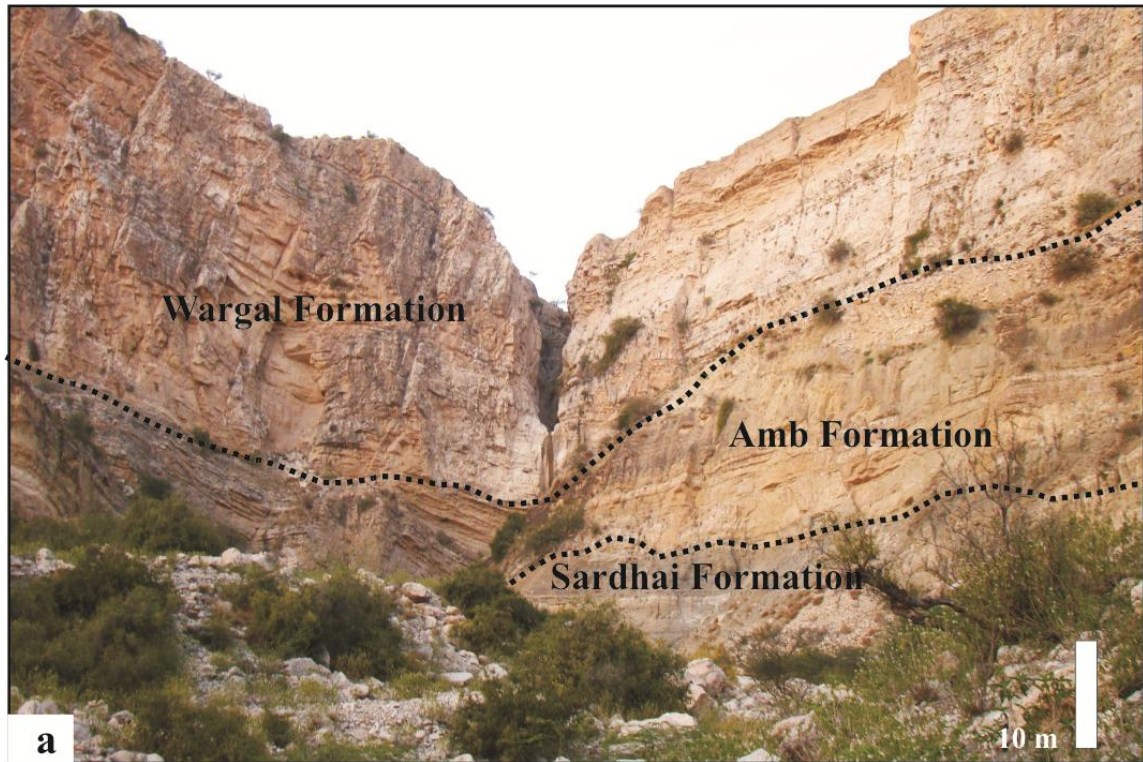


Fig. 1.7 Outcrop of the Warchha gorge section in the central Salt Range. Top and bottom photos show, the Sardhai Formation (i.e. Gondwanan succession) overlain by the Tethyan Zaluch Group (represented by carbonates of the Amb, Wargal and Chiddru formations). View looking northwest.

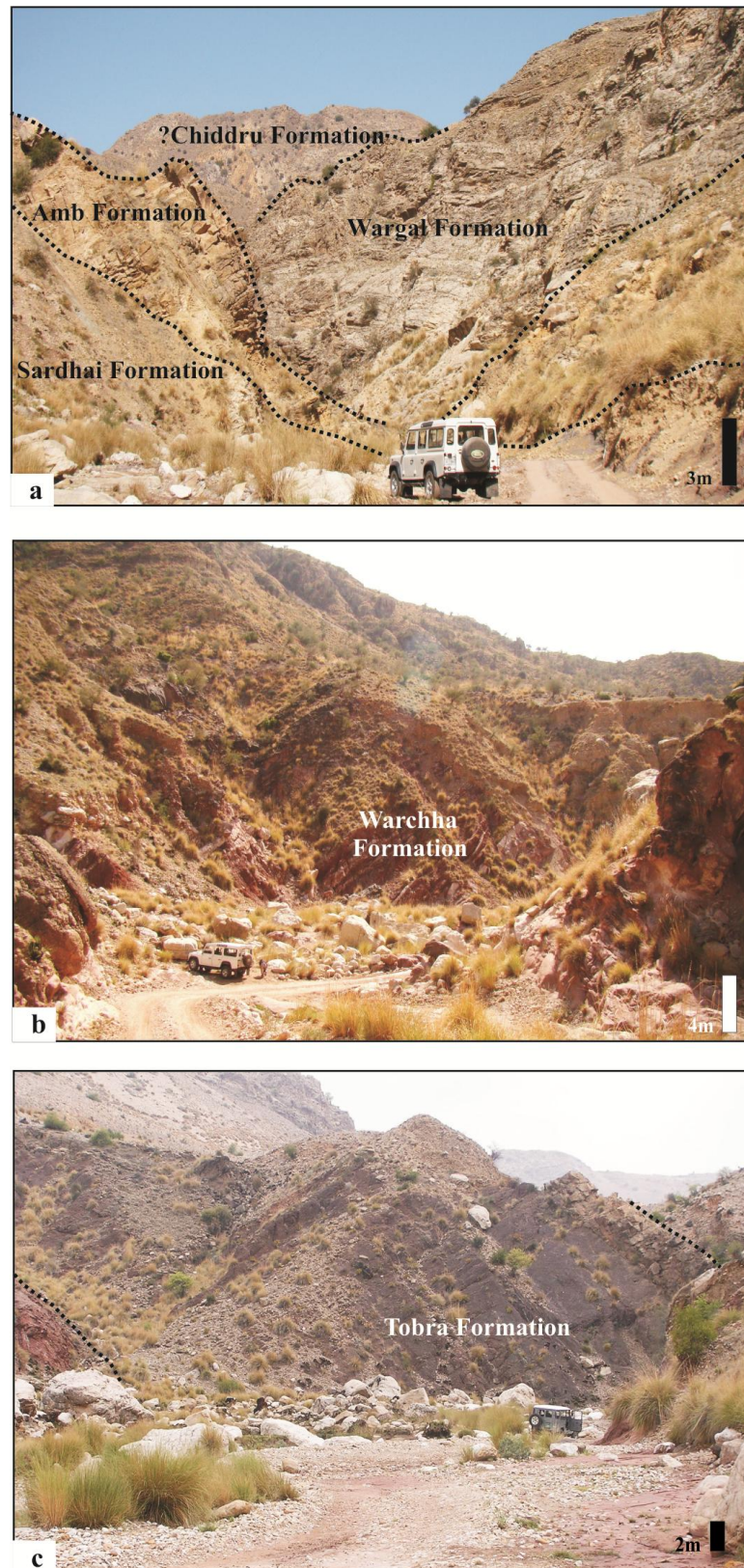


Fig. 1.8 Outcrop of the Zaluch Nala section in the western Salt Range, a. Sardhai Formation overlain by the Zaluch Group (i.e. Amb, Wargal and Chiddru formations), b. Warchha Formation in the Zaluch Nala section, c. Tobra Formation in the Zaluch Nala section. View looking northeast.

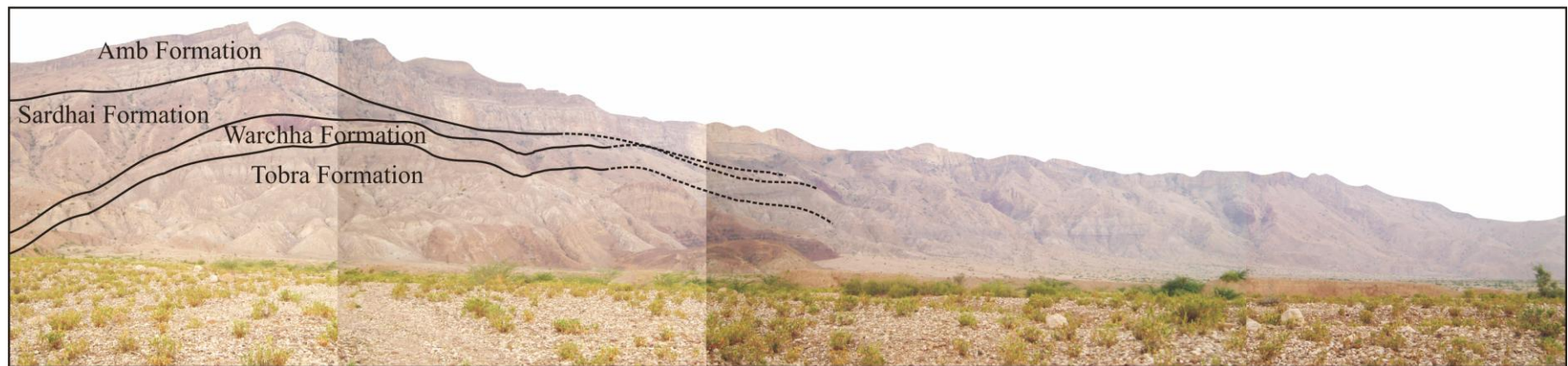


Fig. 1.9 Photomosaic of the Khisor Range showing Tobra, Warchha and Sardhai formations. The Dandot Formation is missing. The cliff is approximately 400 metres. View looking northeast.

SALT RANGE RESEARCH HISTORY	Investigator (s)	Research undertaken
	Elphinstone (1815)	Naming the Salt Range
	Fleming (1848)	Stratigraphic observations and fossil collection
	Theobald (1854)	Introduced the term <i>Productus</i> limestone
	Wynne (1878)	Measured the first stratigraphic section in the Salt Range
	Waagen (1879)	Monograph on the fauna of <i>Productus</i> limestone and <i>Ceratite</i> beds
	Fritz Noetling (1900a, 1900b, 1900c)	Relationship between <i>Productus</i> limestone and <i>Ceratite</i> Formation of the Salt Range
	Tschernyschew (1902)	Correlated and discussed the age of the <i>Productus</i> limestone fauna with Ural and Timan
	Gee (1947)	Mapped the entire Salt Range on scale 2 miles to 1 inch
	Pascoe (1959)	Compiled geological observations in the Salt Range
	Teichert (1967)	Reconnaissance studies of the Tobra Formation
	Kummel & Teichert (1970)	Edited a volume, <i>Stratigraphic boundary problem: Permian and Triassic of west Pakistan</i> . The volume contained very useful papers by various authors
	Pakistani-Japanese Research Group (1985)	Investigated the litho- and biostratigraphy of the marine Permian and the lower Triassic strata of the Salt Range
	Mertmann (1999, 2003)	Developed sequence stratigraphic interpretation of the marine Permian succession

Fig. 1.10 Brief overview of research undertaken in the Salt Range.

Various techniques are used during the maceration process and would usually vary in accordance with the nature and composition of the rock samples to be macerated (Fig. 1.11). These techniques are described in many publications particularly including a detailed review of Wood *et al.* (1996).

The following method has been employed for the palynological processing,

Preparation of samples

1. The sample is cleaned and washed with a brush and water to remove possible contaminants.

2. The sample is crushed to a 4 mm fraction.
3. Approximately 50-100 g is used for processing, which is poured into labelled plastic bottle.

Acid treatment

1. The sample is then dissolved in HCl to remove carbonates if any, no HCl was used in this case as no carbonates were reported.
2. The sample is dissolved in 40% HF to remove silicates. The dissolution process usually takes a week and is conducted in a fume chamber with an extractor to expel gaseous fumes released during the process. During this time the sample is stirred at least twice a day to let the reaction take place successfully.
3. When broken down, the residue is washed 3 times with water leaving to settle each time.
4. It is followed by treatment of residue with HCl to dissolve fluoro-silicates formed during previous reactions.
5. Residue is treated with HNO₃ to remove fine particles.
6. Treatment with KOH to clean the residue.

Sieving

Following the acid treatment, the residue is sieved through a 200 µm sieve to retain larger organic particles, which may contain mega spores and large pollen that could easily break.

Heavy liquid separation and concentration

This involves use of the centrifuge. If the sample is hard to separate into the individual components i.e. the organic material and the heavy minerals, it is centrifuged. Distilled water is added to the sample and put in the centrifuge for 5 minutes involving 4000 rotations per minute. After which the sample is added with zinc bromide (10 mL of 76%

W/W). However, before the zinc bromide is added, the water in the sample has to be removed, since that will form crystals of the zinc hydroxide which can stop the separation process. The sample is then treated with HCl (10 mL of 10%) to stop the crystallisation of zinc hydroxide (ZnOH). After centrifuging, the sample has the organic materials on the surface and the heavy minerals at the base. The organic materials can be skimmed out of the solution.

Slide preparation

For even distribution of the organic materials on the mounted slides, half a tea spoon of PVA (polyvinyl alcohol added and heated in 20 mL water) is mixed with the sample. The sample is then mounted on the slide and the glass is used to stick the slide to cover slip. Finally the covered slip is warmed and dried and is ready for use.

Sedimentology sample preparation

The samples for sedimentology were prepared at the Department of Geology, University of Leicester UK. The sample preparation followed simple procedures:

1. The sample was cut into billets using the cutter machine;
2. These billets are mounted on the glass slides using the “magic fast” and grind using grinder machine;
3. It is then polished with the help of grit (“grit” is a grinding powder, a silicon carbide powder basically, available in different sizes i.e. 100, 220, 400, 600, 800, and 1000 microns);
4. Using grit, the ground billet is polished up to very thin (i.e. 30 microns and >30 microns in carbonate rocks) so that light can pass through it for microscopic examination.

PALYNOLOGICAL PROCESSING FLOW CHART

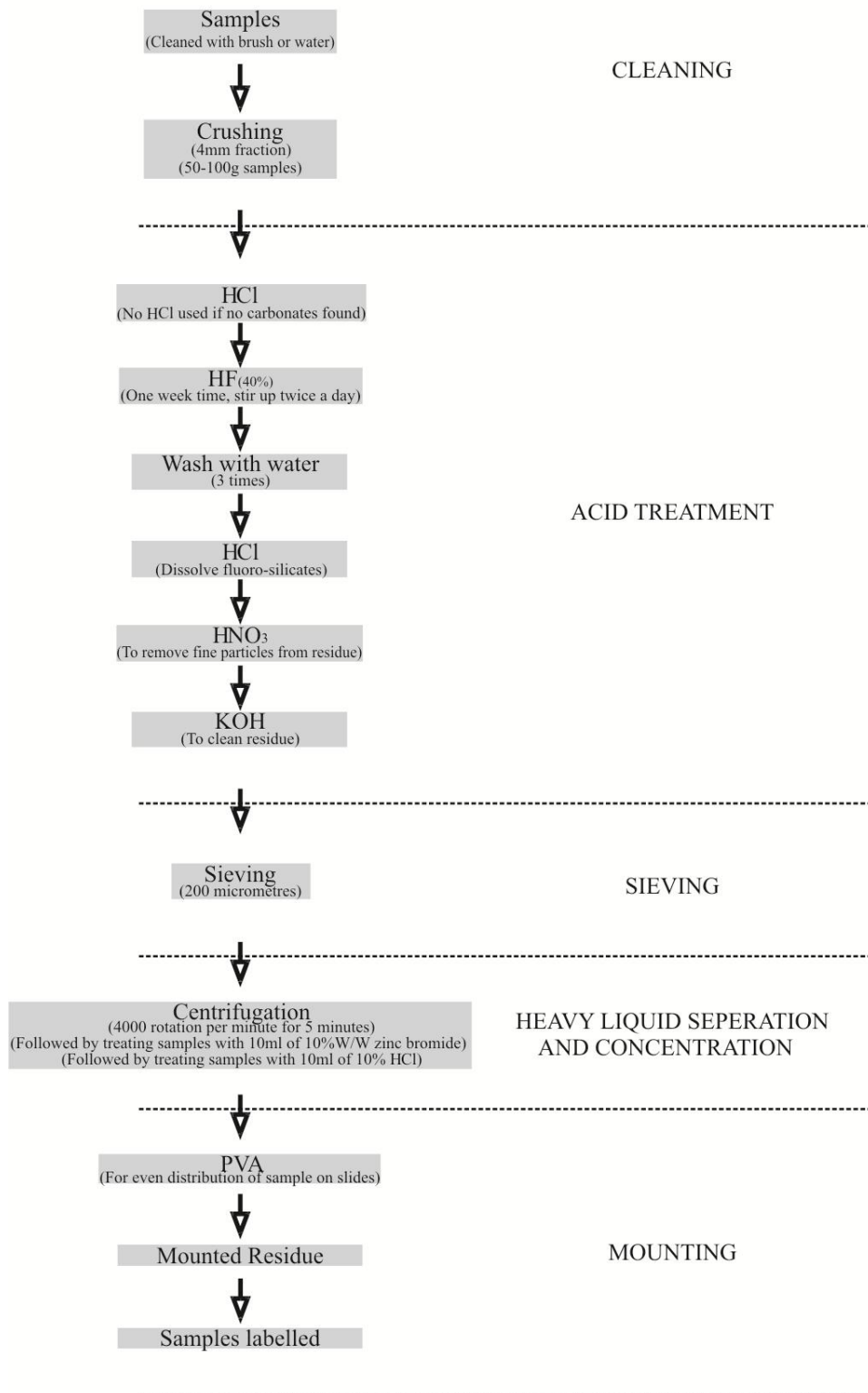


Fig. 1.11 Palynological processing summary chart (Modified after Wood *et al.* 1996).

1.4.2.2 Laboratory analyses

Microscopic palynological analyses

A transmitted-light microscope (Leitz-ARISTOPLAN) at the Department of Geology, University of Leicester was used for the slide analyses, to examine, count and photograph the palynomorphs; however, for the important specimens and publication purposes (see papers in the appendices), the analyses were taken with a Zeiss Universal microscope at the British Geological Survey, Nottingham. These microscopic examinations were conducted using the objective magnifications of x16, x40, x60 and rarely, x100. The magnification of x100 was done with oil immersion to facilitate observation of the fine morphological features of the palynomorphs. Photomicrography was done with a DP11 Olympus digital camera, which stored images in JPEG file format; which were later transferred to computer to photoshop for further analysis and presentation in the thesis chapters or papers. The coordinates for specific palynomorphs on the slide surface, were recorded using the England Finder for future retrieval. The palynological analyses were conducted as outlined below.

Palynological analyses

The study of palynomorphs at generic and specific levels within each sample was conducted to establish the stratigraphic range of each species. These details involved the examination of morphological features as well as the measurements of the important dimensional attributes.

Microscopic sedimentological analyses

Grain identification, modal composition and point counting techniques for a provenance study of the sedimentology samples have been conducted. The petrographic Nikon microscope at the Department of Geology, University of Leicester is used for the

microscopic analyses of these samples and the photomicrographs of these samples are taken using the JVC camera (model KY-F55BE) mounted on the Nikon microscope.

1.4.3 Data representation

1.4.3.1 Palynology data representation

Palynological abundance data representation

The palynomorphs abundance counts were entered into the StrataBugs program at the British Geological Survey to get the abundance charts. These charts, used in palynostratigraphy, have been discussed in the respective chapters 5 and 6.

Palynology range charts representation

The vertical range charts for the palynological data have been constructed using various softwares manually, namely Coreldraw and Freehand.

1.4.3.2 Sedimentology data representation

The sedimentological data from thin sections is represented in the form of frequency histograms and cumulative frequency curves. The plots are made in Microsoft Excel 2007. The QFL ternary plots have been formed using the PAST software (Hammer *et al.* 2001).

2 Chapter 2: The Carboniferous-Permian world and review of Gondwana palynostratigraphy

2.1 Carboniferous-Permian time scales

2.1.1 Carboniferous time scale

The Carboniferous was a time of tremendous diversification in the terrestrial biosphere. This resulted in the development of extensive peat (eventually coal) deposits. The commercial coal mining of these deposits in eastern and western Europe, and North America led to early attempts to study and correlate Carboniferous strata in these regions (Gradstein *et al.* 2004). The original (and informal) classification of this system (after Gradstein *et al.* 2004) in ascending order was as follows.

1. The Old Red Sandstone, which now belongs to the Devonian.
2. The Mountain or Carboniferous Limestone, first proposed by Williams Phillips in 1818.
3. The Millstone Grit, listed by Whitehurst in 1778.
4. The Coal Measure, of Farey in 1807.

These units were formalised by Conybeare & Phillips (1822) as the Carboniferous or Medial Order and by Phillips in 1835 as the Carboniferous System (Gradstein *et al.* 2004). The Carboniferous was sub-divided in other parts of the world (Fig. 2.1) and the North American and Russian subdivisions are discussed briefly below.

2.1.1.1 The North American system

In USA, the Carboniferous is sub-divided into the Mississippian Stage (lower Carboniferous), proposed by Winchell in 1870 and the Pennsylvanian Stage (Upper Carboniferous) proposed by Stevenson in 1888.

PERMIAN	Lopingian	Changhsingian	251.0± 0.4	
		Wuchiapingian	253.8± 0.7	
	Guadalupian	Capitanian	260.4± 0.7	
		Wordian	265.8± 0.7	
		Roadian	268.0± 0.7	
	Cisuralian	Kungurian	270.6± 0.7	
		Artinskian	275.6± 0.7	
		Sakmarian	284.0± 0.7	
		Asselian	294.0± 0.8	
		Gzhelian	299.0± 0.8	
	CARBONIFEROUS	Pennsylvanian	Kasimovian	303.9± 0.9
			Moscovian	306.5± 1.0
Bashkirian			311.7± 1.1	
			318.1± 1.3	

Fig. 2.1 Geological time scale of the Late Carboniferous to Permian (Modified after Gradstein *et al.* 2004).

The predominantly marine deposits of the early Carboniferous were included in the Mississippian stage, with the type locality in the Mississippi valley. The coal-bearing beds in the state of Pennsylvania were assigned to the Pennsylvanian (Gradstein *et al.* 2004). The stratotype section of the base of the Pennsylvanian section is located in Arrow Canyon in the Great Basin Nevada, USA.

The base of the Pennsylvanian Stage coincides with the base of the Bashkirian Stage, established in the early 1930s in the mountains of Bashkiria (southern Urals, Russia),

proposed by Semikhatova in 1934 and is marked by the first appearance datum (FAD) of *Declinognathodus noduliferus s.l.* The radiometric age proposed for the base of the Pennsylvanian and the Bashkirian Stages in the Geological Time Scale is 318.1 ± 1.3 Ma (Gradstein *et al.* 2004).

2.1.1.2 The Upper Carboniferous in Russia

The Upper Carboniferous is further subdivided by Russian geologists, from oldest to youngest, into Moscovian, Kasimovian and Gzhelian Stages and these have become the accepted global standards. The historical developments of these are described as follows.

Moscovian

The Bashkirian-Moscovian boundary is recognised on a global scale by the first appearance datum (FAD) of the conodont species, *Declinognathodus donetzianus* and/or *Idiognathoides postsulcatus* (Nemirovskaya 1999). These conodont species are widely distributed in the Moscow Basin, Urals, Alaska, Canadian Arctic, Japan, North American mid-continent, northwestern Europe, and Spain. The boundary is recognised in North America by the first appearance of *Profusulinella* (Gradstein *et al.* 2004). This conodont zone coincides with the ammonoid zone *Winslowoceras-Diaboloceras* Zone on the Russian Platform and Urals (Gradstein *et al.* 2004).

Kasimovian

Ivanov proposed Kasimovian Stage in 1926 (Gradstein *et al.* 2004), when it was originally included in the Moscovian, based on local correlation. Several attempts have been made thereafter to trace the Moscovian-Kasimovian boundary. The most commonly accepted is suggested by Ruzhenzev in 1950 (Gradstein *et al.* 2004), at the base of the *Dunbarites-Parashumarites* ammonoid zone in the Wewoka Formation of

the upper Desmoinesian (North American Stage; lower Westphalian), this correlates with the proposed *fusulinid* genus *Protriticites* (Davydov *et al.* 1999).

Gzhelian

The stage was proposed by Nikitin in 1890 and is derived and named after a small village called Gzhel near Moscow. The FAD of the conodont *Streptognathodus zethus* in the Moscow Basin was earlier considered by the International Commission on Stratigraphy (ICS) working group to mark the Kasimovian-Gzhelian boundary. However, later Chernykh (2002) found that the FAD of *S. zethus* occurs earlier in the middle Kasimovian and therefore cannot possibly be used to define the base of the Gzhelian Stage (Gradstein *et al.* 2004). Villa (2001) suggested that the first appearance of the conodont *Idiognathodus simulator* can be used as a marker for the Kasimovian-Gzhelian boundary (Gradstein *et al.* 2004).

2.1.2 Permian time scale

The diverse range of deposits in the Ural Mountains of Russia (Murchison 1841) was named Permian after the region of Perm in which it occurs. The post Artinskian Stage deposits, mainly comprising non-marine/hypersaline marine sediments in Russia were inadequate for international correlation (Jin *et al.* 1997) and thus Glenister & Furnish (1961) suggested an integration of faunal schemes from palaeoequatorial marine sequences. However the scheme was not accepted because the sections were geographically separate (Jin *et al.* 1997). Recent improvements in the resolution of Permian conodont stratigraphy (Jin *et al.* 1997) have allowed a threefold subdivision of the Permian.

2.1.2.1 The Cisuralian Series, Lower Permian

The base of Permian was defined in the Ural Mountains of Russia as the base of the Kungurian Stage (Gradstein *et al.* 2004). However this has been lowered to include

three more stages, including, Asselian, Sakmarian and Artinskian. These stages have been put in a series called the Cisuralian (Waterhouse 1982). The Cisuralian (Lower Permian) Series thus constitutes four stages which are described in ascending order.

Asselian

The GSSP for the beginning of the Permian Period and of the Asselian Stage is located at Aidaralash Creek, northern Kazakhstan in the Atobe region (Gradstein *et al.* 2004). The section is located approximately 50 km southwest of the city of Atobe. The position of the GSSP is at the first occurrence of the conodont *Streptognathodus isolatus* and its position is located 27 m above the base of Bed 19, Airdaralash Creek (Davydov *et al.* 1998; Gradstein *et al.* 2004). The first occurrences of *Streptognathodus invaginatus* and *S. nodulinear*, the morphotypes of “*wabaunsensis*” morphocline, nearly coincides with the first occurrence of *S. isolatus* and can thus be used to mark an accessory indicator of the base of the Asselian in other sections (Gradstein *et al.* 2004). The GTS (2004) proposed radiometric age for the onset of the Asselian Stage is 299.0 ± 0.8 Ma, which marks the Carboniferous- Permian boundary. Recently, the radiometric dates of the Rio Bonito Formation of the Paraná Basin, has been assigned as 296.9 ± 1.4 Ma, and 299.1 ± 2.6 Ma by Guerra-Sommer *et al.* (2005) and 298.5 ± 2.6 Ma by Rocha-Campos *et al.* (2006). The Rio Bonito Formation is partly placed in the Asselian (Stephenson 2008a).

Sakmarian

The proposed boundary for the Sakmarian Stage is defined by Ruzhenzev (1950) in Karamurantau, Orenburg Province, Russia (Gradstein *et al.* 2004). Due to the lack of ammonoids, fusulinaceans were originally used as indicators of the base of the Sakmarian Stage. The occurrence of the *Schwagerina (Pseudofusulina) moelleri* Zone was originally used to define the lower boundary. However, this fusulinid is found to occur at higher levels and the proposed base definition is based on the transition of the

conodont *Sweetognathus expansus* to *S. merrilli* (Gradstein *et al.* 2004). This transition occurs at 115 m above Bed 11 of Aidralash Creek, and also it is widespread and seen throughout Kansas in the upper part of the Eiss Limestone of the Bader Limestone. This transition occurs a few meters below the *S. moelleri* beds (Wardlaw *et al.* 1999), and is radiometrically dated as 294.6 ± 0.8 Ma.

Artinskian

Karpinsky in 1874 proposed the stratotype of the Artinskian Stage in the Kashkabash Mountain sandstone on the right bank of the Ufa River, in the village of Arty, Russia. Later, Chuvashov *et al.* (1993) defined the lower boundary of the Artinskian Stage based on the occurrence of the fusulinids *Pseudofusulina*. Jin *et al.* (1997) suggested a redefinition of the lower boundary to be based at the base of the *Sweetognathodus whitei* Zone which marks the base of the Bursevsky Horizon. The Artinskian Stage lower boundary is radiometrically dated as 284.4 ± 0.7 Ma (Gradstein *et al.* 2004).

Kungurian

The lower boundary of this stage was originally included in the Guadalupian Series and then redefined and included in Cisuralian Series by Jin *et al.* (1997). The base of this stage is defined on the basis of the FAD of the conodont *Neostreptognathodus pnevi* in the Saraninsk (Sarana) Horizon. A probable stratotype of the base of this stage is located near the Mechetlino settlement on the Yuryuzan River, Russia (Gradstein *et al.* 2004). The Artinskian-Kungurian boundary is radiometrically dated as 275.6 ± 0.7 Ma (Gradstein *et al.* 2004).

2.1.2.2 The Guadalupian Series, Middle Permian

The Guadalupian was first proposed by Girty for the spectacular fossils found in the Guadalupe and Glass Mountains of West Texas (Gradstein *et al.* 2004). This series has

been established on the basis of the evolution of a single genus of conodont, *Jinogondolella*. The Guadalupian Series constitutes the following three stages.

Roadian

The GSSP for the Roadian is in Stratotype Canyon, Guadalupe Mountains National Park, Texas, USA. The marker horizon for the GSSP is the first appearance of the conodont *Jinogondolella nankingensis* at 42.7 m above the base of the black, thin-bedded limestone of the Cutoff Formation and 29 m below the shale band in the upper part of the El Centro Member (Gradstein *et al.* 2004). The magnetostratigraphy of the Cutoff Formation indicates reverse polarity (Wardlaw *et al.* 2004).

Wordian

The GSSP for the Wordian is located in the Guadalupe Pass, Texas, located at short distance from Stratotype Canyon. The marker horizon is the first evolutionary appearance of *Jinogondolella aserrata* at 7.6 m above the base of the Getaway Ledge outcrop section in Guadalupe Pass, Guadalupe Mountains, National Park, Texas, USA (Wardlaw *et al.* 2004). The magnetostratigraphy of the Wordian Stage limestone of the Guadalupian National Park displayed reverse polarity (Gradstein *et al.* 2004).

Capitanian

The GSSP for the Capitanian is in the Guadalupian National Park. The marker horizon is characterised by the evolutionary appearance of the conodont *Jinogondolella postserrata* within the lineage *nankingensis-aserrata-postserrata* at 4.5 m in the outcrop section at Nipple Hill, in the upper Pinery Limestone Member of the Bell Canyon Formation (Gradstein *et al.* 2004). Normal polarity is indicated by few samples in the Pinery Limestone and overlying Lamar Limestone of the Bell Canyon Formation (Gradstein *et al.* 2004).

2.1.2.3 The Lopingian Series, Upper Permian

Huang (1932) proposed the Lopingian for the uppermost Permian Series. The Lopingian Series is comprised of two stages, The Wuchiapingian and the Changhsingian.

Wuchiapingian

The base of the Lopingian was historically designated to coincide with a global regression, i.e. with the boundary surface between the Middle and the Upper Absaroka Megasequences (Gradstein *et al.* 2004).

The GSSP for the Wuchiapingian Stage coincides with the first occurrence of the conodont *Clarkina postbitteri* within evolutionary lineage *Clarkina postbitteri hongshuiensis* to *Clarkina dukouensis* at the base of Bed 6K of the Panglaitan section (Gradstein *et al.* 2004).

Changhsingian

The former GSSP for the Changhsingian Stage was recommended as the horizon *Clarkina orientalis* and *Clarkina subcarinata*, that was located at the base of the Bed 2, the base of the Changxing Limestone in Section D at Meishan, Changxing Country, Zhejiang Province, China (Gradstein *et al.* 2004). The new GSSP for the Changhsingian Stage is defined by the first occurrence of *Clarkina wangi* within Bed 4 in Section D at Meishan, Chanxing Country, China.

2.2 The Carboniferous-Permian palaeocontinental configuration

The development of the super-continent Pangea is the most distinctive feature of the Late Carboniferous to Early Permian world (Gradstein *et al.* 2004). The Palaeozoic palaeocontinental and palaeogeographical reconstructions are based on Apparent Polar Wander Paths, palaeontological and sedimentological data (Torsvik *et al.* 1990; Frakes *et al.* 1992).

306 Ma
LATE CARBONIFEROUS

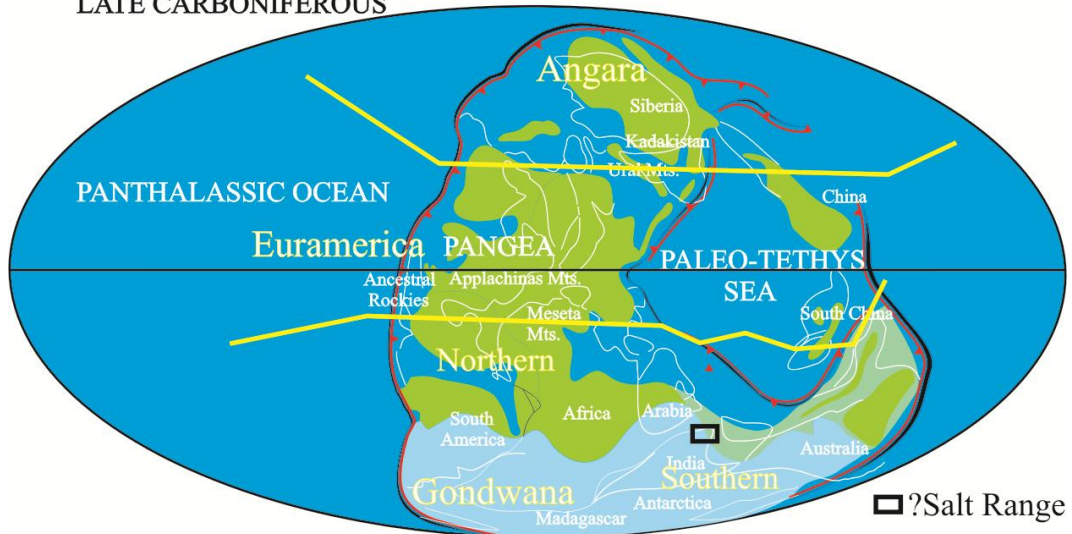


Fig. 2.2 The Late Carboniferous palaeocontinental reconstruction

(Source: <http://www.scotese.com>).

The main mega-continent (e.g. Scotese & McKerrow 1990) that constituted Pangea (Fig. 2.2) are discussed briefly below.

2.2.1 Gondwana

Gondwana was the largest continental mass in the Palaeozoic. It was centred about the South Pole of Pangea and consisted of Africa, Australia, Madagascar, Arabia, Antarctica, South America, New Zealand and India (Scotese *et al.* 1999).

A selective review of the Carboniferous-Permian palynostratigraphic trends in these continental fragments is discussed later in this chapter in detail.

2.2.2 Euramerica

The Euramerican mega-continent was palaeoequatorial and comprised of Laurentia and Avalonia.

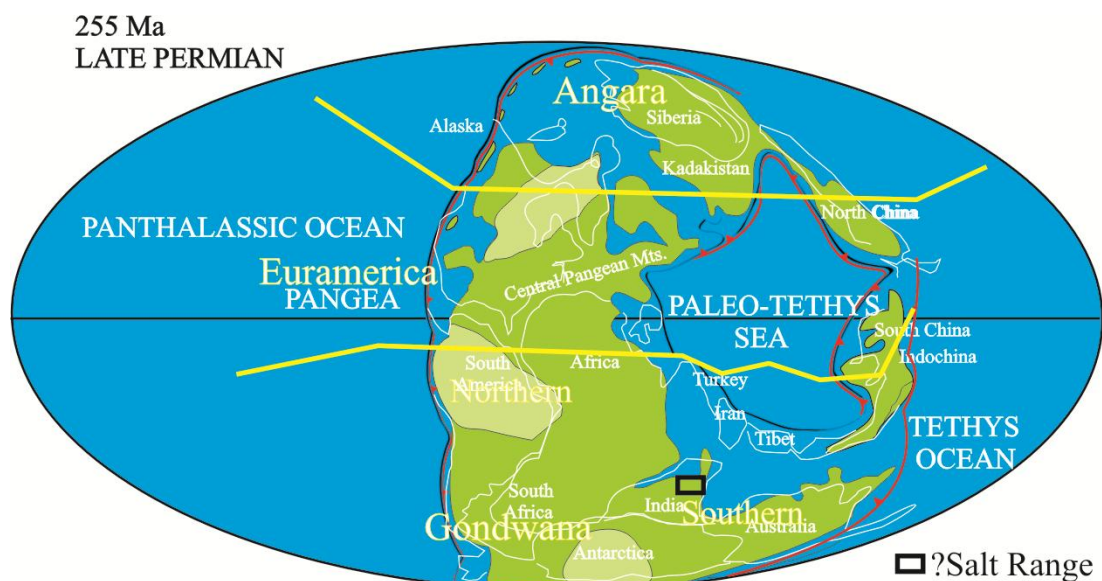


Fig. 2.3 The Late Permian palaeocontinental reconstruction
(Source: <http://www.scotese.com>).

The Laurentian continent consisted of North America, northwest Ireland, Scotland, Greenland, the Chukostsk Peninsula of northeastern USSR, and the northern slope of Alaska (McKerrow & Scotese 1990). The Avalonia comprised of northern France, Belgium, England, Wales, southeastern Ireland, and southern New Brunswick, much of Nova Scotia, the Avalon Peninsula of eastern Newfoundland, and some coastal parts of New England.

2.2.3 Angara

The Angara palaeocontinent was centred about the northern pole and consisted of the following continents, Baltica, Siberia, and Kazakhstan and Cimmeria/Mega Lhasa. The Baltica consisted of the major part of northern Europe. The Siberia was surrounded by the northern half of the Urals and the Irtysh Crush Zone on the west, on the south by the South Mongolian arc, and on the northeast by the Verkhoyansk Fold Belt (McKerrow & Scotese 1990).

The Cimmeria/Mega Lhasa continent consisted of Turkey, Iran, Tibet, Shan Thai-Malaya, and Indo China. It was located along the margins of Gondwana, and thus has glacial-related deposits (McKerrow & Scotese 1990).

2.3 Review of Carboniferous-Permian Gondwana palynostratigraphy

Coal and hydrocarbon exploration resulted in palynological examination of the Carboniferous-Permian Gondwanan sections. Various workers have attempted to review palynology of this region (e.g. Hart 1971; Kemp *et al.* 1977; Anderson 1977; Bharadwaj & Srivastava 1973; Archangelsky *et al.* 1980; Russo *et al.* 1980; Truswell 1980; Foster & Waterhouse 1988; Playford 1990; Backhouse 1991, 1993). Recently, Stephenson (2008a) synthesised the Carboniferous-Permian Gondwanan palynology. A brief history of palynological development in selective Gondwanan regions is given below.

2.3.1 Arabian palynostratigraphy

2.3.1.1 Saudi Arabian palynostratigraphic trends

The initial work by McClure (1980) resulted in the identification of a few palynomorph taxa from the borehole in the Wajid area of southwestern Saudi Arabia. The taxa included *Cyclogranisporites* spp., *Cannanoropollis* spp., *Complexisporites polymorphus*, *Florinites* spp., *Leiotriletes directus*, *Plicatipollenites gondwanensis*, *Potonieisporites novicus* and *Punctatisporites* spp. Subsequently Stump & van der Eem (1995) reported and associated taxa of the Wajid Outcrop Belt of southern Saudi Arabia with Sakmarian to Artinskian, Kazanian and Tatarian. Stephenson *et al.* (2003) established the Oman and Saudi Arabia palynozonation scheme (i.e. extending from OSPZ1 to OSPZ6, fig. 2.4). Stephenson (1998a), Stephenson & Filatoff (2000a, b), Stephenson & Osterloff (2002) and Stephenson *et al.* (2003) correlated the Carboniferous-Permian assemblages in Oman and Saudi Arabia with those from Gondwana.

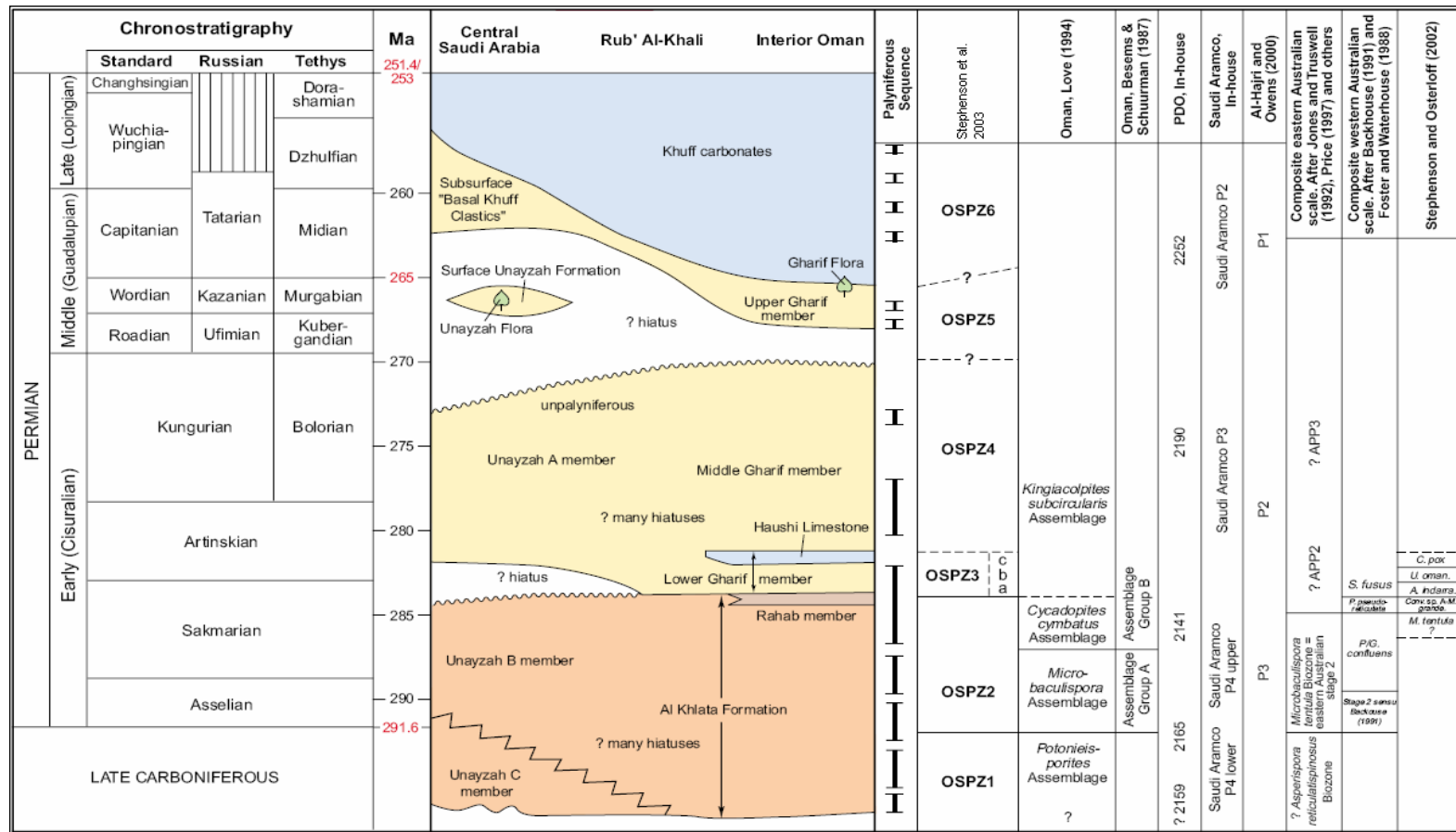


Fig. 2.4 Oman and Saudi Arabia Late Carboniferous to Early Permian palynological schemes (From Stephenson *et al.* 2003).

Stephenson (1998a) and Stephenson & Filatoff (2000a) correlated the upper part of the Al Khlata Formation of Oman and Unayzah B member of central Saudi Arabia, with the *Granulatisporites confluens* Opper-zone (i.e. Foster & Waterhouse 1988), suggesting an Asselian to Sakmarian age. These ages have been recently revised as Pennsylvanian; Gzhelian or Kasimovian (e.g. see Stephenson 2009). Stephenson & Filatoff (2000a) correlated the Arabian Carboniferous-Permian with the South American *Cristatisporites* Zone.

2.3.1.2 Yemen

Very limited palynological studies have been undertaken on the Late Carboniferous to Early Permian rocks of Yemen. Kruck & Thiele (1983) reported the following taxa from the Akbarah Formation, *Apiculatisporis* spp., *A. aff. abditus*, *Acanthotriletes* sp., *Cordaitina* sp., *Kraeuselisporites apiculatus*, *K. punctatus*, *Leiosphaeridia* sp., *Potonieisporites novicus*, *Protohaploxypinus goraiensis*, *P. jacobii*, *Punctatisporites* sp., *Reticulatisporites* sp., *Tympanicysta* sp. and *Vestigisporites* sp. These assemblages were assigned an Early Permian age. El-Nakhal *et al.* (2002) reported palynomorphs from the lower part of the Khalaqah Shale Member (=Akbarah Formation). The taxa recorded were; *Alisporites* cf. *indarraensis*, *Brevitriletes* cf. *cornutus*, *Cristatisporites* cf. *crassilabratus*, ?*Diatomozonotriletes* sp., *Deusilites tentus*, *Leiosphaeridia* sp., *Leiotriletes* cf. *directus*, *Plicatipollenites malabarensis*, *Pteruchipollenites* sp., *Rugospora* sp., *Verrucosisporites* sp., and indeterminate non-taeniate bisaccate pollen. The age suggested for these palynomorphs was only tentatively assigned as Late Carboniferous to Early Permian. Recently Stephenson & Al-Mashaikie (2010) reported diverse and well-preserved palynological assemblages in the lower part of the Kuhlan Formation (Unit A, fig. 2.5).

System/Stage	PERMIAN		Stratigraphy	Biozone	PDO biozones, Penney et al. (2008)	Mukhaizna biozones, Stephenson et al. (2008)	Correlative range of lower Kuhlan Formation	Range of <i>C. confluens</i> in Oman							
	Asselian	Sakmar													
CARBONIFEROUS	Al Khilata Formation	Unayzah B	Unayzah A	OSPZ2	2141B	Biozone A		I?							
									2141A	Biozone B					
											2165B	Hiatus?			
									2165A	Biozone C					
											Unayzah C	OSPZ1	2159	Biozone D	

Fig. 2.5 Correlation of Oman and Arabian Peninsula biozones and a portion of the Khulan Formation of Yemen (From Stephenson & Al-Mashaikie 2010).

2.3.1.3 Oman

Besems & Schuurman (1987) discussed the palynostratigraphy of the Al Khilata Formation using outcrop samples from the Mifrid and Al Khilata localities in Wadi Al Khilata outcrop area and divided the palynological assemblages into two types. Assemblage A and Assemblage B. Assemblage A included commonly occurring monosaccate pollen, represented by *Cannanoropollis* spp., *Plicatipollenites* spp., and *Potonieisporites* spp. The trilete spores in assemblage A are represented by *Cristatisporites* spp., *Horriditriletes* spp., *Lundbladispora braziliensis*, *Microbaculispora* spp., and *Vallatisporites arcuatus*.

The taeniate bisaccate pollen are rare to common in this assemblage (Besems & Schuurman 1987). Assemblage B includes common taeniate bisaccate pollen, *Cycadopites cymbatus*, *Vittatina* spp. and trilete spores (Besems & Schuurman 1987). Love (1994) documented four palynological assemblages from the Haushi Group. From older to younger these assemblages are described as the *Potonieisporites* Assemblage, the *Microbaculispora* Assemblage, the *Cycadopites cymbatus* Assemblage, and the *Kingiacolpites subcircularis* Assemblage.

Penney *et al.* (2008) formulated seven biozones in the Al Khlata Formation of Oman (Fig. 2.6). The biozone 2159 is further divided into lower 2159A and upper 2159B. Biozone 2159A comprises up to 100% *Punctatisporites* Group, represented by *Cyclogranisporites* spp., *Calamospora* spp., *Punctatisporites* spp., and *Retusotriletes* spp. The Monosaccate Group in biozone 2159A comprised less than 5% of the assemblage. Rare occurrences of *Anapiculatisporites concinnus*, *Aratrisporites saharaensis*, *Botryococcus*, *Cristatisporites* spp., *Tetraporina* spp., *Tasmanites* and *Vallatisporites arcuatus* are also found in this biozone. The overlying 2159B biozone is characterised by greater than 10% of the Monosaccate Group, with a proportional decrease in the *Punctatisporites* Group. Less than 5% of the assemblage consists of *Anapiculatisporites concinnus*, *Apiculireticulatispora* spp., *Brevitriletes* spp., *Cyclogranisporites* spp., *Densosporites* spp., *Dibolisporites* spp., *Spelaeotriletes triangulus*, *Vallatisporites arcuatus* and *Verrucosisporites andersonii*. Biozone 2165 is also divided into 2165A and 2165B (Fig. 2.6). Cingulicamerate Group in biozone 2165A is approximately 30% of the assemblages, and *Microbaculispora* Group constitutes 5%. *Punctatisporites* and monosaccate groups are abundant. Bisaccate and *Horriditriletes* groups are rare.

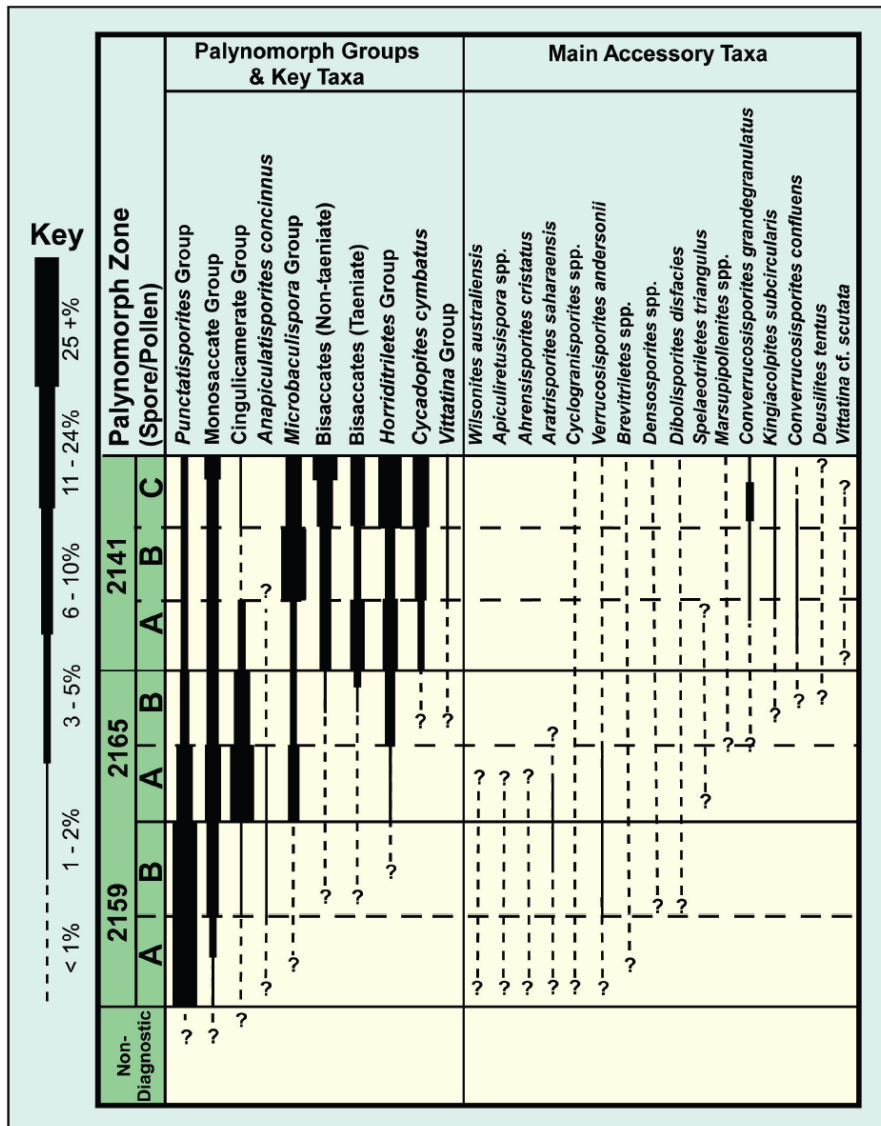


Fig. 2.6 The biozonation of the Al Khlata Formation of South Oman (From Penney *et al.* 2008).

Biozone 2165B is recognised by an increase in *Horriditriletes* Group, generally forming between 5 and 10%, but can form up to 20% of assemblage. *Microbaculispora* Group usually constitutes around 3 to 5% of assemblage, but the group may be absent occasionally. Cingulicamerate Group constitutes 20 to 30% of biozone 2165B. The *Punctatisporites* Group is usually less common than in the biozone below. Bisaccate

groups appear towards the top of this biozone. The Biozone 2141 is subdivided into three biozones i.e. 2141A, 2141B and 2141C (Fig. 2.6).

The diagnostic criteria of the biozone 2141A are; Bisaccate Group represents more than 10% of the assemblage, *Cycadopites cymbatus* is rare at the base, however, it forms 5 to 10% of the assemblage at the top of biozone 2141A. The *Horriditriletes* Group usually represents 10%, but can reach up to 20%. The *Microbaculispora* Group represents approximately 3 to 5% of assemblage, but can be absent occasionally.

The overlying biozone 2141B is defined by containing more than 10% *Microbaculispora* Group, which can become even 60%. The *Cycadopites cymbatus* makes up 5 to 10% of assemblage. Cingulicamerate Group is extremely rare to absent. non-taeniate bisaccate pollen become more important than the taeniate.

Biozone 2141C is marked by more than 10% *Microbaculispora* Group, the *Horriditriletes* Group is more abundant, reaching over 30%. *Cycadopites cymbatus* and the non-taeniate Bisaccate Group are variable and generally reach 60%. The taeniate Bisaccate Group represents 5 to 20%.

Stephenson *et al.* (2008) developed a biozonation in the Mukhaizna field, Oman, based on the first downhole appearance (FDA) of certain taxa using cutting samples. The documented biozones from younger to older are; A, B, C, and D (Fig. 2.7). The top of Biozone A is characterised by an abrupt downhole increase in *Cycadopites cymbatus* and *Microbaculispora tentula* and comprises 15-30% of the assemblages.

Other characteristic taxa of Biozone A include, *Alisporites indarraensis*, *Microbaculispora grandegrnulata* and *Vittatina* cf. *V. scutata* (Fig. 2.7).

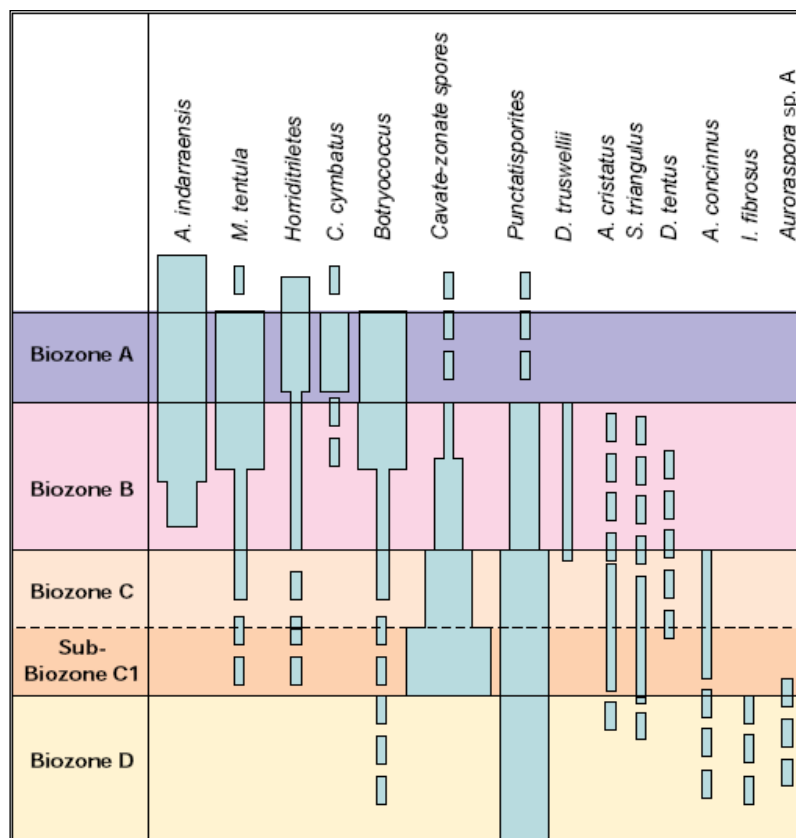


Fig. 2.7 Al Khlata Formation palynostratigraphic scheme proposed in the Mukhaizna Field in south Oman (From Stephenson *et al.* 2008).

The top of the Biozone B is defined downhole by the first appearance of cingulicamerate spores as, *Cristatisporites* spp., *Lundbladispora* spp., *L. braziliensis*, *Vallatisporites* spp., and *V. arcuatus*. Other species with first downhole appearance within Biozone B include, *Ahrensia* *crispatus*, *Deusilites tentus* and *Spelaotriletes triangulus*. The top of Biozone C is defined by the first downhole appearance of *Anapiculatisporites concinnus* and an increase in cingulicamerate spores to up to 40%.

appear and become common. The younger successions (i.e. Stage 3/Unit III) are comprised of (taeniate and non-taeniate) bisaccate pollen (Stephenson 2008a).

2.3.2.1 Western Australian palynostratigraphy

In Western Australia, eight palynozones (Units I to VIII) have been recognised in the Late Carboniferous to Late Permian in the Canning Basin (Kemp *et al.* 1977). The Carboniferous-Permian boundary was proposed to exist between Units II and III by Balme (1980), however, later Backhouse (1991, 1993) amended and repositioned the boundary lower than previously suggested by Balme (1980) in the Collie Basin.

Powis (1984) assigned Stage 1 as Late Carboniferous, characterised by low diversity of palynomorphs and comprised mainly of fern spores (e.g. *Calamospora* spp., and *Punctatisporites* spp.). Powis (1984) correlated Stage 1 with Unit I of Kemp *et al.* (1977).

The base of Stage 2 was originally defined on the appearance of taeniate bisaccate pollen (Evans 1969), however Powis (1984) redefined Stage 2, characterised by the collective first appearance of *Cycadopites cymbatus*, *Horriditriletes ramosus*, *Horriditriletes tereteangulatus*, *Microbaculispora* spp., *Striatoabeites multistriatus* and *Striatopodocarpites cancellatus*.

The base of Stage 3a (Powis 1984) is marked by the first appearance of *Verrucosisporites pseudoreticulatus* and the base of Stage 3b is marked by the first appearance of *Microbaculispora trisina*, *Vittatina* spp., and *Tiwarisporites simplex*.

Foster & Waterhouse (1988) erected the *Converrucosisporites confluens* Opper-zone in the Grant Group of the Canning Basin to replace Stage 2 (of Powis 1984), however, Backhouse (1991, 1993) working on the Collie Basin, Western Australia showed that *Converrucosisporites confluens* Opper-zone is not a replacement of the Stage 2, and he considered it as a separate biostratigraphic unit preceded by Stage 2 (*sensu* Backhouse

1991) and followed by Stage 3. Backhouse (1991, 1993) correlated *Pseudoreticulatispora pseudoreticulata* Zone to Unit III (Kemp *et al.* 1977) and with the Stage 3a of Powis (1984). Unit IV of Kemp *et al.* (1977) is equivalent to *Striatopodocarpites fusus* Zone of Backhouse (1991) and to Stage 3b of Powis (1984, fig. 2.8). The *Striatopodocarpites fusus* Zone of Backhouse (1991) is characterised by the abundance of taeniate and non-taeniate bisaccate pollen, and Unit IV (Kemp *et al.* 1977) is characterised by an abundance of cingulicamerate spores.

2.3.2.2 Eastern Australian palynostratigraphy

The same interval in eastern Australia has been incorporated into five assemblage biozones (Stages 1-5) and a broad similarity can be drawn between the eastern and Western Australian palynozones (Stephenson 2008a). The eastern Australian palynological scheme was proposed by Evans (1969). Five palynological stages were recognised. The base of Stage 2 is marked by the first appearance of taeniate bisaccate pollen grains. Jones & Truswell (1992) worked on the palynology of the Galilee Basin, eastern Australia and proposed, *Spelaeotriletes queenslandensis* Superzone consisting of *Verrucosiporites basiliscutis* Opper-zone (A), *Brevitriletes leptocaina* Opper-zone, *Diatomozonotriletes birkheadensis* Opper-zone (C), *Asperispora reticulatispinosus* Opper-zone (D) and *Microbaculispora tentula* Opper-zone (E).

The base of the *Spelaeotriletes queenslandensis* Superzone (Jones & Truswell 1992) is characterised by the appearance of *Spelaeotriletes queenslandensis*.

The *Verrucosiporites basiliscutis* Opper-zone (A) is characterised by the occurrence of the monosaccate pollen e.g. *Cannanoropollis janaki*, *Potonieisporites novicus* and trilete spores as *Apiculiretusispora arcuatus*, *Cyclogranisporites firmus*, *Spelaeotriletes queenslandensis* and *Verrucosiporites basiliscutis*.

The base of the overlying *Brevitriletes leptocaina* Oppel-zone (B) is marked by FAD of *Brevitriletes leptocaina* and first appearance of *Ahrensisporites cristatus*, *Reticulatisporites bifrons* and *Striatomonosaccites*, and the presence of *Caheniasaccites elephas*, *Dibolisporites disfacies* and *Potonieisporites elongatus*. The *Brevitriletes leptocaina* Oppel-zone (B) is dated as Namurian to early Westphalian.

The succeeding biozone i.e. *Diatomozonotriletes birkheadensis* Oppel-zone (C), is marked by the first appearance of *Diatomozonotriletes birkheadensis* and *Protohaploxypinus goraensis*. The *Diatomozonotriletes birkheadensis* Oppel-zone (C) is dated as Late Namurian to Westphalian D. The succeeding *Asperispora reticulatispinosus* Oppel-zone (D) is Late Westphalian to early Asselian in age and is characterised by the increase in *Cannanoropollis janakii* and appearance of the cavate spores. *Asperispora reticulatispinosus*, *Apiculatisporis pseudoheles*, *Horriditriletes ramosus* and *Retusotriletes* spp., appear at the top of this zone. The *Microbaculispora tentula* Oppel-zone (E) is early Asselian to Sakmarian in age. The base of this zone is defined by the introduction of *Microbaculispora tentula*. This zone was correlated with Stage 2 of Powis (1984).

2.3.3 South African palynostratigraphy

Much of the palynological research in the Karoo basin successions is linked with the correlation of the coal seams (Stephenson 2008a). Anderson (1977) established a comprehensive palynological scheme for the Dwyka and lower Ecca formations of South Africa and established seven biozones for the Late Carboniferous to Permian periods of Karoo basin (Fig. 2.9).

The Dwyka Formation, assigned to Palynozone 1, is dominated by monosaccate pollen and rare occurrence of bisaccate pollen and cavate/zonate spores.

System/Stage		Karoo Basin biozones, Anderson (1977)		Collie Basin biozones, Backhouse (1991)
		Strat	Biozone	
Permian ?	Artinskian	ME	3a	<i>Microbaculispora trisina</i>
		Lower Ecca	2d	<i>Striatopodocarpites fusus</i>
			2c	
	Sakmarian	2b	<i>Pseudoreticulatispora pseudoreticulata</i>	
		2a		
	Asselian	Dwyka	1	<i>Converrucosisporites confluens</i>
Stage 2				
Carboniferous				

Fig. 2.9 Correlation of palynozonations for the two main Carboniferous-Permian basins of South Africa (Modified after Stephenson 2008a).

Palynozone 1 (Anderson 1977) comprises taxa including *Cycadopites cymbatus*, *Microbaculispora* spp., *Indotriradites splendens*, *Punctatisporites* spp., *Plicatipollenites* spp., *Potonieisporites* spp., *Pityosporites* spp., and *Vestigisporites* spp., and is correlated with Stage 2 of eastern Australia (Kemp *et al.* 1977; Backhouse 1991, 1993).

The succeeding Lower Ecca Formation is assigned to Palynozone 2 (Anderson 1977).

This palynozone is divided into four subzones, i.e. 2a, 2b, 2c, and 2d. The base of Palynozone 2 is defined by the appearance of *Microbaculispora micronodosa* and *Pseudoreticulatispora pseudoreticulata*. Palynozone 2a is characterised by the increase in zonate/cavate spores and decrease in monosaccate pollen. Palynozone 2b is characterised by low diversity in zonate/ cavate spores, numerical increase in

Microbaculispora spp., and absence of *Cycadopites cymbatus* and *Vittatina* spp. The base of Palynozone 2c is recognised by the first appearance of *Horriditriletes* spp., *Pachytriletes densus* and *Striatopodocarpites fusus* and FDA of *Gondisporites braziliensis*. Palynozone 2d is characterised by low diversity and a collective increase of non-taeniate bisaccate pollen e.g. c.f. *Alisporites* spp. Palynozone 2 is correlated with Stage 3a of eastern Australia (Kemp *et al.* 1977) and zones *P. pseudoreticulata* and *S. fusus* (Backhouse 1991, 1993).

2.3.4 South American palynostratigraphy

The earliest Late Carboniferous palynological assemblages (e.g., Palynozone I of Azcuy 1979) are dominated by monosaccate pollen (i.e. *Potonieisporites*) and zonate spores (e.g. *Lundbladispota*). Both taeniate and non-taeniate bisaccate pollen are rare (Fig. 2.10). The Permian palynological assemblages (e.g. Palynozone II and III of Azcuy 1979) contain more taeniate bisaccate pollen such as *Vittatina* and *Cristatisporites* (Stephenson 2008a). Most of the South American palynological work has been undertaken on Argentinean and Brazilian sections.

2.3.4.1 Brazil

Most of the palynostratigraphic work in Brazil has been undertaken on the Paraná and Amazonas basins.

Paraná Basin

Daemon & Quadros (1970) proposed six, Late Carboniferous to Early Permian palynozones in the Paraná Basin, Brazil. These biozones in ascending order (i.e. older to younger) are designated as, G, H (H1, H2, H3), I (I1, I2+I3+I4), J, K, L (L1, L2, L3, fig. 2.11). Later, Dias (1993) brought about improvements in the stratigraphic ranges of certain taxa described by Daemon & Quadros (1970).

System/ sub system	South America Azcuay (1979)	Chaco-Paraná, Argentina Playford and Dino (2002) Vergel (1993)		NW Argentina Césari and Gutiérrez (2000)	N Argentina, Bolivia Tarija Basin, Di Pasquo (2003)		Brazil, Paraná Basin Souza (2006)	Brazil, Amazonas Basin Playford and Dino (2000)	
					Strat	Biozone		Strat	Biozone
Lower Permian (Cisuralian)		Striatites Zone		LW			<i>L. virkkiae</i>	Andirá Fm.	<i>V. costabilis</i>
	Palynozone IV	Cristatisporites Zone	Upper						
			Middle						
	Palynozone III		Lower	FS					
?									
Carboniferous (Pennsylvanian)	Palynozone II	Potomcisporites- Lundbladispora Zone	Upper	DM	Tarija Fm. E. Fm.	S. T. Fm.	<i>C. monoletus</i>	Nova Olinda Fm.	<i>R. cephalata</i>
	Palynozone I		Lower				Itaituba F.		<i>I. unicus</i>
									<i>S. incrass.</i>
								<i>S. triangulus</i>	

Fig. 2.10 Correlation of palynozonations for the main basins of South America

(From Stephenson 2008a).

Marques-Toigo (1991) working on southern part of the Paraná Basin, recognised two biozones, in ascending order (older to younger), i.e. *Cannanoropollis korbaensis* Interval Zone and *Lueckisporites virkkiae* Interval Zone. The *Cannanoropollis korbaensis* Interval Zone was further subdivided into three subzones, *Protohaploxylinus goraiensis* Subzone, *Caheniasaccites ovatus* Subzone and *Hamiapollenites karrooensis* Subzone (Fig. 2.11). Souza & Marques-Toigo (2003, 2005) and Souza (2006), further developed the Late Carboniferous to Early Permian biostratigraphic scheme of the Paraná Basin, Brazil (Fig. 2.11). These workers divided the Late Carboniferous to Early Permian into four biozones, which in ascending order are comprised of, *Ahrensiporites cristatus* Interval Zone, *Crucisaccites monoletus* Interval Zone, *Vittatina costabilis* Interval Zone, and *Lueckisporites virkkiae* Interval Zone.

Geochronology *				Palynostratigraphy				
Period	Epoch	Stage	Age (Ma)	Daemon and Quadros (1970)		Marques-Toigo (1988, 1991)	Souza and Marques-Toigo (2003,2005), Souza (2006)	Main palynological features
PERMIAN	Lopingian	Changhsingian	251.0 ± 0.4					
		Wuchiapingian	253.8 ± 0.7					
	Guadalupian	Capitanian	260.4 ± 0.7	L	L ₃	Lueckisporites virkkiae Interval Zone	Lueckisporites virkkiae Interval Zone	<ul style="list-style-type: none"> • Appearance of Lueckisporites • Dominance of taeniate and polyplicate pollen grains (Lueckisporites, Lunatisporites, Weylandites) • Rare spores (Laevigatosporites, Thymospora, Convolutispora) and monosaccate pollen grains
		Wordian	265.8 ± 0.7		L ₂			
		Roadian	268.0 ± 0.7		L ₁			
	Cisuralian	Kungurian	270.6 ± 0.7					
		Artinskian	275.6 ± 0.7					
		Sakmarian	284.4 ± 0.7		J	Cannanoropollis korbaensis Interval Zone HamiapolLENites karoensis Subzone Caheniasaccites ovatus Subzone Protohaploxylinus goraiensis Subzone	Vittatina costabilis Interval Zone HamiapolLENites karoensis Subzone Protohaploxylinus goraiensis Subzone	<ul style="list-style-type: none"> • Appearance of Vittatina and Illinites • Low to high frequency of taeniate and polyplicate pollen grains • Local dominance of trilete spores (coal beds in RS and SC)
		Asselian	294.6 ± 0.8		I			
	UPPER CARBONIFEROUS	Pennsylvanian	Gzhelian	299.0 ± 0.8		H ₃		
Kasimovian			303.9 ± 0.9		H ₂			<ul style="list-style-type: none"> • Dominance of trilete spores and monosaccate pollen grains (Plicatipollenites, Potonieisporites, Caheniasaccites, Cannanoropollis)
Moscovian			306.5 ± 1.0		H ₁			
Bashkirian		311.7 ± 1.1		G			Ahrensisporites cristatus Interval Zone	<ul style="list-style-type: none"> • Rare taeniate pollen grains (Protohaploxylinus, Meristocarpus)
			318.1 ± 1.3					

* according to Gradstein et al. (2004)

Fig. 2.11 Brazilian Late Carboniferous to Early Permian palynological scheme

(From Souza & Marques-Toigo 2005).

The *Ahrensisporites cristatus* Interval Zone is dated as Late Bashkirian to Kasimovian, and its base is identified by the first appearance of the taxa, *Anapiculatisporites argentinensis*, *Ahrensisporites cristatus*, *Brevitriletes levis*, *Cannanoropollis* spp., *Caheniasaccites* spp., *Convolutispora ordonenzii*, *Cristatisporites* spp., *Foveosporites hortonensis*, *Granulatisporites varigranifer*, *Limitisporites* spp., *Psomospora detecta*, *Protohaploxylinus* spp., *Potonieisporites* spp., *Plicatipollenites* spp., *Raistrickia rotunda* and *Raistrickia pinguis*. Other taxa occurring commonly in this zone include, *Cristatisporites* spp., *Cannanoropollis janakii*, *Calamospora* spp., *Caheniasaccites flavatus*, *Limitisporites* spp., *Punctatisporites* spp., *Plicatipollenites malabarensis*,

Plicatipollenites gondwanensis, *Potonieisporites novicus*, *Potonieisporites brasiliensis*, *Protohaploxypinus* spp., *Vallatisporites arcuatus* and *Vallatisporites validus*.

The upper limit of this zone and the base of the succeeding biozone (i.e. *Crucisaccites monoletus* Interval Zone), is defined by the disappearance of *Ahrensisporites cristatus*, *Anapiculatisporites argentinensis*, *Granulatisporites varigranifer*, *Foveosporites Hortonensis*, *Psomospora detecta* and *Raistrickia pinguis*.

The overlying *Crucisaccites monoletus* Interval Zone is considered extending from Kasimovian to Gzhelian and the base is defined by the first appearance of *Crucisaccites monoletus* and *Scheuringipollenites maximus*. Other taxa common to this zone include *Cycadopites* spp., *Cristatisporites* spp., *Calamospora* spp., *Horriditriletes* spp., *Limitisporites* sp., *Punctatisporites* spp., *Protohaploxypinus*, *Spelaeotriletes ybertii* and *Vallatisporites* spp.

The succeeding *Vittatina costabilis* Interval Zone is characterised by *Illinites unicus*, *Protohaploxypinus goraiensis*, *Protohaploxypinus limpidus*, *Protohaploxypinus amplus*, *Striatopodocarpites* spp., *Vittatina* spp., and cavate/zonate spores. Monosaccate pollen are less important at this stage.

The succeeding *Lueckisporites virkkiae* Interval Zone is considered as Artinskian to Capitanian (Souza & Marques-Toigo 2003, 2005). The base of this zone is defined by the first appearance of *Lueckisporites virkkiae* which is coincident with the last appearance of *Hamiapollenites karooensis* and *Stellapollenites talchirensis*. Other species which occur in this zone are *Protohaploxypinus* spp., *Striatopodocarpites* spp., *Lunatisporites* spp., and *Marsupipollenites* spp. Monosaccate pollen are less common in this zone, while spores are very rare.

Amazonas Basin

Playford & Dino (2000) recognised six palynozones in the Late Carboniferous to Early Permian sections in the Tapajós Group of the Amazonas Basin, Brazil. The oldest zone i.e. *Spelaeotriletes triangulus* Zone (Playford & Dino 2000) comprises *Florinites occultus*, *Florinites pellucidus*, *Protohaploxypinus amplus*, *Striomonosaccites ovatus*, *Spelaeotriletes triangulus*, *Spelaeotriletes arenaceus*, and *Waltzispora polita* and is dated as Westphalian (A-B; Playford & Dino 2000).

The *Striomonosaccites incrassatus* Zone (Playford & Dino 2000) is dated as Westphalian C and comprises *Costatascyclus crenatus*, *Cannanoropollis janakii*, *Illinites unicus*, *Protohaploxypinus amplus*, *Striomonosaccites ovatus*, *Spelaeotriletes triangulus* and *Spelaeotriletes arenaceus*.

The *Illinites unicus* Zone is dated as late Westphalian C (Playford & Dino 2000) and includes *Barakarites rotatus*, *Cycadopites follicularis*, *Cannanoropollis janakii*, *Florinites occultus*, *Florinites pellucidus*, *Illinites unicus*, *Protohaploxypinus* spp., *Striomonosaccites ovatus*, *Spelaeotriletes triangulus*, *Spelaeotriletes arenaceus* and *Vallatisporites arcuatus*.

The base of the overlying *Striatosporites heyleri* Zone (Playford & Dino 2000) is defined by the first appearance of *Apiculatasporites daemonii* and *Striatosporites heyleri*. Additional taxa in this zone include, *Crucisaccites* spp., *Illinites unicus*, *Mabuitasaccites crucistriatus*, *Protohaploxypinus* spp., and *Striatopodocarpites* spp.

This zone is dated as Westphalian (C-D). The *Raistrickia cephalata* Zone is dated as Westphalian D (Playford & Dino 2000). The base of the zone is marked by occurrence of *Peppersites ellipticus* and *Raistrickia cephalata*. Other species that occur in this zone are, *Apiculatasporites daemonii*, *Cycadopites follicularis*, *Limitisporites* spp.,

Protohaploxylinus spp., *Striatosporites heyleri*, *Striatopodocarpites* spp.,
Spelaeotriletes triangulus and *Spelaeotriletes arenaceus*.

The base of the overlying *Vittatina costabilis* Zone (Playford & Dino 2000) is defined by the first appearance of *Vittatina* species. Associated taxa of the zone include *Corisaccites alutas*, *Hamiapollenites* spp., *Lueckisporites virkkiae* and *Pakhapites fusus*, *Pakhapites ovatus*. This zone is dated as Early Permian (Playford & Dino 2000).

2.3.4.2 Argentina

Azcuy (1979) and Archangelsky *et al.* (1980) discussed palynology of most of the South American Late Palaeozoic basins. Palinozone II (Azcuy 1979), defined on the basis of monosaccate pollen and dated as Late Carboniferous, is correlated with the *Potonieisporites* Palinozone (Azcuy & Jelin 1980; fig. 2.12). Palinozone III (Azcuy 1979) is correlated with *Cristatisporites* Zone (e.g. Archangelsky *et al.* 1980). The base of *Cristatisporites* Zone is characterised by the first appearance of *Apiculatisporites cornutus* and *Converrucosisporites confluens* and the high abundance of cingulicamerate spores. *Caheniasaccites ovatus*, *Potonieisporites brasiliensis*, *Potonieisporites novicus* and *Plicatipollenites malabarensis* constituted the dominant monosaccate pollen of this zone, while bisaccate pollen are rare.

The base of the overlying *Striatites* Zone (Archangelsky *et al.* 1980) is defined by the sharp increase in striate bisaccate pollen and comprises mainly *Hamiapollenites bullaeformis* and *Protohaploxylinus limpidus*. Other taxa in this biozone include, *Convolutispora ordonezi*, *Lueckisporites virkkiae* and *Striatoabieites* spp.

Later Russo *et al.* (1980) established three biozones for the Late Carboniferous to Early Permian of Argentina, i.e. the *Potonieisporites-Lundbladispota* Zone, *Cristatisporites* Zone and *Striatites* Zone. These zones were redefined later by Vergel (1993) and the *Cristatisporites* Zone was further divided into lower, middle and upper parts.

Syst em	Serie	Zone [1]	Azcuy and Jelin, 1980	Azcuy 1979	Azcuy 1986	Césari, 1986 Paganzo Basin Chacoparanense Basin		Russo et al. 1980	Vergel, 1993	Megafloristic Zone [2]	Paleoclimatic Stage [3]		
P E R M I A N C A R B O N I F E R O U S	Lower	LW						Striatites Zone	Striatites Zone		V		
		FS	Palinozone III	Palinoz. III	Palinozone III	Cristatisporites Zone		Cristatisporites Zone	Cristatisporites Zone	upper middle lower		upper lower	IV
			C	Palinozone III	Palinozone III	Palinozone III	Transition Subzone					Interval	
	Upper	DM	Potoneisporites Palinozone	II	Potoneisporites Palinozone	Raistrickia/ Plicatipol- lenites	Potoneis- porites / Lundblad- dispora Zone	Potoneisporites Lundbladispora Zone	Potoneisporites Lundbladispora Zone	N B G	IIIb IIIa		
		A	Ancistrospora Palinozone	Palinoz. I	Ancistrospora Palinozone								
	Lower	CV										II	
											A F	I	

**Fig. 2.12 Argentinian Late Carboniferous to Early Permian palynological schemes
(From Césari & Gutiérrez 2000).**

Césari & Gutiérrez (2000) reviewed the Late Carboniferous to Early Permian palynology of central-western Argentina (Fig. 2.12). Three palynozones were defined, i.e. the *Raistrickia densa-Convolutispora muriornata* Assemblage Biozone (DM), *Fusacolpites fusus-Vittatina subsaccata* Interval Biozone (FS) and the *Lueckisporites-Weylandites* Assemblage Biozone (LW).

The lowermost *Raistrickia densa-Convolutispora muriornata* Assemblage Biozone (DM) comprises *Anapiculatisporites argentinensis*, *Cannanoropollis* spp., *Convolutispora murionata*, *Crucisaccites* spp., *Cristatisporites* spp., *Limitisporites* spp., *Potoneisporites* spp., *Platysaccus* spp., *Raistrickia rotunda*, *Raistrickia densa* and *Vallatisporites ciliaris*. This zone is divided into three subzones i.e. A, B and C. The

base of subzone A is recognised by the first appearance of *Potonieisporites* spp., the base of subzone B is defined by the first appearance of *Protohaploxylinus* spp., while the base of the overlying subzone C is characterised by the appearance of *Quadrisporites* spp., scolecodonts and some acritarchs.

The base of the overlying *Fusacolpites fusus-Vittatina subsaccata* Interval Biozone (Césari & Gutiérrez 2000) is recognised by the first appearance of *Pakhapites fusus* and occurrence of other striate pollen like *Apiculatisporis cornutus*, *Barakarites rotatus*, *Distriatites insolitus*, *Granulatisporites trisinus*, *Hamiapollenites fusiformis*, *Krauselisporites sanluisensis*, *Lophotriletes rarus*, *Latusipollenites quadrisaccatus*, *Latusipollenites cursus*, *Marsupipollenites striatus*, *Striatoabieites multistriatus* and *Vittatina subsaccata*.

The base of the *Lueckisporites-Weylandites* Assemblage Biozone (LW) is defined by the first appearance of *Lueckisporites* spp., and occurrence of other striate pollen, *Lunatisporites* spp., *Marsupipollenites* spp., *Vittatina* spp., and *Weylandites* spp (Césari & Gutiérrez 2000).

Azcuy *et al.* (2002) investigated the palynology of the Late Carboniferous Tarma Formation of Peru and assigned Westphalian C age to the Tarma Formation, based on the abundance of *Illinites unicus* and compared it to the Amazonas Basin palynozonation scheme.

Playford & Dino (2002) discussed the palynology of the Ordóñez and Victoriano Rodríguez formations from south of the Chaco-Paraná Basin, northeastern Argentina. They investigated three palynozonations originally established by Russo *et al.* (1980) which from older to younger represented by the *Potonieisporites-Lundbladisporea* Zone, *Cristatisporites* Zone and *Striatites* Zone.

The base of the *Potonieisporites-Lundbladispota* Zone of Russo *et al.* (1980) is characterised by the dominance of trilete spores (60%) such as, *Cyclogranisporites* spp., *Cristatisporites* spp., *Punctatisporites* spp., and *Vallatisporites arcuatus*.

Monosaccate pollen comprise 20% of the assemblages and are represented by *Caheniasaccites ovatus*, *Potonieisporites brasiliensis*, *Potonieisporites novicus*, *Plicatipollenites malabarensis* and *Plicatipollenites densus*.

Bisaccate pollen are represented by 15-20% of the assemblages, mainly comprised of *Limitisporites rectus* and *Protohaploxypinus* spp.

The base of the *Cristatisporites* Zone of Russo *et al.* (1980) is defined by the abundance of cingulicamerte spores, represented by *Cristatisporites* spp., and *Vallatisporites* spp., and first appearance of *Apiculatisporites cornutus*, *Converrucosisporites confluens* and *Microbaculispora tentula*.

Monosaccate pollen are common in this zone and are represented by *Caheniasaccites*, *Potonieisporites brasiliensis*, *Potonieisporites novicus* and *Plicatipollenites malabarensis*.

The base of the overlying *Striatites* Zone of Russo *et al.* (1980) is marked by the abundance of taeniate and non-taeniate bisaccate pollen (80%) and are represented by *Marsupipollenites striatus*, *Lunatisporites variesectus*, *Lueckisporites virkkiae*, *Striomonosaccites cicatricosus* and *Striatoabietites* spp. Trilete spores in this biozone are rare, represented only by *Convolutispora ordenezi*.

2.3.5 Peninsula Indian palynostratigraphy

Much of Indian palynomorph taxonomic work in 1960s concentrated on correlation between Carboniferous-Permian coal seams. Tiwari & Tripathi (1992) and Vijaya & Awatar (2001) attempted to synthesise the Permian palynostratigraphic scheme for all of India and correlations of Indian palynostratigraphy with the International stages have

been made by Tiwari (1996), Veevers & Tewari (1995, fig. 2.13) and Vijaya (1994). Veevers & Tewari (1995) synthesised and correlated the Gondwanan basins of India and the Salt Range Pakistan, with Australian biozones (Fig. 2.13). The *Potonieisporites neglectus* Assemblage-Zone (Tiwari & Tripathi 1992) is recognised in the lower parts of the Talchir Formation. This zone is dominated by monosaccate pollen, e.g. *Cannanoropollis* spp., *Potonieisporites* spp., and *Plicatipollenites* spp., and lacks taeniate bisaccate pollen. These authors correlated this zone with the *Plicatipollenites-Parasaccites* Zone of Tiwari & Tripathi (1988).

The base of the overlying palynozone (Tiwari & Tripathi 1992), i.e. *Plicatipollenites gondwanensis* Assemblage-Zone is marked by sudden increase in diversity of pollen and spores. Monosaccate pollen are dominant in this zone and are represented by *Caheniasaccites densus*, *Cristatisporites* spp., *Plicatipollenites* spp., *Potonieisporites* spp., and *Parasaccites* spp. The top of this zone is marked by the first occurrence datum of *Microbaculispora tentula*. Taeniate bisaccate pollen appear in this zone. The base of overlying *Parasaccites korbaensis* Assemblage-Zone (Tiwari & Tripathi 1992) is characterised by the first appearance of *Divarisaccus lelei*, *Microbaculispora tentula* and *Microfoveolatispora foveolata*. This zone is characterised by an increase in diversity of apiculate and lycopsid spores, e.g. *Horriditriletes* spp. and *Jayantisporites* spp. Bisaccate and monosaccate pollen are also common in this zone, represented by *Crucisaccites monoletus*, *Cannanoropollis korbaensis*, *Potonieisporites* spp., *Plicatipollenites* spp., and *Sahnites* spp.

TIME		PALYNOMORPH ZONES		SALT RANGE PAKISTAN	
		EASTERN AUSTRALIA Kemp <i>et al.</i> 1977 Helby <i>et al.</i> 1987	INDIA		
208	TRIASSIC	LATE	<i>P. crenulatus</i>	Supra-Panchet	Kingriali Formation
210			<i>Rotundus</i>		
220		MIDDLE	<i>Senectus</i>	Tredian Formation	
230			<i>Parvispinosus</i>		
240	EARLY	<i>Tenuispinosub</i>	Panchet	Mianwali Formation	
		<i>Samoilovichi</i>			
		<i>Pellucious</i>			
250	PERMIAN	LATE	<i>M. bitriangularis</i>	Raniganj	Chiddru Formation
			<i>D. parvitholus</i>		Wargal Formation
260		EARLY	<i>D. granulata</i>	BM	Amb Formation
			4	Barakar	Sardi (Sardhai) Formation
270			3b	Karharbari	Warchha Formation
			<i>C. confluens</i> ^{3a}	Marine	Dandot Formation
280			2		Talchir
290	CARB.	LATE	1		

Fig. 2.13 Correlation of the Carboniferous-Permian (and Triassic) formations and palynology events of India, eastern Australia and Pakistan. The shaded portion represents the Carboniferous to Permian time interval (Modified after Veevers & Tewari 1995).

The base of the overlying *Crucisaccites monoletus* Assemblage-Zone (Tiwari & Tripathi 1992) is defined by the first appearance of *Marsupipollenites triradiatus* and *Welwitschiapites magnus*. Tiwari & Tripathi (1992) assigned the entire Karharbari Formation to their *Crucisaccites monoletus* Assemblage-Zone.

Geochronology and Chronostratigraphy after Gradstein et al. (2004)		Brazil, Parana Basin, Souza (2006)	Argentina Vergel (1993); Playford and Dino (2002)	Australia		South Africa Anderson (1977)	India Tiwari and Tripathi (1992)	Antarctica Playford (1990)	Arabia Stephenson et al. (2003)	
				West Backhouse (1991)	East Jones and Truswell (1992)					
Lower Permian (Cisuralian)	Kungurian 275.6	<i>Lueckisporites virkkiae</i>	<i>Striatites</i>	<i>S. fusus</i>		3a	<i>Faunipollenites varius</i>	<i>Protolaploxytinus</i>	OSPZ3	
	Artinskian 284.4					2d 2c 2b 2a	<i>S. barakarensis</i>			
	Sakmarian 294.6	<i>Vittatina costabilis</i> ?	<i>Cristatisporites</i>	<i>P. pseudo</i>	<i>Microbaculispora tentula</i>	1	<i>Crucisaccites monoletus</i>			OSPZ2
	Asselian 299			<i>C. confluens</i> Stage 2 of Backhouse						
Pennsylvanian pars	Gzhelian 303.9	<i>Crucisaccites monoletus</i>	<i>Potonieisporites-Lundbladispora</i>		<i>Asperispora reticulatispinosus</i>		<i>Parasaccites korbaensis</i>	OSPZ1		
	Kazimovian 306.5						<i>Plicatipollenites gondwanensis</i>		<i>Parasaccites</i>	
	Moscovian 311.7	<i>Ahrensiporites cristatus</i>			<i>Diatomozonotrites birkheadensis</i>	<i>Potonieisporites neglectus</i>				
	Bashkirian 318.1									

Fig. 2.14 Comparison of the main Carboniferous-Permian palynozones of the Gondwana regions (Modified after Stephenson 2008a).

Stephenson (2008a) attributed that the assemblages from the *Potonieisporites neglectus* Assemblage-Zone of Tiwari & Tripathi (1992) from the lowest glaciogenic sediments of the Talchir Formation are dominated by monosaccate pollen lacking taeniate bisaccate pollen. The succeeding *Plicatipollenites gondwanensis* Assemblage-Zone is marked by the diversification and the appearance of taeniate bisaccate pollen and the biozone above (*Parasaccites korbaensis* Assemblage-Zone) in the upper Talchir Formation is marked by fern spores such as *Microbaculispora tentula*. Stephenson (2008a) correlated the Peninsula Indian palynozones with the Gondwana biozones (Fig. 2.14).

3 Chapter 3: Sedimentological analyses of the Carboniferous-Permian succession of the Salt Range

3.1 Abstract

The sedimentology of the Carboniferous-Permian Nilawahan Group is analysed. Detailed lithofacies, facies association and grain size analyses were performed on exposures at several localities in the Salt Range and Khisor Range. In a cumulative 472.5 m thick succession, 12 lithofacies types and ten facies associations have been recognised. The Tobra Formation exhibits three distinctive facies association: debris flow deposits (DFFA), streamflow deposits (SFFA) and overbank deposits (OFA). These facies associations extend from the Khisor Range, through the western and central Salt Range and into the eastern Salt Range. Two depositional models have been proposed for this succession; an alluvial fan depositional setting and a glacio-fluvial setting. The timing of deposition suggests the latter as the most likely depositional setting. The Tobra Formation in the eastern and central Salt Range is overlain by the Dandot Formation, which encompasses one facies association and represents sedimentation in an intertidal to shallow marine setting. This association has not been observed in any other measured section of the Salt and Khisor ranges, e.g. the Zaluch Nala section (western Salt Range) and Saiyiduwali section (Khisor Range), indicating that the marine incursion only prevailed in the eastern part of the area. The Warchha Formation conformably overlies the Dandot Formation in the east and unconformably overlies the Tobra Formation in the central, western Salt Range and Khisor Range. It is represented by five facies associations which represent the accumulation of the Warchha Formation in a fluvial system, associated with the development of an arid palaeoclimate in the area. The Sardhai Formation represents one facies association and is interpreted as a shallow marine depositional unit.

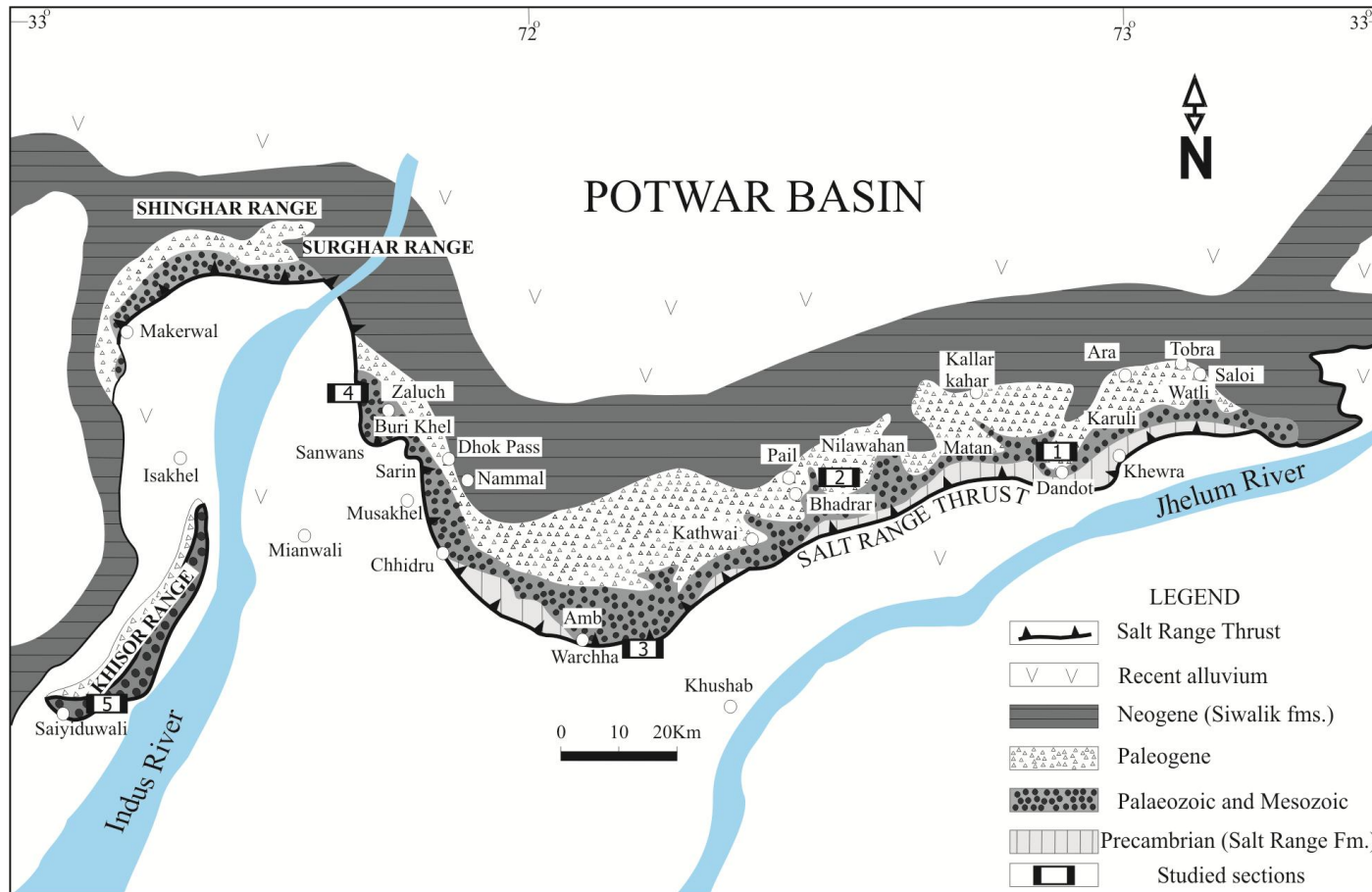


Fig. 3.1 Geological map of the Salt Range and Khisor Range, showing the locations selected for sedimentological investigations. 1. Khewra-Choa section (eastern Salt Range), 2. Pail section (central Salt Range), 3. Warchha gorge section (central Salt Range), 4. Zaluch Nala section (western Salt Range) and 5. Saiyiduwali section (Khisor Range; modified after Jan & Stephenson 2011).

KEY			
	Lenticular bedding		Hummocky cross-stratification
	Red layer		?Rippled/wavy lamination
	Burrows		Normally graded units
	Fissile mudstone		Siltstone
	Jointed /blocky concoidal sediments		Laminated mudstone
	Trough cross-bedded sandstone		Massive mudstone
	Planar cross-bedded sandstone		Clast-supported conglomerate
	Thin-bedded limestone		Matrix-supported conglomerate
Gmc	Clast-supported massive conglomerate	RSFA	Red mudstone interbedded with thin sandstone and calcretes
Gmm	Matrix-supported massive conglomerate	PSFA	Pebbly sandstone
Sf	Fining upwards pebbly sandstone	ACF	Abandoned channel fill deposits
Sm	Massive sandstone	DLSFA	Deep lacustrine to shallow marine facies association
Fss	Fine-grained sandstone and siltstone	TZ	Tobra Formation at the Zaluch Nala
St	Trough cross-bedded sandstone	TW	Tobra Formation at the Warchha gorge
Sp	Planar cross-bedded sandstone	TKC	Tobra Formation at the Khewra-Choa section
Sr	Ripple-laminated sandstone and interlaminated mudstone	WZ	Warchha Formation at Zaluch Nala
Sh	Hummocky cross-stratified sandstone	UeQ	Undulose extinction quartz
Fm	Massive mudstone	PsmQ	Polycrystalline sutured margin quartz
Fl	Laminated mudstone	Pg	Plagioclase
Lsf	Thin-bedded sandy limestone	M	Microcline
DFFA	Debris flow-dominated alluvial plain facies association	PcQ	Polycrystalline quartz
SFFA	Stream flow dominated alluvial plain facies association	Sk ₁	Skewness
OFA	Overbank facies association	○ ₁	Sorting
ISFA	Intertidal to shallow marine facies association	Mz	Mean
ECS	Erosive-based cross-bedded sandy bedform element	φ ₅₀	Median
LCS	Lenticular cross-bedded sandstone bodies with erosional bases		

Fig. 3.2 Key for the lithologies and sedimentary structures documented in the study.

3.2 Previous sedimentological work

The Salt Range and the Trans-Indus ranges of Pakistan are regarded as important reference areas for Carboniferous-Permian strata and though the regional geology and structure of the area is well established (Fatmi 1973; Shah 1977; Gee 1989), the sedimentology of the Nilawahan Group has received limited detailed analysis.

Koken (1907) believed the boulder beds were uniform throughout the entire Salt Range, but later detailed mapping by Gee (in Pascoe 1959), showed that the beds varied considerably in thickness and facies.

Later investigations by Teichert (1967) at Zaluch Nala and Khan Zaman Nala (Salt Range and the trans-Indus Khisor Range) showed that the Tobra Formation has three distinctive facies. He described a tillitic facies in the easternmost Salt Range, which grades upwards into marine sandstone containing the bivalve *Eurydesma* and the conularid *Conularia* (Reed 1936; Pascoe 1959). In the central Salt Range, he described a freshwater facies of palyniferous (sic) siltstone and shale, with scattered clasts. The third facies described by Teichert (1967) was a mixture of diamictite, sandstone and boulder beds which shows westward thickening in the western Salt Range and in the Khisor Range. At Zaluch Nala, Teichert (1967) reported the thickness of the Tobra Formation to be 122 m and divided the formation into three facies: the A-, B- and C-members (sic).

At Zaluch Nala, the A-member is 55 m thick and has a uniform brownish-grey matrix including clay, silt, and sand grains up to 1 mm in diameter. The extrabasinal clasts are approximately 10 mm in diameter. Most of the extrabasinal clasts are angular to subangular while a few are subrounded and well rounded. Compositionally the extrabasinal clasts comprise quartz, quartzite and a variety of other rock types. Larger pebbles and small boulders up to 150 mm in diameter are present but rare. Some of the larger boulders have poorly preserved striated faceted surfaces. The B-member is 8.5 m thick and is a dark to light olive, medium to coarse-grained thick-bedded sandstone with a conglomerate bed present at its base. The C-member is similar to the A-member, with a slightly less uniform lithology, and is divided into three units. Unit 1 represents the lowermost 4.6 m. This unit has a pale grey matrix with clasts up to 228 mm in diameter.

The contact with overlying Unit 2 is sharp. Unit 2 is 11.3 m thick. This unit has a dark greenish grey friable claystone matrix and pebble-sized clasts. The matrix is coarser towards the top of the unit. The colour of Unit 2 is medium dark grey in outcrop and brown on a freshly broken surface. Unit 3 is a dark greenish-grey friable claystone, 15.9-57.9 m thick. The member contains rare pebbles of quartz and feldspar in its basal portion (Teichert 1967).

Ghauri *et al.* (1977) made a petrographic study of the Tobra Formation in the eastern Salt Range and divided the formation into six units: rusty brown sandstone, coarse sandstone, gritstone, carbonaceous shale, and siltstone, yellowish green sandstone and boulder bed. Ghauri *et al.* (1977) suggested that the extrabasinal clasts of the Tobra Formation were derived from southern India. There is no study known that pertains to the sedimentology of the Dandot Formation, though some work on the palaeontology of the formation has been conducted (e.g. Reed 1936). Sedimentological work on the Warchha Formation is scarce; Ghazi & Mountney (2009, 2011) studied the Warchha Formation at various localities in the eastern and central Salt Range and identified seven lithofacies types and nine architectural elements. Ghazi & Mountney (2009) interpreted the deposition of the Warchha Formation in terms of a meandering river system. There is no published work on the sedimentology of the Sardhai Formation.

3.3 Present sedimentological analysis

A sedimentological analysis of the Carboniferous-Permian Nilawahan Group of Pakistan (Figs. 3.1 & 3.3) was completed to develop depositional models for the evolution of palaeoenvironments in this region during the late Palaeozoic icehouse.

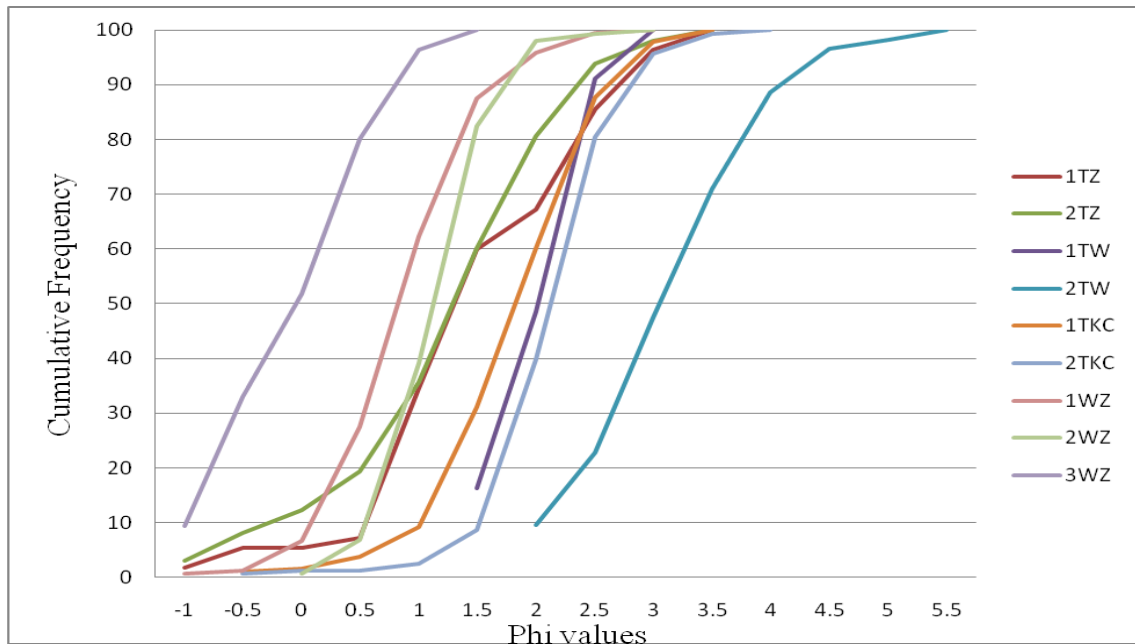


Fig. 3.4 Percentage cumulative frequency curves of the Nilawahan Group samples. See Appendix 2 for sample locations and Fig. 3.2 for sample codes.

Samples for petrography and grain size analysis from some of these units have been collected (Appendix 2). Optical microscopic studies of the samples have helped in determining various grain size parameters of the lithofacies (Fig. 3.4, Table 3.1). These parameters with the field observations have produced a refined interpretation of the lithofacies.

3.3.1 Facies analysis

The formations of the Nilawahan Group have been studied at the Khewra-Choa section (eastern Salt Range), the Zaluch Nala section (western Salt Range), Pail, and the Warchha gorge sections (central Salt Range) and Saiyiduwali section (Khisor Range, figs. 3.1 & 3.3.) These sections represented various levels in the succession and were easily accessible (Figs. 3.1 & 3.3). Twelve facies types have been recognised in the exposures studied of the Nilawahan Group.

Lithofacies types	Representative sample	Unit	Location	Grain size parameters			
				ϕ_{50}	Mz	σ_1	SK_1
Gmc	1TZ		Western Salt Range (Zaluch Nala)	1.333	1.486	0.998	-0.629
Gmm	2TZ			1.333	1.249	0.971	-0.359
Sm (no extrabasinal clasts)	2TW	Tobra Formation	Central Salt Range (Warchha Gorge section)	3.083	3.069	0.784	0.642
Sm (no extrabasinal clasts)	1TW			2	1.992	0.408	0.628
Sf	2TKC		Eastern Salt Range (Khewra-Choa section)	0.625	0.624	0.27	-0.038
Sm (with extrabasinal clasts)	1TKC			1.75	1.75	0.534	0.125
Sm (no extrabasinal clasts)	3WZ			0.833	0.833	0.291	0.019
Sm (no extrabasinal clasts)	2WZ	Warchha Formation	Western Salt Range (Zaluch Nala)	0.625	0.589	0.214	-0.191
Sm (no extrabasinal clasts)	1WZ			-0.1	-0.078	0.39	-0.095

Table 3.1 Graphic measures from the grain size analyses of some of the Nilawahan Group samples. See Appendix 2 for the sample details and Fig. 3.2 for sample and facies codes.

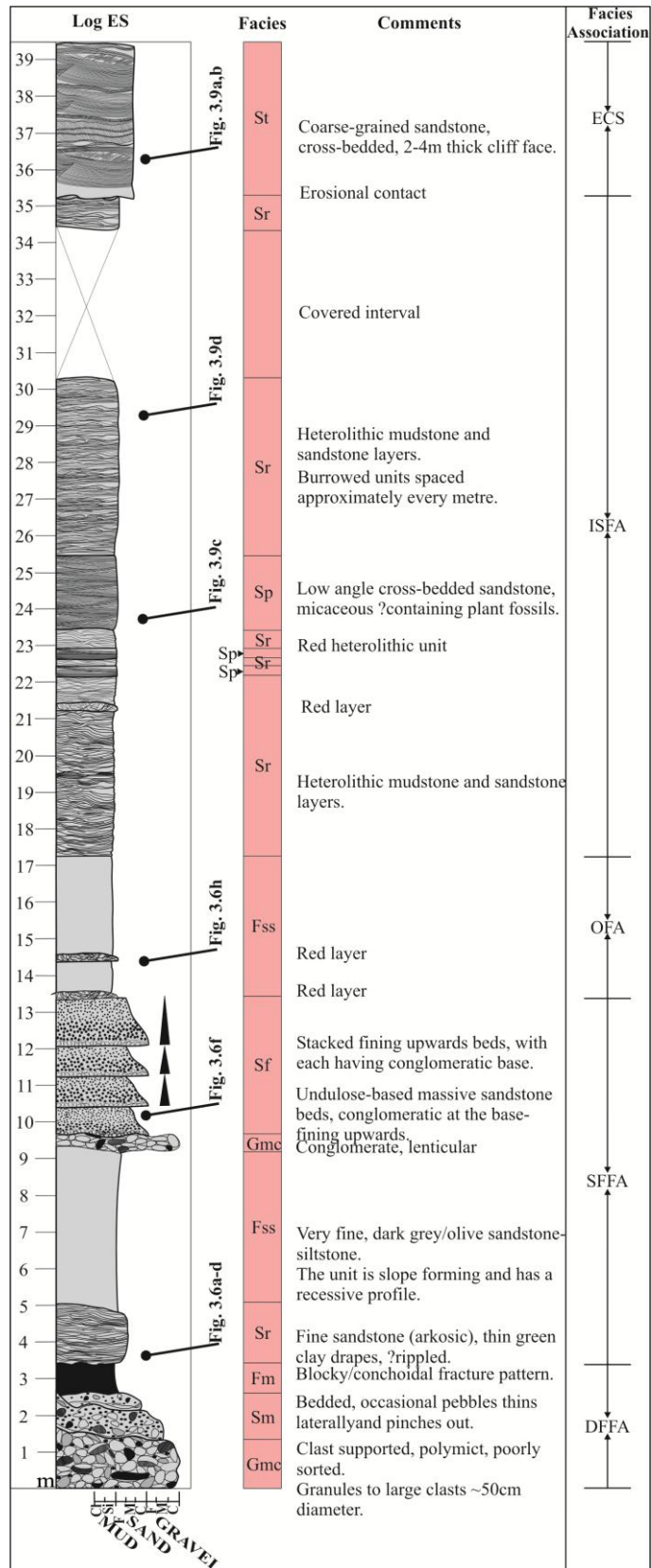


Fig. 3.5 Log ES-The distribution of lithofacies types and facies associations in the Carboniferous-Permian succession of the Khewra-Choa section (eastern Salt Range). For detailed stratigraphic location of the units (formations), refer to Fig. 3.3. For key, refer to Fig. 3.2.

Conglomeratic facies dominate, followed by the sandstone-dominated facies.

Mudstone-dominated facies are less common or locally even absent in individual exposures. The facies make up variable proportions of the sections studied and are discussed below in detail.

3.3.1.1 Conglomeratic facies

3.3.1.1.1 Gmc: Clast-supported massive conglomerate

Description. This facies comprises moderately to poorly sorted (Table 3.1) and angular to subrounded extrabasinal clasts ranging in size from granules (1 mm) to large boulders up to ~500 mm in diameter, in a coarse-grained green-grey sandstone matrix (Fig. 3.5, Log ES, basal 2 m, Fig. 3.7, Log WS1). Extrabasinal clasts dominate this facies comprising more than 65% of the clast assemblage. The extrabasinal clasts include granite, gneiss, schist and quartzite. There are also intraclasts, such as locally-derived sandstone and siltstone, that form a more minor component (less than 25%). The matrix constitutes 10% of the facies. Approximately 55% of the extrabasinal clasts are faceted (Figs. 3.6a-d). The facies has a structureless appearance. The Gmc facies at the Khewra-Choia section (eastern Salt Range, fig. 3.6a), overlies the Cambrian Baghanwala Formation, which has an irregular relief of 2-3.5 m on the outcrop scale and the Gmc facies appears to infill that relief. Elsewhere the Gmc facies overlies erosion surfaces, where the facies is found in thinner beds (0.5 m) as in Log WS1 (Fig. 3.7) and the facies has a much smaller basal relief. The Gmc facies is found throughout the outcrops of the Salt Range and Khisor Range studied.

Interpretation. The presence of sub-rounded clasts and the conspicuous relief associated with the basal surface of this facies suggest deposition from stream flows (Collinson 1996). The moderately to poorly sorted clasts, absence of clast imbrication and absence of horizontal stratification, however, suggest a clast-rich high-strength

debris flow process (Opluštil *et al.* 2005). The presence of abundant faceted clasts could indicate a glacial origin; however faceting of clasts may also be produced by the tectonic or mass flow process (Collinson 1996). Thus, on balance, an interpretation of deposition from debris flows is suggested for facies Gmc.

3.3.1.1.2 Gmm: Matrix-supported massive conglomerate

Description. This facies comprises moderately to poorly sorted (Table 3.1) and rounded clasts in an abundant matrix. The facies is a uniform brownish grey. The matrix consists of clay, silt and sand grains up to 1 mm in diameter. The extrabasinal clasts are predominantly angular to subangular, a small (10%) proportion of the clasts are subrounded and only rarely (<2%) well rounded (Fig. 3.7, Log WS1). Pebbles, ranging from a few millimetres to rarely more than 10 mm, are dominated by vein quartz and quartzite (Fig. 3.6e). Scattered larger pebbles and smaller boulders, up to 150 mm in diameter, occasionally show crude alignment, but overall the facies is structureless. At the Zaluch Nala section (western Salt Range) and the Saiyiduwali section (Khisor Range), the facies shows an increase in clast size upwards and includes boulders ranging from 10 to 230 mm in size. At the outcrop scale, the facies forms a lenticular to tabular body. The Gmm facies has similarities with Teichert's A- and C-members (Teichert 1967). Teichert (1967) also recognised parallel bedding, undisturbed bedding features and graded bedding, which were not observed in this study.

Interpretation. The general absence of sedimentary structures, moderate to poor sorting, and poorly rounded grains, variable sizes of the extrabasinal clasts in coarse-grained matrix, mixing of fine and coarse materials, lack of both internal bedding and clast imbrication, suggest that the facies Gmm was deposited by gravity flow processes, probably debris flows (Howard *et al.* 2003; Opluštil *et al.* 2005).

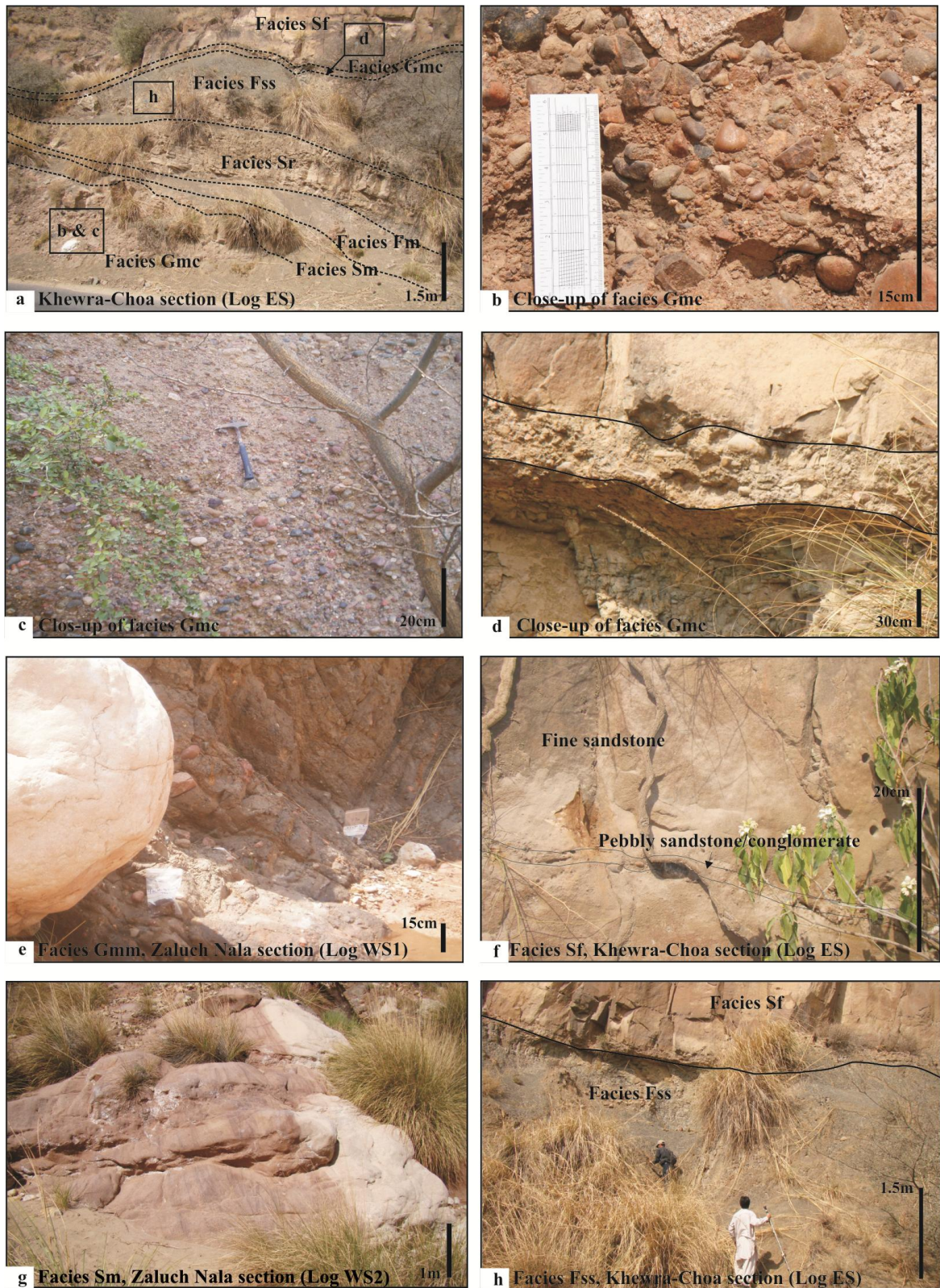


Fig. 3.6 Characteristic examples of lithofacies present in the Carboniferous-Permian succession of the Salt Range. Stratigraphic location given on Figs. 3.5, 3.7 and 3.8.

3.3.1.2 Sandstone-dominated facies

3.3.1.2.1 Sf: Fining upwards pebbly sandstone

Description. This facies comprises fining upwards 0.5-1 m-thick tabular beds. The scattered extrabasinal clasts are subangular to sub-rounded and include pink granites and volcanics. Intraclasts of red mudstone are present. The facies is very well sorted (Table 3.1). The base of the facies in each stacking pattern is represented by a coarse-grained pebbly sandstone or conglomerate, which fines upwards into fine-grained sandstone (Fig. 3.5, Log ES, 10 to 14 m, Fig. 3.6f & Fig. 3.8, Log WS2, 55-61 m). The facies is found in the Tobra Formation in the Khewra-Choa section (eastern Salt Range) and in the Warchha Formation in the Zaluch Nala section (western Salt Range). Lower and upper bed contacts are sharp and the lower contact is commonly undulose and indicates erosion of the underlying bed. The facies can be traced for a few metres laterally.

Interpretation. The basal part of the facies can be interpreted as channel lag deposits (Walker & Cant 1984; Howard *et al.* 2003; Tanoli *et al.* 2008), produced during the onset of a new stream channel or during increased flow conditions. As the initial intensity of the flow decreased, the coarser sediments were deposited. The very good sorting of the facies further suggests long-distance transportation of the sediments. The facies fines upwards into fine-grained sandstone, which was deposited by streams during subsequent relatively steady flow conditions, possibly of lower flow regime (Tanoli *et al.* 2008).

3.3.1.2.2 Sm: Massive sandstone

Description. This facies includes all very well to moderately sorted (Table 3.1) sandstone units that lack primary sedimentary structures. There are two representatives of this facies.

Firstly, massive sandstones with extrabasinal clasts, for example in the Tobra Formation (Fig. 3.5, Log ES, 2 m above the base of the log & Fig. 3.7, Log WS1, 72 m to 79 m above base of the log). Secondly, other massive sandstones which have no extrabasinal clasts and are matrix-supported, for example in the Warchha Formation (Fig. 3.8, Log WS2, 46 m to 47 m & 68 to 70 above base of the log). Rare extrabasinal clasts of granite, gneiss, and quartzite, and clasts of claystone and sandstone are present (Fig. 3.6g). The extrabasinal clasts within this massive sandstone are a range of sizes and are partly sub-rounded. Size broadly relates to composition, with granite clasts typically largest on average (2 mm to 50 mm and occasionally 100 mm), followed by gneiss and quartzites (Fig. 3.7, Log WS1, intermediate level). The massive sandstone with no extrabasinal clasts is the most common facies representative and is present in variable proportions in the measured stratigraphic units of the Tobra and Warchha formations. Some of the beds show a distinctive weathering pattern (Fig. 3.8, Log WS2, 0 m to 3 m above base of the log), possibly as a result of calcareous cement. The lower contact of the facies is erosive and sharp. The upper contact is mostly sharp. The facies is traceable for a few metres and is typically represented by a geometrically lenticular body. Some tabular bodies are also observed (particularly in the Warchha Formation). Individual bodies are 3 m to 8 m thick.

Interpretation. Massive sandstones can be produced as a result of dispersive pressures such as in subaqueous debris flows (Boggs 2001; Finzel & McCarthy 2005; King 2008), however weathering could also possibly remove evidence of internal structures (King 2008). The first type of the massive sandstone facies, with extrabasinal clasts, can be attributed to a sediment gravity flow process such as in debris flows. The active erosion and weathering of nearby lithologies contributed a variety of clast types at the site of deposition of this facies.

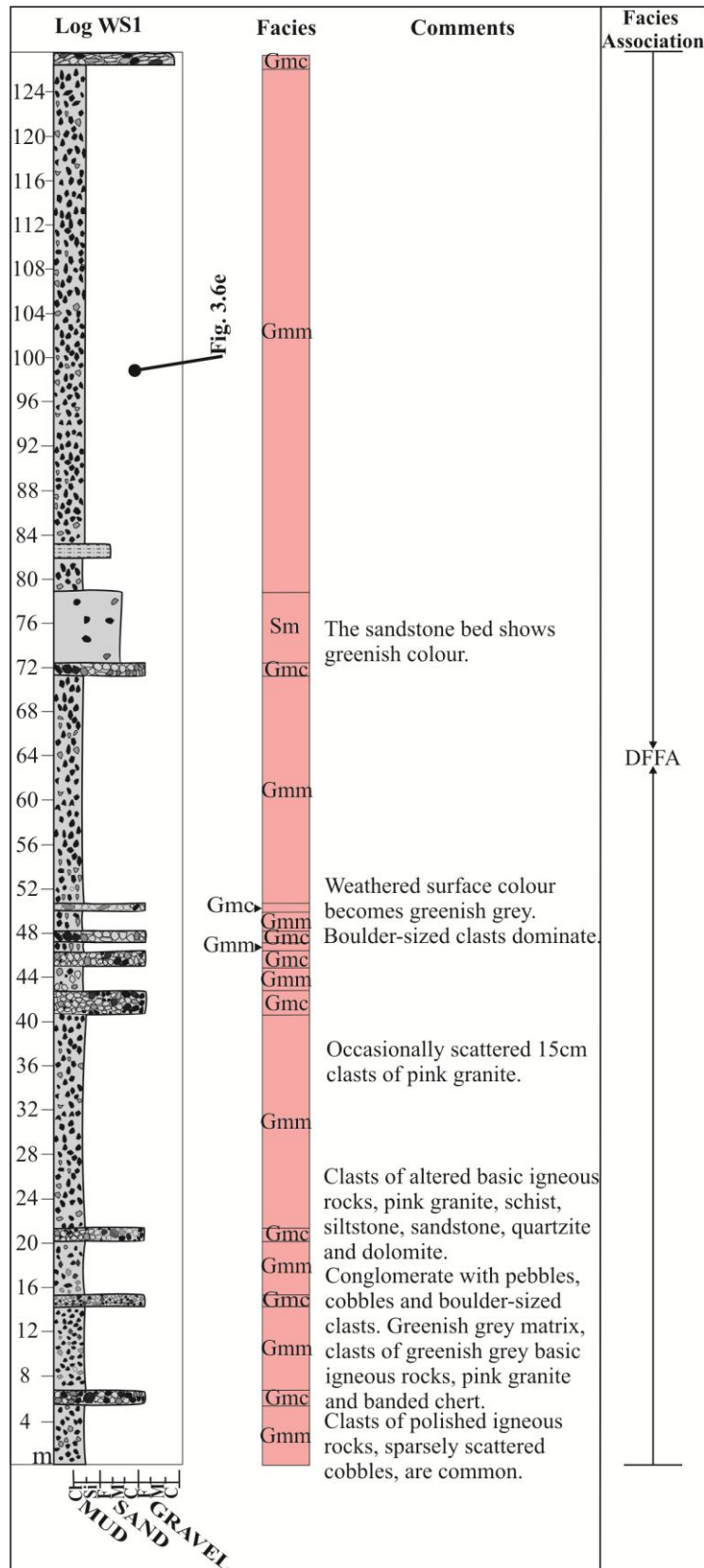


Fig. 3.7 Log WS1-The distribution of lithofacies types and facies associations in the Tobra Formation (Zaluch Nala section, western Salt Range). For detailed stratigraphic location of the unit (formation), refer to Fig. 3.3. For key refer to Fig. 3.2.

The locally present sub-rounded extrabasinal clasts in this facies suggest stream flow deposition (Collinson 1996). However, the absence of any clast imbrication or horizontal stratification is contrary to this interpretation. The sub-rounded extrabasinal clasts could have been deposited in an area of active erosion and weathering, away from the site of the deposition of this facies, and may have been resedimented as debris flows. The distinctive weathering pattern may have obscured evidence of internal structures in the massive sandstone, whether it included extrabasinal clasts or not (King 2008). However, even away from the weathered areas, the sandstones appear structureless. The massive sandstone facies without extrabasinal clasts are locally associated with trough cross-bedded sandstone (i.e. Fig. 3.8, Log WS2, top 4 m) and therefore could be interpreted as collapse liquefaction of the channel banks or bars (Collinson 1996). The lenticular form is consistent with this interpretation. The massive sandstone facies is also observed with the massive and laminated sandstone facies (e.g. Fm and Fl, fig. 3.8, Log WS2) in the form of tabular bodies and these are interpreted as representing rapid deposition from tractional currents during floods (Collinson 1996).

3.3.1.2.3 Fss: Fine-grained sandstone and siltstone

Description. This facies consists of fine-grained sandstone with siltstone interbeds. The colour of the facies is dark grey overall, though it includes rare associated, less conspicuous (<300 mm), red layers (Fig. 3.5, Log ES, 5 to 9 m & 13 to 17 m & Fig. 3.6h). The facies has a mainly massive appearance with no obvious sedimentary structures other than the interbedding of the two lithologies. The outcrop expression of the facies is typically slope-forming with a recessive profile, typical of less competent lithologies. Laterally the facies does not extend for more than a few metres.

Interpretation. This facies is interpreted as representing the settling of fine-grained sand and silt away from the main channel, following flooding events (Miall 1992;

Howard *et al.* 2003; Tanoli *et al.* 2008). The presence of red layers and the red colouration may be attributed to well-drained and oxygenated floodplain conditions (Tanoli *et al.* 2008).

3.3.1.2.4 St: Trough cross-bedded sandstone

Description. This facies is characterised by trough cross-bedded sandstones of a range of grain sizes. The cross-beds are commonly highlighted by grains of different shade or slightly different size (Figs. 3.9a & b). The facies shows trough cross-bedded sets and cosets in mainly fine-grained sandstone (Fig. 3.8, Log WS2, Figs. 3.9a & b). The facies is red on weathered surfaces and light pink to red on fresh surfaces. The beds are lenticular to tabular and the cosets are typically 2 to 4 m in thickness. The cross-beds show variable sizes with sets varying from 200 mm to 500 mm thickness to large units of 1 m thickness. The boundaries between individual cross-sets are marked by thin (<30 mm) siltstone beds. The cross-bedded sets are commonly grouped though occur more rarely as solitary sets.

This facies is commonly associated with facies Sm (especially in the Warchha Formation), association with other facies types being less common. Both lower and upper contacts are sharp. The lower contacts are erosive, with 1 to 2 m relief. The facies can be traced for tens of metres.

Interpretation. This facies is interpreted as deposited by the migration of sinuous-crested dunes in the lower flow regime (Miall 1996; Ghazi & Mountney 2009). The lenticular geometry also supports the fluvial bedform interpretation (Collinson 1996; Ghazi & Mountney 2009). The facies has similarities with the coarse-grained trough cross-bedded sandstone facies of Ghazi & Mountney (2009).

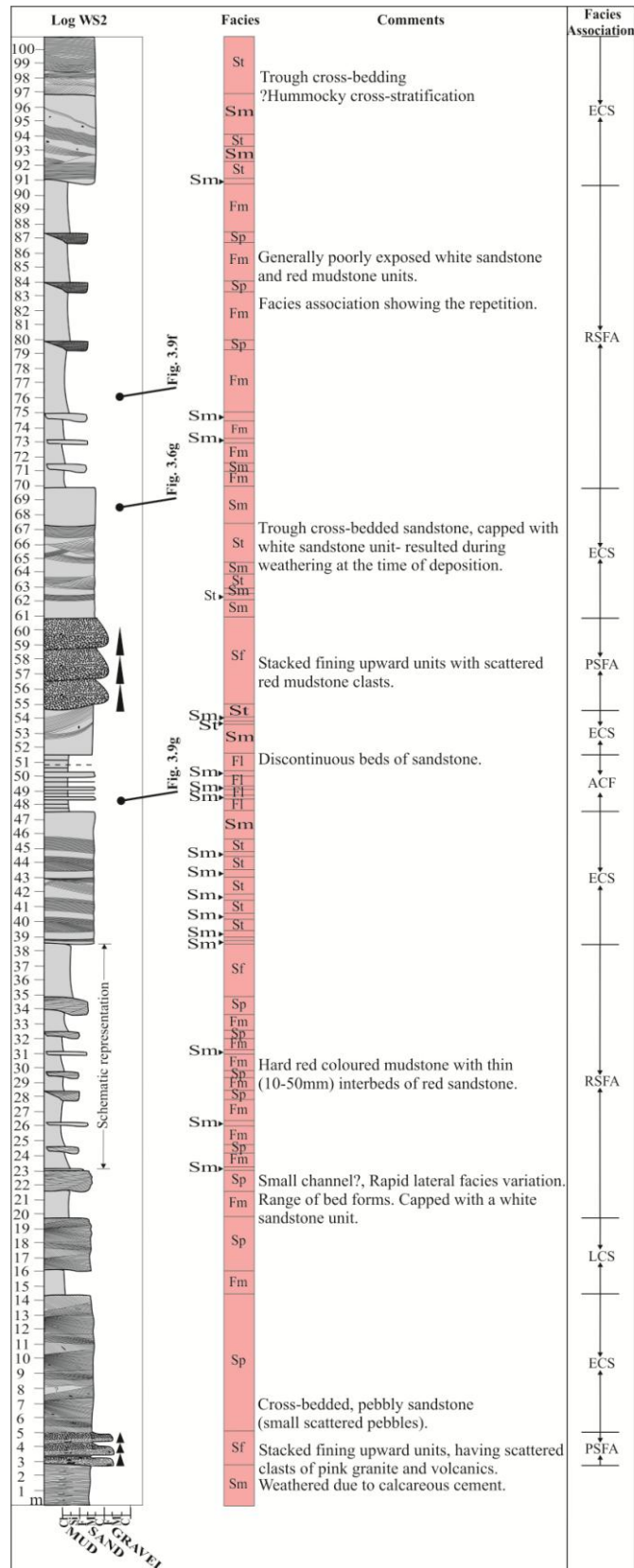


Fig. 3.8 Log WS2-The distribution of lithofacies types and facies associations in the Warchha Formation (Zaluch Nala section, western Salt Range). For detailed stratigraphic location of the unit (formation), refer to Fig. 3.3. For key refer to Fig. 3.2.

3.3.1.2.5 Sp: Planar cross-bedded sandstone

Description. This facies consists of poorly sorted sandstone with lower sharp and erosive contacts and upper sharp contacts. Internally the beds are characterised by planar cross-beds that are arranged in multi-storey cosets, exhibiting a fining-upwards grain size profile. Occasionally the sandstones are micaceous (Fig. 3.8, Log WS2, Fig. 3.9c). The individual cross-sets vary from 100 mm to 200 mm in thickness; both low (8-13°) and high angle (10-30°) stratification is observed. Weathered surfaces are light brown and fresh surfaces are white or pink. The beds comprise lenticular to wedge-shaped bodies that usually thin at both margins and form convex-up bodies. Laterally the facies can be traced for a few metres.

Interpretation. The facies is interpreted to have formed from the migration of straight-crested dunes or bars, deposited under lower flow regime conditions (Miall 1996; Ghazi & Mountney 2009). A similar facies in the Warchha Formation has been identified by Ghazi & Mountney in the eastern Salt Range (Fig. 3.1).

3.3.1.2.6 Sr: Ripple-laminated sandstone and interlaminated mudstone

Description. This facies consists of very fine-grained sandstone lenses interlaminated with more continuous dark grey mudstone (Fig. 3.9d). The sandstone is well sorted and light grey in colour and is present in the form of thin wedge-shaped lenses that pinch out laterally within a few centimetres. Mudstone laminations are more continuous and could be traced for few metres or as far laterally as the exposure can be traced. The interlamination of lensoidal sandstone interbedded with more continuous mudstone beds produces structures that resemble symmetrical ripples. Occasional red layers, vertical burrows and cross-laminae (<150 mm in thickness) have also been observed in this facies.

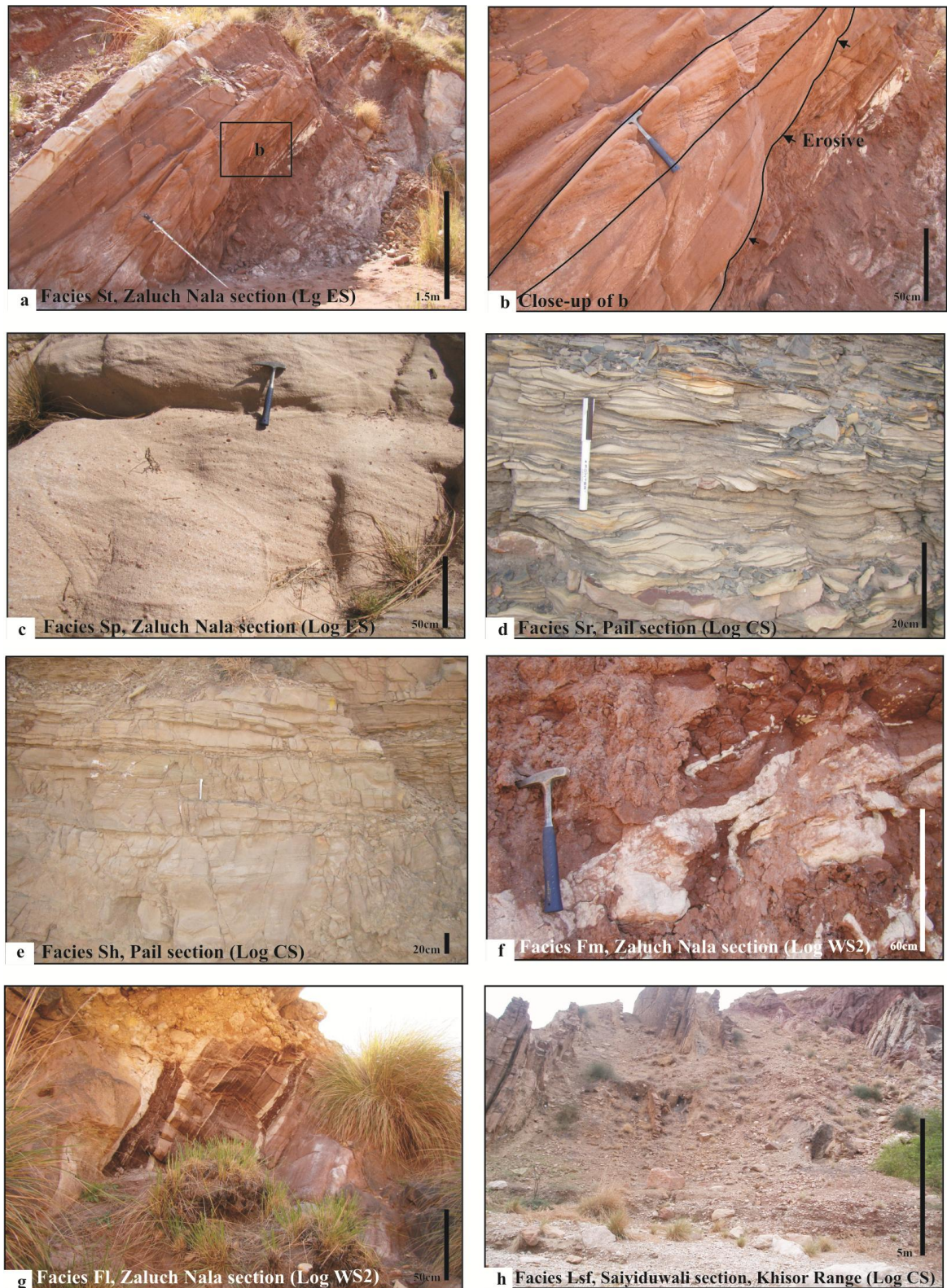


Fig. 3.9 Characteristic examples of lithofacies present in the Carboniferous-Permian succession of the Salt Range and Khisor Range. Stratigraphic location given on Figs. 3.5, 3.8 and 3.11.



Fig. 3.10 Burrows in facies Sr (Ripple-laminated sandstone and interlaminated mudstone).

Vertical burrows are observed to increase in abundance upwards, i.e. at the top of the measured sections at the above-mentioned localities (Figs. 3.10a-d). The facies is frequently found in the Dandot Formation of the Khewra-Choa section (eastern Salt Range, fig. 3.5, Log ES, interval 3.5 to 5 m), Pail section (central Salt Range, fig. 3.11, Log CS interval 8 to 21 m) and is only rarely found in the Tobra Formation of the Khewra-Choa section (eastern Salt Range, fig. 3.5, Log ES).

Interpretation. The presence of burrows is consistent with relatively slow sedimentation and indicates environments suitable for burrowing organisms. These and the presence of wave ripples in this facies suggest an intertidal to shallow marine setting.

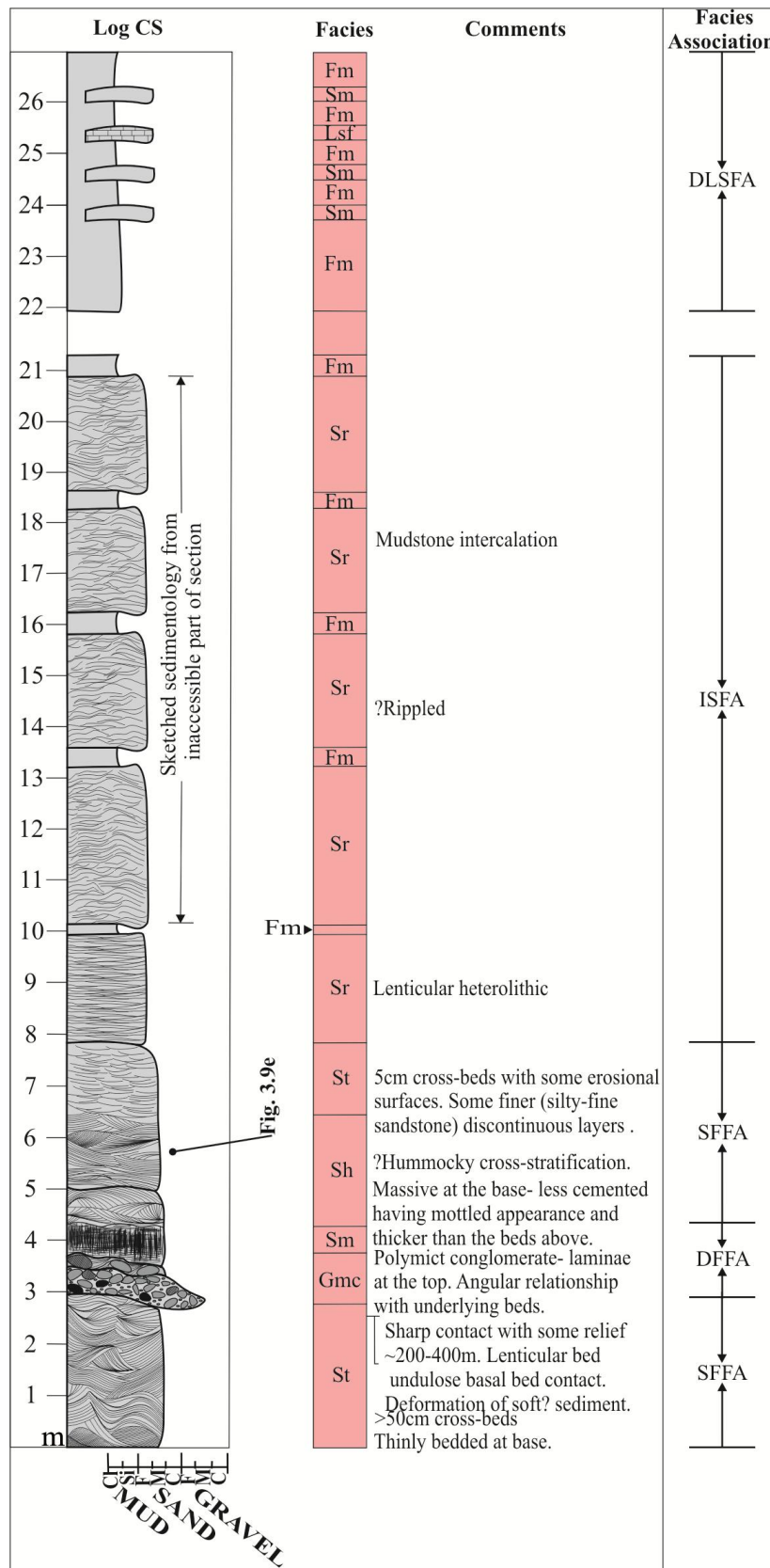


Fig. 3.11 Log CS-The distribution of lithofacies types and facies associations in the Carboniferous-Permian succession of the Pail section (central Salt Range). For detailed stratigraphic location of the units (formations), refer to Fig. 3.3. For key refer to Fig. 3.2.

3.3.1.2.7 Sh: Hummocky cross-stratified sandstone

Description. Thin-bedded, moderately sorted and rounded sandstones with hummocky cross-stratification characterise this facies. The individual hummocks are 2 m in length, 280 mm high and approximately 140 mm in set thickness. Interbedded with the sandstones are dark grey, thin mudstone laminae, in the form of layers and lenses. Typically the basal contact of the facies is sharp (Fig. 3.11, Log CS, interval 4 to 6 m). The facies is represented by tabular bodies that can be traced for a few metres along the road cut (Fig. 3.9e).

Interpretation. The absence of trace fossils, wave ripples and wave ripple cross-lamination in this facies argue against the interpretation of the facies by oscillatory flow. The presence of current-formed sedimentary structures (i.e. trough cross bedding and current ripples) in the immediately overlying facies (i.e. St, Log CS, interval 6 to 8 m), suggest rather the deposition of the facies by unidirectional flow (Johnson & Baldwin 1996). The formation of the hummocky cross-stratification by unidirectional flows has been discussed by various workers in the context of a fluvial system carrying a large amount of fine sands in suspension (e.g. Cotter & Graham 1991). The deposition of the subsequent mudstone layers represent settling out from suspension in a steady and calm depositional setting.

3.3.1.3 Mud-dominated facies

3.3.1.3.1 Fm: Massive mudstone

Description. This facies is represented by generally structureless red, brown, green and light to dark grey mudstones. Desiccation cracks, calcretes and rain-drops were observed on some bedding planes in the Warchha Formation. The facies occurs as thick lenticular bodies of a few metres thickness that could be traced laterally over a few metres (Fig. 3.11, Log CS, Fig. 3.9f). The facies represents a significant proportion of

the Warchha Formation and is associated with the massive sandstone facies (Sm).

However, when present in the Sardhai Formation, the massive mudstone is dark grey to black and occasionally includes some carbonaceous content. Desiccation cracks, calcretes and rain drops are absent.

Interpretation. The absence of laminae could be attributed to the following factors,

1. The muds may have been subjected to burrowing, modifying or destroying the original laminae (Howard *et al.* 2003).
2. The deposition of mud could have occurred as aggregates (Rust & Nanson 1989; Howard *et al.* 2003). This would produce a “clotted texture” and laminae would not form during this process.
3. The muds were deposited by rapid settling from suspension, which would not produce any laminae (Howard *et al.* 2003).

The absence of plant fossils and woody debris alongside the presence of calcretes in a similar facies, studied in the eastern Salt Range, the Warchha Formation, was interpreted by Ghazi & Mountney (2009) to represent semi-arid conditions. In this setting, the absence of plant matter could relate either to rapid channel migration and sediment instability or to a lack of water and subsequently oxidising conditions, which would inhibit both plant growth and preservation. Two samples investigated for palynology from this facies in the Warchha Formation (Appendices 2 & 6), showed an absence of palynomorphs, which may be related to the oxic environment, unsuitable for sustaining plant communities. If such vegetation was limited, as also proposed by Ghazi & Mountney (2009), disturbance of the mud by plant roots would seem unlikely. Therefore, a more likely reason for the massive mudstone in the Warchha Formation is deposition by mass flow processes. The massive mudstone in the Sardhai Formation, however, shows different properties to that in the Warchha Formation.

3.3.1.3.2 Fl: Laminated mudstone

Description. This facies is represented by parallel-laminated red clay-rich mudstones with occasional silty mudstone units. These units reach a few centimetres to over a metre in thickness. The facies is only found in the Warchha Formation, where the lower and upper contacts are erosional and sharp. Geometrically the beds are arranged in 1 m thick-sheet like bodies, extending over a few metres (Fig. 3.8, Log WS2, Fig. 3.9g).

Interpretation. Sediments of these facies are interpreted as reflecting deposition during waning stage floods in overbank areas. They most probably represent infills of abandoned channels as indicated by the erosional surfaces at the base and the association with the sandstone interbeds.

3.3.1.4 Limestone-dominated facies

3.3.1.4.1 Lsf: Thin-bedded sandy limestone

Description. This facies comprises very thin-bedded sandy limestones and is often associated with facies Fm. The facies has only been observed in the Sardhai Formation in this study. No fossils have been observed in the facies during the present investigation (Fig. 3.11, Log CS, Fig. 3.9h). However, from the sandy limestone beds in the Sardhai Formation of the Saiyiduwali section (Khisor Range, fig. 3.1), Hussain (1967) described the marine macrofossils *Anastompora* sp., *Fenestella* sp., *Athyris* sp., and *Spirifer* sp. The Sardhai Formation as a whole is very rarely exposed in the Salt Range, because of the incompetent character of the formation which is hence more prone to recessive erosion.

Interpretation. The sandy limestone facies shows deposition in a shallow-marine environment (Banerjee 1959; Qureshi *et al.* 2008). The thin beds reflect periodic influxes of sediments. The lithofacies demonstrated in these stratigraphic units (i.e. Tobra, Dandot, Warchha and Sardhai formation) have been summarised in Table 3.2.

Facies group	Facies types	Formation (unit)			
		Tobra	Dandot	Warchha	Sardhai
Conglomeratic facies	Gmc	+			
	Gmm	+			
Sandstone-dominated facies	Sf	+		+	
	Sm	+		+	+
	Fss	+			
	St	+		+	
	Sp		+	+	
	Sr	+	+		
	Sh	+			
Mudstone-dominated facies	Fm	+	+	+	+
	Fl			+	
Limestone-dominated facies	Lsf				+

Table 3.2 Summary of lithofacies types present in each stratigraphic unit (formation) in the Carboniferous-Permian succession of the Salt Range. A positive sign indicates that the lithofacies is present. See Fig. 3.2 for key to lithofacies.

3.4 Tobra Formation facies association

A cumulative 228 metre-thick succession of the Tobra Formation is exposed at a number of locations in the Salt and Khisor ranges. The nine distinctive lithofacies types recognised (Fig. 3.12, Table 3.2), are grouped into the following three facies associations.

3.4.1 DFFA: Debris flow-dominated alluvial plain facies association

The debris flow facies association (DFFA) is characterised by facies Gmm, Gmc, Sm, and Fm and is found in all measured sections of the Tobra Formation during the present investigation, i.e. extending from the Saiyiduwali section (Khisor Range), through the

Zaluch Nala section (western Salt Range) and into the Khewra-Choa section (eastern Salt Range, fig. 3.12). The Tobra Formation in the Saiyiduwali section (Khisor Range), Zaluch Nala section (western Salt Range) and partly in the central Salt Range, Warchha gorge section is entirely represented by the DFFA facies association, which at the Zaluch Nala section (western Salt Range) reaches a maximum thickness of 125 m (Fig. 3.12). However at the Pail section (central Salt Range) and Khewra-Choa section (eastern Salt Range), the DFFA facies association is represented by less than 1.5 m thick beds and thus a lateral decrease in its thickness is observed. At these latter locations, the DFFA occupies various stratigraphic positions (Fig. 3.12).

3.4.2 SFFA: Stream flow dominated alluvial plain facies association

The stream flow facies association (SFFA) includes facies St, Sh, Sr, Fss, and Sf and is restricted to the Tobra Formation at the Pail and Warchha gorge sections (central Salt Range) and the Khewra-Choa section (eastern Salt Range, fig. 3.12). Facies suggestive of stream flow processes have not been observed in the Saiyiduwali section (Khisor Range) or the Zaluch Nala section (western Salt range). The SFFA facies association is present at various stratigraphic levels in the Tobra Formation and the maximum thickness reached is 12 m.

3.4.3 OFA: Overbank facies association

The overbank facies association (OFA) is characterised by the facies Fss. The OFA facies association is restricted to the eastern Salt Range, i.e. Khewra-Choa section (eastern Salt Range, fig. 3.12). The facies association reaches a maximum thickness of 5 m.

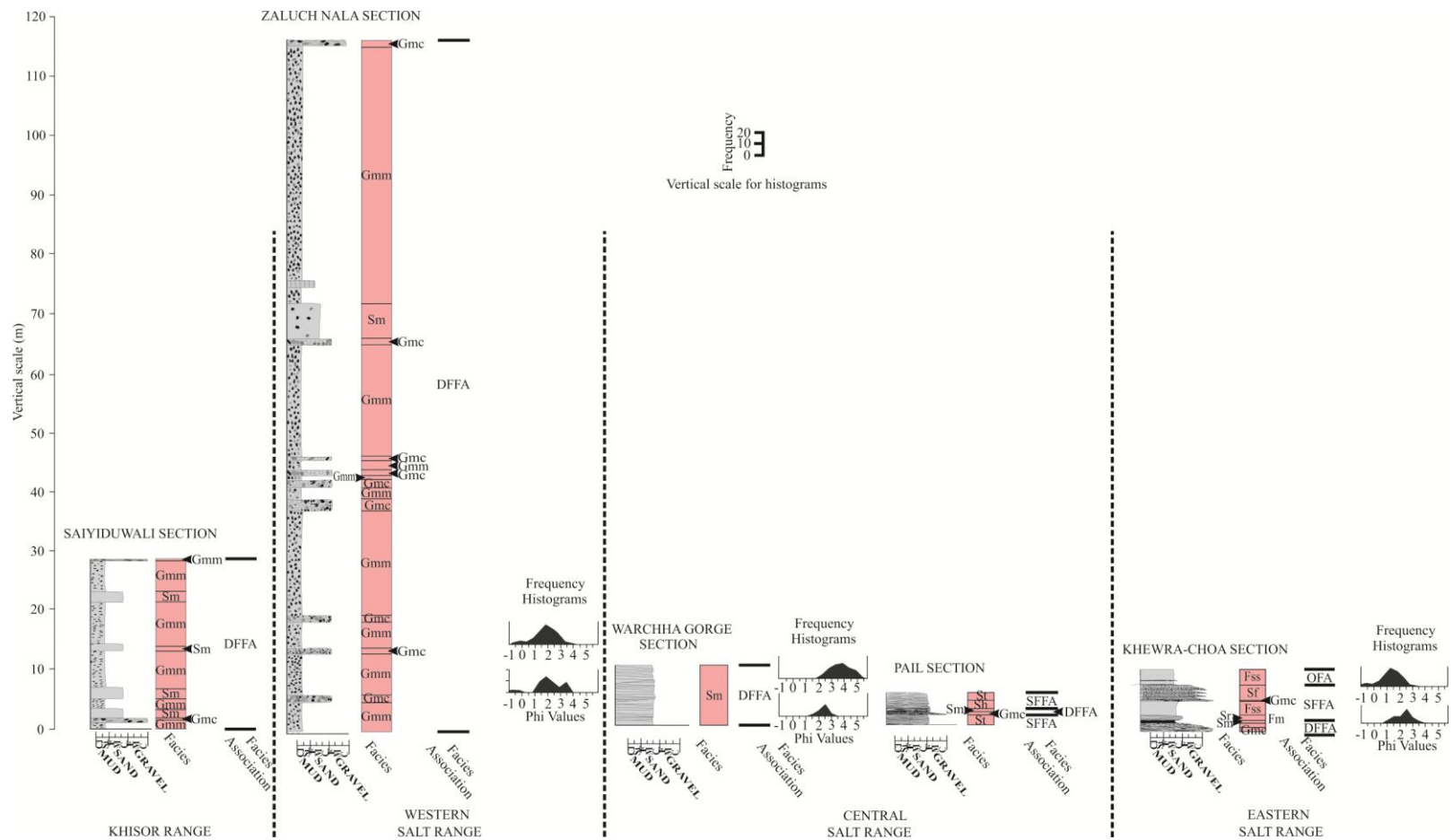


Fig. 3.12 The facies and facies associations variations in the Tobra Formation from the Saiyiduwali section (Khisor Range), through the Zaluch Nala section (western Salt Range) Pail, and Warchha gorge sections (central Salt Range) and into the Khewra-Choa section (eastern Salt Range). The histograms of the sedimentology samples are also shown. For sedimentology sample locations refer to Appendix 2. Refer to Fig. 3.1 for locations of these units and Fig. 3.2 for key.

3.5 Grain size analyses and provenance of the Tobra Formation

The frequency histograms (Fig. 3.12) of representative samples from the Tobra Formation (Appendix 2, Table 3.1), show that the deposits possess a wide range of grain sizes, from the western to the eastern Salt Range (Fig. 3.3).

In the Zaluch Nala section (western Salt Range i.e. sample 1TZ and 2TZ, Table 3.1, fig. 3.4), the sediments range from very fine- to very coarse-grained sand. The mean composition (i.e. Mz) corresponds to medium-grained sand. These sediments are moderate to poorly sorted and show a well-developed coarse tail (Fig. 3.13a-e, Table 3.1). In the Warchha gorge section (central Salt Range), a general decrease in the grain sizes is observed. Two samples (i.e. 1TW and 2TW, Table 3.1), studied from the Tobra Formation at the Warchha gorge section show that the constituent sediments range between very coarse-grained silt and medium-grained sand. The mean composition corresponds to fine-grained sand. The sediments are moderately well-sorted and more material occurs in the fine tail (Table 3.1).

Further east, i.e. in the Khewra-Choa section (eastern Salt Range i.e. 1TKC and 2TKC, Table 3.1, Appendix 2), the sediments range from very coarse-grained silt to very coarse-grained sand, with a mean composition of coarse-grained sand. The sediments are well sorted and show a tendency for more material in the fine tail (Table 3.1). A general increase in the sorting of the constituent grains of the Tobra Formation is observed from the western to the eastern Salt Range (Fig. 3.13f-h, Table 3.1).

Associated changes in the sphericity and roundness of the grains in these locations have also been observed, with the former parts of the Salt Range showing a dominance of grains having less sphericity and more angularity (Fig. 3.14). In the latter parts (i.e. central and eastern Salt Range) these grains show a greater degree of sphericity and more grains fall in the sub-rounded to rounded categories (Fig. 3.14).

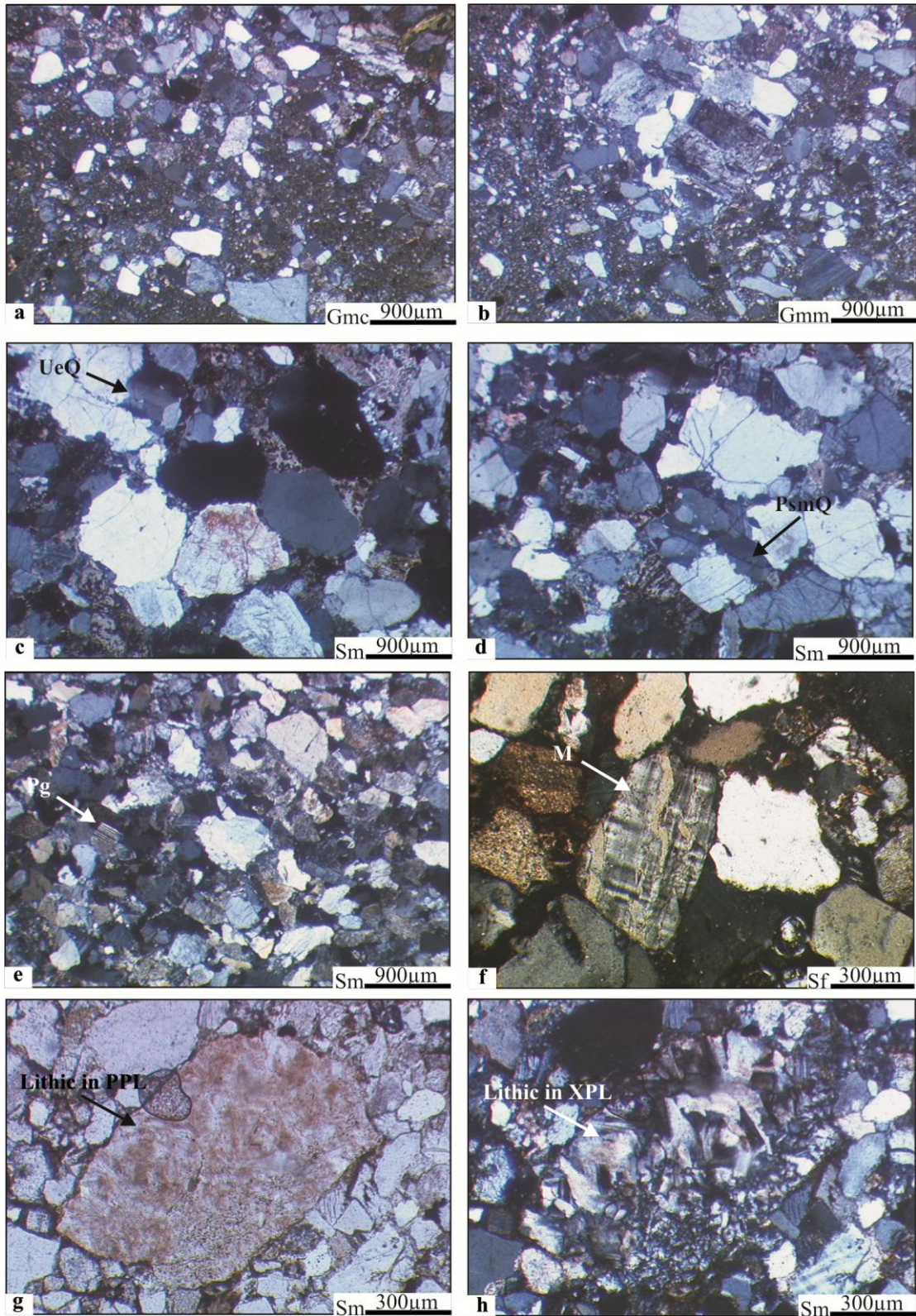


Fig. 3.13 Photomicrographs of some of the lithofacies in the Tobra Formation. For facies codes and mineral symbols refer to Fig. 3.2.

Plots of the Tobra Formation samples on the QFL triangular diagram show that detrital material was likely derived from recycled orogenic belts and cratonic interiors (Dickinson 1985, fig. 3.15). Mineralogically the most dominant component is quartz, and both monocrystalline and polycrystalline varieties are present (Fig. 3.13c & d). The polycrystalline quartz grains with undulose extinction shows its derivation from either a metamorphic or igneous source (Adams *et al.* 1991, fig. 3.13c). The polycrystalline quartz grains with sutured margins are derived from metamorphic sources, whereas those with straight margins originated from igneous sources (Fig. 3.13d). The monocrystalline quartz is likely derived from the weathering of granites (Pettijohn *et al.* 1987). Feldspar represents the second most dominant detrital mineral. Alkali feldspars (Fig. 3.13e & f) are more frequent than calcic plagioclase and thus show probable derivation from either granites or gneisses. Very rare perthite is found (Fig. 3.13e & f). Mica is represented by muscovite and very rarely biotite. Occasionally, highly birefringent sericite was also found. The lithics represent igneous, metamorphic and sedimentary categories (Fig. 3.13g & h). Gahuri *et al.* (1970) conducted comparative petrographic studies of the Tobra Formation and those of the Aravalli System exposed in the Udaipur, Rajasthan India, which is situated approximately 600 km southeast of the Salt Range and demonstrated differences in the sediments of the Aravalli System and the Tobra Formation. Recently the source area of the Tobra Formation has been discussed by Ghazi & Mountney (2011) as the Malani Range, which forms a series of volcanic porphyritic rhyolites lavas, situated more than 500 km south of the Salt Range and extending into the Sindh Province of Pakistan.

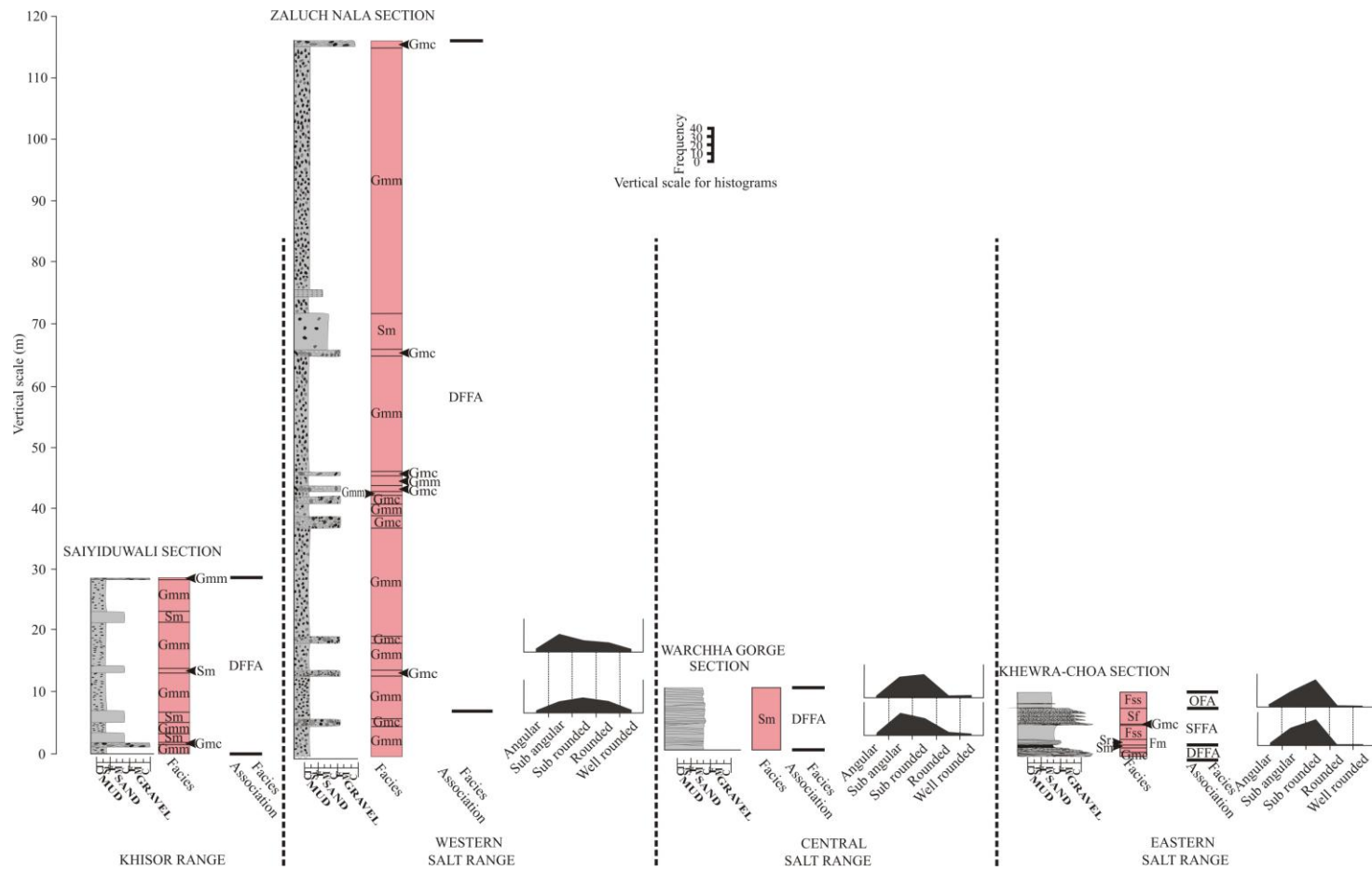


Fig. 3.14 Variation in the grain roundness (histograms) from the Saiyiduwali section (Khisor Range), through the Zaluch Nala section (western Salt Range), Warchha gorge sections (central Salt Range) and into the Khewra-Choa section (eastern Salt Range). Sedimentology sample locations refer to Appendix 2. Refer to Fig. 3.1 for locations of these units and to Fig. 3.2 for key.

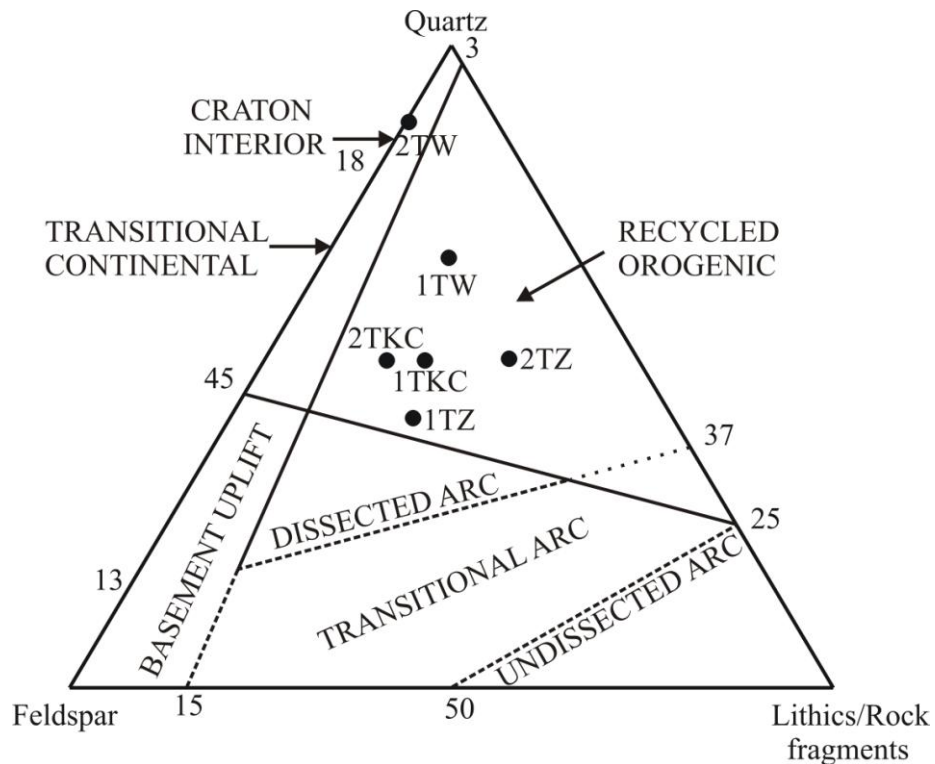


Fig. 3.15 The QFL diagram for the Tobra Formation and interpretation of provenance (c.f. Dickinson 1985). See Fig. 3.2 for key to samples.

3.6 Tobra Formation depositional environment

The succession of the Tobra Formation studied is interpreted as comprising debris flow, stream flow and overbank deposits. The three facies associations (i.e. DFFA, SFFA and OFA) partly overlie each other eastwards in the Salt Range. There is a repetitive alternation of the facies Gmc, Gmm and Sm in the Khisor Range and western Salt Range. In the central and eastern Salt Range, this type of facies succession is usually rare.

Two possible depositional models can be inferred for the Tobra Formation. The first is that of an alluvial fan setting (Dasgupta 2006), in an undisturbed tectonic region, in which a slight decrease in the lateral profile can be assumed from the Khisor Range, through the western Salt Range and in the eastern Salt Range (Figs. 3.16 & 3.17). The

sorting of the constituent grains increases from the western to the eastern Salt Range (Figs. 3.4 & 3.12). Given an alluvial fan setting, the following three episodes of development might have resulted,

1. The debris flow facies association (DFFA) marks the initial episode of sedimentation on an alluvial fan, which is extensive in geographical extent, extending from a proximal to a distal fan setting (i.e. from the western Salt Range to the eastern Salt Range, fig. 3.16). The thickness of the debris flow deposits decreases eastwards in the Salt Range, which represents a decrease in flow strength from west to east. The massive sandstone facies (Sm) in the DFFA facies association, observed sporadically in the Khisor Range (Saiyiduwali section) and western Salt Range (Zaluch Nala section) and more frequently in the central (Warchha gorge and Pail sections) and eastern Salt Range (Khehra-choa section), overlying the facies Gmm and Gmc, shows the initiation of subaqueous debris flows related to fluid input (Dasgupta 2006). During this episode of deposition, the fine fractions of the debris flows are winnowed out to down-fan locations and the resulting sediments are concentrated in larger clasts (Collinson 1996).
2. The next episode of sedimentation is represented by the development of the stream flow facies association (SFFA), which marks the initiation of stream flow processes in the central and eastern Salt Range, as the debris flow processes waned, (Fig. 3.11). Downslope on the proximal fan, the deposition of ripple laminated sandstone and interlaminated mudstone facies (Sr), fine-grained sandstone and siltstone facies (Fss) and trough cross-bedded sandstone facies (St) took place. The high sand content down the slope of the proximal fan also results in the development of hummocky cross-stratified sandstone facies (Sh) in

the central Salt Range (Pail section) and the waning flow conditions resulted in the development of a fining-upwards pebbly sandstone facies (Sf) further east, i.e. in the eastern Salt Range (Khewra-Choa section). The SFFA facies association thus shows an interval away from the proximal fan setting, where the major debris flow processes gradually waned and are followed by stream flow processes (Collinson 1996) in the mid and distal fan settings. The mid and distal fan areas are thus only confined to the central and eastern Salt Range (Fig. 3.16).

3. In the distal fan setting, submergence of the floodplain of the alluvial fan occurred, as a result of the flooding and overtopping of the streams, and the water flowed out of the main stream courses, resulting in the development of an Overbank Facies Association (OFA).

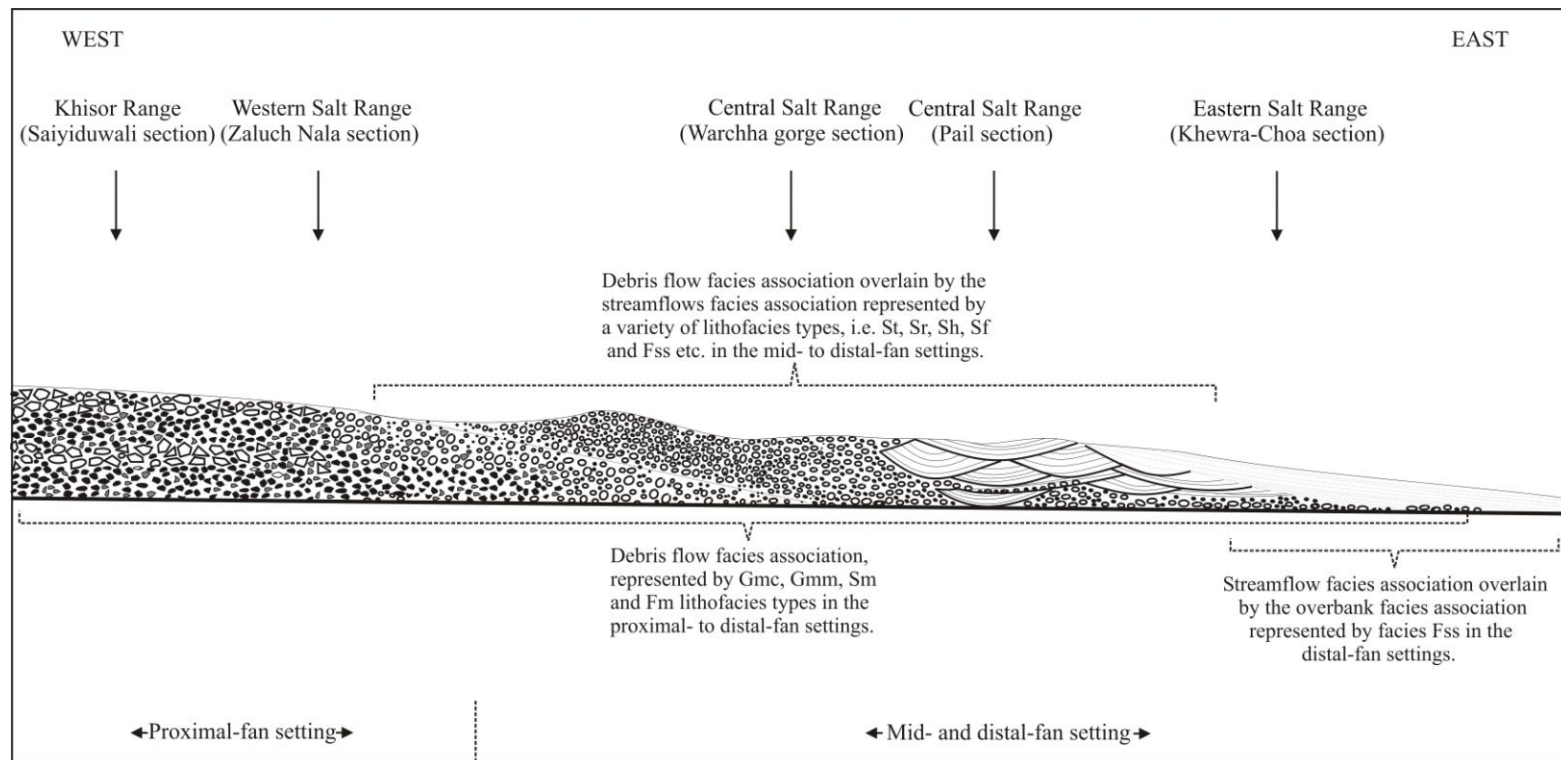


Fig. 3.16 Depositional model 1 of the Tobra Formation in an alluvial fan setting showing the distribution of the major facies associations. See Fig. 3.2 for key. The figure is not to scale.

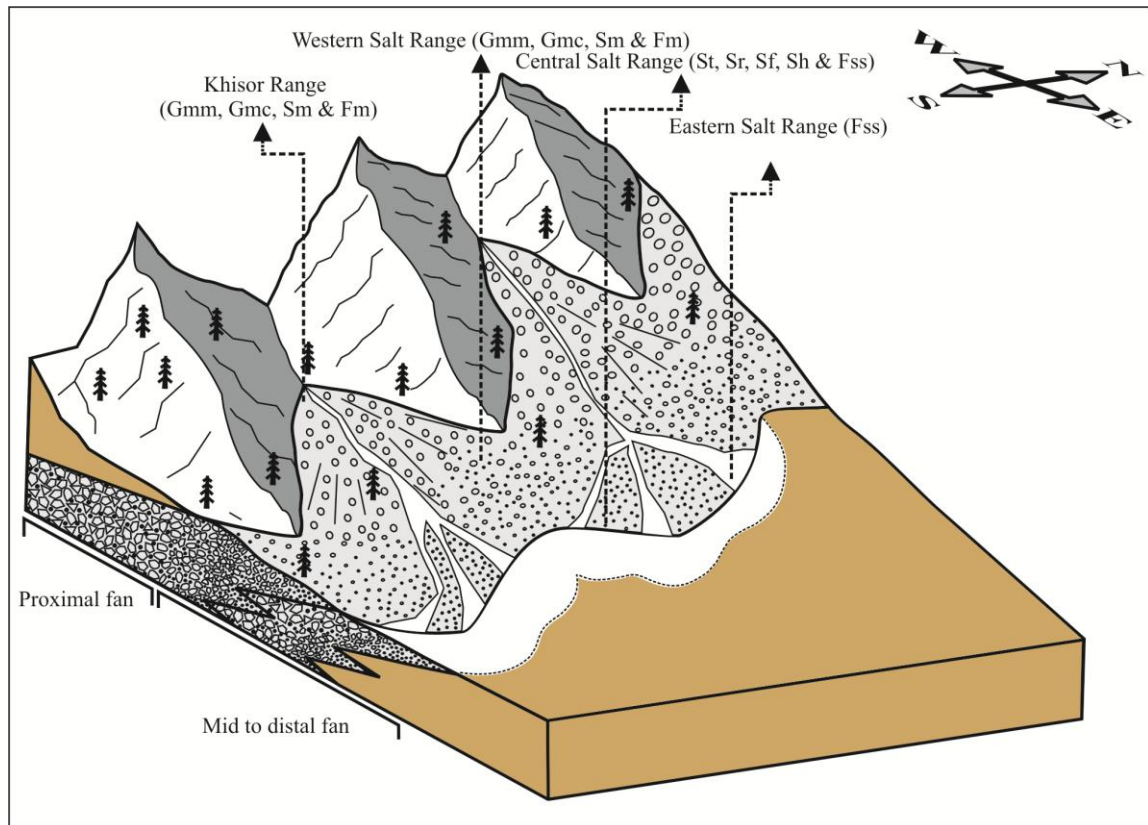


Fig. 3.17 Block diagram of the idealised depositional model 1 of the Tobra Formation. See Fig. 3.2 for facies codes.

The second model represents development of these facies associations in a tectonically active region, where the deposition of the Tobra Formation took place on uneven relief (Fig. 3.18). The outcrop-scale 2-4 m relief supports this depositional model. The lateral variability of the Tobra Formation (Teichert 1967), is also best described by this model. The presence of faceted clasts and correlation of the Tobra Formation with the glaciogenic Al Khlata Formation of Oman and Saudi Arabia (Jan & Stephenson 2011), support that the Tobra Formation represents deposition in the proximity of the South Polar glaciations. However, the absence of the features like glacial striations and grooves, rather support that the Tobra Formation deposited ice-marginally, being

deposited by glacio-fluvial processes associated with the final stages of the Gondwana glaciation.

Given a glacio-fluvial setting, the deposition of the Tobra Formation at the Trans-Indus Khisor Range (i.e. Saiyiduwali section) and western Salt Range (i.e. Zaluch Nala section, fig. 3.1) took place continuously from glacial outwash. This resulted in the development of the debris flow facies association (DFFA) in these areas. These deposits (DFFA) also extended into the central (Pail and Warchha gorge sections) and eastern (Khewra-Choa section) Salt Range, probably as a result of intermittent facies belt advances associated with glacial maxima.

Eastwards, in the central Salt Range (Pail and Warchha gorge sections), the deposition of the stream flow facies association (SFFA) took place, which in the eastern Salt Range developed into the overbank facies association (OFA).

The systematic sorting of the constituent grains support this model, as the debris flow facies association (DFFA) is characterised by moderate to poorly sorted grains and the stream flow facies association (SFFA) by moderately well-sorted to well-sorted grains (Table 3.1).

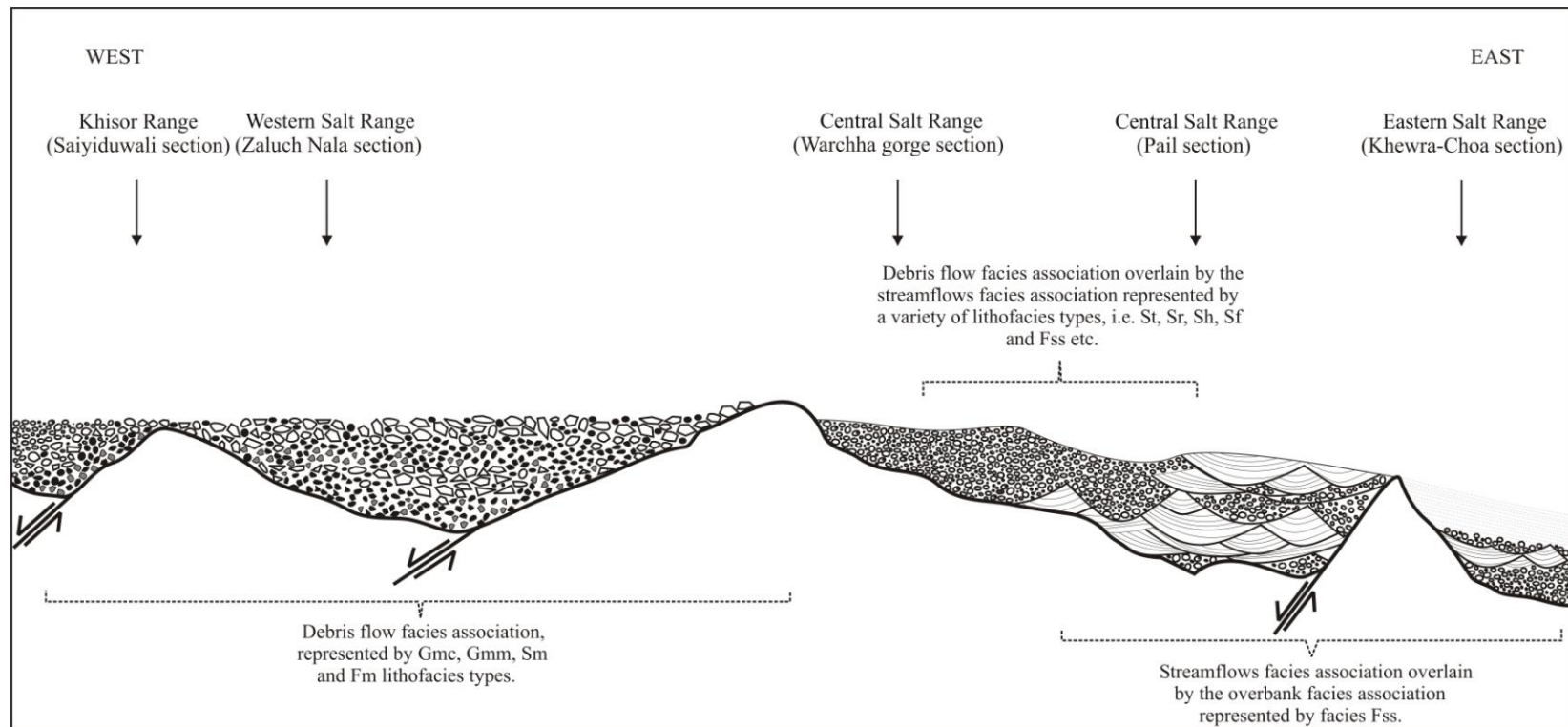


Fig. 3.18 Depositional model 2 of the Tobra Formation in a tectonically active region showing the distribution of the major facies associations. See Fig. 3.2 for key. The figure is not to scale.

3.7 Dandot Formation facies association

In the measured cumulative 31.5 m-thick succession of the Dandot Formation, the facies observed at the Khewra-Choa section (eastern Salt Range) and Pail section (central Salt Range) have been summarised in Fig. 3.19. Three lithofacies types have been recognised in this stratigraphic unit (Table 3.2) in the central and eastern Salt Range. Westwards (i.e. in the western Salt Range and Khisor Range), this facies association is non-existent.

3.7.1 ISFA: Intertidal to shallow marine facies association

The ISFA facies association is represented by a ripple-laminated sandstone and interlaminated mudstone facies (Sr), which is occasionally interbedded with a massive mudstone facies (Fm) and a planar cross-bedded sandstone facies (Sp, fig. 3.19). This facies is underlain by the stream flow facies association (SFFA) of the Tobra Formation at the Pail section (central Salt Range, fig. 3.11), however at the Khewra-Choa section (eastern Salt Range), the ISFA directly overlies the overbank facies association (i.e. OFA) of the Tobra Formation (Fig. 3.5). The deposits of the ISFA facies association are up to 2 m thick, with individual units being 10 cm thick. Wavy and lenticular bedding that is discontinuous and pinches out laterally is common in this facies association (Maejima *et al.* 2004). Common sedimentary structures include wave ripples, cross-bedding and cross-lamination. Laminae are commonly disturbed by burrows (Collinson 1996).

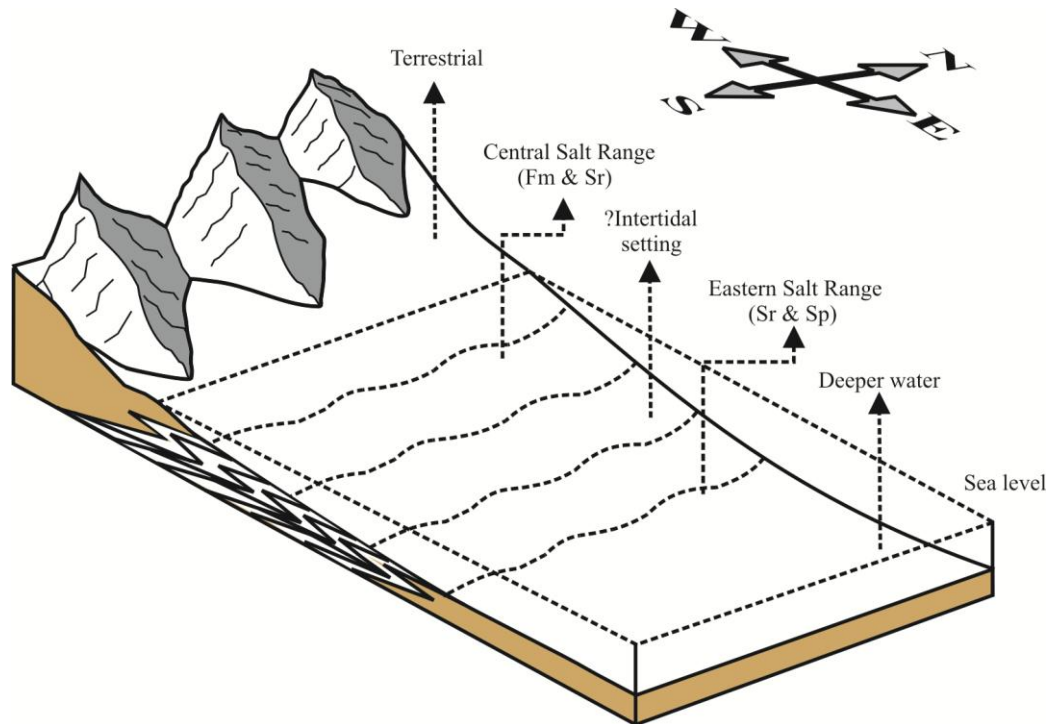


Fig. 3.20 Idealised depositional model of the Dandot Formation. See Fig. 3.2 for facies codes.

3.8 Dandot Formation depositional environment

The heterolithic lithology with ripple lenses, separated by mud flasers, support the idea that the Dandot Formation represents facies progression to a basinal setting (i.e. ISFA facies association, fig. 3.20). The occurrence of marine fauna in the same suite of lithologies (Reed 1936), further suggests deposition of these strata in an intertidal to shallow marine settings (Fig. 3.20). Though, no such fauna has been found during the present work, the given information, i.e. the presence of flaser bedding, heterolithic lithology and lenticular bedding suggest the deposition of the unit in the intertidal to shallow marine setting (Chakrabarti 2005).

The absence of the ISFA facies association, i.e. the Dandot Formation from the western Salt Range and Khisor Range may have resulted from either one or a combination of the following factors.

1. Post-depositional tectonism and subsequent removal of the unit from these locations, before the deposition of the overlying unit i.e. the Warchha Formation (Fig. 3.3).
2. Only local marine incursion occurred into the central and eastern part of the Salt Range. Pre-depositional tectonics might have played a role in the development of such a basin in these areas. However, tectonic activity was only local and not sufficient to develop a basin across the entire Salt Range.

3.9 Warchha Formation facies association

During this investigation a cumulative 153.5 m-thick section of the Warchha Formation has been studied (Fig. 3.21). Six lithofacies types have been recognised in the Warchha Formation (Table 3.2). These have been summarised in four architectural elements/facies associations.

3.9.1 ECS: Erosive-based cross-bedded sandy bedform element

Sandy bedform elements are characterised by erosively-based units that locally cut down to the fine-grained deposits of facies Fm and fine-grained floodplain sediments of facies Fl. Occasional lower and upper contacts with the massive sandstone facies (Sm) are also found. The element is represented by cross-bedded sandstones in amalgamated vertically stacked units of 5-10 m thickness. They are usually present at different stratigraphic levels in the measured sections of the Saiyiduwali section (Khisor Range), Zaluch Nala section (western Salt Range), and Khewra-Choa section (eastern Salt Range, fig. 3.21) and are separated by units of mudstone and sandstone. The elements at these sections are lenticular to wedge-shaped in geometry and are laterally traced only for few metres. Thus, the precise lateral relationship of the elements is hard to interpret. The erosively-based cross-bedded sandstone elements represent deposition in a multi-storey fluvial system (Fig. 3.9c).

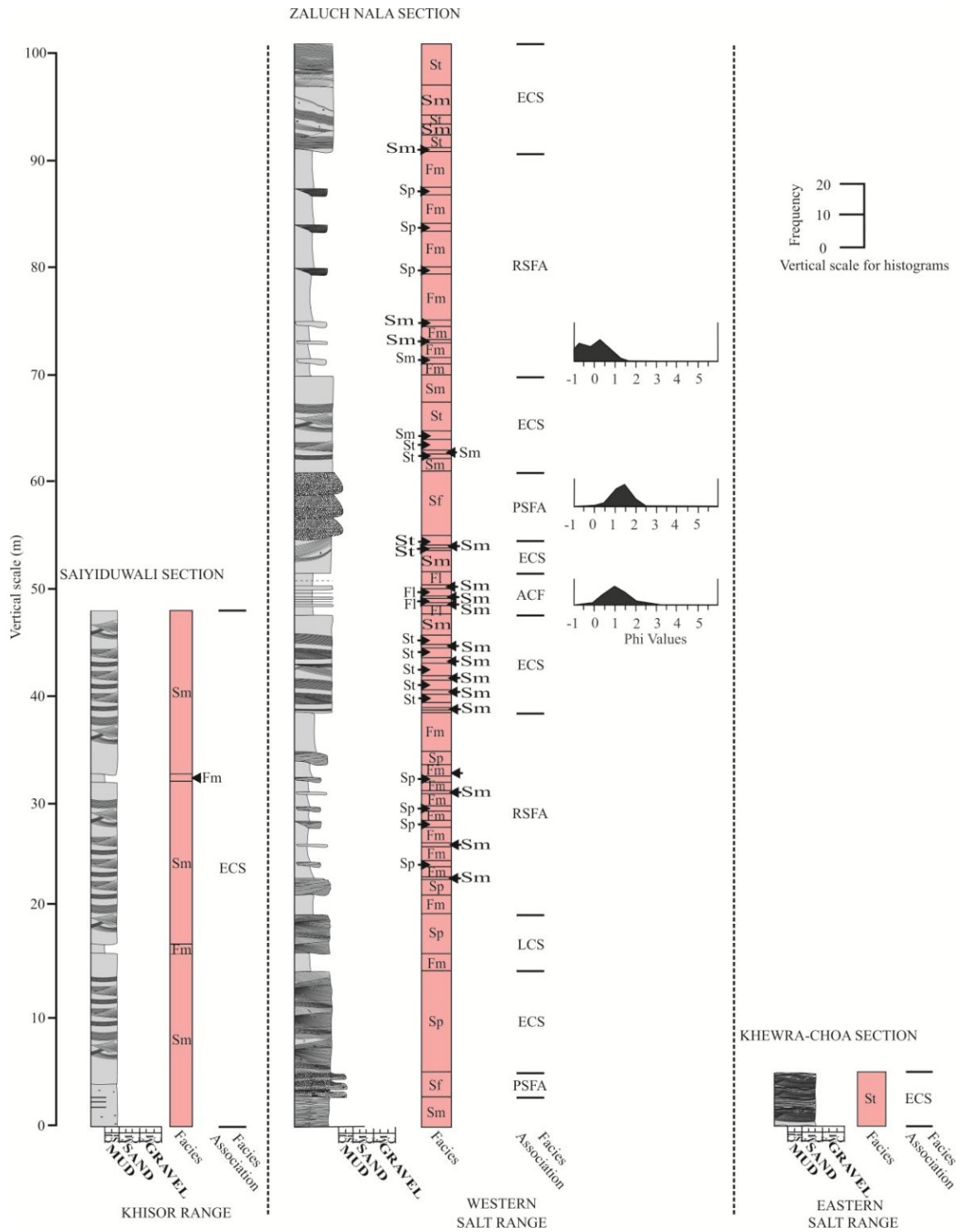


Fig. 3.21 The facies and facies association variation in the Warchha Formation from the Saiyiduwali section (Khisor Range), through the Zaluch Nala section (western Salt Range) and into the Khewra-Choa section (eastern Salt Range). Refer to Fig. 3.1 for locations of these units and Fig. 3.2 for key.



Fig. 3.22 Characteristic examples of facies associations in the Warchha Formation.

3.9.2 LCS: Lenticular cross-bedded sandstone bodies with erosional bases

These elements are represented by lenticular bodies with sharp erosional bases. The sedimentary structures include cross-bedding and low angle cross-stratification. The elements are normally associated with mudstones and are usually present in the lower part of the measured stratigraphic level in the Warchha Formation, at the Zaluch Nala section (western Salt Range, fig. 3.21). The elements are represented as isolated channel deposits on a flood plain (Figs. 3.9a & b).

3.9.3 RSFA: Red mudstone interbedded with thin sandstone and calcretes

The elements are represented by a red mudstone succession that is commonly associated with thin sandstone and calcretes.

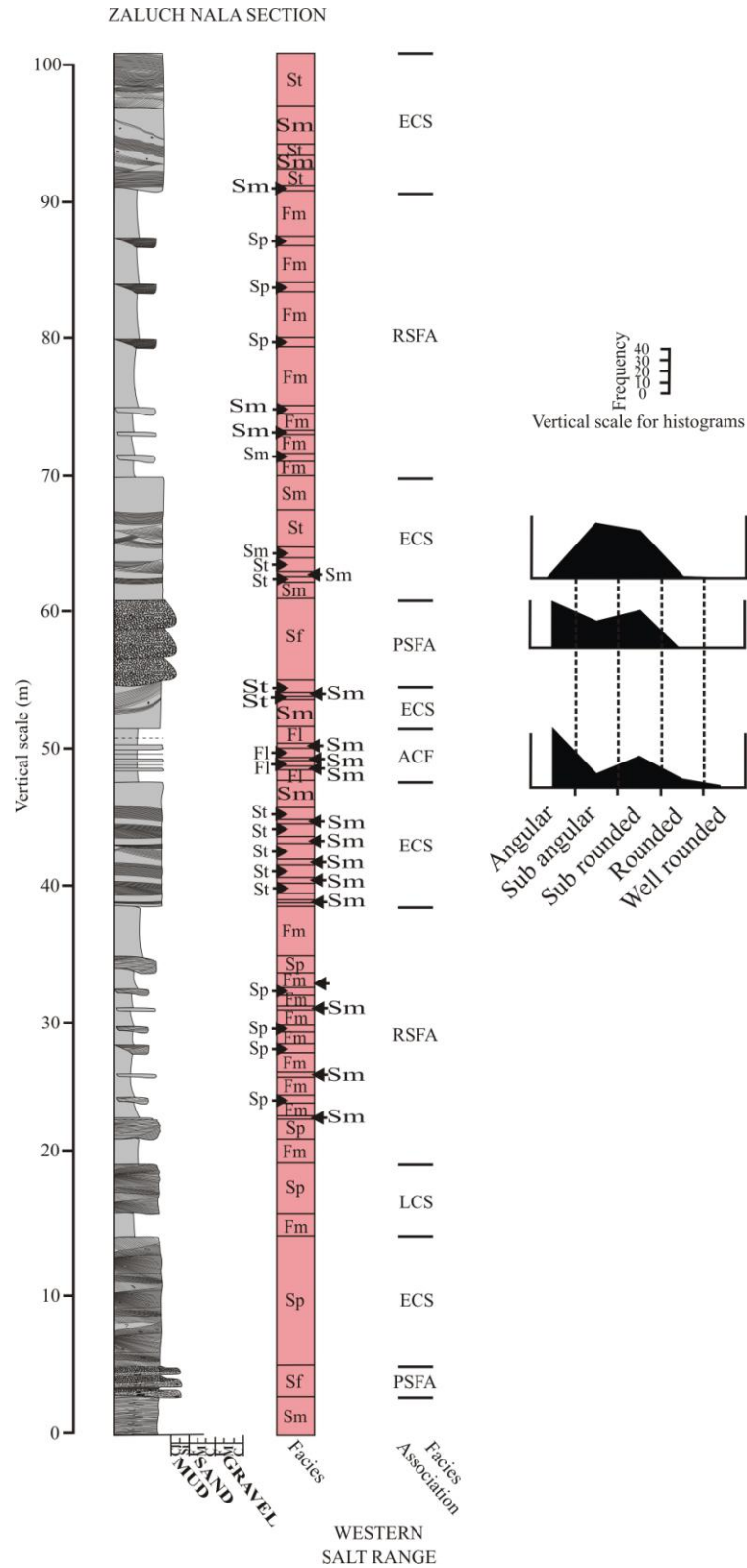


Fig. 3.23 Variation in the grain roundness (histograms) of the Warchha Formation at the western Salt Range, Zaluch Nala section. Refer to Fig. 3.1 for location of this unit and Fig. 3.2 for key.

The elements occur at various stratigraphic levels in the Warchha Formation at the Zaluch Nala section (western Salt Range) and the Saiyiduwali section (Khisor Range). The elements represent deposition as overbank deposits on a flood plain (Figs. 3.22a & b).

3.9.4 PSFA: Pebbly sandstone

The pebbly sandstone elements make up the lowest percentage in the measured succession and are mostly present in the Warchha Formation, Zaluch Nala section (western Salt Range). The pebbly sandstone element contains conglomerate showing fining-upwards trends. The element represents deposition in a fluvial setting (Fig. 3.22c).

3.9.5 ACF: Abandoned channel fill deposits

This facies association is represented by 4-5 m-thick units of interbedded, and parallel-laminated red clay-rich mudstones and silty mudstone units. These units are represented by sheet-like bodies that are traceable for a few metres. The erosional lower contact of the association represents infill in the abandoned channels of a flood plain, during the waning stage of a flood.

3.10 Grain size analyses and provenance of the Warchha Formation

Three samples (Table 3.1) have been studied from the Warchha Formation at the Zaluch Nala section (western Salt Range, figs. 3.1 & 3.3). The frequency histograms (Fig. 3.23) of the sedimentology samples (Appendix 2), show that the sediments range from fine- to coarse-grained sand. The average mean composition of these deposits corresponds to the coarse-grained sand category. These sediments are very well sorted to well sorted. The skewness ranges from the near symmetrical (i.e. at the stratigraphically lowest sample) to coarse- to fine-skewed upwards.

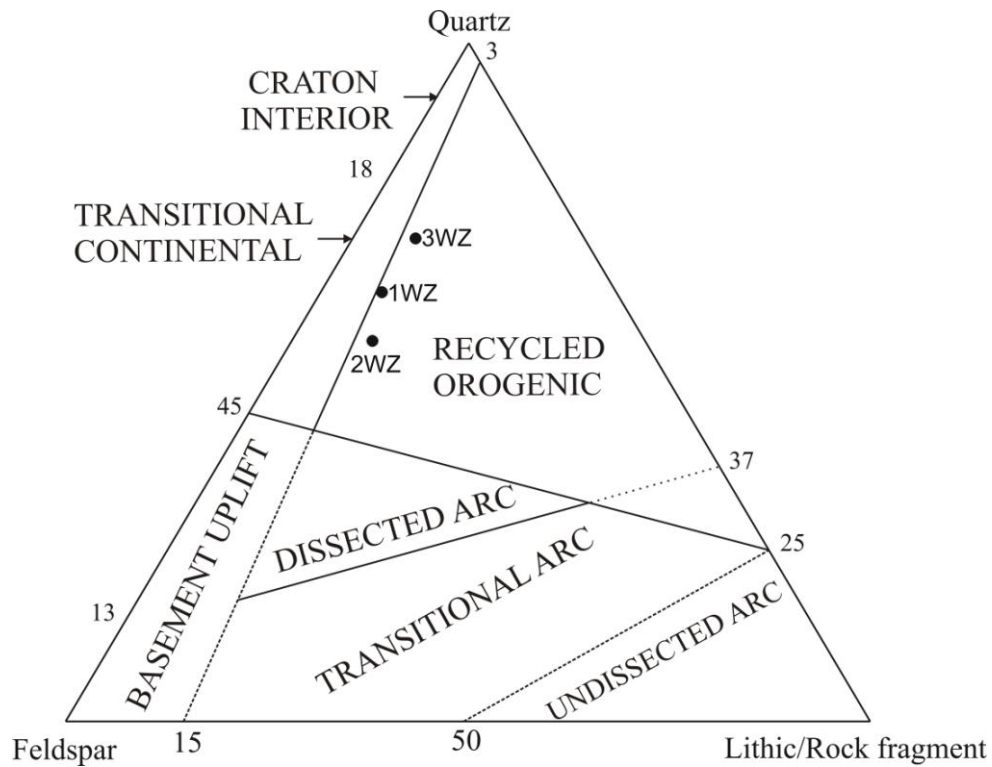


Fig. 3.24 The QFL diagram for the Warchha Formation samples and interpretation of provenance. See Fig. 3.2 for key to samples.

Overall the constituent sediments show distribution of the grains in the angular and sub-rounded categories, very rarely rounded to well-rounded grains were observed (Fig. 3.23). The QFL plot of the Warchha Formation samples show that the material was likely derived from recycled orogenic belts (Dickinson 1985, fig. 3.24). Mineralogically quartz dominates the constituent grains, followed by feldspar and lithics (Fig. 3.25). The accessory minerals include mica and opaque minerals. Quartz is shown by monocrystalline and polycrystalline varieties (Fig. 3.25a & b). The former is likely derived from weathering of granites (Pettijohn *et al.* 1987; Ghazi & Mountney 2011), whereas the latter type shows derivation from the metamorphic source rocks (Blatt 1967; Ghazi & Mountney 2011). Feldspar is represented by plagioclase, orthoclase, microcline and perthite. Perthite is very low in concentration (Fig. 3.25c & d).

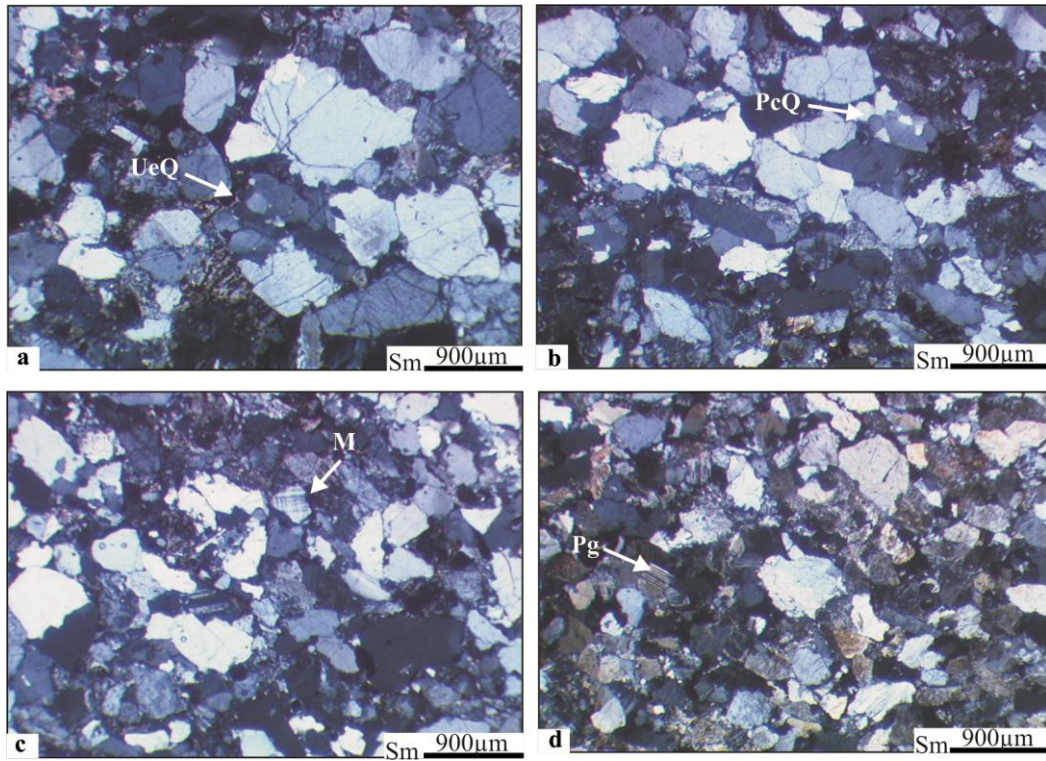


Fig. 3.25 Photomicrographs of some of the lithofacies of the Warchha Formation. For facies codes and mineral symbols refer to Fig. 3.2.

The K-feldspar represents derivation from plutonic and metamorphic sources (Ghazi & Mountney 2011). The lithics are represented by igneous, metamorphic and sedimentary types. Mica is shown by muscovite. Ghazi & Mountney (2011) recently conducted a provenance study of the Warchha Formation and concluded the source areas were situated in the south to the southeast of the then Salt Range. These areas include the Aravalli System and Malani Range in India respectively, with some more local source areas (Ghazi & Mountney 2011).

ECS, LCS, RSFA, PSFA & ACF facies association

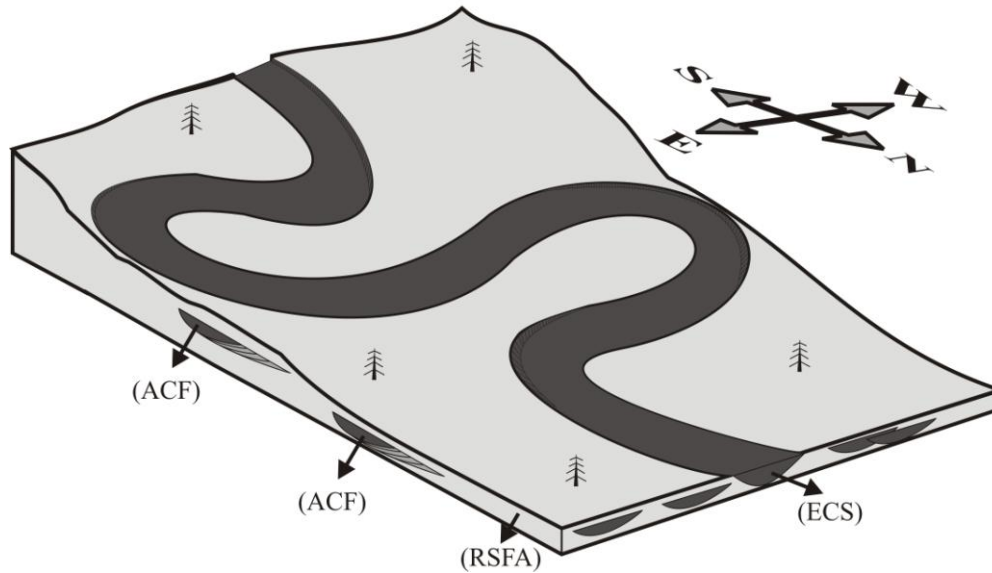


Fig. 3.26 Idealised depositional model for the Warchha Formation sedimentation. The palaeocurrent directions of the river system are after Ghazi & Mountney (2009). See Fig. 3.2 for facies associations.

3.11 Warchha Formation depositional environment

The facies association in the Warchha Formation suggest deposition in an alluvial setting (Fig. 3.26); however due the nature of the exposures of the Warchha Formation in the sections studied, it is difficult to establish the lateral extent of these deposits and therefore to establish whether the system was meandering or braided. In the Warchha Formation further east of the eastern Salt Range (Fig. 3.1), lateral accretion surfaces have been identified, which prompted interpretation of at least some of the system as meandering (Ghazi & Mountney 2009). The sedimentology of the Warchha Formation in this study closely corresponds to that outlined by Ghazi & Mountney (2009) although no lateral accretion surfaces were identified.

3.12 Sardhai Formation facies association

During the present investigation, a 59.5 m-thick succession of the Sardhai Formation was studied (Fig. 3.27). Three lithofacies types have been recognised (Fig. 3.27, Table 3.2). These lithofacies have been summarised into one facies association.

3.12.1 DLSFA: Deep lacustrine to shallow marine facies association

The facies association is represented by the interlamination of the massive mudstone facies (Fm), and occasional massive sandstone facies (Sm) rarely with a thin-bedded sandy limestone facies (Lsf). The facies association dominantly shows rapid deposition from suspension in the form of facies Fm, with some subsequent mass flow sedimentation (facies Sm). The thin-bedded sandy limestone facies (Lsf), that is rarely found in the Sardhai Formation suggests periodic inundation by a shallow marine environment at the site of deposition.

3.13 Sardhai Formation depositional environment

In contrast to the massive mudstone facies in the Warchha Formation, variation in the massive mudstone facies in the Sardhai Formation has been observed. The colouration, shows anoxic conditions suitable for the preservation of organic matter and may thus represent water-logged conditions (Collinson 1996). The most suitable environment depicted for the preservation of the facies Fm in the Sardhai Formation is in an extensive lacustrine to shallow marine setting and under humid conditions via deposition from suspension (Collinson 1996). The rarely present interlaminated sandy limestone in the DLSFA facies association shows the proximity of the depositional site to the sea (Fig. 3.28).

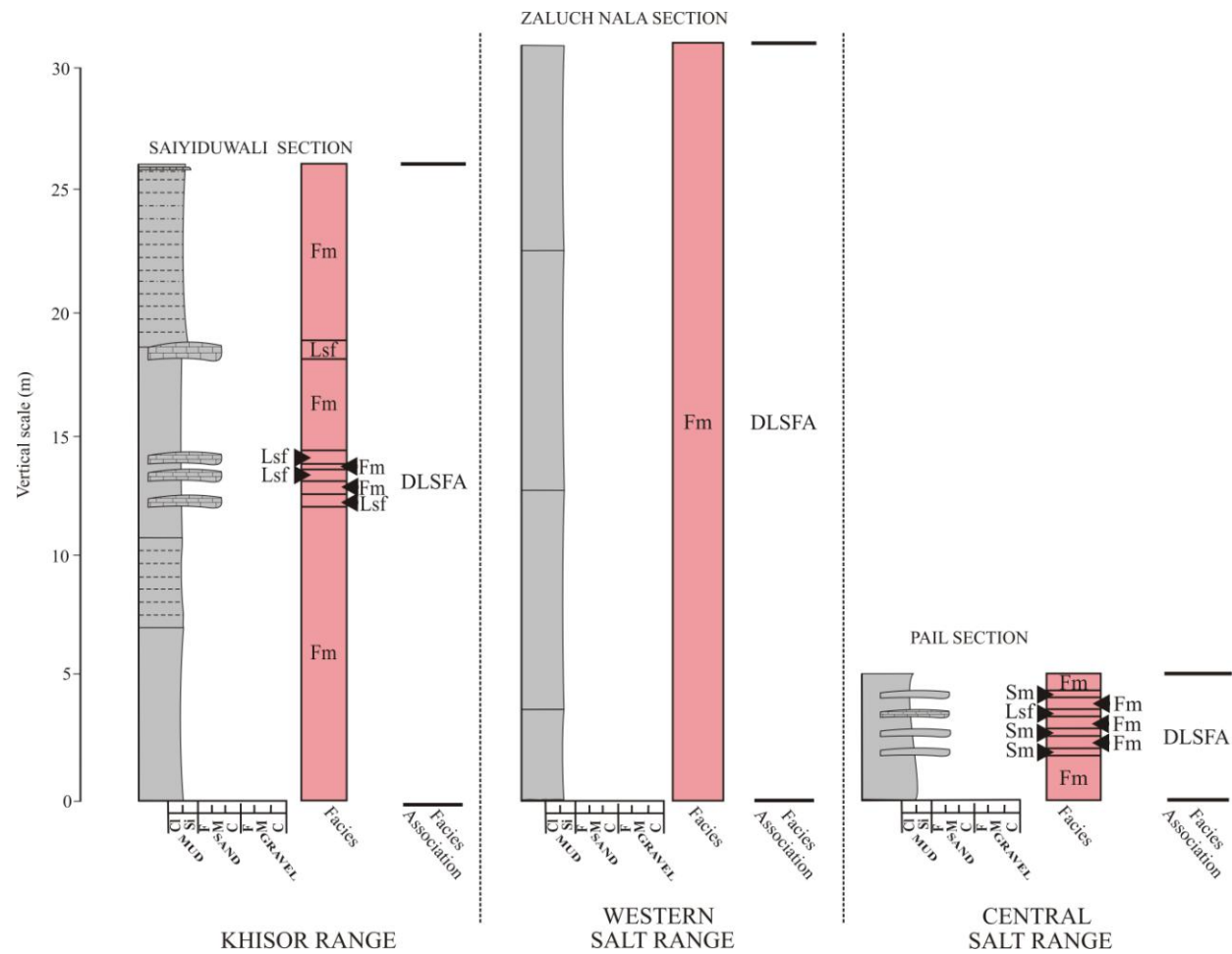


Fig. 3.27 The facies and facies association variation in the Sardhai Formation from the Khisor Range, through the western Salt Range and into the central Salt Range. Refer to Fig. 3.1 for locations of these units and Fig. 3.2 for key.

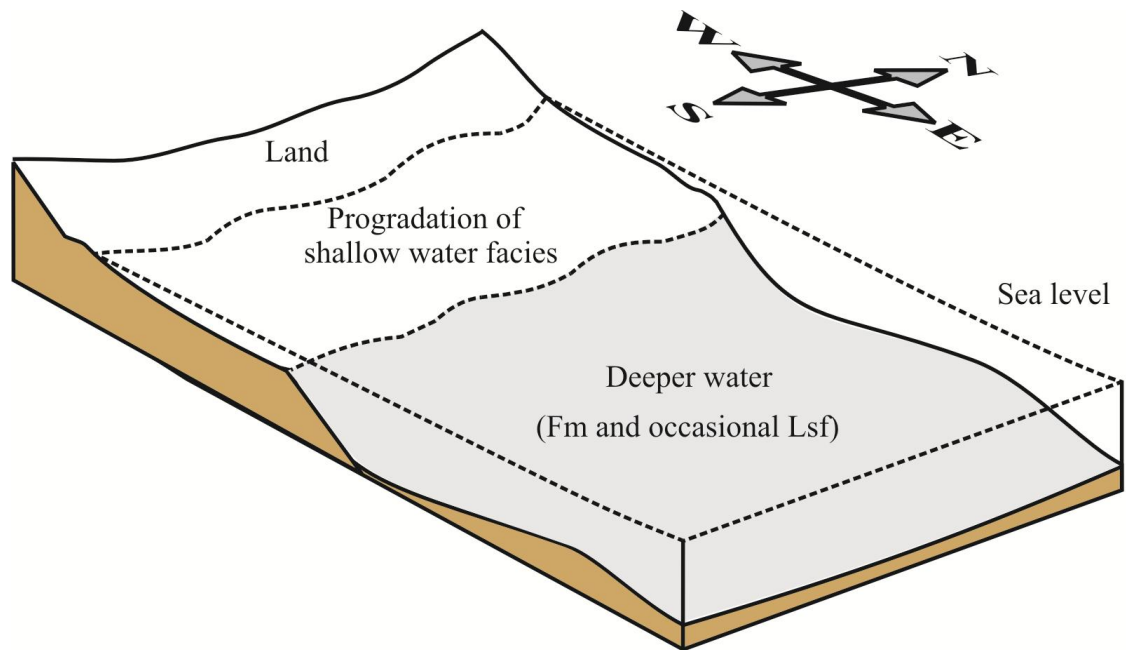


Fig. 3.28 Idealised depositional model for sedimentation of the Sardhai Formation. See Fig. 3.2 for facies codes.

3.14 Sedimentological synthesis

During the Carboniferous-Permian, the Salt Range occupied a palaeogeographic position east of the main mass of Gondwanaland at the Tethys margin (Jan *et al.* 2009; Ghazi & Mountney 2011). The long period of non-deposition in the Salt Range, since the early Palaeozoic, came to an end with the Carboniferous-Permian Gondwanan deposition of the Tobra Formation that overlies the Cambrian Baghanwala Formation (Fig. 3.3). These deposits are biostratigraphically correlated with the far-off Gondwana continent, particularly India and Arabia (Jan & Stephenson 2011). The deposits of the Tobra Formation in the study area, in contrast to most of the coeval successions on Gondwana lack direct glacial signatures, e.g. glacial grooves and striations. However, the presence of faceted clasts and correlation with the Al Khlata Formation of Oman and Saudi Arabia suggest that they may be better regarded as proglacial.

Comparison with the correlative deposits in India (see chapter 5, section 5.4.4) indicates that the Tobra Formation has lithological similarity with the upper part of the Talchir Formation, which was deposited during the deglaciation event via remobilisation of the earlier glacial deposits of peninsular India, giving rise to alluvial fan deposits (Dasgupta 2006). The brecciated conglomerate representing the upper part of the Talchir Formation bears true glacial signatures, e.g. particularly clasts with striations at the base (Veevers & Tewari 1995; Dasgupta 2006). These features have not been demonstrated by the Tobra Formation during the present work. This work assumes that Tobra Formation represents a depositional setting similar to the upper part of the Talchir Formation and formed as a result of reworking of sediments of earlier glacial deposits. The materials in the Tobra Formation are attributed to have been transported from India (Ghauri *et al.* 1977; Ghazi & Mountney 2011). However, in the Tobra Formation, these earlier sedimentary deposits were either not deposited, or were eroded and resedimented as locally present faceted clasts (i.e. facies Gmc).

Comparison with the palaeogeographically nearby and biostratigraphically related deposits of the Al Khilata Formation of Oman and Saudi Arabia (e.g. see Jan & Stephenson 2011) also shows lithological similarities with the Tobra Formation. The glacio-fluvial deposits of the Al Khilata Formation which comprise conglomerate-dominated facies and sandstone-dominated facies (Osterloff *et al.* 2004) are represented by the Tobra Formation facies associations DFFA and SFFA. The glacio-lacustrine deposits of the Al Khilata Formation, comprising glacio-lacustrine mudstones (Osterloff *et al.* 2004) show similarity with the facies association OFA. In the absence of evidences for a glaciogenic origin of the Tobra Formation, the presence of faceted clasts, which in part show the glacial influence and a systematic sorting of sediments of

from the western Salt Range to the eastern Salt Range proposes a glacio-fluvial nature of the Tobra Formation.

The demise of the Gondwana-wide Carboniferous-Permian glaciers as climate ameliorated (Ghazi & Mountney 2011) and Gondwana drifted northward (Stephenson *et al.* 2007; Jan *et al.* 2009), resulted in subsequent sea level rise and transgression (Angiolini *et al.* 2003a). This transgression resulted in the development of the overlying Dandot Formation in an intertidal to shallow marine setting. This transition in the depositional environment has been observed in most, if not all of the Gondwanan basins (e.g. Australia, India, Africa and Arabia). In India for example, a similar transition at the top of the Talchir Formation is observed, whereby the basin evolution is controlled by deglaciation as a result of climatic warming (Maejima *et al.* 2004). The Talchir Formation deposits are thus represented by mudstone with intercalations of sandstone and siltstone. The mudstone shows discrete beds of ripple cross- or climbing-ripple cross-laminated siltstone. The presence of a marine incursion at the top of the Talchir Formation in India is attributed to an increase in the eustatic sea level rise associated with the Carboniferous-Permian deglaciation (Maejima *et al.* 2004). A similar marine transgression has been observed in the Carboniferous-Permian deposits of Australia with the development of marine fauna (Foster & Waterhouse 1988). The presence in the Dandot Formation of marine fauna, e.g. *Fenestella fossula*, *Dielasma dadanense*, *Pterinea cf. lata*, *Nucula pidhensis* sp. nov. *Cardiomorpha?* *Pusilla*, *Maeonia cf. gracilis*, *Astartila cf. ovalis* and *Eurydesma cordatum*, reported by Reed (1936) has been correlated with the “Lower Marine Series” of New South Wales, Australia (Kummel & Teichert 1970). This fauna has been attributed by Reed (1936) to the development of contemporaneous marine conditions in Australia and Salt Range, Pakistan. However, the event has not necessarily affected all of the Gondwana basins

equally and the marine incursion is only rarely present in some of the basins (e.g. Australia; Stephenson *et al.* 2007).

By Early Permian times the Gondwanian-wide fluvial system had also established itself in this region. In the Salt Range, the uplift of the basement rocks resulted in sub-aerial exposure and contributed to the development of a semi-arid palaeoclimate in the region. The fluvial system was generated in the highlands located south-southeast of the Salt Range as a result of the seasonally hot climate and heavy rainfall in the south of the Salt Range, i.e. the Aravalli System and Malani Range and discharged into the marine embayment lying to the north of it, depositing the fluvial Warchha Formation (Ghazi & Mountney 2009, 2011).

The northwards drift of the Mega Lhasa Block/Cimmerian blocks (comprising Iran, Afghanistan, Karakorum and Sibumasu, Thailand) in the Middle Permian, i.e. Wordian and the resultant opening of the neo-Tethys (Angiolini *et al.* 2003b; Jan *et al.* 2009; Muttoni *et al.* 2009) resulted in a major transgression along the Gondwana margin. In the Salt Range, the transgression resulted in the development of the shallow-marine Sardhai Formation and the overlying Zaluch Group. The Amb Formation of the Zaluch Group above the Sardhai Formation (Fig. 3.3) is associated palaeontologically and lithologically with the lower part of the Arabian Khuff Formation and is widely considered its temporal and sedimentological equivalent (see Angiolini & Bucher 1999). Both have been formed by essentially the same marine transgression associated with neo-Tethyan sea floor spreading (Angiolini *et al.* 2003b; Mertmann, 2003; Jan *et al.* 2009).

4 Chapter 4: Systematic palynology

4.1 Introduction

This chapter discusses the taxonomical part of the research. Species are assigned to turma divisions, which is an artificial suprageneric grouping of the morphology of fossil spores and pollen (Punt *et al.* 2007).

Description

Descriptions are those of the present author. The present author concentrated more on the descriptions of the taxa that have stratigraphic significance and are best preserved.

Best reference specimens

The best reference specimens for photography are given in the present study.

Dimensions

The dimensional attributes of the palynomorphs used are modified from Modie (2007) and are shown in Figs. 4.1 to 4.5.

Selected previous records

Refer to the most recent selected previous records of taxa in the Gondwanan continents and are not exhaustive.

4.2 Pollen/Spore classification

The spores and pollen are classified based on the suprageneric Anteturma PROXIGERMINANTES Potonié (1970), and Anteturma VARIEGERMINANTES Potonié (1970). This is followed by subdivisions; turma, supraturma, subturma and infraturma.

During this study, the scheme of Neves & Owens (1966, fig. 4.6) for spore classification has been employed. For pollen various other classifications have been used.

4.3 Descriptive terminologies

The descriptive terminologies used in this chapter are those of Kremp (1965), Foster (1979), MacRae (1978), Playford & Dettmann (1996), Millstead (1999) and Punt *et al.* (1994, 2007).

The following are some explanations to the terms used in this work,

4.4 Pollen

Saccus onlap

Stephenson (1998b) described saccus onlap as the distance, measured along the latitudinal meridian, between the distal (or proximal) root of the saccus and the outer margin of the corpus.

Cappa

The thick-walled proximal side of the corpus of a saccate pollen grain.

Cappula

The thin-walled distal side of the corpus of a saccate pollen grain between the distal roots of the sacchi.

Sulcus

An elongated latitudinal ectoaperture situated at the distal or proximal pole of a pollen grain.

Exoexine (synonym of sexine)

The outer layer of the exine of the spore, which lies above the intexine.

Intexine

The inner, non-sculptured part of the exine of the spore, which lies below the exoexine.

Diploxytonoid

Pollen in which the sacchi outlining the bisaccate pollen is discontinuous with the corpus outline (Fig. 4.7a).

Haploxytonoid

Pollen in which the sacchi outline of bisaccate pollen is continuous with the corpus outline (Fig. 4.7b).

4.5 Spores

Amb

The shape of the spore equatorial outline.

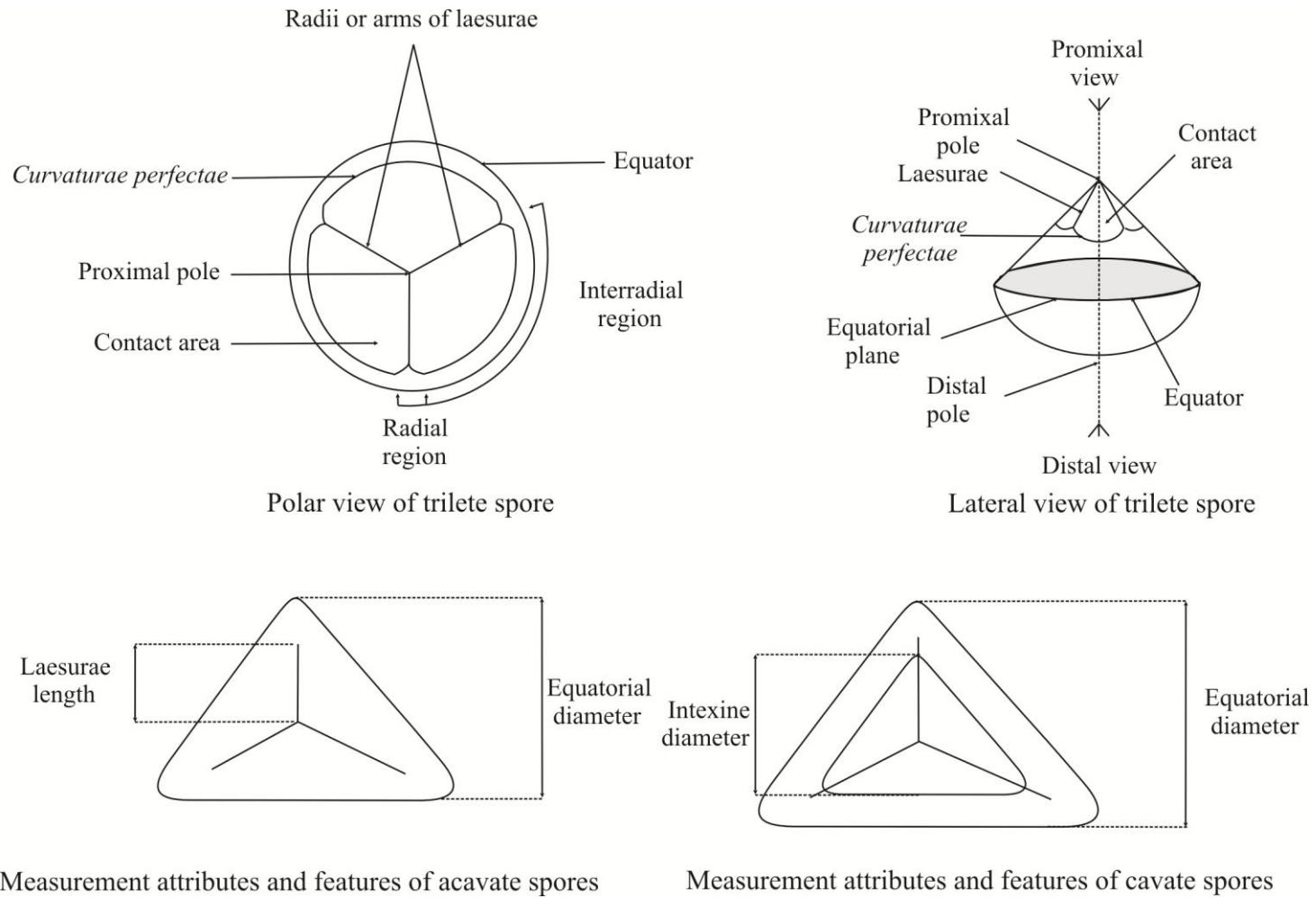
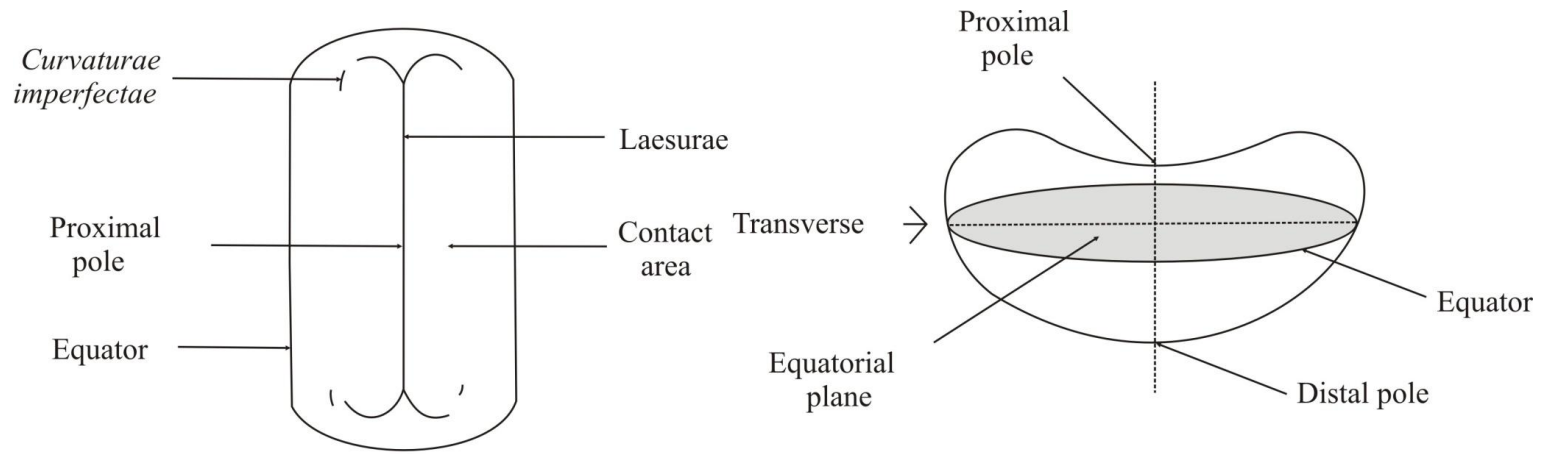


Fig. 4.1 Orientation and dimensional attributes of trilete spore (From Modie 2007).



Polar view of monolete spore

Equatorial longitudinal view of monolete spore

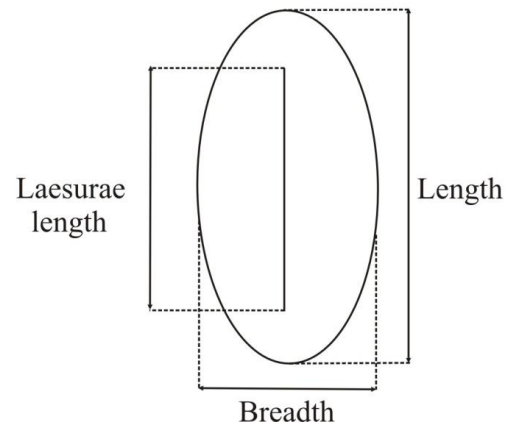
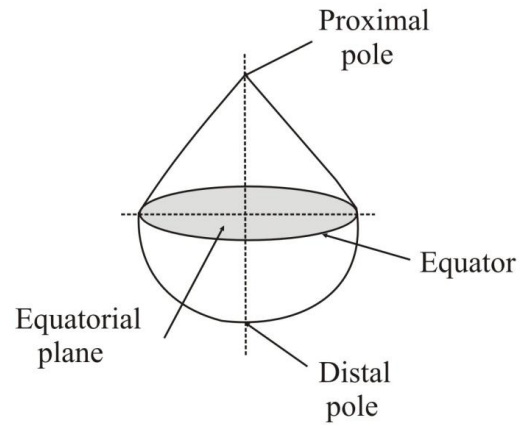


Fig. 4.2 Orientation and dimensional attributes of monolete spore (From Modie 2007).

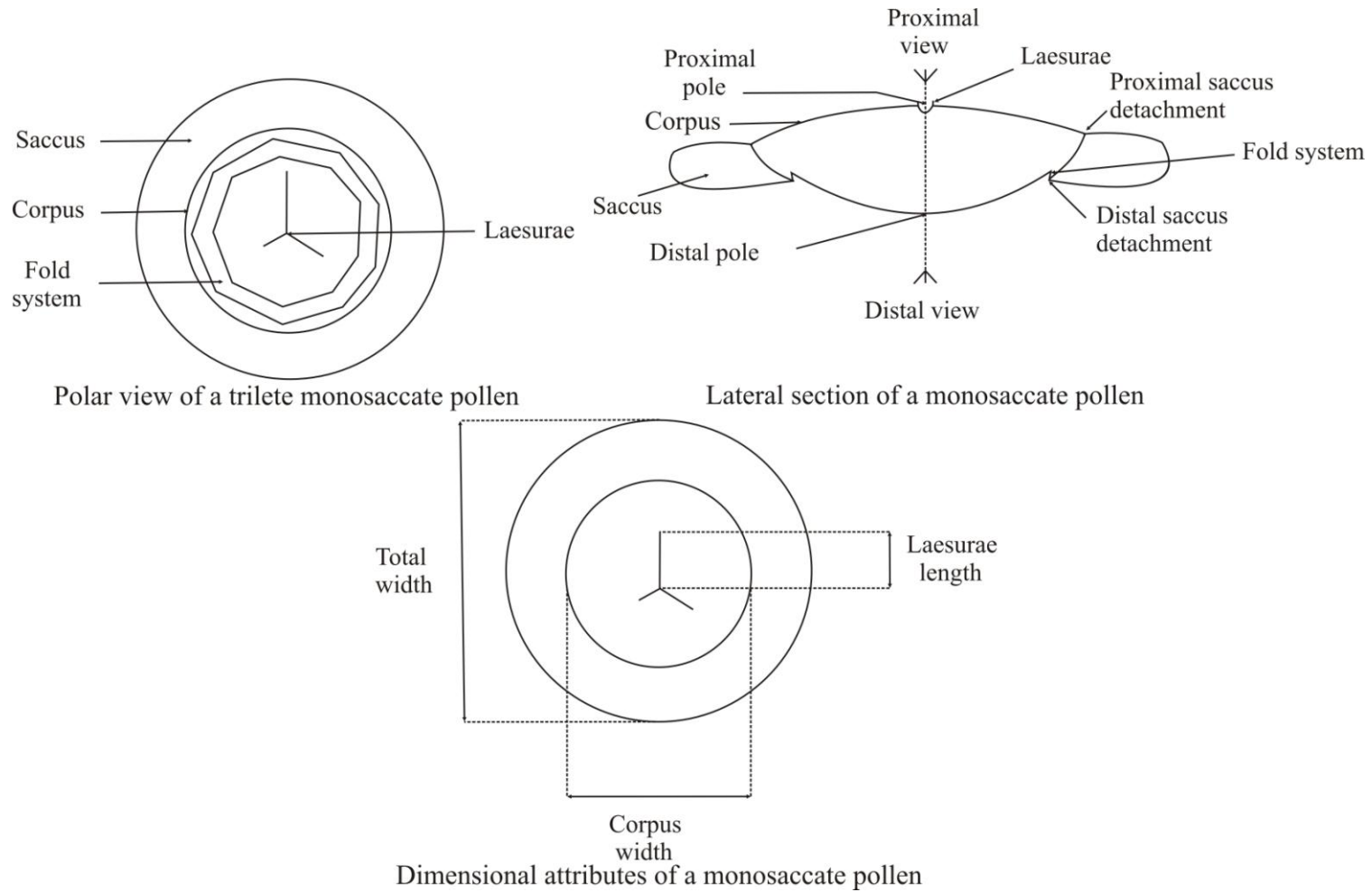


Fig. 4.3 Orientation and dimensional attributes of monosaccate pollen (From Modie 2007).

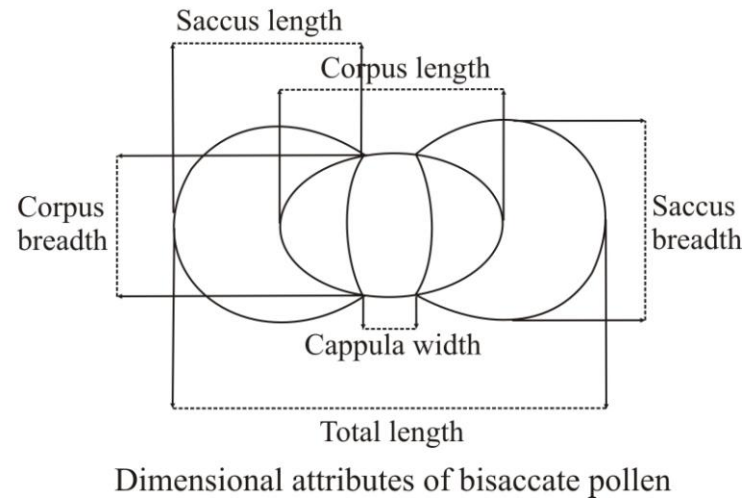
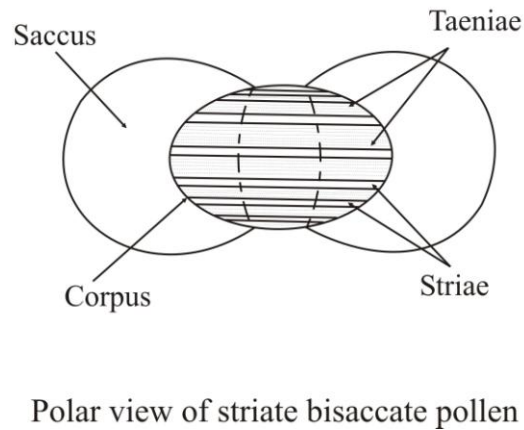
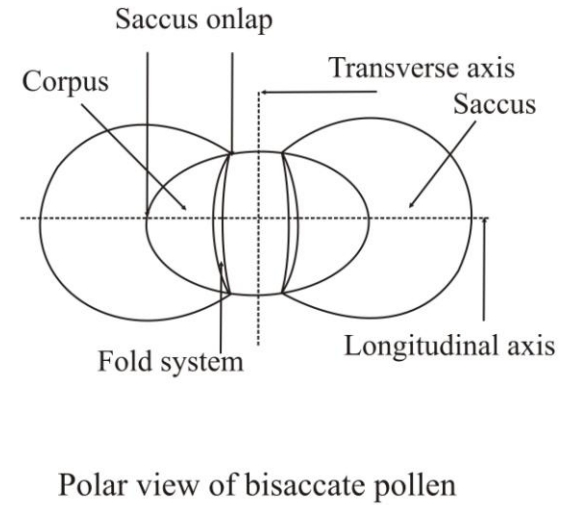
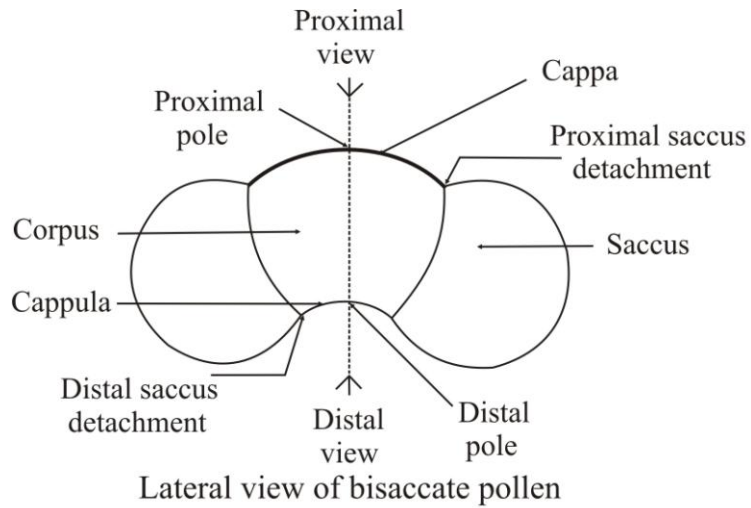


Fig. 4.4 Orientation and dimensional attributes of bisaccate pollen (From Modie 2007).

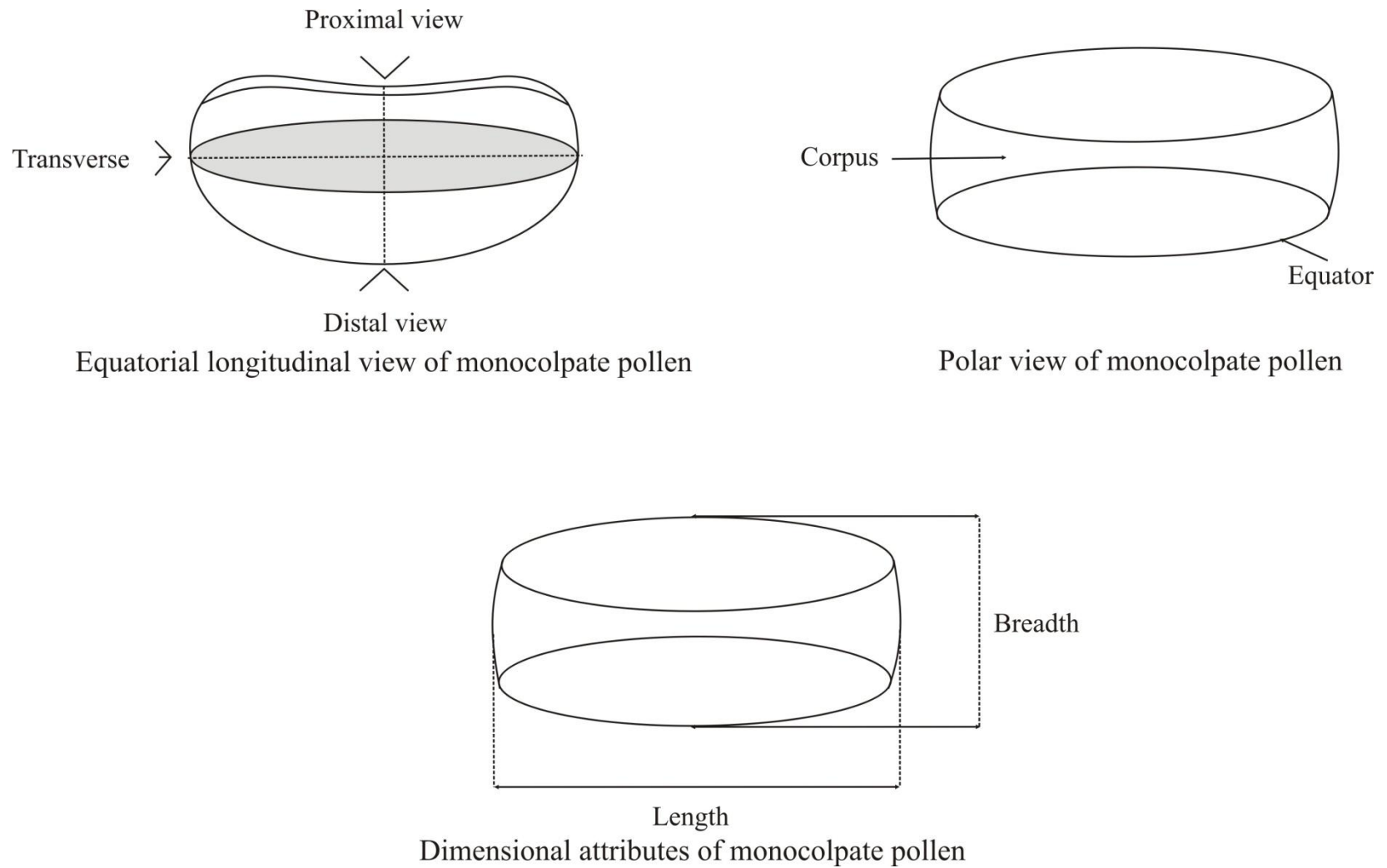


Fig. 4.5 Orientation and dimensional attributes of monocolpate pollen (From Modie 2007).

Diagnostic features	Category										Rank	
	Sporites										Anteturma	
Apertura	Triletes								Monol-etes	Hilates	Turma	
Stratification	Acameratitriletes		Cameratitriletes					Perino-triletes			Suprasub-turma	
Equatorial features	Azonotriletes	Zonotriletes	Solutitriletes	Membranatitriletes								Sub-turma
Membrane attachment												
Sculpture	Laevigati, Apiculati Murornati etc.	Tricassiti, Cingulati, Zonati etc.	Planati	Decorati	Continuati	Cingulicamerati	Membranati	Polycamerati				
Equatorial thickening &/or extension												

Fig. 4.6 Spore classification scheme (From Neves & Owens 1966).

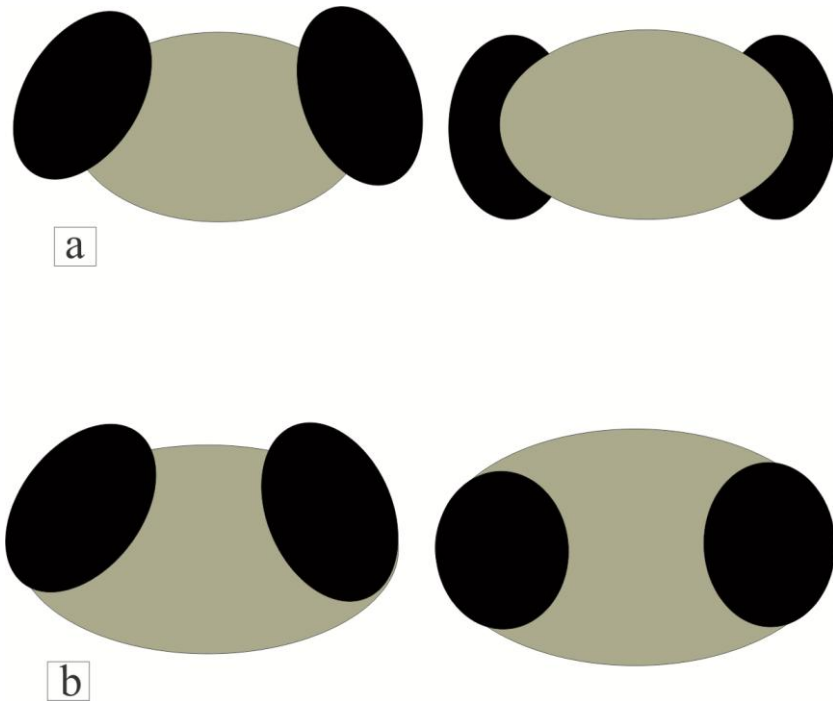


Fig. 4.7 a. Shows a diploxytonoid outline for bisaccate pollen, b. Shows a haploxytonoid outline for bisaccate pollen (From Punt *et al.* 2007).

4.6 Systematic description

Anteturma PROXIGERMINATES Potonié 1970

Turma TRILETES Reinsch *emend.* Dettmann 1963

Suprasubturma ACAVATITRILETE Dettmann 1963

Subturma AZONOTRILETES Luber *emend.* Dettmann 1963

Infraturma LAEVIGATI Bennie & Kidston *emend.* Potonié 1970

***Punctatisporites ubischii* Foster 1979**

Plate 1, Fig. 1

Description

Spores, radial, trilete; amb circular to sub circular. Laesurae distinct, straight, extend 50% to 75% of the spore radius; third ray comparatively shorter. Exine thick; infrareticulate.

Best reference specimens

W23/3, MPA58394/1; G23/1, MPA58394/1; Y33/5, MPA58395/2

Dimension

Equatorial diameter; 56(57)58 μm ; 3 specimens

Selected previous records

Australia, Permian (Foster 1979); Antarctica, Permian (Lindström 1995); Pakistan, Carboniferous-Permian (Jan & Stephenson 2011).

Infraturma APICULATI Bennie & Kidston *emend.* Potonié 1956

***Brevitriletes leptocaina* Jones & Truswell 1992**

Plate 1, Fig. 2

Description

Spores, radial, trilete; amb mostly rounded with sparsely projecting spinae and pila. Laesurae distinct, straight, often gaping; extend 90%-100% of the spore radius; with labra. Laesurae may connect with the curvatural ridges at the outer margin of the spore. Exine 1-2 μm thick; proximal face laevigate, low in the contact area. Distal face sparsely and evenly sculptured with pila and slender spinae, 3-6.5 μm high, evenly spaced (5 μm apart). 20 to 25 elements may project from the spore margin.

Best reference specimens

T33, MPA57511/2; X13/1, MPA57511/1; X13, MPA57512/1; M27/2, MPA57512/1; O18, MPA57517/1

Dimensions

Equatorial diameter (excluding ornament); 22(36)44 μm ; 5 specimens

Remarks

The ornament in the present specimens is sparser (i.e. 5 μm apart) and longer (1 to 2 μm) than those previously described (e.g. Jones & Truswell 1992; Stephenson 2004). Stephenson (2004) considered that some specimens assigned to *Apiculatisporites cornutus* by MacRae (1988) and to *Brevitriletes levis* by Backhouse (1991), are better assigned to *Brevitriletes leptocaina*.

Selected previous records

Australia, Carboniferous-Permian (Backhouse 1991; Jones & Truswell 1992), Oman and Saudi Arabia, Carboniferous-Permian (Stephenson & Filatoff 2000a; Stephenson &

Osterloff 2002; Stephenson *et al.* 2003; Stephenson 2004 & references therein), Pakistan, Carboniferous-Permian (Jan & Stephenson 2011).

***Brevitriletes parmatus* (Balme & Hennelly) Backhouse 1991**

Plate 1, Fig. 3

Basionym *Verrucosisporites parmatus* Balme & Hennelly 1956b

Description

Spores, radial, trilete; amb subcircular to circular. Laesurae distinct, straight or curved; without labra; commissures gape in many specimens. Laesurae extend more or less to the equator. Exine <1µm thick; proximal face laevigate or finely punctate. Distal face ornamented with scattered verrucae, 2-4 µm apart and 1 µm high. Verrucae concentrated at and around distal pole; smaller and more scarce towards spore margin (i.e. only occasionally projecting at the equator).

Best reference specimens

Q11/2, MPA57512/1; U9, MPA57512/2; U15, MPA57520/1; T9/2, MPA57520/1; K29/4, MPA57560/1; S23/3, MPA57511/1; H31/2, MPA57514/1

Dimensions

Equatorial diameter (excluding ornament); 20(26)28 µm; 7 specimens

Selected previous records

Australia, Early Permian (Backhouse 1991), Oman and Saudi Arabia, Carboniferous-Permian (Stephenson & Filatoff 2000a; Stephenson & Osterloff 2002; Stephenson *et al.* 2003; Stephenson 2004 & references therein), Yemen, Carboniferous-Permian (Stephenson & Al-Mashaikie 2010, 2011), Pakistan, Carboniferous-Permian (Jan *et al.* 2009; Jan & Stephenson 2011).

***Brevitriletes cornutus* (Balme & Hennelly) Backhouse 1991**

Plate 1, Fig. 4

Basionym *Apiculatisporites cornutus* Balme & Hennelly 1956b

Description

Spores, radial, trilete; amb circular. Laesurae distinct, with narrow labra (0.5 µm thick) that are sinuous; extend to the spore margin. Exine thin 0.5 µm; proximal face granulate. Distal face sparsely but regularly ornamented with both horn-shaped spinae and flat-headed bacula (the latter being less represented in numbers); elements 2µm wide at the base, 2-3 µm apart and 2-4 µm long.

Best reference specimens

T11, MPA57512/2; C27, MPA57514/1; N10, MPA58394/1

Dimensions

Equatorial diameter; 21(24)26 µm; 3 specimens

Remarks

The distinction between the spina and baculum is much pronounced at the equator of the spore. The sparsely distributed ornaments make the contact area visible. Some ornamentation elements merge to give volcano-like profile.

Backhouse (1991) described occasional bifurcation of sculpture elements on the distal face and around the equator. The present specimens however do not show any such bifurcation of ornaments.

Selected previous records

Africa, Permian (Anderson 1977), Australia, Permian (Foster 1979; Backhouse 1991), Oman, Early Permian (Besems & Schuurman 1987), Oman and Saudi Arabia, Carboniferous-Permian (Stephenson & Filatoff 2000a; Stephenson & Osterloff 2002; Stephenson *et al.* 2003; Stephenson 2004 & references therein; Stephenson *et al.* 2008),

Argentina, Carboniferous-Permian (Césari *et al.* 1995; Vergel 1986, 1987), Argentina, Late Carboniferous (Césari & Gutiérrez 2000), West Papua, Permian (Playford & Rigby 2008), Yemen, Carboniferous-Permian (Stephenson & Al-Mashaikie 2010), Pakistan, Carboniferous-Permian (Jan *et al.* 2009; Jan & Stephenson 2011).

***Horriditriletes tereteangulatus* (Balme & Hennelly) Backhouse 1991**

Plate 1, Fig. 5

Basionym *Acanthotriletes tereteangulatus* Balme & Hennelly 1956b

Description

Spores, radial, trilete; amb rounded triangular, with mostly concave sides. Some rare specimens also have convex sides. Spinae project from the spore margin. Laesurae distinct, straight to slightly sinuous, commissures often gaping; extend 80-85% of the spore radius. Exine thin (<1 µm), spinae 1-3 µm high, <1 µm basal diameter with or without some subordinate coni.

Best reference specimens

U5, MPA57511/1; X28/2, MPA57514/1, Y25, MPA57514/1

Dimension

Equatorial diameter; 26(28)35 µm; 3 specimens

Remarks

The distinction of *Horriditriletes tereteangulatus* and other morphologically closely related taxa, e.g. *Horriditriletes ramosus* and *Horriditriletes uruguiensis*, with secondary spinae, is difficult. This is partly because these end members are very closely related to each other and might require and detailed high magnification studies.

Selected previous records

Australia, Permian (Backhouse 1991; Foster 1979), Pakistan, Permian (Balme 1970), Oman ?Late Carboniferous-Permian (Besems & Schuurman 1987), Oman and Saudi Arabia, Early Permian (Stephenson & Filatoff 2000a; Stephenson & Osterloff 2002; Stephenson *et al.* 2003; Stephenson 2004 & references therein; Penney *et al.* 2008), West Papua, Permian (Playford & Rigby 2008), Pakistan, Carboniferous-Permian (Jan *et al.* 2009; Jan & Stephenson 2011).

***Horriditriletes ramosus* (Balme & Hennelly) Bhardwaj & Salujah 1964**

Basionym *Acanthotriletes ramosus* Balme & Hennelly 1956b

Plate 1, Fig. 6

Description

Spores, radial, trilete; amb triangular with mostly convex sides, however slight concavity is also seen in some specimens, with projecting bacula. Laesurae distinct, with labra, gaping; extend 80%-85% of the spore margin. Exine <1 µm, comprehensively ornamented. Ornamentation denser on the distal surface, dominant elements bacula (2-8 µm high, 1-1.5 µm basal diameter).

Best reference specimens

H11, MPA57520/1; X12/1, MPA58384/1; W20/3, MPA57511/2

Dimensions

Equatorial diameter (excluding ornaments); 26(28)35 µm; 3 specimens

Remarks

Most specimens have convex sides. Laesurae have elevated labra. Balme & Hennelly (1956b) described bifurcation of the ornaments at their upper ends and fusion at the bases. No such features are observed in the present specimens.

Selected previous records

Australia, Late Carboniferous-Permian (Backhouse 1991; Jones & Truswell 1992), Oman and Saudi Arabia, Early Permian (Stephenson & Osterloff 2002; Stephenson *et al.* 2003; Stephenson 2004 & references therein; Penney *et al.* 2008), South Africa, Permian (Anderson 1977), Argentina, Late Carboniferous-Early Permian (Césari *et al.* 1995), West Papua, Permian (Playford & Rigby 2008), Yemen, Carboniferous-Permian (Stephenson & Al-Mashaikie 2010), Pakistan, Carboniferous-Permian (Jan & Stephenson 2011).

***Horriditriletes uruguayensis* (Marques-Toigo) Archangelsky & Gamero 1979**

Basionym *Neoraistrickia uruguayensis* (Marques-Toigo) 1974

Plate 1, Fig. 7

Description

Spores, radial, trilete; amb triangular with rounded apices and slightly concave or straight sides. Laesurae indistinct, with no labra. Exine thin, <1 µm; ornament projects from sides. Ornament denser on the distal face and on the spore margin. Distal ornament dense, dominated by bacula (2-3 µm high, and 1 µm broad at the base), with common spinae, coni and irregularly-shaped elements.

Best reference specimens

G24, MPA57511/1; X19/2, MPA57511/2; S17/4, MPA57512/1; Q11, MPA57512/2;
W7, MPA57519/1

Dimensions

Equatorial diameter (excluding ornament) 27(28)34 µm; 5 specimens

Remarks

Horriditriletes uruguiensis has shorter bacula than *Horriditriletes ramosus*, and more dense and heterogeneous ornament.

Selected previous records

Oman and Saudi Arabia, Early Permian (Stephenson & Filatoff 2000a; Stephenson & Osterloff 2002; Stephenson *et al.* 2003; Stephenson 2004 & references therein; Penney *et al.* 2008), Argentina, Carboniferous-Permian (Césari *et al.* 1995; Archangelsky & Gamero 1979), Yemen, Carboniferous-Permian (Stephenson & Al-Mashaikie 2010), Pakistan, Carboniferous-Permian (Jan & Stephenson 2011).

Microbaculispora tentula Tiwari 1965

Plate 1, Fig. 8

Description

Spores, radial, trilete; amb rounded triangular, with broad apices and straight sides. Laesurae distinct, sinuous, often with thin labra; extend to the apices. Exine 1-2 μm thick; proximal face laevigate. Distal face ornamented with regularly spaced grana, accompanied by some irregular puncta. Grana are 0.5-1 μm apart.

Best reference specimens

V14, MPA57511/2; T26, MPA57511/2; X14, MPA57512/1; U15/4, MPA57514/1

Dimensions

Equatorial diameter; 28(30)31 μm ; 4 specimens

Selected previous records

Oman and Saudi Arabia, Carboniferous-Permian (Stephenson & Filatoff 2000a; Stephenson & Osterloff 2002; Stephenson *et al.* 2003; Stephenson 2004 & references therein; Penney *et al.* 2008), West Papua, Permian (Playford & Rigby 2008), Yemen,

Carboniferous-Permian (Stephenson & Al-Mashaikie 2010), Australia, Permian (Segroves 1970; Foster & Waterhouse 1988, Kemp *et al.* 1977; Backhouse 1991 1993; Jones & Truswell 1992), South Africa, Early Permian (Millstead 1999), Botswana, Late Palaeozoic (Modie & Hérissé 2009), India, Permian (Tiwari & Tripathi 1992), Pakistan, Carboniferous-Permian (Jan & Stephenson 2011).

***Converrucosisporites grandegranulatus* (Anderson) Lindström 1995**

Plate 2, Fig. 1

Basionym *Microbaculispora grandegranulata* Anderson 1977

Description

Spores radial, trilete; amb rounded triangular with slightly concave sides. Laesurae distinct, extend to the apices in most of the specimens; straight; with or without labra. Exine 1 µm, thick; proximal face laevigate; distal face ornamented with regularly spaced, rounded verrucae and grana 1-1.5 µm basal diameter, 1-2 µm high, 1 µm apart.

Best reference specimens

F17/1, MPA57518/1; S17/1, MPA57518/1; H19/2, MPA57518/2

Dimension

Equatorial diameter; 33(45)52 µm; 3 specimens

Selected previous records

South Africa, Early Permian (Anderson 1977), Namibia, South Africa, Early Permian (Stephenson 2009), Oman and Saudi Arabia, Early Permian (Stephenson & Osterloff 2002; Stephenson *et al.* 2003; Stephenson 2004), West Papua, Permian (Playford & Rigby 2008), Antarctica, Early Permian (Lindström 1995), Australia, Permian, Asselian-Sakmarian (Foster & Waterhouse 1988), Pakistan, Carboniferous-Permian (Jan & Stephenson 2011).

Infraturma MURORNATI Potonié & Kremp 1954

***Camptotriletes warchianus* Balme 1970**

Plate 2, Fig. 2

Description

Spores, radial, trilete; amb rounded triangular with straight to concave sides. Laesurae distinct, straight to slightly curved, without labra; extend to the spore margin; often gaping. Exine very thick, 2-4 μm , rigid; proximal face sparsely and irregularly granulate or cristate. Distal face with extensive cristae and rarely discrete ornament. Ornaments coarseness variable (most cristae 1-2 μm high, 1-2 μm wide at the base); the ornaments protrude at the margin of the spore giving a serrated amb.

Best reference specimens

S21, MPA57528/2; W18/3, MPA57528/1; O14/4, MPA58401/1

Dimension

Equatorial diameter; 60(74)75 μm ; 3 specimens

Selected previous records

Pakistan, Permian (Balme 1970), Israel, Late Permian (Singh 1964), Iraq, Late Permian (Nader *et al.* 1993), Turkey, Permian (Stolle *et al.* 2011), Oman, Permian (Stephenson 2008b; Stephenson 1998b, PhD thesis & references therein), Oman and Saudi Arabia, Permian (Stephenson 2006), Pakistan, Permian (Jan *et al.* 2009).

Suprasubturma CAMERATRILETES Neves & Owens 1966

Subturma MEMBRANATRILETES Neves & Owens 1966

Infraturma CINGULICAMERATI Neves & Owens 1966

***Cristatisporites crassilabratus* Archangelsky & Gemerro 1979**

Plate 2, Fig. 3

Description

Spores, radial, trilete, cavate; amb rounded triangular and spinose at the margin.

Intexinal body prominent, distinct; Intexine thick, ?punctate. Laesurae poorly discernible (due to thick intexinal body). Proximal face planar; exoexine laevigate.

Distal face convex; exoexine thin, strongly ornamented with spinae at the distal pole.

Size of elements increase in length from proximal to distal pole, often bifurcating. Zona varies in width, mostly continuous. Intexine-exoexine separation distinct.

Best reference specimens

H20, MPA57511/1; R14/2, MPA57511/1; V30/2, MPA57761/1; T38, MPA57764/1;

D11/3, MPA58394/1

Dimension

Equatorial diameter (excluding ornaments); 50(57)80 µm; 5 specimens

Selected previous records

South America, Late Carboniferous-Permian (Archangelsky & Gamerro 1979;

Marques-Toigo & Klepziq 1995), Argentina, Carboniferous-Permian (Archangelsky &

Gamerro 1979; Césari *et al.* 1995; Césari & Gutiérrez 2000; Playford & Dino 2002),

Brazil, Late Carboniferous (Souza *et al.* 2006), Oman and Saudi Arabia, Late

Carboniferous-Permian (Stephenson & Filatoff 2000a; Stephenson *et al.* 2003;

Stephenson 2004; Penney *et al.* 2008), West Papua, Permian (Playford & Rigby 2008), Pakistan, Carboniferous-Permian (Jan & Stephenson 2011).

***Vallatisporites arcuatus* (Marques-Toigo) Archangelsky & Gamarro, 1979**

Plate 2, Fig. 4

Description

Spores, radial, trilete, cavate; amb rounded triangular to slightly circular, slightly uneven due to the projecting grana and spinae at the margin. Laesurae indistinct, with raised labra. Exine two layered, Intexine body distinct, laevigate, thick; forming rounded triangular inner body; separated from exoexine in the equatorial plane forming a narrow (1 µm or less wide), continuous equatorial cavum. Proximal face planar to depressed in the contact area. Distal face convex in shape; variously ornamented with grana, spinae and coni. Zona wide, width approximately 30-35% of the spore width, different layers can be identified in the zona. The outer part is sparsely granulate.

Best reference specimens

T34/4, MPA57511/1; X13/1, MPA57511/1; M27/2, MPA57512/1; T32/1,
MPA57511/1; X13/1, MPA57511/1

Dimension

Equatorial diameter; 30(34)54 µm; Intexine diameter; 22(23)36 µm; 5 specimens

Selected previous records

Argentina, Late Carboniferous-Permian (Archangelsky & Gamarro 1979; Césari *et al.* 1995; Césari & Gutiérrez 2000; Playford & Dino 2000), Brazil, Early Permian (Souza *et al.* 1997; Souza & Callegari 2004), Oman and Saudi Arabia, Late Carboniferous-Permian (Stephenson 1998b, PhD thesis; Stephenson & Osterloff 2002; Stephenson *et al.* 2003; Stephenson 2004), West Papua, Permian (Playford & Rigby 2008), Yemen,

Carboniferous-Permian (Stephenson & Al-Mashaikie 2010), Pakistan, Carboniferous-Permian (Jan & Stephenson 2011).

Subturma SOLUTITRILETES Neves & Owens 1966

Infraturma PLANATI Neves & Owens 1966

Turma MONOLETES Ibrahim 1933

Subturma AZONOMONOLETES Luber 1935

Infraturma LAEVIGATOMONOLETES Dybova & Jachowitz 1957

***Laevigatosporites callosus* Balme 1970**

Plate 2, Fig. 5

Description

Spores, bilateral, monolete; amb oblate oval (pumpkin-shaped). Laesurae very distinct, length 75%-80% of the spore length; commissure margins upturned and resemble labra. *Curvaturae imperfectae* in some specimens. Exine thickness 1-2 μm , slightly brighter than the flanked commissure and mostly bright yellow coloured, comprehensively laevigate and very rarely punctate; occasional thickened areas found at the distal pole. Proximal face flatter or slightly concave, distal face convex.

Best reference specimens

K21, MPA57533/1; U4/1, MPA57528/2; N13/3, MPA57533/2; W5, MPA58402/1

Dimension

Length; 38(47)49 μm ; breadth; 22(24)28 μm ; 5 specimens

Selected previous records

Pakistan, Late Permian (Balme 1970; Jan *et al.* 2009), Permian (Nader *et al.* 1993), Saudi Arabia. Late Permian (Stump & Van der Eem 1995), Oman and Saudi Arabia,

Carboniferous-Permian (Stephenson 1998b, PhD thesis & references therein; Stephenson *et al.* 2003).

Infraturma SCULPTATOMONOLETI Dybova & Jachowitz 1957

***Thymospora opaqua* Singh 1964**

Plate 2, Fig. 6

Description

Spores, bilateral, monolete; amb circular to subcircular. Monolete slit distinct, straight, 50- 70% of the spore radius. Exine yellowish to dark brown, verrucose; ornamented with variable sizes verrucae, mostly in the range of 1-2 μm high and 2 μm broad, non-bifurcating at the spore margin. Verrucae confluent/diffused at the bases.

Best reference specimens

O18/2, MPA58399/2; O18, MPA18399/2; Q15/1, MPA58399/2; S22, MPA587528/1

Dimension

Length; 13(14)16 μm ; 4 specimens

Selected previous records

Iraq, Permian (Singh 1964), Oman and Saudi Arabia, Carboniferous-Permian (Stephenson 2006, 2008b; Stephenson *et al.* 2003), Southeast Turkey-Northern Iraq, Permian (Stolle 2007, Stolle *et al.* 2011), Pakistan, Permian (Jan *et al.* 2009).

Anteturma VARIEGERMINANTES Potonié 1970

Turma SACCITES Erdman 1947

Subturma MONOSACCITES Chitaley *emend.* Potonié & Kremp 1954

Infraturma MONPOLSACCITI Hart 1965

***Florinites? balmei* Stephenson & Filatoff 2000**

Plate 3, Figs. 1 to 8

Description

Pollen, monosaccate, bilaterally symmetrical; amb oval. Corpus almost imperceptible; the presence is suggested by a narrow uneven to oval fold structure in the saccus. Long axis of the corpus parallel to the long axis of the grain; diameter of corpus almost half of the grain diameter. Saccus coarsely infrareticulate; brochi 1-2 μm in diameter, muri width less than 1 μm .

Best reference specimens

V8/1, MPA57533/2; V33/2, MPA57533/2; N3/2, MPA57533/2; R6/1, MPA57533/2;
R6, MPA57513/2; W 12/3, MPA57533; Y11, MPA57533; W25, MPA57533

Dimension

Total width; 20(28)42 μm ; corpus width; 10(18)22 μm ; 8 specimens

Selected previous records

Saudi Arabia and Oman, Permian (Stephenson & Filatoff 2000b; Stephenson 2006; Stephenson 2008b), Southeast Turkey, Permian (Stolle *et al.* 2011, Stolle 2007), Iraq, Permian (Singh 1964; Nader *et al.* 1993), Kuwait, Permian (Tanoli *et al.* 2008), Pakistan, Permian (Jan *et al.* 2009).

Infraturma TRILETESACCITI Leschik 1955

***Barakarites rotatus* (Balme & Hennelly) Bharadwaj & Tiwari 1964**

Plate 4, Fig. 1

Basionym *Nuskoisporites rotatus* Balme & Hennelly 1956b

Description

Pollen, radially symmetrical, monosaccate, trilete; amb circular, margin smooth to very slightly wavy. Corpus distinct; circular, exine relatively thick, with distal circumpolar annular tenuitas, close to the corpus outer margin, cracks in the cappa exine; radius of corpus 50% of the total grain radius. Saccus annular, regular in width around the corpus, finely infrareticulate. Corpus with trilete mark (Laesurae 14 µm long).

Best reference specimens

P3, MPA57512/1; X17/1, MPA57511/2; T3, MPA57512/1; O13/3, MPA57512/2;
J30/1, MPA57514/1; N22/4, MPA57515/1; J19, MPA57515/1; D24/2, MPA57514/1;
W31/3, MPA57513/1

Dimension

Total width; 57(127)143 µm; corpus width; 34(85)71 µm; 9 specimens

Selected previous records

South Africa, Permian (Anderson 1977; Milstead 1999), Australia, Permian (Balme & Hennelly 1956b; Foster 1975), India, Permian (Bharadwaj & Tiwari 1964), Antarctica, Permian (Balme & Playford 1967), Oman and Saudi Arabia, Carboniferous-Permian (Stephenson 1998b, PhD thesis & references therein; Stephenson & Filatoff 2000a & b; Stephenson *et al.* 2003; Penney *et al.* 2008), Pakistan, Carboniferous-Permian (Jan *et al.* 2009; Jan & Stephenson 2011).

***Cannanoropollis janakii* Potonié & Sah 1960**

Plate 4, Fig. 2

Description

Pollen, radially symmetrical, monosaccate, trilete; amb circular with crenulated margins. Corpus circular, intexine imperceptible to faintly visible; exine thin; laevigate to micropunctate; trilete rays 15% of the total corpus length. Saccus distally inclined. Proximal saccus detachment equatorial; distal saccus detachment subequatorial.

Best reference specimens

S32, MPA57511/1; X21/3, MPA58401/1; R15/2, MPA58403/1

Dimension

Total width; 122 µm; corpus width 71 µm; 1 specimen

Selected previous records

South Africa, Late Carboniferous to Late Permian (Anderson 1977; Milstead 1999), Australia, Late Carboniferous to Late Permian (Balme & Hennelly 1956b; Foster 1979; Jones & Truswell 1992), South America, Late Carboniferous to Early Permian (Archangelsky & Gamberro 1979; Marques-Toigo & Klepzig 1995), Oman and Saudi Arabia, Carboniferous-Permian (Stephenson & Filatoff 2000a & b; Stephenson & Osterloff 2002; Stephenson *et al.* 2003), West Papua, Permian (Playford & Rigby 2008), Yemen, Carboniferous-Permian (Stephenson & Al-Mashaikie 2010), Pakistan, Carboniferous-Permian (Jan *et al.* 2009; Jan & Stephenson 2011).

***Plicatipollenites malabarensis* (Potonié & Sah) Foster 1979**

Plate 4, Fig. 3

Basionym *Cannanoropollis malabarensis* Potonié & Sah 1960

Description

Pollen, radially symmetrical, monosaccate, trilete; amb circular to rarely oval, margin wavy or smooth. Corpus distinct; circular, exine thick. Cappula circular to slightly ellipsoidal, smaller than the corpus (cappa) due to the saccus onlap on distal side, delineated by the circular distal intexinal fold. Laesurae length 50% of the corpus length, some specimens however show laesurae extending to corpus margin. Saccus distally inclined (concave), rigid, coarsely infrareticulate.

Best reference specimens

K11/1, MPA57513/1; D4/2, MPA57515/1; V16/4, MPA57516/1; Q16/3, MPA57516/1

Dimensions

Total width; 71(85)143 µm; corpus width; 42(44)57 µm; 4 specimens

Selected previous records

Gondwana, Permian (Foster 1979; Lindström 1995; Archangelsky & Gamarro 1979; Lele 1964), Oman and Saudi Arabia, Carboniferous-Permian (Stephenson & Osterloff 2002; Stephenson *et al.* 2003; Stephenson 2004; Penney *et al.* 2008), Argentina, Permian (Playford & Dino 2002), Yemen, Carboniferous-Permian (Stephenson & Al-Mashaikie 2010), Pakistan, Carboniferous-Permian (Jan & Stephenson 2011).

***Cannanoropollis densus* (Lele) Bose & Maheshwari, 1968**

Plate 4, Fig. 4

Description

Pollen, monosaccate, radially symmetrical, amb circular to slightly subcircular. Corpus distinct, dark, outline well-defined, circular to occasionally oval. Laesurae not clear. Saccus infrareticulate to infrapunctate, brochi are arranged in a radial pattern.

Best reference specimens

X31, MPA57528/1

Dimension

Total width; 59 μm ; corpus width; 32 μm ; 1 specimen

Selected previous records

Oman and Saudi Arabia, Carboniferous-Permian (Stephenson 1998b, PhD thesis & references therein), India, Early Permian (Lele 1964), Africa, Early Permian (Bose & Maheshwari 1968; MacRae 1988), Argentina, Permo-Carboniferous (Archangelsky & Gamero 1979).

Infraturma VESICULOMONORADITES Pant 1954

***Potonieisporites brasiliensis* (Nahuys, Alpern & Ybert) Archangelsky & Gamero 1979**

Plate 4, Fig. 5

Basionym *Vestigisporites brasiliensis* Nahuys, Alpern & Ybert 1968

Description

Pollen, bilaterally symmetrical, monosaccate, monolete (occasionally dilete and very rarely trilete); amb oval. Corpus circular, small, dark; intxine thick (1-2 μm). Monolete

or dilete (or trilete) distinct to indistinct, usually short and hardly 50% of the corpus length; mostly between 25%-50%; exine within commissure intact but thin. Saccus distally inclined; proximal saccus detachment equatorial; distal saccus detachment closer to distal pole; marked by single circular intexinal folds in the longitudinal direction of corpus. Cappula small, oval. Bordered by intexinal folds; cappula width 50% of corpus length. Saccus oval; exoexine thick, rigid.

Best reference specimens

P18/3, MPA57512/1; N9/2, MPA57513/2; O6, MPA57514/1; D30/3, MPA57514/1

Dimension

Total width; 112(140)147 μm ; corpus width; 55(63)70 μm ; 4 specimens

Selected previous records

South America, Late Carboniferous to Late Permian (Archanglesky & Gamero 1979; Marques-Toigo & Klepzig 1995), Argentina, Carboniferous-Permian (Archanglesky & Gamero 1979), Australia, Carboniferous-Permian (Powis 1979), Oman and Saudi Arabia, Carboniferous-Permian (Stephenson & Filatoff 2000a; Stephenson & Osterloff 2002; Penney *et al.* 2008), West Papua, Permian (Playford & Rigby 2008), Pakistan, Carboniferous-Permian (Jan & Stephenson 2011).

***Potonieisporites novicus* Bharadwaj 1954**

Plate 4, Fig. 6

Description

Pollen, bilaterally symmetrical, monosaccate, monolete; amb oval having smooth outlines (margin). Corpus transversely elongate and longitudinally little squashed; Intexine sufficiently thicker or darker, compared to saccus; micropunctate. Cappula bounded by intexinal folds. Saccus inclined distally; proximal saccus detachment

subequatorial. Distal saccus detachment marked by distal intexinal folds. Saccus oval, annular in shape; saccus having radial/non radial folds. Brochi of variable sizes (1-2 μm). Monolete, dilete or trilete mark present; distinct; length 75% of the corpus radius.

Best reference specimens

H11/4, MPA57513/1; X28, MPA57515/1; M3/3, MPA57515/1; U5, MPA58394/1

Dimension

Total width; 62(155)163 μm ; corpus width; 37(85)86 μm ; 4 specimens

Selected previous records

Australia, Late Carboniferous to Late Permian (Foster 1979), South Africa, Late Carboniferous to Late Permian (Marques-Toigo & Klepzig 1995), Oman and Saudi Arabia, Carboniferous-Permian (Stephenson & Filatoff 2000a & b, Stephenson & Osterloff 2002; Stephenson *et al.* 2003; Penney *et al.* 2008), Yemen, Carboniferous-Permian (Stephenson & Al-Mashaikie 2010), West Papua, Permian (Playford & Rigby 2008), Pakistan, Carboniferous-Permian (Balme 1970; Jan & Stephenson 2011).

Anteturma VARIAGERMINANTES Potonié 1970

Turma SACCITES Erdman 1947

Subturma DIACCITES Cookson 1947

Infraturma DISACCIATRILETI Leschik 1955

***Limitsporites rectus* Leschik 1956**

Plate 4, Fig. 7

Description

Pollen, bilaterally symmetrical, bisaccate, monolete (or rarely dilete); amb slightly diploxylonoid. Intexinal body transversely elongate, thick, dark; laevigate to finely

micropunctate. Occasionally irregularly shaped areas of expanded infra-reticulate exoexine occur on cappa. Cappula distinct; width equal to the corpus width. Commonly a pair of distal intexinal folds mark cappa margin. Proximal saccus detachment equatorial; distal saccus detachment subequatorial; saccus distally inclined, lunate, to semi-circular, rigid; saccus infra-reticulum coarse (brochi 1-2 μm). Monolete mark distinct, 50-90% of the corpus length.

Best reference specimens

U17/1, MPA57513/1; R15/2, MPA58401/1; E16/1, MPA58403/1

Dimension

Total length; 57(65)125 μm ; corpus length; 28(34)71 μm ; corpus breadth; 37(42)65 μm ; saccus breadth 37(42)80 μm ; 3 specimens

Selected previous records

South America, Early Permian (Marques-Toigo & Klepzig 1995; Playford & Dino 2002), Gondwana, Permian (Foster 1979; Londström 1995), Oman and Saudi Arabia, Carboniferous-Permian (Stephenson 1998b, PhD thesis & references therein; Stephenson & Filatoff 2000a; Stephenson & Osterloff 2002; Stephenson *et al.* 2003), South eastern Turkey, Permian (Stolle 2010), Pakistan, Carboniferous-Permian (Jan & Stephenson 2011).

Infraturma STRIATITI Pant 1954

***Corisaccites alutas* Venkatachala & Kar 1966**

Plate 4, Fig. 8

Description

Pollen, bilaterally symmetrical, bisaccate, monolete; amb slightly diploxylonoid to haploxylonoid. Corpus distinct, dark in colour, longitudinally oval shaped; split into two more or less uniform halves by a central longitudinal furrow (?cavity or sulcus). Corpus exine thick (1-2 μm); Intexine discernible in the floor of the medial furrow, light in colour, laevigate. Saccus larger than the corpus, semicircular in shape; distally inclined, light in colour, unstructured.

Best reference specimens

T31/3, MPA588397/2; Q33/3, MPA57528/2; M20/4, MPA58397/1; Q33/3,
MPA57528/1

Dimension

Total length; 45(50)77 μm ; corpus length; 43(48)76 μm ; corpus breadth; 32(38)56 μm ;
saccus breadth; 34(40)57 μm ; 4 specimens

Selected previous records

India, Early Permian (Venkatachala & Kar 1966), Iran, Permian (Ghavidel-Syooki 1996), Pakistan, Permian (Balme 1970; Jan *et al.* 2009), Oman and Saudi Arabia, Carboniferous-Permian (Stephenson 1998b, PhD thesis & references therein; Stephenson & Osterloff 2002; Stephenson *et al.* 2003), south eastern Turkey, Permian (Stolle 2010, Stolle *et al.* 2011).

***Protohaploxylinus* cf. *uttingii* Stephenson & Filatoff 2000**

Plate 5, Fig. 1

Description

Pollen, bilaterally symmetrical, taeniate, bisaccate, haploxylinoid to weakly diploxylinoid; amb oval elongate. Corpus indistinct, longitudinally oval. Intexinal body distinct, appears as circular dark coloured areas in the centre of the corpus. Distal saccus overlap 20-75% of the corpus width. Sacci sub-circular in outline, approximately 75% of the corpus size.

Best reference specimens

S35, MPA57528/1; T32, MPA57532/1

Dimension

Total length; 57 μm , 50 μm ; corpus length; 28 μm ; 30 μm ; corpus breadth; 20 μm , 31 μm ; saccus breadth 10 μm , 14 μm ; 2 specimens

Remarks

The thick exoexine and the elongation of the corpus in the longitudinal axis rather than the transverse axis, make the present specimens different than the *Protohaploxylinus utiingii* Stephenson & Filatoff (2000). The present specimen has been identified as *Protohaploxylinus utiingii* in Jan *et al.* (2009), however cf. has been used here to account for the obvious differences in these specimens.

Selected previous records

Pakistan, Permian (Jan *et al.* 2009).

***Protohaploxylinus hartii* Foster 1979**

Plate 5, Fig. 2

Description

Pollen, bilaterally symmetrical, bisaccate, taeniate; amb haploxylinoid to weakly diploxylinoid. Corpus distinct, latitudinally elongate; cappa 1-1.5 μ m thick, with 5-8 teniae, each approximately 2 μ m wide. Saccus semi-circular in outline, attached to exoexine by a narrow bladder, saccus exoexine 1 μ m thick, weakly reticulate. Proximal saccus detachment equatorial; distal saccus detachment subequatorial.

Best reference specimens

K9/4, MPA58387/1; G29/2, MPA58384/2; K15/1, MPA58384; V28/1, MPA58401/1;
R22/2, MPA58401/1

Dimension

Total length; 56(70)90 μ m; corpus length; 35(36)38 μ m; corpus breadth; 28(34)35 μ m;
saccus breadth; 10(18)21 μ m; 5 specimens

Selected previous records

South America, Permian (Marques-Toigo & Klepzig 1995), Pakistan, Carboniferous-Permian (Jan & Stephenson 2011).

***Striatopodocarpites fusus* (Balme & Hennelly) Potonié 1958**

Plate 5, Fig. 3

Description

Pollen, bilaterally symmetrical, bisaccate, taeniate; amb diploxylinoid. Corpus distinct, circular, dark. Saccus much larger than corpus, sub-circular to circular in outline. Proximal saccus detachment equatorial; distal saccus detachment subequatorial.

Best reference specimens

N24, MPA57528/1

Dimension

Total length; 70 µm; corpus length; 20 µm; corpus breadth; 20 µm; saccus breadth; 30 µm; 1 specimen

Selected previous records

Gondwana, Permian (Balme & Hennelly 1955; Bharadwaj & Salujah 1964; Anderson 1977; Foster 1979; Marques-Toigo & Klepzig 1995; Milstead 1999), Oman and Saudi Arabia, Carboniferous-Early Permian (Stephenson & Osterloff 2002; Stephenson *et al.* 2003), South eastern Turkey, Permian (Stolle 2010), Pakistan, Permian (Jan *et al.* 2009).

Lueckisporites virkkiae* Potonié & Klaus 1954*Plate 5, Fig. 4****Description**

Pollen, bilaterally symmetrical, bisaccate, alete, ?trilete; amb diploxytonoid. Corpus distinct. Latitudinal oval; proximal cap divided into half by narrow cleft that generally narrows on either side, and extends full diameter of corpus, along its longitudinal axis; a monolete mark may be visible. Sacci semi-circular in shape. Proximal saccus detachment equatorial; distal saccus detachment subequatorial. Saccus infra-structure fine to micro-punctate or vermiculate.

Best reference specimens

T23/3, MPA57528/1

Dimension

Total length; 65 µm; corpus length; 45 µm; corpus breadth; 40 µm; saccus breadth; 20 µm; 1 specimen

Selected previous records

Southeast Turkey and Northern Iraq, Permian (Stolle *et al.* 2011), Oman and Saudi Arabia, Permian (Stephenson *et al.* 2003), southwest Iraq, Permo-Triassic (Nader *et al.* 1993), Pakistan, Permian (Jan *et al.* 2009), south Africa, Permian (Anderson 1977; Milstead 1999).

Turma PLICATES Naumova *emend.* Potonié 1960

Subturma MONOCOLPATES Iverson & Troels-Smith 1950

***Cycadopites cymbatus* (Balme & Hennelly) Segroves 1970**

Plate 5, Fig. 5

Description

Pollen, monosulcate; amb elongate to spindle-shaped i.e. fusiform, with mostly pointed longitudinal extremities, some specimens have flat ends. Distal furrow runs the entire length of the grain, narrower at the centre and opening at the ends, before joining together at the ends again. Exoexine laevigate, 1 µm thick, translucent; intexine thick, darker, punctate.

Best reference specimens

V4/3, MPA57518; P16/2, MPA58403/1; U29/3, MPA58401/1

Dimensions

Length; 41(50)60 µm, 3 specimens

Selected previous records

Gondwana, Permian (Segroves 1970), Oman, Early Permian (Besems & Schuurman 1987), Carboniferous-Early Permian (Stephenson & Filatoff 2000a; Stephenson & Osterloff 2002; Stephenson 2000; Stephenson *et al.* 2003; Stephenson 2004; Penney *et al.* 2008; Stephenson *et al.* 2008), Australia, Permian (Balme & Hennelly 1956a; Segroves 1970; Foster & Waterhouse 1988), Antarctica, Permian (Lindström 1995), West Papua, Permian (Playford & Rigby 2008), South Africa, Late Permian (MacRae 1988), Pakistan, Carboniferous-Permian (Jan & Stephenson 2011).

4.7 Plates explanation

Figures, England Finder coordinates, slide representation and formation in which found are given.

Plate 1

(1). *Punctatisporites ubischii* Foster 1979 comb. nov.

W23/3, MPA- 58394/1, Tobra Formation.

(2). *Brevitriletes leptocaina* Jones & Truswell 1992

T11/4, MPA-57512/2, Tobra Formation.

(3). *Brevitriletes parmatus* (Balme & Hennelly) Backhouse 1991

O18, MPA-57517/1, Tobra Formation.

(4). *Brevitriletes cornutus* (Balme & Hennelly) Backhouse 1991

N10, MPA-58394/1, Tobra Formation.

(5). *Horriditriletes tereteangulatus* (Balme & Hennelly) Backhouse 1991

S17/1, MPA-57512/1, Tobra Formation.

(6). *Horriditriletes ramosus* (Balme & Hennelly) Bhardwaj & Salujah 1964

W20/3, MPA-57511/2, Tobra Formation.

(7). *Horriditriletes uruguayensis* (Marques-Toigo) Archangel'sky & Gamarro 1979

W20/3, MPA-57511/2, Tobra Formation.

(8). *Microbaculispora tentula* Tiwari 1965

V14, MPA-57511/2, Tobra Formation.

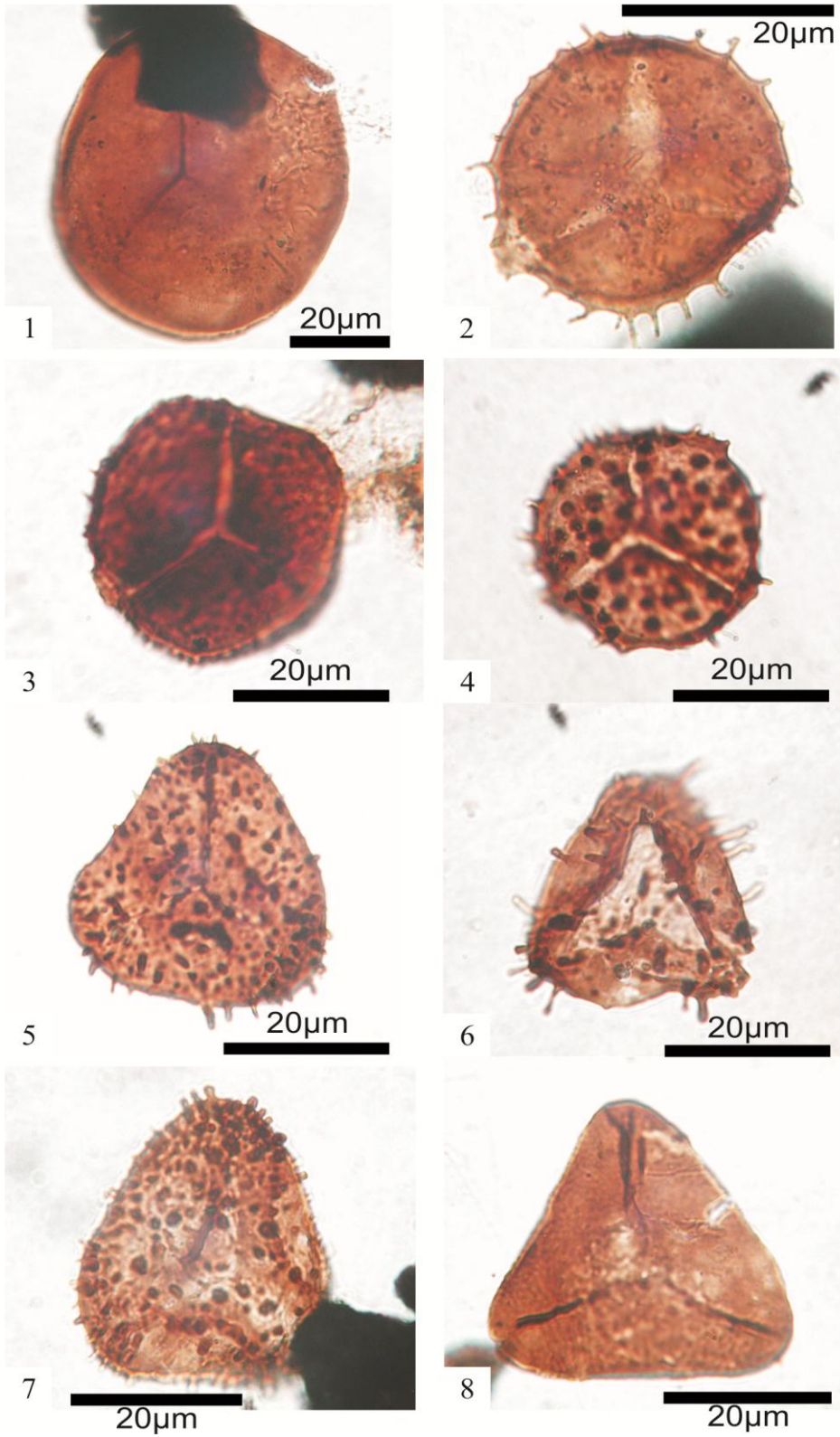


Plate 1

Plate 2

(1). *Converrucosisporites grandegrnulatus* (Anderson) Lindström 1995

K27/3, MPA-57519/1, Tobra Formation (distal focus).

(2). *Camptotriletes warchianus* Balme 1970

S21, MPA-57528/2, Sardhai Formation.

(3). *Cristatisporites crassilabratus* Archangelsky & Gemerro 1979

V30/2, MPA-57761/1, Tobra Formation.

(4). *Vallatisporites arcuatus* Archangelsky & Gamerao 1979

X13/1, MPA-57511/1, Tobra Formation.

(5). *Laevigatisporites callosus* Balme 1970

N13/3, MPA-57533/2, Sardhai Formation.

(6). *Thymospora opaqua* Singh 1964

S22, MPA-57728/1, Sardhai Formation.

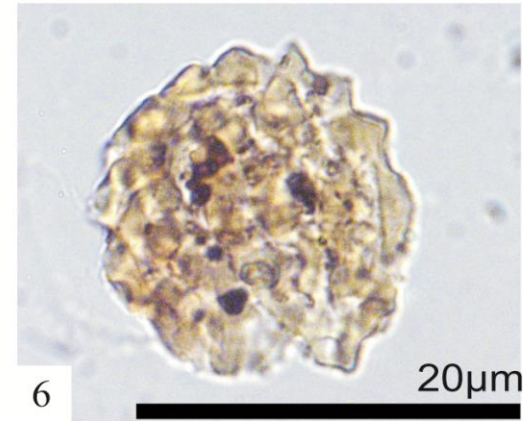
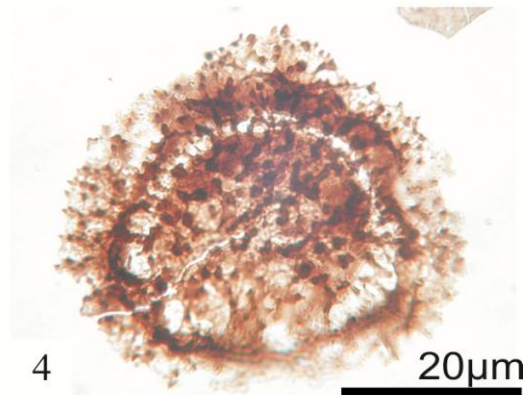
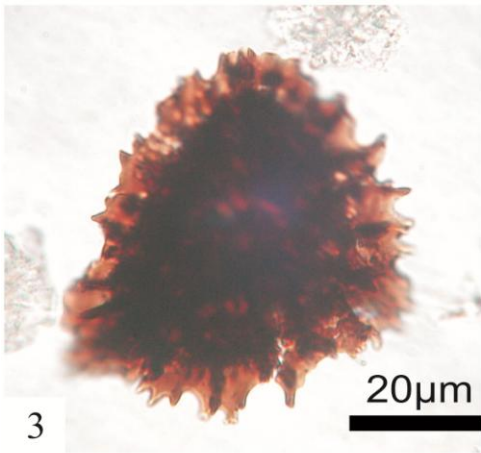
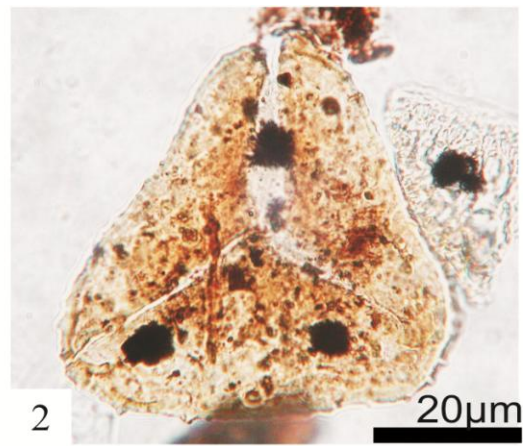
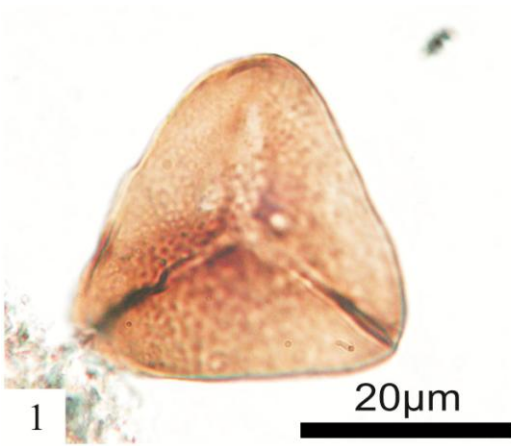


Plate 2

Plate 3

(1). *Florinites? balmei* Stephenson & Filatoff 2000

W25, MPA-57533/1, Sardhai Formation.

(2). *Florinites? balmei* Stephenson & Filatoff 2000

V8/1, MPA-57533/1, Sardhai Formation.

(3). *Florinites? balmei* Stephenson & Filatoff 2000

V29/1, MPA-57533/1, Sardhai Formation.

(4). *Florinites? balmei* Stephenson & Filatoff 2000

U3/3, MPA-57533/1, Sardhai Formation.

(5). *Florinites? balmei* Stephenson & Filatoff 2000

L29/3, MPA-57533/1, Sardhai Formation.

(6). *Florinites? balmei* Stephenson & Filatoff 2000

V33/2, MPA-57533/1, Sardhai Formation.

(7). *Florinites? balmei* Stephenson & Filatoff 2000

O12, MPA-57533/1, Sardhai Formation.

(8). *Florinites? balmei* Stephenson & Filatoff 2000

S17/4, MPA-57533/1, Sardhai Formation.

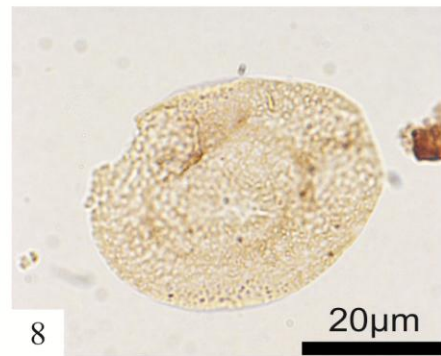
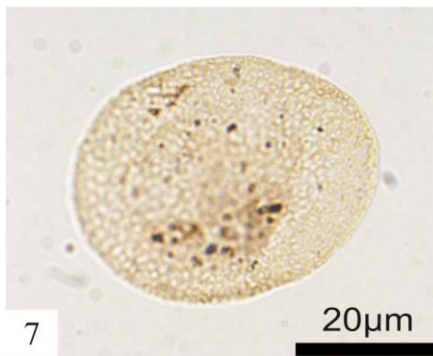
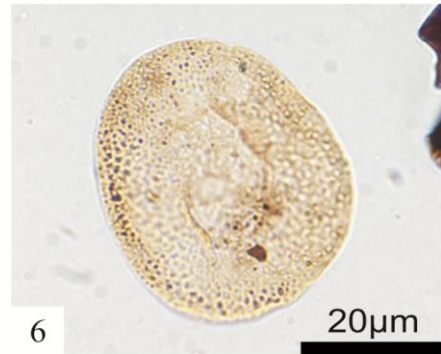
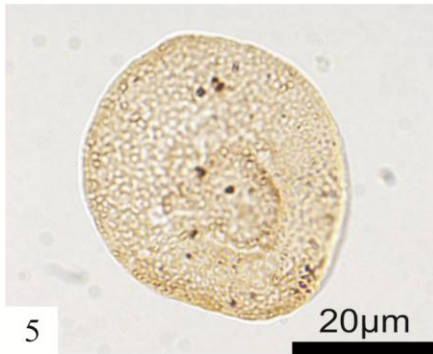
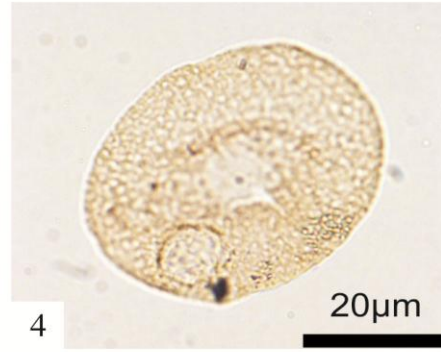
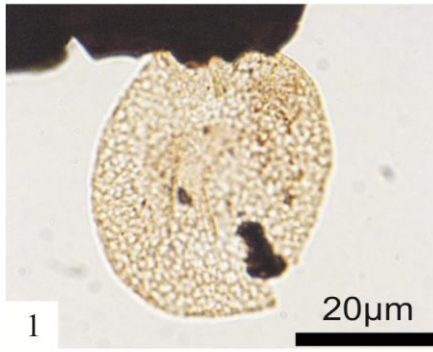


Plate 3

Plate 4

(1). *Barakarites rotatus* (Balme & Hennelly) Bharadwaj & Tiwari 1964

O13/3, MPA-57512/2, Tobra Formation.

(2). *Cannanoropollis janakii* Potonié & Sah 1960

X21/3, MPA-58401/1/1, Tobra Formation.

(3). *Plicatipollenites malabarensis* (Potonié & Sah) Foster 1979

K11/1, MPA-57513/1, Tobra Formation.

(4). *Cannanoropollis densus* (Lele) Bose & Maheshwari, 1968

X31, MPA-57528/1, Sardhai Formation.

(5). *Potonieisporites brasiliensis* (Nahuys, Alpern & Ybert) Archangelsky & Gamarro 1979

K19/2, MPA-57513/2, Tobra Formation.

(6). *Potonieisporites novicus* Bharadwaj 1954

O6, MPA-57514/1, Tobra Formation.

(7). *Limitsporites rectus* Leschik 1956

E16/1, MPA-58403/1, Tobra Formation.

(8). *Corisaccites alutas* Venkatachala & Kar 1966

T31/3, MPA-58397/2, Sardhai Formation.

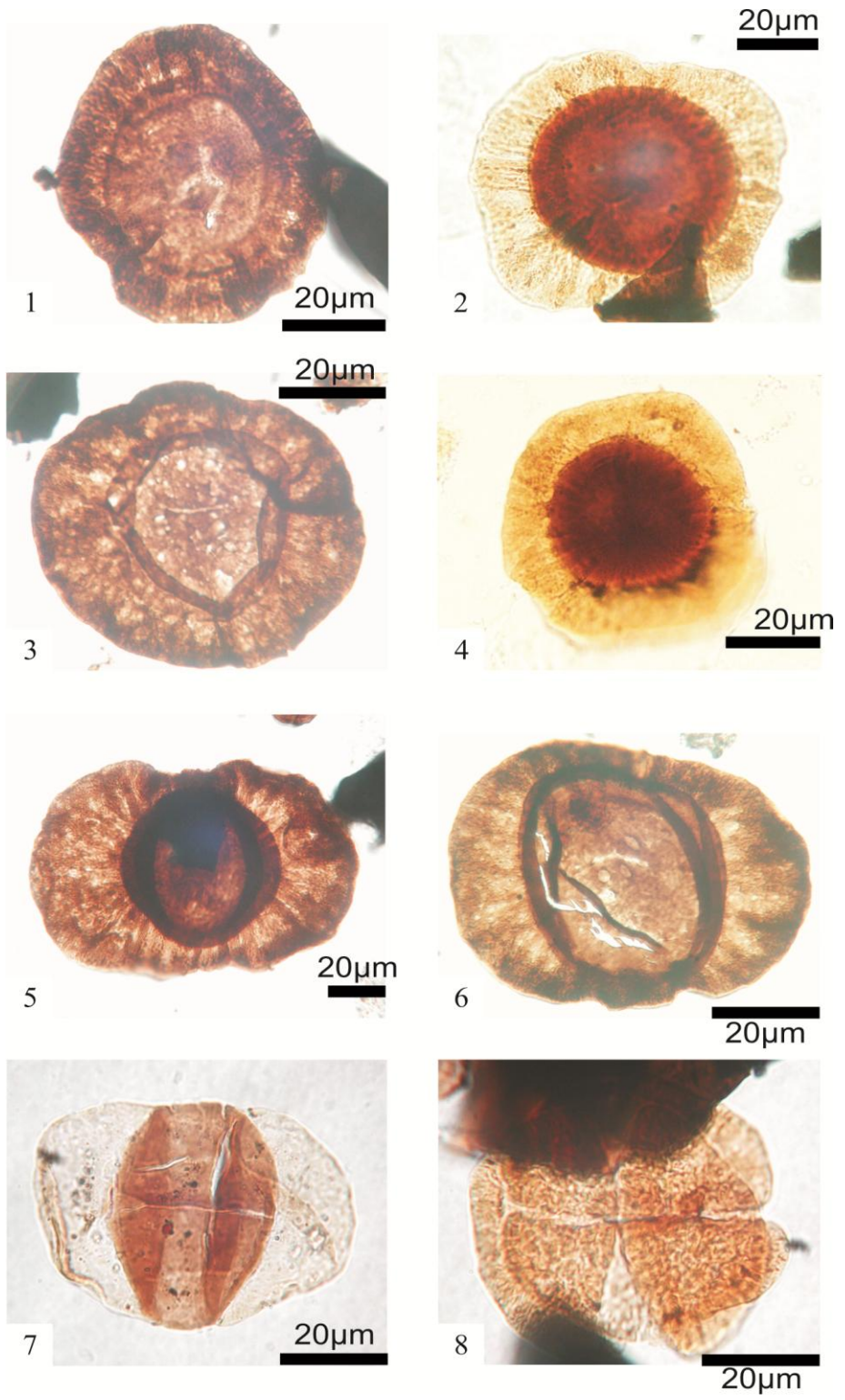


Plate 4

Plate 5

(1). *Protohaploxypinus cf. uttingii* Stephenson & Filatoff 2000

S35, MPA-57528/1, Sardhai Formation.

(2). *Protohaploxypinus hartii* Foster 1979

R22/2, MPA-58401/1, Tobra Formation.

(3). *Striatopodocarpites fusus* (Balme & Hennelly) Potonié 1958

N24, MPA-57528/2, Sardhai Formation.

(4). *Lueckisporites virkkiae* Potonié & Klaus 1954

W12/1, MPA-57528/1, Sardhai Formation (distal focus).

(5). *Cycadopites cymbatus* (Balme & Hennelly) Segroves 1970

V4/3, MPA-57519/1, Tobra Formation.

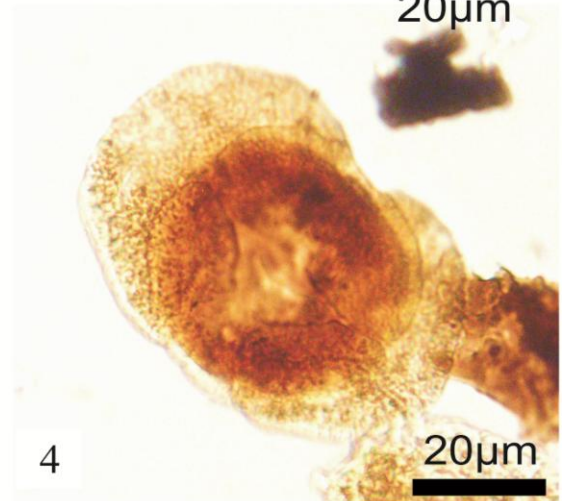
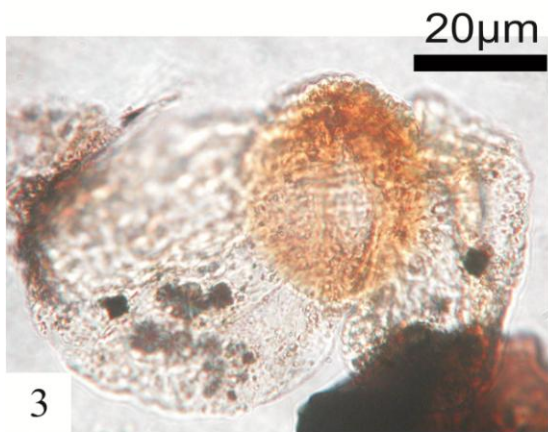
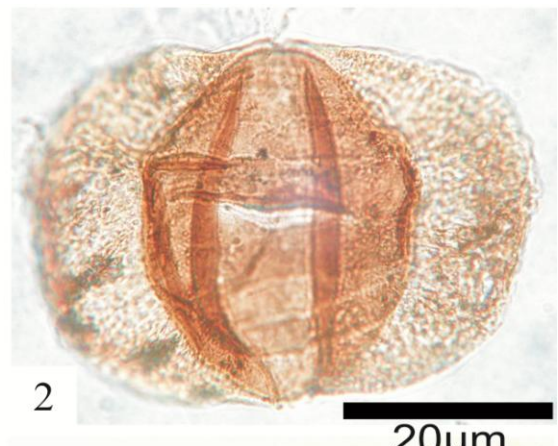
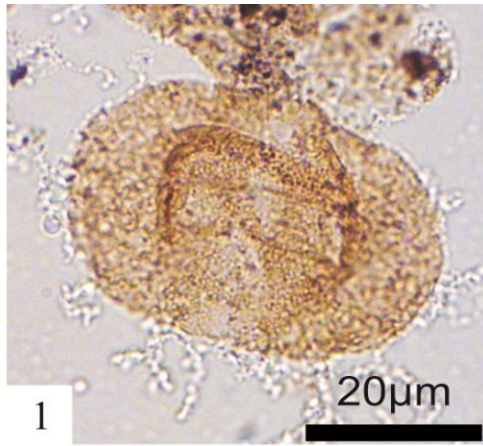


Plate 5

5 ¹Chapter 5: Palynology and palynostratigraphy of the Upper Pennsylvanian Tobra Formation

5.1 Abstract

Samples from the upper 84 m of a 125 metre-thick section of the Tobra Formation at Zaluch Nala section (western Salt Range), Pakistan yielded significant palynomorph taxa including the spores *Horriditriletes* sp., and *Microbaculispora tentula*; abundant monosaccate pollen including *Barakarites* cf. *rotatus*, *Cannanoropollis janakii* and *Plicatipollenites malabarensis*, and rare taeniate and non-taeniate bisaccate pollen. *Converrucosisporites grandegrnulatus*, *Cycadopites cymbatus*, *Horriditriletes ramosus*, *Horriditriletes tereteangulatus* and *Microbaculispora tentula* indicate the South Oman 2165B Biozone (Pennsylvanian), suggesting that the Tobra Formation in the Zaluch Nala section (western Salt Range) is equivalent to the middle part of the Al Khlata Formation of South Oman (PDO Al Khlata production unit AK P5). *Brevitriletes leptocaina*, *Brevitriletes parmatus*, *Horriditriletes ramosus* and *Microbaculispora tentula* indicate the lower part of the Oman and Saudi Arabia Palynological Zone 2 (OSPZ2). The Tobra Formation assemblages are also correlated with those from Stage 2 (*sensu* Backhouse 1991) and the eastern Australian *Microbaculispora tentula* Oppelzone, based on the occurrence of *Brevitriletes cornutus*, *Brevitriletes parmatus*, *Cycadopites cymbatus*, *Horriditriletes ramosus*, *Horriditriletes tereteangulatus* and *Microbaculispora tentula*. The Tobra Formation in the Zaluch Nala section (western Salt Range) lacks the deglaciation sequence that is present in several other palaeogeographically-nearby basins such as those of south Arabia and Western

¹ This chapter is modified from the paper that is published in the American Association of Stratigraphic Palynologists' journal "*Palynology*". The published paper is included as Appendix 3.

Australia, indicating either non-deposition during the deglaciation period, or erosion associated with the unconformity between the Tobra Formation and the overlying Warchha Formation.

5.2 Previous palynological work on the Carboniferous-Permian succession of the Salt Range, Pakistan

Balme (in Teichert 1967) described assemblages from Unit 2 of the C-member of the Tobra Formation at Zaluch Nala (Figs. 5.1 & 5.2), and assigned them to the Permian. The palynomorphs reported were *Apiculatisporis* sp., *Acanthotriletes* cf. *A. tereteangulatus*, ?*Cymatiosphaera* sp., *Kraeuselisporites* sp., *Leiosphaeridia* spp., *Leiotriletes* sp., cf. *Nuskoisporites* sp., *Punctatisporites* cf. *gretensis*, *Punctatisporites* spp., *Protohaploxypinus* sp., *Potonieisporites* sp., and *Striatopodocarpites* sp. Kemp (1975) examined two unlocated samples from the Tobra Formation at Zaluch Nala and reported *Brevitriletes* sp., *Brevitriletes* cf. *unicus*, *Dentatisporites* sp., *Horriditriletes* sp., *Lophotriletes* sp., *Lophotriletes* cf. *scotinus*, *Lophotriletes* sp., and *Potonieisporites neglectus* along with the acritarch *Cymatiosphaera* sp. Khan *et al.* (2001) indentified *Cannanorpollis niazuddinii*, *Densipollenites indicus*, *Nuskoisporites* cf. *Nuskoisporites dulhuntyi*, *Plicatipollenites indicus* and *Plicatipollenites trigonalis* from the Tobra Formation at Nilawahan Gorge (central Salt Range, fig. 5.1) and assigned an Early Permian age to the assemblages. Virkki (1946) examined samples collected by E.R. Gee in 1936, from a carbonaceous shale about 7.6 m (25 feet) above the top of the Tobra Formation in Kathwai in the central Salt Range (Fig. 5.1), and reported bisaccate taeniate and monosaccate pollen. Later Venkatachala & Kar (1966, 1968) reinvestigated these assemblages in more detail and erected the saccate pollen genus *Corisaccites* and the species *Corisaccites alutas* and *Corisaccites vanus*.

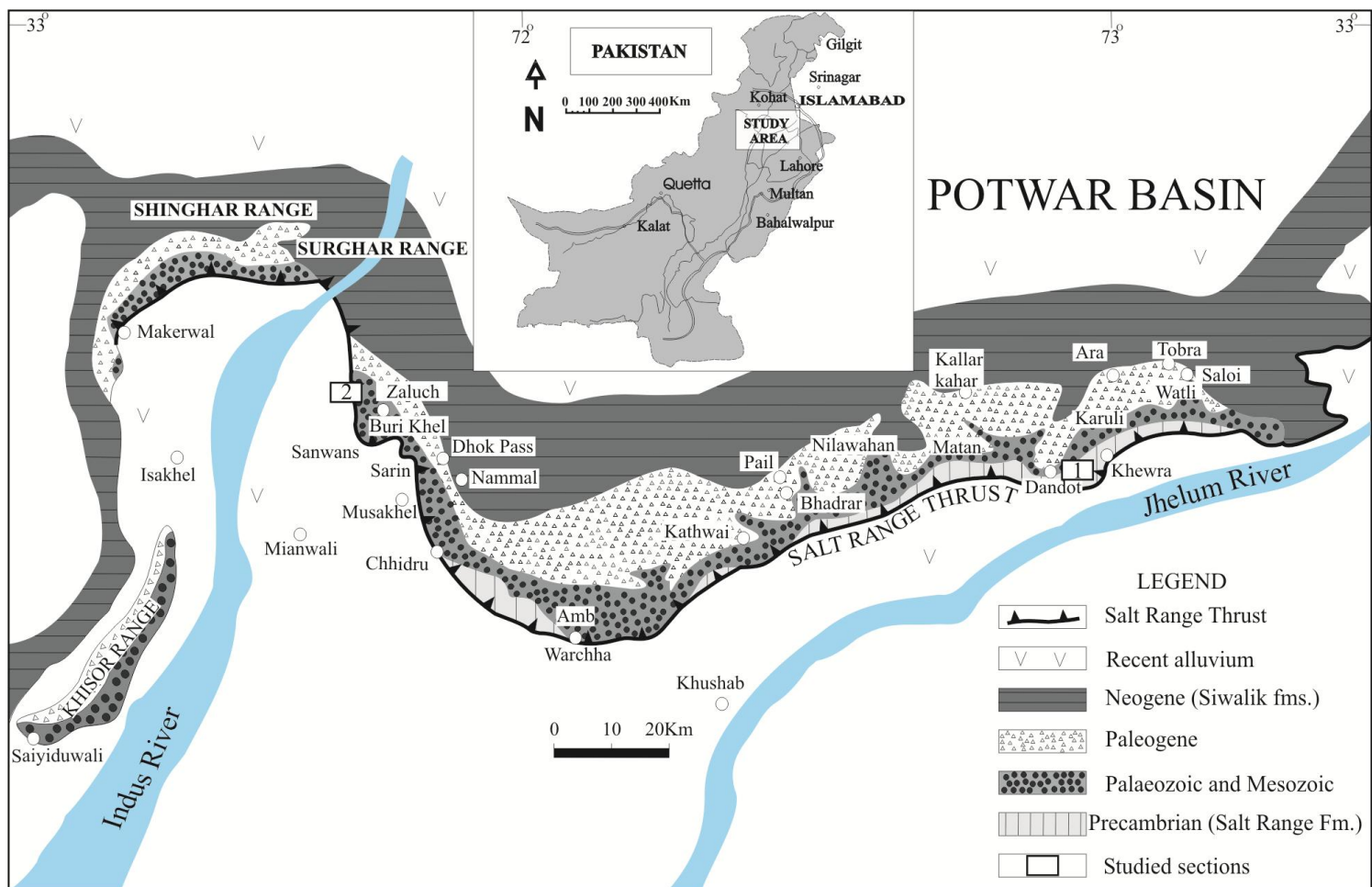


Fig. 5.1 Location map of the, 1. Khewra-Choa section (eastern Salt Range) and 2. Zaluch Nala section (western Salt Range)

(Modified after Gee 1989; Ghazi & Mountney 2009; Jan *et al.* 2009; Jan & Stephenson 2011).

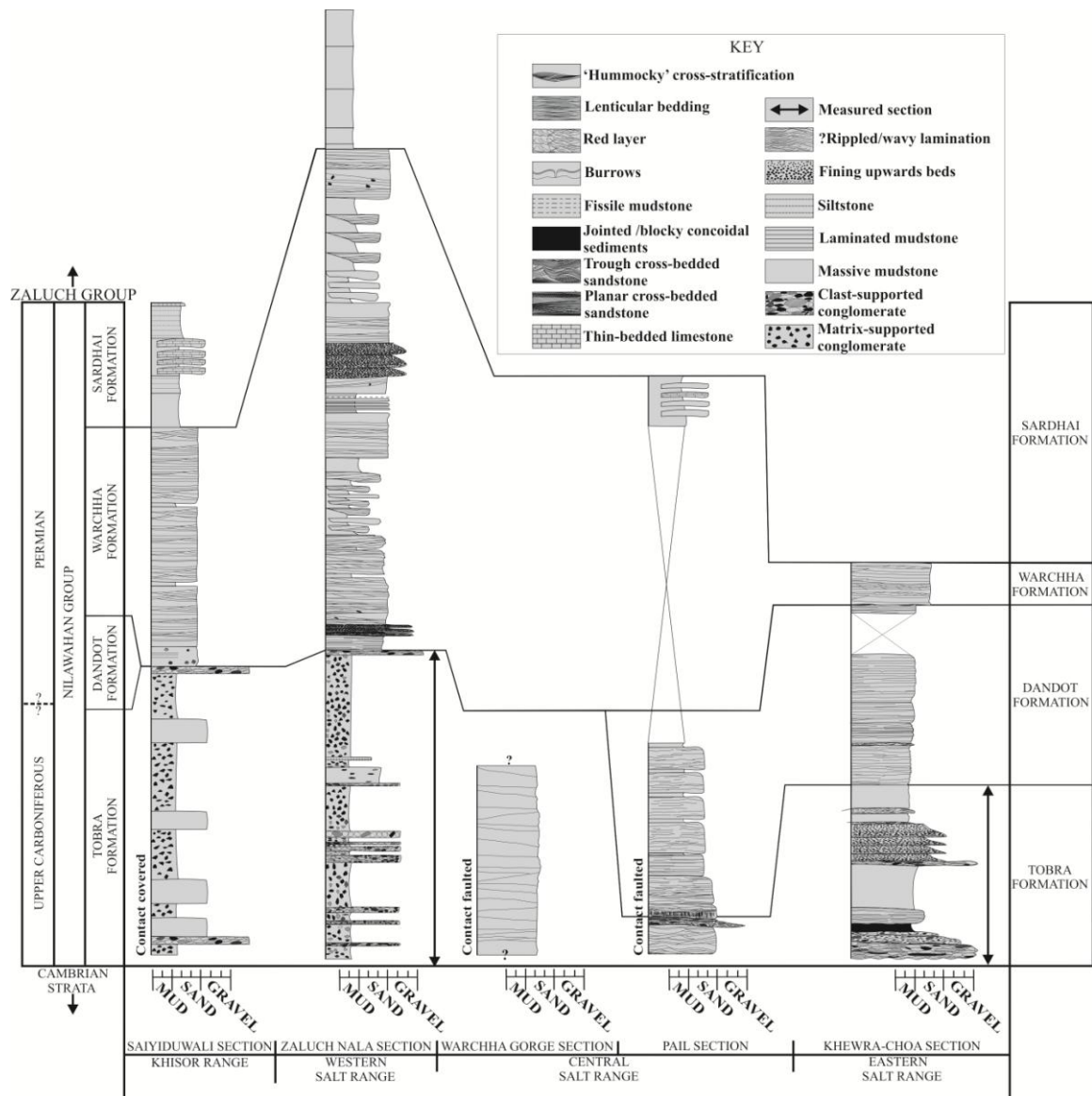


Fig. 5.2 Carboniferous-Permian stratigraphy of the Salt Range, Pakistan, showing the measured section of the Tobra Formation at Khewra-Choa section (eastern Salt Range) and Zaluch Nala section (western Salt Range; modified after Jan & Stephenson 2011).

Jan *et al.* (2009) investigated the Sardhai Formation in Zaluch Nala section (western Salt Range) and the Saiyiduwali section (Khisor Range, fig. 5.1) and reported spores, monosaccate and bisaccate pollen. Based on the presence of *Florinites? balmei*, *Thymospora opaqua* and *Camptotriletes warchianus*, the Sardhai Formation was correlated with the Khuff transition beds of Oman and the basal Khuff clastics of Saudi

Arabia (Jan *et al.* 2009). A Middle Permian (Wordian) age was assigned to the Sardhai Formation (Jan *et al.* 2009).

Balme (1970) made a detailed taxonomic survey of the carbonate-dominated succession of the overlying Amb, Wargal and Chhidru formations. He recovered pollen and spores from the plant-bearing horizons of the Amb Formation at three localities in the Salt Range: Zaluch Nala, Dhodha Wahan, and near the Warchha Water Tank. Trilete spores represented were: *Acanthotriletes tereteangulatus*, *Camptotriletes warchianus*, *Leiotriletes cf. adnatus*, *Lophotriletes novicus* and *Verrucosisporites sp. cf. V. planiverrucatus*, while *Reticuloidosporites warchianus* was the only monolete spore taxon. The monosaccate pollen included *Plicatipollenites indicus* and *Potonieisporites novicus*. Balme (1970) reported a high diversity of bisaccate pollen including the taeniate taxa *Corisaccites alutas*, *Guttulapollenites hannonicus*, *Hamiapollenites insolitus*, *Lueckisporites singhii*, *Protohaploxylinus limpidus*, *P. goraiensis*, *P. diagonalis*, *P. varius*, *Striatopodocarpites cancellatus*, *S. rarus* and *S. pantii*. Non-taeniate bisaccate taxa included *Alisporites tenuicarpus*, *Falcisporites nuthallensis*, *Pinuspollenites thoracatus*, *Sulcatisporites ovatus*, *S. nilssoni* and *Vitreisporites pallidus*.

5.3 Present palynological investigation

The Carboniferous-Permian succession of the Salt Range represents the southern side of a rift flank basin, along the northern Gondwanan coastal margin (Wardlaw & Pogue 1995) and this palaeogeographically important area has been the focus of a number of studies (e.g. Pakistani-Japanese Research Group 1985; Wardlaw & Pogue 1995; Mertmann 1999; Jan *et al.* 2009).

Most of the previous palaeontological work has been concentrated on the taxonomy of various palaeontological groups and Permian-Triassic boundary problems (e.g. Waagen

1882-1885; Noetling 1901; Diener 1912; Grabau 1931; Balme 1970; Kummel & Teichert 1970; Rowell 1970; Grant 1970; Glenister & Furnish 1970; Kummel 1970; Sohn 1970; Sweet 1970; Sarjeant 1970).

The aim is to correlate the lowest of the Carboniferous-Permian Salt Range lithostratigraphic units, the Tobra Formation, with the palaeogeographically-nearby (Sengör 1979; Ricou in Dercourt *et al.* 1993; Ziegler *et al.* 1998; Gaetani *et al.* 2000; Angiolini 2001; Jan *et al.* 2009) and stratigraphically best-resolved Arabian (Stephenson *et al.* 2003; Penney *et al.* 2008) and Australian sections (Backhouse 1991; Jones & Truswell 1992). The present palynological investigation was carried out on samples of the Tobra Formation at two localities in the Salt Range, these being the Khewra-Choa section (eastern Salt Range) and the Zaluch Nala section (western Salt Range, figs. 5.1 & 5.2). Forty-one samples were collected from a 125 metre-thick section of the Tobra Formation at Zaluch Nala (western Salt Range, figs. 5.1. & 5.3). Three additional samples of the Tobra Formation at the Khewra-Choa section (eastern Salt Range) were also investigated (Figs. 5.1 & 5.4).

5.3.1 Palynology of the Tobra Formation at Zaluch Nala section, western Salt Range

Assemblages from the Tobra Formation at Zaluch Nala section (western Salt Range) are shown in Fig. 5.5 and some important taxa are shown in Plates 6 & 7. Two palynological assemblages are identified from the Tobra Formation. The lower assemblages, i.e. between 84 and 73 m (5 samples), are dominated by the *Punctatisporites* Group of Penney *et al.* (2008) (*Punctatisporites* spp., and *Retusotriletes* sp.) constituting an average 20% of the assemblages.

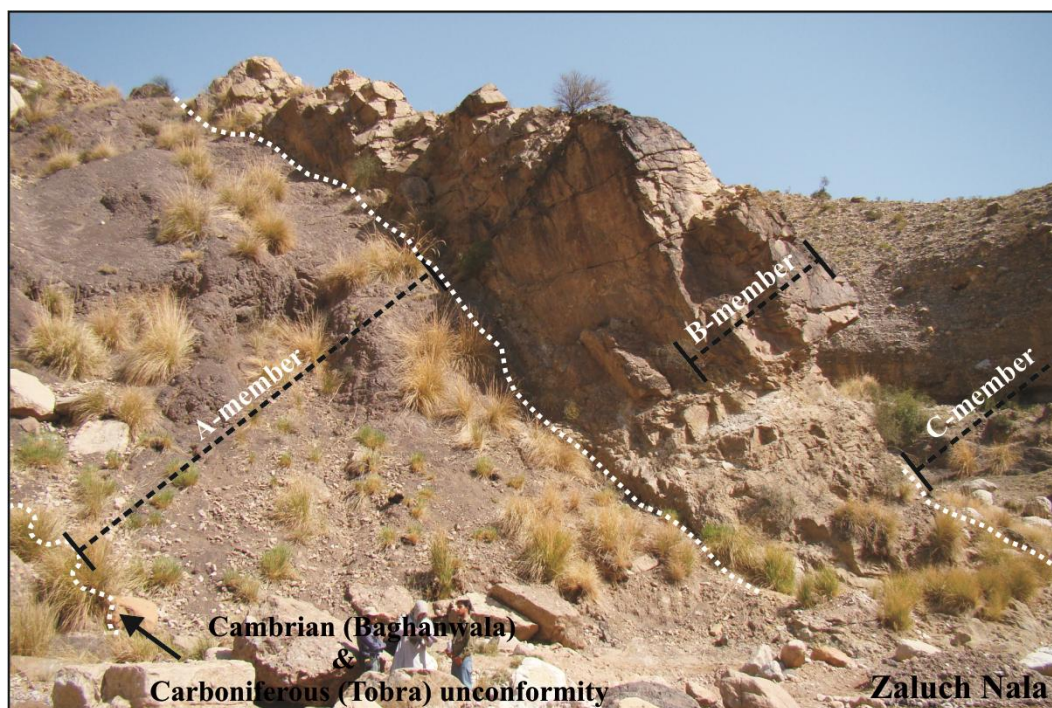


Fig. 5.3 Tobra Formation near the entrance to the Zaluch Nala section
(From Jan & Stephenson 2011).

Cingulicamerate spores (see Penney *et al.* 2008) represent 18% of assemblages (*Cristatisporites crassilabratus*, *Cristatisporites* spp., *Lundbladispora braziliensis*, *Vallatisporites arcuatus* and *Vallatisporites* spp.). Indeterminate spores also make up 18% of this lower assemblage. The monosaccate pollen *Cannanoropollis janakii*, *Plicatipollenites malabarensis*, *Potonieisporites novicus* and *Potonieisporites* spp. make up 6% of these lower assemblages (Fig. 5.5). The *Horriditriletes* Group (*Horriditriletes tereteangulatus*, *Horriditriletes ramosus* and *Horriditriletes uruguiensis*) and the *Microbaculispora* Group (mostly *Microbaculispora tentula*) make up 1% each. The upper assemblages, i.e. between 47 and 0 m (29 samples), are dominated by the *Punctatisporites* Group which makes up on average 17% of the assemblages, followed by the cingulicamerate spores, which represent 13%.

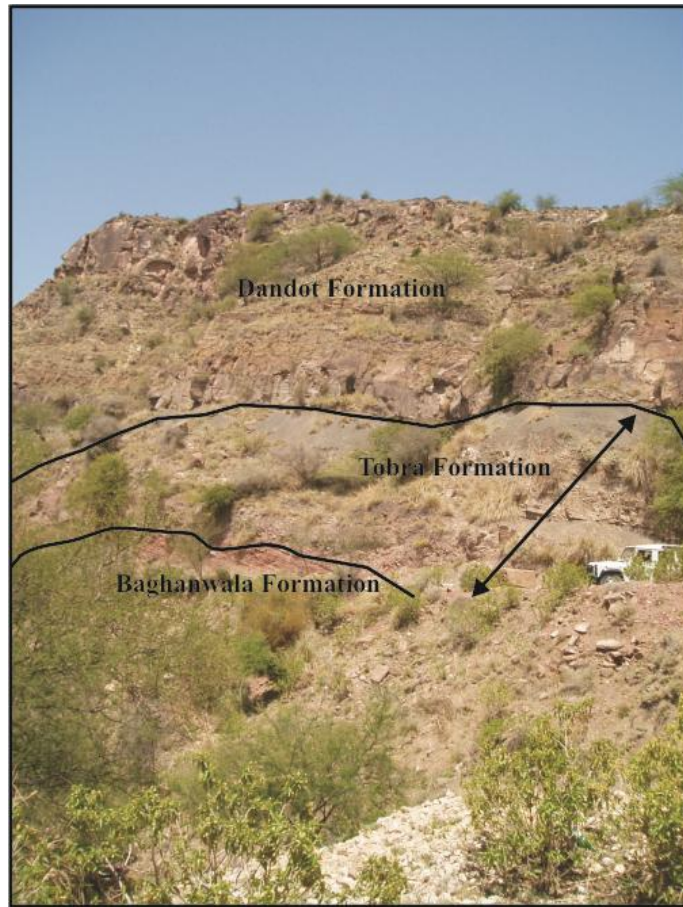


Fig. 5.4 The Tobra Formation in the Khewra-Choa section (eastern Salt Range).

The *Horriditriletes* Group makes up 11% of the upper assemblages and the *Microbaculispora* Group (*Microbaculispora tentula* and *Converrucosisporites grandegranulatus*) represent 4%. *Brevitriletes cornutus*, *Brevitriletes parmatus* and *Brevitriletes leptocaina* are generally rare, but from 23 m, *Brevitriletes leptocaina* becomes common. Radially- and bilaterally-symmetrical monosaccate pollen are represented by poorly-preserved common *Barakarites* cf. *rotatus* and *Plicatipollenites malabarensis*. *Cannanoropollis janakii* is also present. Taeniate and non-taeniate bisaccate pollen are represented by *Hamiapollenites* spp., *Limitisporites rectus*, *Protohaploxylinus* cf. *hartii* and *Striatopodocarpites* spp. *Cycadopites cymbatus* and

Converrucosisporites grandegranulatus also occur first in these assemblages.

Indeterminate monosaccate and bisaccate pollen (taeniate and non-taeniate) and spores are present throughout (Fig. 5.5).

5.3.2 Palynology of the Tobra Formation at Khewra-Choa section, eastern Salt Range

The analyses of three samples of the Tobra Formation at the Khewra-Choa section (eastern Salt Range, fig. 5.4), near Dandot village resulted in the identification of taxa that resembled the palynological assemblages of the Tobra Formation at Zaluch Nala section (western Salt Range, fig. 5.3). The yield of the samples was not very good;

however it was possible to count 200 taxa in each slide (Fig. 5.6). The assemblages are mostly dominated by the *Punctatisporites* Group, constituting about 20% of the assemblages, followed by the *Horriditriletes* Group, representing about 16% (Fig. 5.6).

The monosaccate pollen, represented mainly by *Barakarites* cf. *rotatus*, *Plicatipollenites malabarensis*, *Cannanoropollis* sp., and *Potonieisporites novicus*, constituted about 16% of the assemblages. The indeterminate spores were represented by 10%, followed by 5% *Microbaclispora* Group (mainly *Microbaculispora tentula* and *Converrucosisporites grandegranulatus*).

The palynological yields of the Tobra Formation within the Zaluch Nala section (western Salt Range) are better represented than those of the Tobra Formation in the Khewra-Choa section (eastern Salt Range). Therefore the Zaluch Nala section is considered as a reference section for palynostratigraphic investigation of the Tobra Formation in a regional context.

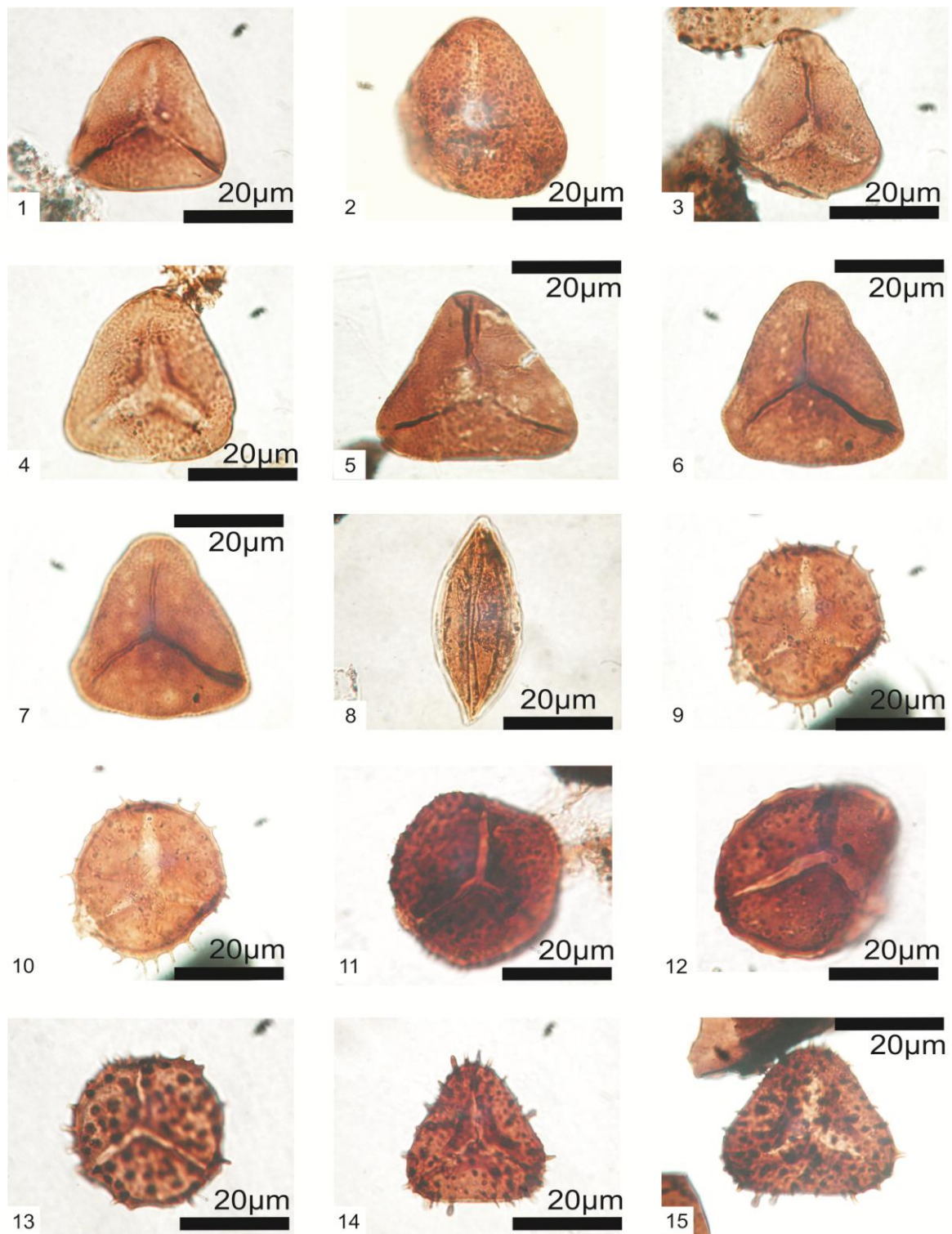


Plate 6

Plate 6 Selected palynomorphs from the Tobra Formation, Zaluch Nala section (western Salt Range), followed by slide number and England Finder coordinates.

- (1). *Converrucosisporites grandegranulatus*, MPA-57518, S17/1.
- (2). *Converrucosisporites grandegranulatus*, MPA-57518, H19/2.
- (3). *Microbaculispora tentula*, MPA-57517, W15/1.
- (4). *Microbaculispora tentula*, MPA-57519, K27/3.
- (5). *Microbaculispora tentula*, MPA-57511, V14.
- (6). *Microbaculispora tentula*, MPA-57511, T26 (proximal focus).
- (7). *Microbaculispora tentula*, MPA-57511, T26 (distal focus).
- (8). *Cycadopites cymbatus*, MPA-57518, V4/3.
- (9). *Brevitriletes leptocaina*, MPA-57512, T11/4 (proximal focus).
- (10). *Brevitriletes leptocaina*, MPA-57512, T11/4 (distal focus).
- (11). *Brevitriletes parmatus*, MPA-57517, O18.
- (12). *Brevitriletes parmatus*, MPA-57512, Q11/2.
- (13). *Brevitriletes cornutus*, MPA-58394, N10.
- (14). *Horriditriletes ramosu*, MPA-57520, H11.
- (15). *Horriditriletes ramosus*, MPA-58384, X12/1.

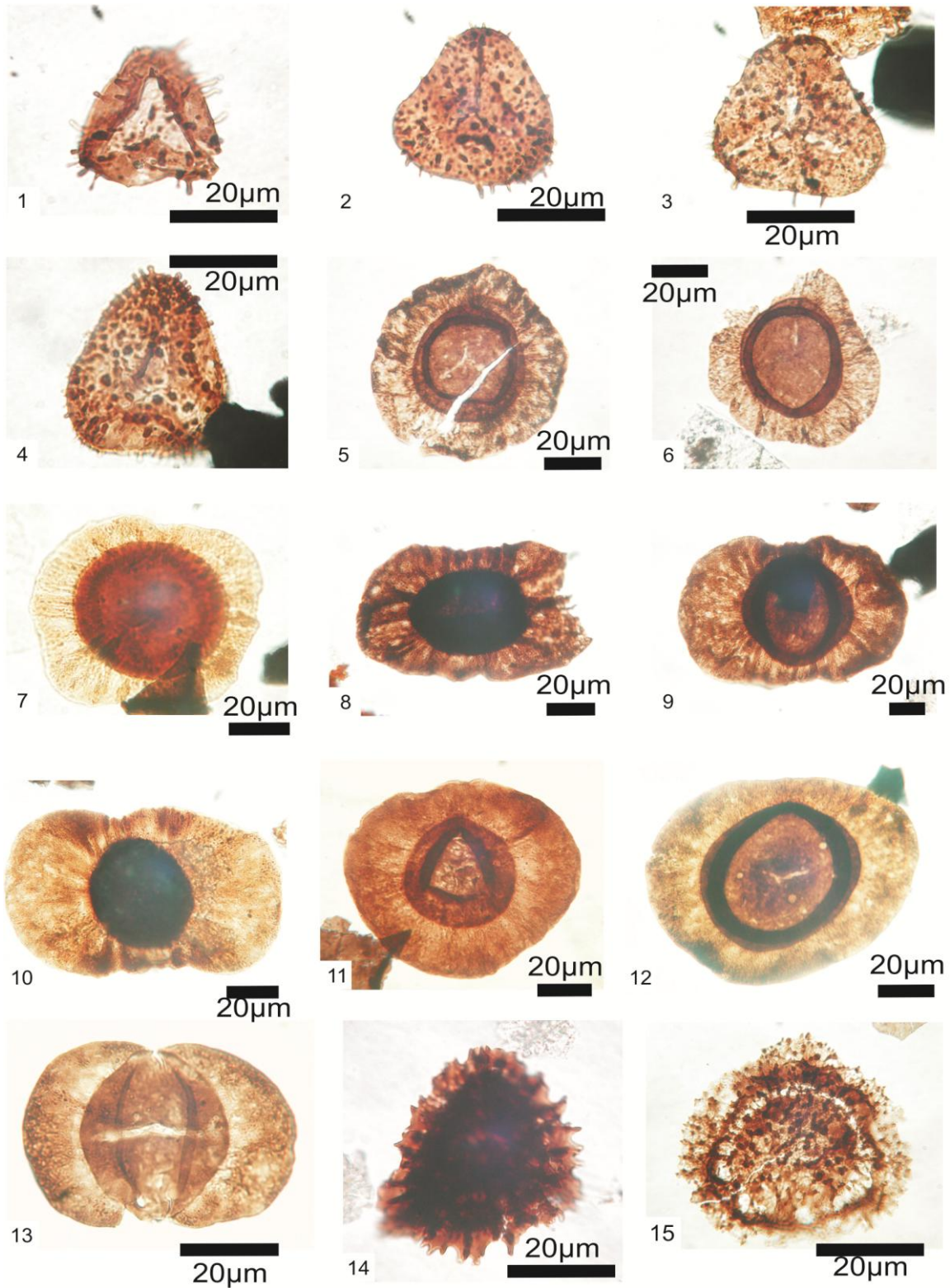


Plate 7

Plate 7 Selected palynomorphs from the Tobra Formation, Zaluch Nala section (western Salt Range), followed by slide number and England Finder coordinates.

- (1). *Horriditriletes ramosus*, MPA-57511, W20/3.
- (2). *Horriditriletes tereteangulatus*, MPA-57512, S17/4.
- (3). *Horriditriletes tereteangulatus*, MPA-57519, W7.
- (4). *Horriditriletes uruguiensis*, MPA-57511, W20/3.
- (5). *Plicatipollenites malabarensis*, MPA-57513, K11/1.
- (6). *Plicatipollenites malabarensis*, MPA-57515, P4/2.
- (7). *Cannonoropollis janakii*, MPA-58401, X21/3.
- (8). *Potonieisporites brasiliensis*, MPA-57512, P18/3.
- (9). *Potonieisporites brasiliensis*, MPA-57513, K19/2.
- (10). *Potonieisporites brasiliensis*, MPA-57514, O6.
- (11). *Potonieisporites* sp., MPA-57765, U28/4.
- (12). *Plicatipollenites* sp., MPA-58384, U5.
- (13). *Limitisporites rectus*, MPA-58401, R22/2.
- (14). *Cristatisporites crassilabratus*, MPA-57761, V30/2.
- (15). *Vallatisporites arcuatus*, MPA-57511, X12/1.

5.4 Correlation of the Tobra Formation

Much palynological work in the Carboniferous-Permian Gondwanan basins is concerned with exploration for coal, oil and gas (Playford & Dino 2005; Stephenson 2008a). The absence of a Gondwana-wide biostratigraphic framework has hampered inter-basinal correlation and correlation with the international chronostratigraphic stages (Stephenson 2008a). Rare marine intervals in the Australian and Arabian Carboniferous-Lower Permian succession allow limited calibration of palynological biozones with the International stages (e.g. Leonova 1998; Archbold 1999; Stephenson 2008a), and Australian and Arabian palynological biozones are generally well-documented (Backhouse 1991; Jones & Truswell 1992; Stephenson *et al.* 2003; Penney *et al.* 2008).

5.4.1 Correlation with Arabia

5.4.1.1 Correlation with Oman

A detailed biozonation of the Al Khlata Formation of South Oman was presented by Penney *et al.* (2008), based on quantitative trends of spore and pollen groups and the ranges of a few single taxa (Fig. 5.7). The *Horriditriletes* Group of Penney *et al.* (2008), represented by *Horriditriletes tereteangulatus*, *Horriditriletes ramosus* and *Horriditriletes uruguayensis*, constitutes 5 to 10 % (rarely 20%) of the 2165B Biozone. The *Horriditriletes* Group is present throughout the Zaluch Nala assemblages; however it becomes dominant and consistent in the upper assemblages, between 46 and 4 m (Fig. 5.5). Similar percentages of the *Microbaculispora* Group occur in the Zaluch Nala upper assemblages and in 2165B Biozone. However *Converrucosisporites confluens* which is present towards the top of 2165B is absent from Zaluch Nala.

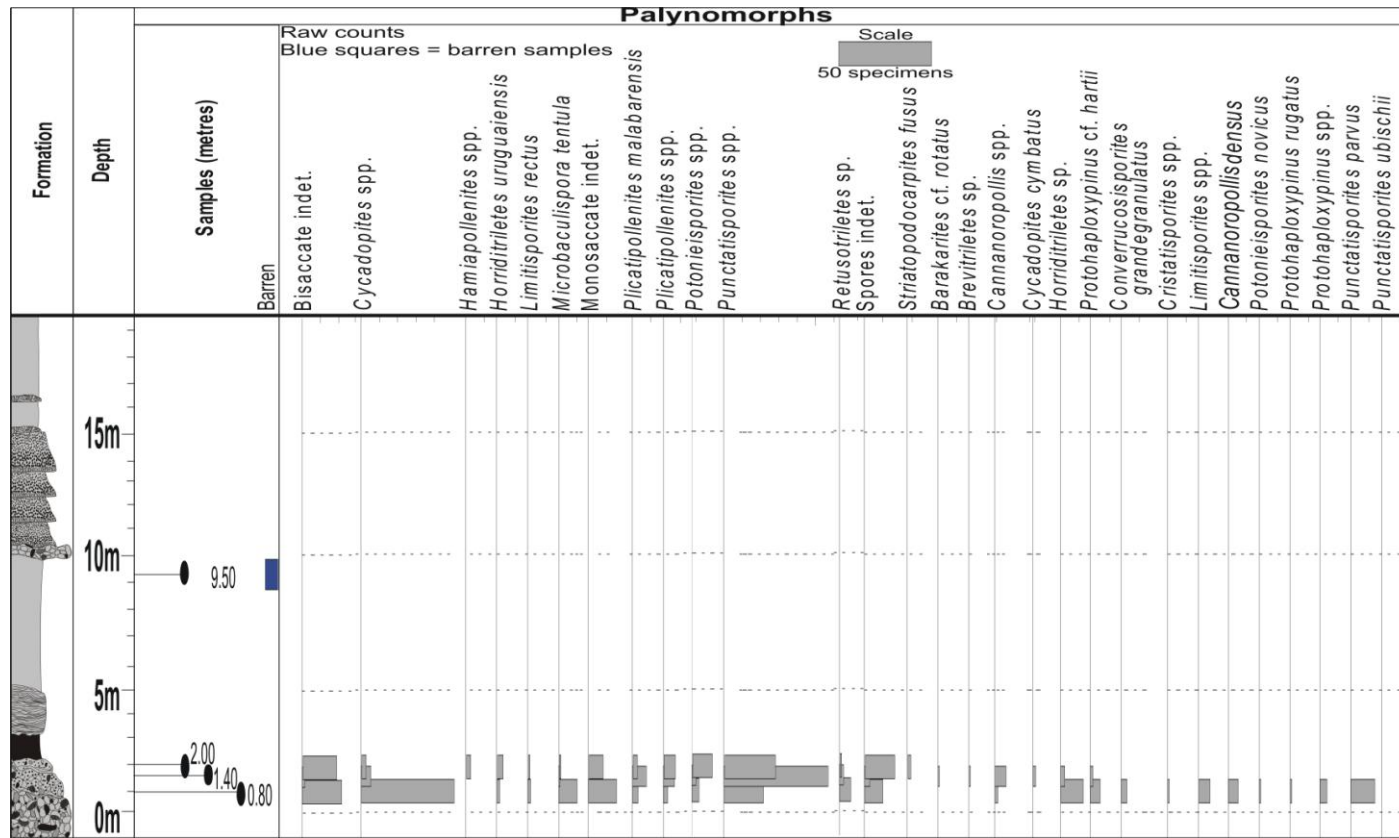


Fig. 5.6 Abundance chart for the Tobra Formation, Khewra-Choa section (eastern Salt Range).

Converrucosisporites grandegrnulatus and *Cycadopites cymbatus* first occur within 2165B but these taxa are not present in 2165A which supports the correlation with 2165B. This suggests that the upper assemblages from Zaluch Nala correspond to the 2165B Biozone of South Oman, probably below the stratigraphic level where *Converrucosisporites confluens* appears first (Fig. 5.5). The 2165A Biozone, underlying 2165B, is identified by rare to 5% presence of the *Microbaculispora Group* and 30% presence of cingulicamerate spores (Penney *et al.* 2008). This biozone also contains 5% *Anapiculatisporites concinnus* and rare *Horriditriletes Group*. Monosaccate pollen and members of the *Punctatisporites* group are abundant (Penney *et al.* 2008, fig. 5.7). These data suggest that the lower Zaluch Nala assemblages are similar to those of 2165A because the samples contain 20% *Punctatisporites* spp., 18% cingulicamerate spores and 6% monosaccate pollen. However, the stratigraphically lower assemblages of Zaluch Nala differ from those of the 2165A Biozone by lacking *Anapiculatisporites concinnus*. The Zaluch Nala section does not correlate with the 2141A Biozone (which overlies the 2165B Biozone) because that biozone contains 5 to 10% *Cycadopites cymbatus* and 10% non-taeniate and taeniate bisaccate pollen.

The 2141A Biozone also contains the first occurrences of *Circumstriatites talchirensis*, *Kingiacolpites subcircularis*, *Marsupipollenites striatus*, *Pakhapites fusus*, *Striatites tectus*, *Vittatina subsaccata* and *Vittatina cf. scutata*, none of which were recorded in the Zaluch Nala section. Thus, the upper Zaluch Nala assemblages correlate with the 2165B Biozone which corresponds to the upper part of the Biozone C and lower part of the Biozone B of the Mukhaizna Field of Oman (Stephenson *et al.* 2008, fig. 5.8). The 2165B Biozone also corresponds with the P5 production unit of Petroleum Development Oman (Penney *et al.* 2008). At present, the lower Zaluch Nala assemblages are only tentatively correlated with the 2165A Biozone.

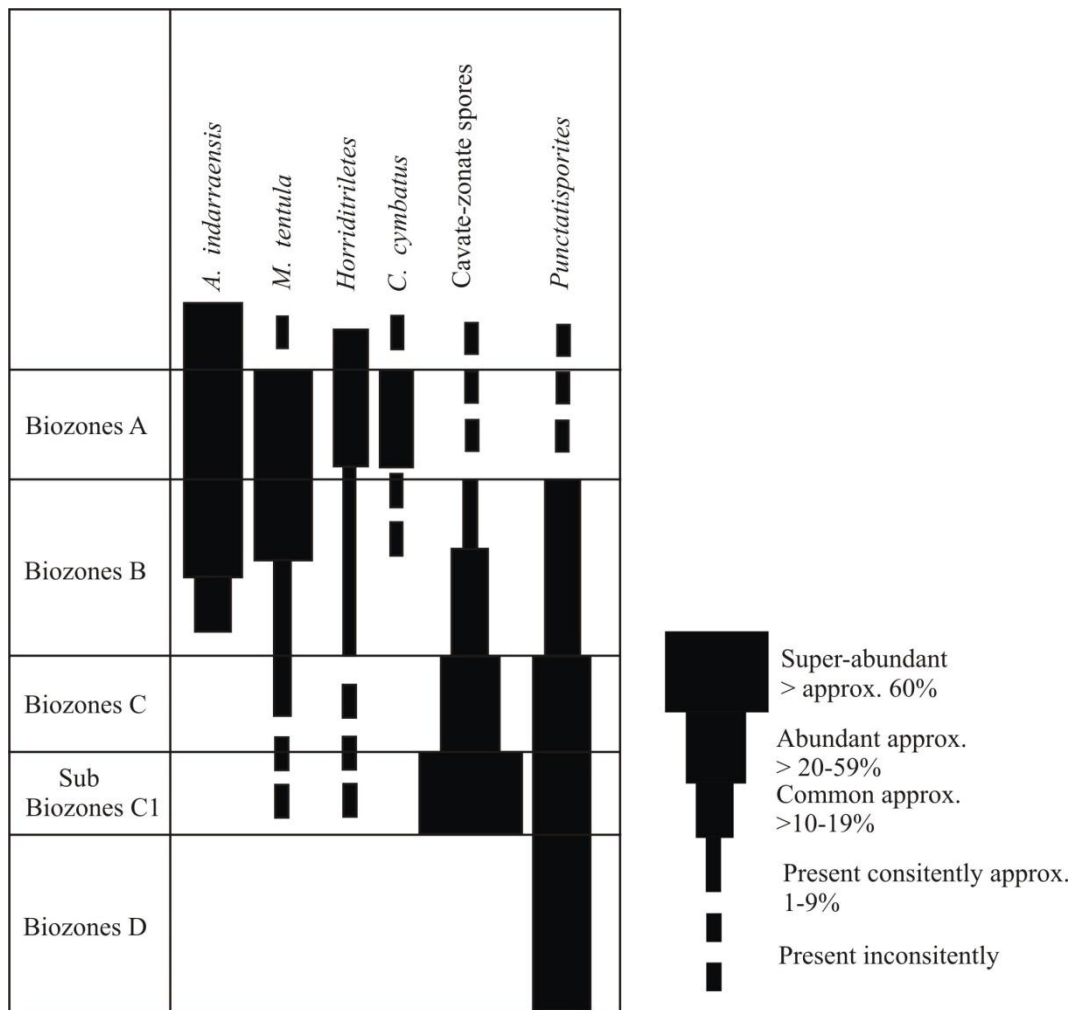


Fig. 5.8 The Mukhaizna Field, south Oman biozonation, showing stratigraphically important taxa (Modified after Stephenson *et al.* 2008).

5.4.1.2 Correlation with Saudi Arabia

The base of the Oman and Saudi Arabia Palynological Zone 2 i.e. OSPZ2 (Stephenson *et al.* 2003) is defined by the first occurrence of *Horriditriletes* spp. and *Microbaculispora tentula*, these taxa make up about 20-30% of the assemblages in OSPZ2 (Fig. 5.9). In the Zaluch Nala section (in both lower and upper assemblages; fig. 5.5), *Horriditriletes* spp. constitute an average of 8% of assemblages, and *Microbaculispora tentula* 2% of the assemblages.

Palynostratigraphy		OSPZ1	OSPZ2	OSPZ3			OSPZ4	OSPZ5	OSPZ6
				a	b	c			
Schematic ranges of selected palynomorphs	<i>Angulisporites cf. splendidus</i>	■							
	<i>Anapiculatisporites concinnus</i>								
	<i>Granulatisporites confluens</i>		■						
	<i>Horriditriletes ramosus</i>		■						
	<i>Microbaculispora tentula</i>		■						
	Common <i>Alisporites indarraensis</i>			■	■	■			
	<i>Ulanisphaeridium omanensis</i>				■				
	<i>Divarisaccus sp. A</i>					■			
	<i>Cyclogranisporites pox</i>					■			
	<i>Corisaccites alutas</i>						■	■	■
	Common <i>Barakarites rotatus</i>						■	■	■
	<i>Distriatites sp. A</i>							■	■
	<i>Distriatites insolitus</i>							■	■
	<i>Cedripites sp. A</i>								■
	<i>Indotriradites sp. C</i>								■
	<i>Playfordiaspora cancellosa</i>								■
	<i>Lueckisporites virkkiae</i>								■
	<i>Triplexisporites cf. Playfordii</i>								■
	<i>Pyramidosporites cyathodes</i>								■
	<i>Camptotriletes warchianus</i>								■
<i>Protohaploxypinus uttingii</i>								■	
? <i>Florinites balmei</i>								■	

Fig. 5.9 Oman and Saudi Arabia Palynological Zone schemes

(From Stephenson *et al.* 2003).

Other taxa of OSPZ2 are *Brevitriletes parmatus*, *Brevitriletes leptoacaina* and *Cycadopites cymbatus*, which are also found in Zaluch Nala. *Converrucosisporites confluens* occurs first in the upper part of the OSPZ2, but this is absent from Zaluch Nala. Thus the qualitative and quantitative character of the Zaluch Nala assemblages suggests correlation with the lower part of OSPZ2 (Stephenson *et al.* 2003).

The Zaluch Nala assemblages do not correlate with the OSPZ1 Biozone (Stephenson *et al.* 2003, fig. 5.9) because they do not contain *Angulisporites cf. splendidus* and because *Punctatisporites* spp., and *Retusotriletes* spp., are more common (50% of the assemblages) in the OSPZ1 Biozone than in the Zaluch Nala assemblages, for example *Retusotriletes* spp., rarely reaches 3% at Zaluch Nala. Likewise the OSPZ3 Biozone (Stephenson *et al.* 2003) contains very numerous non-taeniate and taeniate bisaccate

pollen (e.g. *Alisporites indarraensis*) and the Zaluch Nala assemblages contain few pollen of this type and *Alisporites indarraensis* is not recorded.

5.4.1.3 Correlation with Yemen

The palynology of the Khulan Formation of Yemen has been recently studied by Stephenson & Al-Mashaikie (2010, 2011). The palynological assemblages are represented by brown, moderately- to well-preserved palynomorphs, woody, and cellular material and AOM. The most commonly present taxa included, indeterminate monosaccate pollen (e.g. *Cannanoropollis*, *Potonieisporites* and *Plicatipollenites*), *Cristatisporites* spp., *Cannanoropollis janakii*, *Deusilites tentus*, *Leiosphaeridia* sp., and *Punctatisporites* spp. Other commonly found taxa are; *Anapiculatisporites concinnus*, *Brevitriletes cornutus*, *B. parmatus*, *Dibolisporites disfacies*, *Horriditriletes uruguayensis*, *H. ramosus*, *Lundbladispora braziliensis*, *Microbaculispora tentula*, *Spelaeotriletes triangulus*, *Verrucosisporites andersonii* and *Vallatisporites arcuatus*. The taxa in the Khulan Formation are identical to those of the Al Khlata Formation's 2165A to 2141A biozones (Stephenson & Al-Mashaikie 2010). Their quantitative characters helped interpret part of the Khulan Formation equivalent to the lower part of the OSPZ2, and biozone C and B of South Oman Mukhaizna field (Stephenson & Al-Mashaikie 2010, their Fig. 4).

The Tobra Formation assemblages are tentatively correlated to the Khulan Formation of Yemen, with the portion where taxa like *Brevitriletes cornutus*, *B. parmatus* and *Microbaculispora tentula* occur, however these assemblages diverge from the Khulan Formation assemblages by not having *Anapiculatisporites concinnus*, *Deusilites tentus*, *Dibolisporites disfacies* and *Spelaeotriletes triangulus*.

5.4.2 Correlation with Australia

In eastern Australia, the base of Stage 2 was originally defined by Evans (1969) as the horizon at which taeniate bisaccate first appear, however Powis (1984) redefined the base of Stage 2 as the collective first appearance of such cheilocardioid spores as *Horriditriletes ramosus*, *Horriditriletes tereteangulatus* and *Microbaculispora tentula*. Jones and Truswell (1992) correlated their *Microbaculispora tentula* Opper-zone (E) based in the Galilee Basin, eastern Australia with Powis' Stage 2 and erected four lower (Carboniferous) Biozones.

The base of the eastern Australian *Microbaculispora tentula* Opper-zone is defined by the first occurrence of *Microbaculispora tentula*, constituting 0.5% of the assemblages (Jones & Truswell 1992). *Microbaculispora tentula* in the Zaluch Nala (collectively in the lower and upper assemblages) constitutes 2%. Other taxa common to the Zaluch Nala assemblages and the *Microbaculispora tentula* Opper-zone are: *Brevitriletes leptocaina*, *Cannanoropollis janakii*, *Cristatisporites* spp., *Horriditriletes ramosus*, *Cannanoropollis densus* and *Punctatisporites* spp. (Fig. 5.5). The Zaluch Nala assemblages (both lower and upper), differ from the *Asperispora reticulatispinosus* Opper-zone (Jones & Truswell 1992), that underlies the *Microbaculispora tentula* Opper-zone, in lacking *Asperispora reticulatispinosus*, *Retusotriletes nigrifellus*, and *Apiculatisporis pseudoheles*. Thus, the Zaluch Nala section assemblages are correlated to the eastern Australian *Microbaculispora tentula* Opper-zone.

In Western Australia, Foster & Waterhouse (1988) established the *Converrucosisporites* (*Granulatisporites*) *confluens* Opper-zone in the Calytrix No. 1 borehole in the Canning Basin. They believed the zone to be the biostratigraphic equivalent of Stage 2 of Powis (1984). Backhouse (1991, 1993) reported that *C. confluens* does not have a stratigraphic range consistent with that of Stage 2 in the Collie and southern Perth Basins, Western

Australia. In the latter basins Backhouse indicated that *C. confluens* is preceded by Stage 2 assemblages (without *G. confluens*) and succeeded by Stage 3 assemblages. Backhouse therefore considered the *C. confluens* Oppel-zone to be a separate biostratigraphic unit to Stage 2.

The Zaluch Nala assemblages are similar to Stage 2 (*sensu* Backhouse 1991), because they contain *Cycadopites cymbatus*, *Horriditriletes ramosus* and *Microbaculispora tentula* and because they lack *Converrucosisporites confluens* (Fig. 5.5).

5.4.3 Correlation with South American

5.4.3.1 Correlation with Chacoparana Basin, Argentina

The palynozonation scheme of the Chacoparana Basin, Argentina was established by Russo *et al.* (1980). These workers formulated 3 palynozones in the upper Palaeozoic Ordóñez and Victoria Rodríguez formations, namely, *Potonieisporites-Lundbladispota*, *Cristatisporites* and *Striatites* zones. The refinement of this scheme by Vergel (1993) and later by Playford & Dino (2002), shows that the base of the upper part of *Potonieisporites-Lundbladispota* Zone is represented by the first occurrence of *Cristatisporites crassilabratus* and *Horriditriletes uruguayensis*. The biozone also contains *Caheniasaccites ovatus*, *Cannanoropollis janakii*, *Granulatisporites austroamericanus* (= *Microbaculispora tentula*), *Potonieisporites brasiliensis*, *Potonieisporites novicus*, *Plicatipollenites malabarensis*, *Cannanoropollis densus* and *Plicatipollenites malabarensis*. However, these taxa are extended from the lower part of the *Potonieisporites-Lundbladispota* Zone. The overlying *Cristatisporites* Zone has abundant zonate-cavate spores, e.g. *Converrucosisporites micronodosus*, *Converrucosisporites confluens*, *Lundbladispota braziliensis* and *Vittatina saccata*. The Tobra Formation Zaluch Nala section assemblages are represented by 11% cingulicamerate spores, represented by *Cristatisporites* spp., *Vallatisporites arcuatus*,

Vallatisporites spp., *Lundbladispora braziliensis* and *Cristatisporites crassilabratus*. *Horriditriletes uruguayensis* constitutes about 3% of the Tobra Formation Zaluch Nala section assemblages and *Microbaculispora tentula* is present throughout the section. *Converrucosisporites confluens* present at the base of the *Cristatisporites* Zone is not present in the Tobra Formation, Zaluch Nala assemblages. This shows that the Tobra Formation Zaluch Nala assemblages can be correlated with the upper part of the *Potonieisporites-Lundbladispora* Zone, based on the presence of *Cristatisporites crassilabratus* and *Horriditriletes uruguayensis*. Tobra Formation Zaluch Nala assemblages differ from the overlying *Cristatisporites* Zone by lacking *Converrucosisporites confluens*.

The Tobra Formation, Zaluch Nala assemblages are different than the underlying i.e. the lower part of the *Potonieisporites-Lundbladispora* Zone, as the latter shows 20% monosaccate pollen and 15-20% bisaccate pollen in the assemblages. In the case of Tobra Formation Zaluch Nala section, the monosaccate pollen constitute about 6% of the assemblages, whereas taeniate and non-taeniate bisaccate pollen are represented by poorly preserved *Hamiapollenites* spp., *Limitisporites rectus*, *Protohaploxypinus* cf. *hartii* and *Striatopodocarpites* spp., which rarely reach 1% of the assemblages. Also taxa like *Potonieisporites neglectus*, which is present exclusively in the lower part of the *Potonieisporites-Lundbladispora* Zone, are not found in the Tobra Formation, Zaluch Nala assemblages.

5.4.3.2 Correlation with central-western Argentina

The *Raistrickia densa-Convolutispora muriornata* (DM) Assemblage Biozone (Césari & Gutiérrez 2000), is characterised by monosaccate pollen particularly *Plicatipollenites* spp., *Potonieisporites* spp., and *Cannanoropollis* spp. This biozone is also represented by the bisaccate pollen *Protohaploxypinus* spp. The Tobra Formation, Zaluch Nala

palynological assemblages can be correlated with the *Raistrickia densa-Convolutispora muriornata* (DM) Assemblage Biozone, as they contain *Cannanoropollis* spp., *Plicatipollenites* spp., *Protohaploxypinus* spp.

The difference between the Tobra Formation, Zaluch Nala palynological assemblages and the *Raistrickia densa-Convolutispora muriornata* (DM) Assemblage Biozone is however, the absence of certain taxa, e.g. *Apiculiretusispora variornata*, *A. alonsoi*, *A. teuberculata*, *Anapiculatisporites argentinensis*, *Convolutispora muriornata*, *Cristatisporites inconstans*, *Foveosporites hortonensis*, *Granulatisporites varigranifer*, *Raistrickia rotunda*, *R. densa* and *Vallatisporites ciliaris*.

The base of the overlying *Fusacolpites fusus-Vittatina subsaccata* (FS) Interval Biozone (Césari & Gutiérrez 2000), is marked by first appearance of *Fusacolpites fusus* and increase in the striate pollen grain. The taxa typical to this biozone include, *Barakarites rotatus*, *Vittatina subsaccata*, *Hamiapollenites fusiformis*, *Striatoabieites multistriatus*, *Granulatisporites* sp. *Lophotriletes rarus* and *Apiculatisporis cornutus*. The presence in the Tobra Formation, Zaluch Nala assemblages of *Barakarites* cf. *rotatus* also characterises the tentative correlation of the assemblages with the *Fusacolpites fusus-Vittatina subsaccata* (FS) Interval Biozone.

No common taxa are found between the Tobra Formation, Zaluch Nala palynological assemblages and the stratigraphically lower *Cordylosporites-Verrucosisporites* (CV) Assemblage Biozone.

5.4.3.3 Correlation with Amazonas Basin, Brazil

The *Illinites unicus* Zone is defined by the association of *Illinites unicus*, *Spelaeotriletes triangulus*, *S. arenaceus* and spores like *Vallatisporites* and *Cristatisporites*.

Protohaploxypinus spp., show an increase from the lower palynozone, i.e.

Striomonosaccites incrassatus Zone (Playford & Dino 2000). The lower limit of the

Illinites unicus Zone is well delineated by the incoming of taxa such as, *Barakarites rotatus*, *Cycadopites* sp., and *Vallatisporites arcuatus*, whereas the top of this biozone (and the base of the overlying *Stratosporites heyleri* Zone, is marked by the introduction of *Apiculatasporites daemonii*.

The Tobra Formation Zaluch Nala assemblages representing *Barakarites* cf. *rotatus*, *Vallatisporites arcuatus* and *Cycadopites* sp., and lacking *Apiculatasporites daemonii*, can be correlated tentatively with the *Illinites unicus* Zone (Playford & Dino 2000).

5.4.4 Correlation with India

The base of the *Parasaccites korbaensis* Assemblage-Zone (Tiwari & Tripathi 1992) is defined by the first occurrence of *Microbaculispora tentula* and *Microfoveolatispora foveolata*. Other taxa common in this biozone are; *Parasaccites korbaensis*, *Callumispora gretensis*, *Circumstriatites obscurus* and *C. talchirensis*. The top of this biozone is defined by the oldest occurrence of *Crucisaccites monoletus*. At present only a tentative correlation of the Tobra Formation Zaluch Nala palynological assemblages can be suggested with the *Parasaccites korbaensis* Assemblage-Zone. Based on the presence of *Microbaculispora tentula* in Tobra Formation Zaluch Nala assemblages, it can be assumed that the assemblages are at least not older than the *Parasaccites korbaensis* Assemblage-Zone, which is represented by the FAD of *Microbaculispora tentula* (Tiwari & Tripathi 1992, fig. 5.10).

5.5 Age of the Tobra Formation Assemblages

The age of the South Oman 2165A to 2141A biozones was originally considered Early Permian (Penney *et al.* 2008), based mainly on the distribution of *Converrucosisporites confluens* in faunally-calibrated sections in Western Australia.

The *Converrucosisporites confluens* Opper-zone of Western Australia was originally considered mid- to late Asselian in age (Foster & Waterhouse 1988; Stephenson 2009). However, recent investigation of a radiometrically-dated section in Namibia (Stephenson 2009), which contains *Converrucosisporites confluens* has shown the age of the deposits as 302 ± 3.0 Ma (i.e. Upper Pennsylvanian; Gzhelian or Kasimovian), suggesting that the *C. confluens* Opper-zone is older than previously suggested and hence that the 2165A to 2141A biozones could be older than previously thought (Césari 2007; Stephenson 2009).

The Zaluch Nala assemblages correlate with those of the middle part of the Al-Khlata Formation, below sections containing *C. confluens*, (Fig. 5.10), and thus are likely Late Pennsylvanian in age.

5.6 Conclusions

The palynology samples studied from the Tobra Formation contained *Converrucosisporites grandegrulatus*, *Cycadopites cymbatus*, *Horriditriletes ramosus* and *Microbaculispora tentula*, but lacked *Converrucosisporites confluens*. This suggests that the Tobra Formation correlates to the South Oman 2165B Biozone (Penney *et al.* 2008) and the lower part of the OSPZ2 Biozone (Stephenson *et al.* 2003), and is therefore Late Pennsylvanian in age.

The Zaluch Nala assemblages are also correlated with Stage 2 (*sensu* Backhouse 1991) and the eastern Australian *Microbaculispora tentula* Opper-zone (Jones & Truswell 1992), South American Chacoparana Basin, Argentina *Potonieisporites-Lundbladispora* Zone, central-western Argentina *Raistrickia densa-Convolutispora muriornata* (DM) Assemblage Biozone and *Fusacolpites fusus-Vittatina subsaccata* (FS) Interval Biozone and Amazonas Basin, Brazil *Illinites unicus* Zone. The Zaluch Nala assemblages are also correlated with the Indian *Parasaccites korbaensis* Assemblage-Zone. The

correlation of the Zaluch Nala Tobra assemblages with the South Oman 2165B Biozone and lower part of the Oman and Saudi Arabia OSPZ2, indicates that the upper part of the glacial sequence that is commonly preserved in southern Arabia and Western Australia, including the deglaciation sequence (see Stephenson *et al.* 2007), is not represented by the Tobra Formation in Zaluch Nala. The red-bed character of the overlying Warchha Formation from which the Tobra Formation is separated by a marked unconformity, strongly suggests that the deglaciation sequence is not present above the Tobra Formation in the Zaluch Nala location. This in turn suggests that the deglaciation sequence was either never deposited or has been removed by erosion associated with the pre-Warchha Formation unconformity.

In the Khewra-Choa section (eastern Salt Range), the Dandot Formation is found above the Tobra Formation (Fig. 5.2). The Dandot Formation thus might represent deglaciation here, however the formation is barren of any palynomorphs in this study and thus it is hard to test the hypothesis.

6 ²Chapter 6: Palynology and palynostratigraphy of the Middle Permian Sardhai Formation

6.1 Abstract

Palynological assemblages from the Sardhai Formation (Permian), lying between the Warchha Formation and the Amb Formation in the Salt and Khisor ranges of Pakistan contain abundant bisaccate pollen grains and few spores. In particular, well-preserved specimens of *Florinites? balmei*, a bilaterally symmetrical monosaccate pollen grain, are common. The presence of this pollen and the stratigraphic context suggest that the Sardhai Formation correlates with the Khuff transition beds of Oman and the basal Khuff clastics of central Saudi Arabia. *Florinites? balmei* was first described by Stephenson & Filatoff in 2000 from the basal Khuff clastics of Saudi Arabia, and it has since been reported from Oman, Kuwait, southeastern Turkey, Iraq, United Arab Emirates and Qatar. This suggests that the plant that produced *Florinites? balmei* had a rather limited palaeogeographic distribution in the Mid-Permian which may be useful in reconstructing the problematic tectonic and palaeogeographic history of this complex region.

6.2 Description of the Sardhai Formation assemblages

For the present study, five samples were collected from a 22 metre-thick exposure of the Sardhai Formation at the Saiyiduwali section (Khisor Range) at N32° 11' 52.1" E 70° 59' 18.0" (Figs. 6.1, 6.2, 6.3 & 6.4), and three samples were collected from the 30 metre-thick outcrop of Sardhai Formation at Zaluch Nala section (western Salt Range) at N32° 46' 58.4" E 71° 38' 49.4" (Figs. 6.1, 6.2 & 6.5).

² This chapter is modified from the paper that is published in the Elsevier journal “*Review of Palaeobotany and Palynology*”. The published paper is included as Appendix 4.

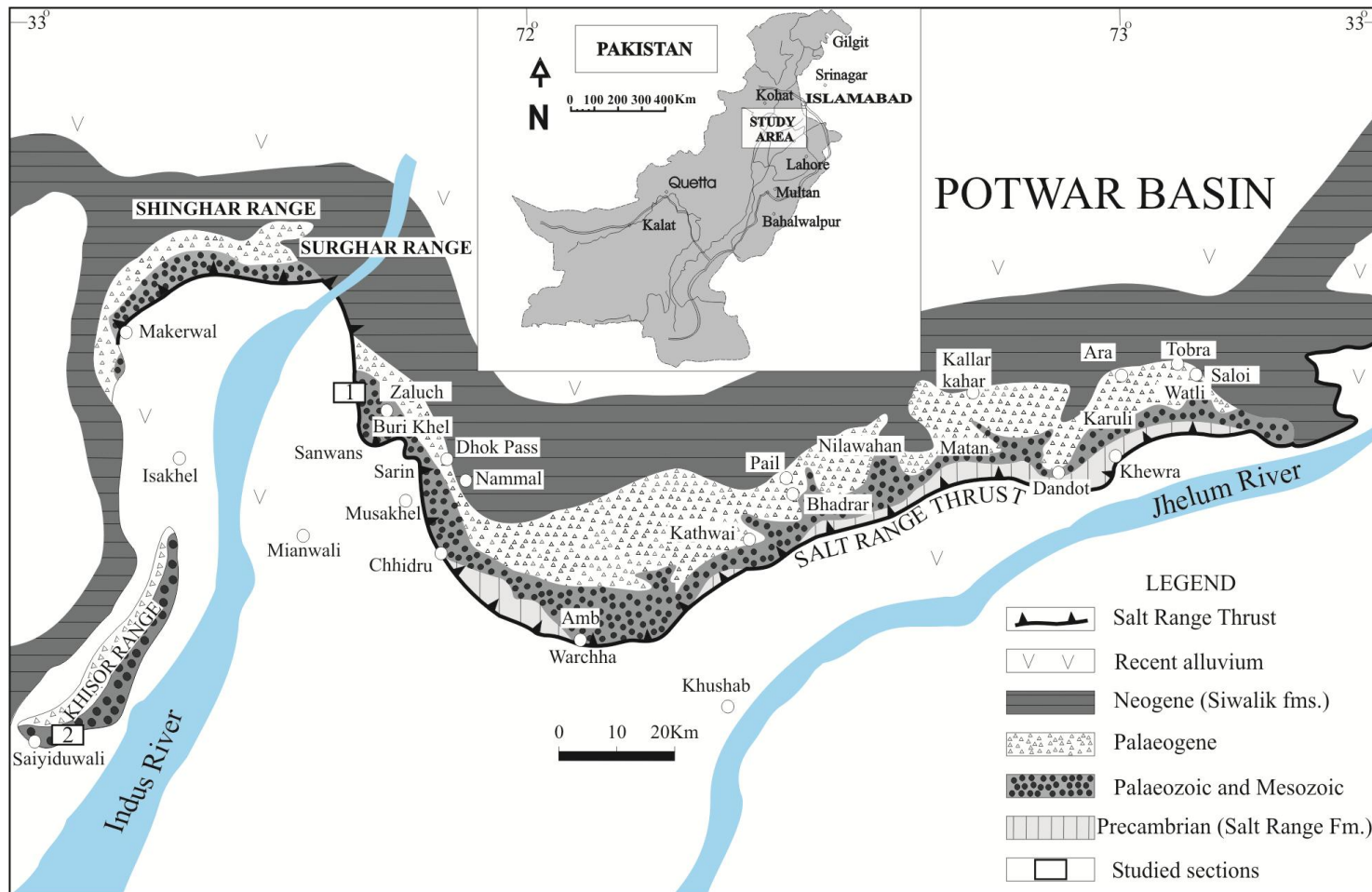


Fig. 6.1 Location map of the, 1. Zaluch Nala section (western Salt Range) and 2. Syidiuwali section (Khisor Range; modified after Gee 1989; Ghazi & Mountney 2009; Jan *et al.* 2009; Jan & Stephenson 2011).

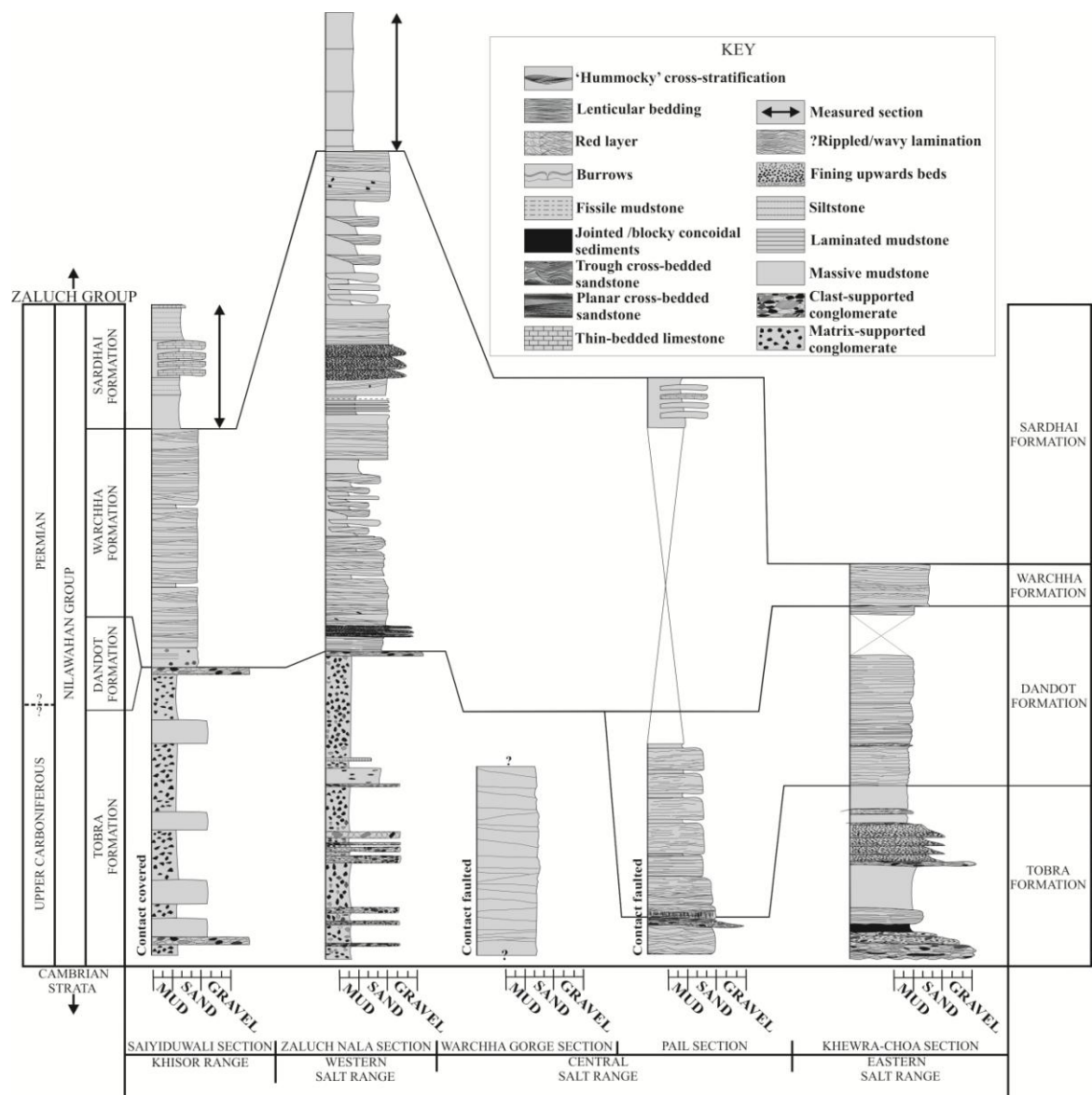


Fig. 6.2 Carboniferous-Permian stratigraphy of the Salt Range, showing the measured section of the Sardhai Formation at Zaluch Nala section (western Salt Range) and Saiyiduwali section (Khisor Range; modified after Jan & Stephenson 2011).

The yield of the samples was mainly poor, however it was possible in most cases to count at least two hundred specimens per slide. Thirty five taxa were identified from these samples, including the palynostratigraphically important *Camptotriletes warchianus*, *Florinites? balmei* and *Lueckisporites virkkiae*.



Fig. 6.3 Vertical beds of the Sardhai Formation underlain by red beds of the Warchha Formation (to the right in the photo). Rock outcrop to the left (represented by arrow) is 5 m high (Modified after Jan *et al.* 2009).

The quantitative character of assemblages from the Sardhai Formation at the Saiyiduwali section (Khisor Range) and Zaluch Nala section (western Salt Range) is shown in Figs. 6.6 and 6.7 respectively, and some assemblages are shown in Plates 8 and 9. The dominant palynomorph taxa in the Sardhai Formation are *Alisporites indarraensis*, *Corisaccites alutas*, *Florinites? balmei*, *Laevigatosporites callosus* and *Protohaploxylinus uttingii*. Rare taxa include *Alisporites nuthallensis*, *Camptotriletes warchianus*, *Distriatites* sp., *Kingiacolpites subcircularis*, *Lueckisporites virkkiae*, *Strotersporites indicus* and *Thymospora opaqua*.

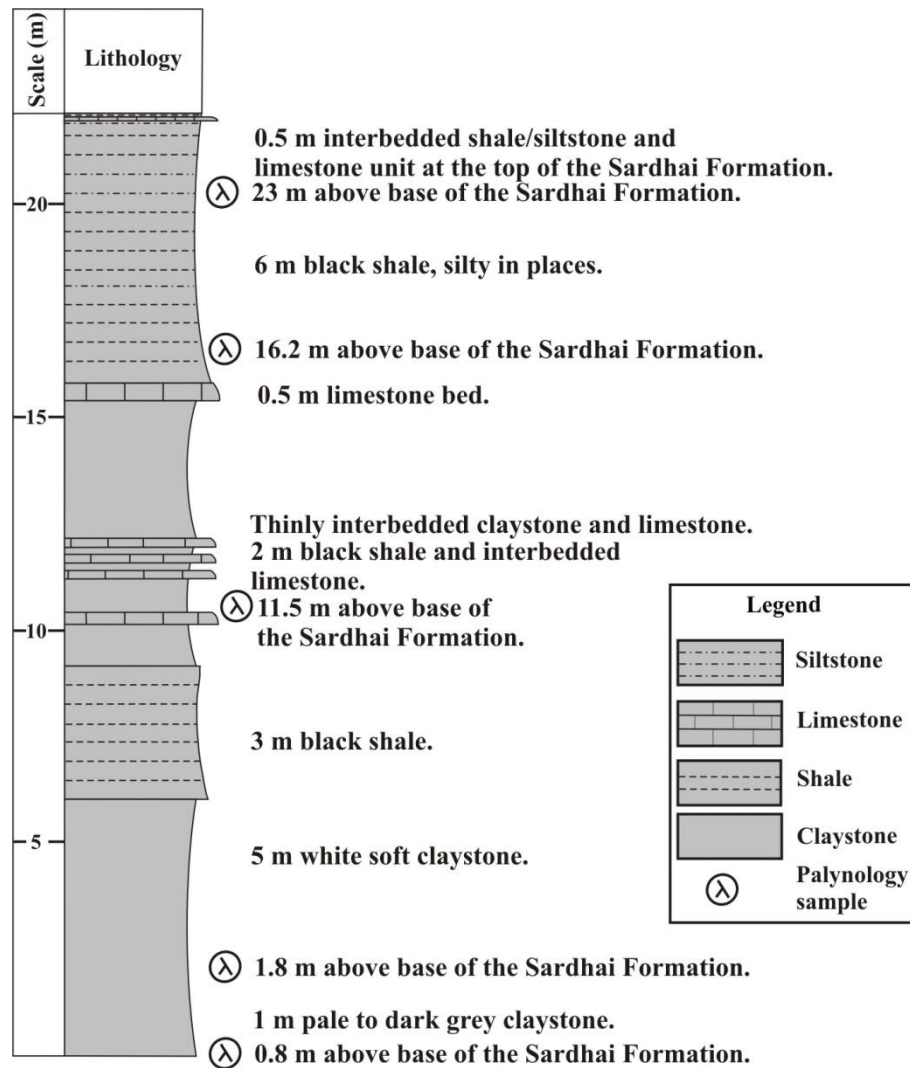


Fig. 6.4 Measured section of the Sardhai Formation at the Saiyiduwali section (Khisor Range; modified after Jan *et al.* 2009).

6.3 Correlation of the Sardhai Formation with other Permian Tethys successions

6.3.1 Correlation with Arabia

The composition of the assemblage suggests correlation with the Arabia. The most extensively studied Tethyan Permian sections are those of Oman and Saudi Arabia (Stephenson & Filatoff 2000a & b; Stephenson 2008b).

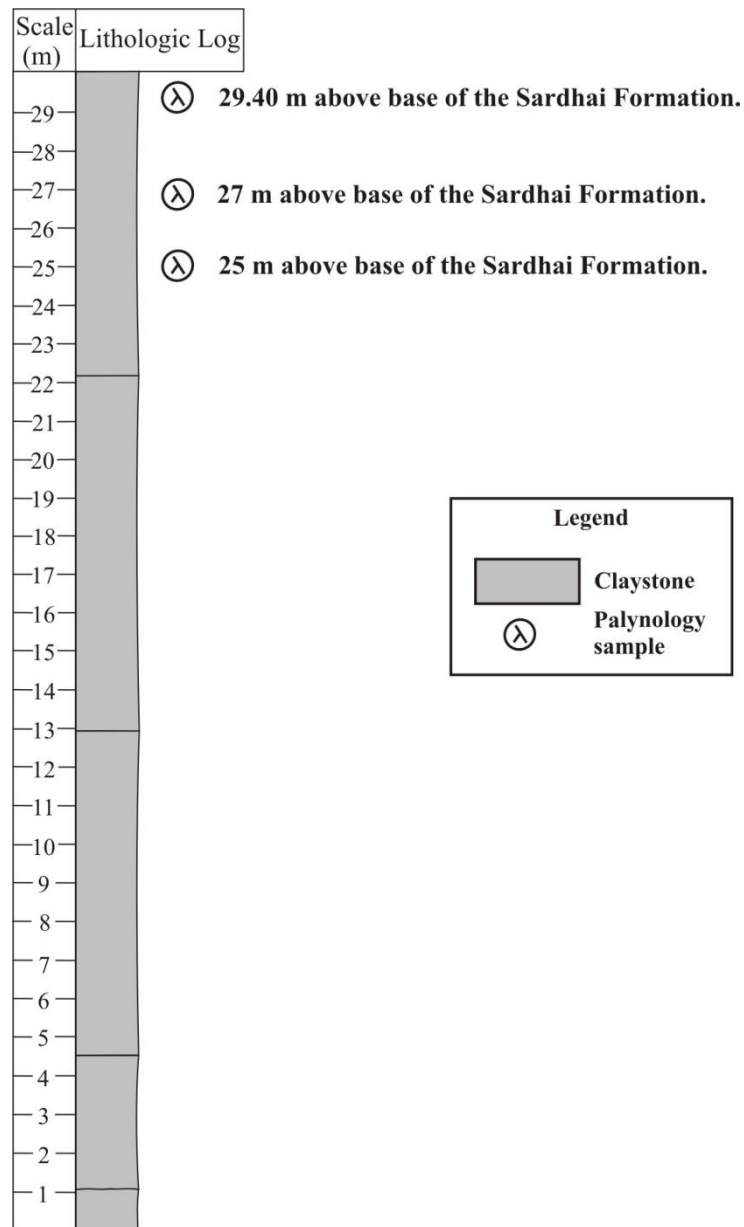


Fig. 6.5 Measured section of the Sardhai Formation within the Zaluch Nala section (western Salt Range).

Stephenson *et al.* (2003) and Stephenson (2006) established eight palynological biozones (OSPZ 1 to OSPZ6); and OSPZ5 and OSPZ6 are considered Mid- and Late Permian in age. OSPZ5, associated with the lower to middle parts of the Upper Gharif member in Oman, is dominated by distally-taeniate bisaccate pollen including *Distriatites insolitus* and *Hamiapollenites dettmannae*, but also contains

Densiopollenites indicus, *Platysaccus* cf. *queenslandi*, *Playfordiaspora cancellosa* and *Thymospora opaqua*. The base of the succeeding biozone, OSPZ6, represents a considerable palynological change because a number of taxa appear for the first time at this level, and because diversity increases. The base of OSPZ6 is defined by the first occurrence of *Florinites? balmei* which is usually very common. Other taxa of OSPZ6 include *Camptotriletes warchianus*, *Pyramidosporites cyathodes* and *Protohaploxylinus uttingii*, though many taxa such as *Alisporites nuthallensis*, *Laevigatosporites callosus*, *Lueckisporites virkkiae*, *Thymospora opaqua* and *Reduviasporonites chalastus* persist from OSPZ5 (Stephenson *et al.* 2003; Stephenson 2006, 2008b). The base of OSPZ6 occurs in the highest parts of the Upper Gharif member in Oman, a few meters below the base of the succeeding carbonate Khuff Formation in beds sometimes referred to as the Khuff transition beds (see Stephenson 2006, 2008b) and the biozone extends into the Khuff Formation. In central Saudi Arabia, assemblages assigned to OSPZ6 (i.e. containing *Florinites? balmei*) also occur in clastic sedimentary rocks below the base of the Khuff Formation.

The lower age limit of OSPZ6 is difficult to constrain since no independent palaeontological data are available from the clastic sedimentary rocks of the Upper Gharif member. In Oman the base of OSPZ6 occurs consistently a few metres below the base of the carbonate Khuff Formation (see Stephenson 2006, 2008b), and the lower beds of the Khuff Formation are dated as early Wordian in age (Angiolini *et al.* 2003b). Since no significant hiatus is present between the Upper Gharif member and the lower Khuff Formation the lower limit of the age of OSPZ6 is likely to be Wordian. The upper age limit of OSPZ6 in Oman and Saudi Arabia is yet to be defined but the assemblages that characterise it are not known to extend into the Triassic.

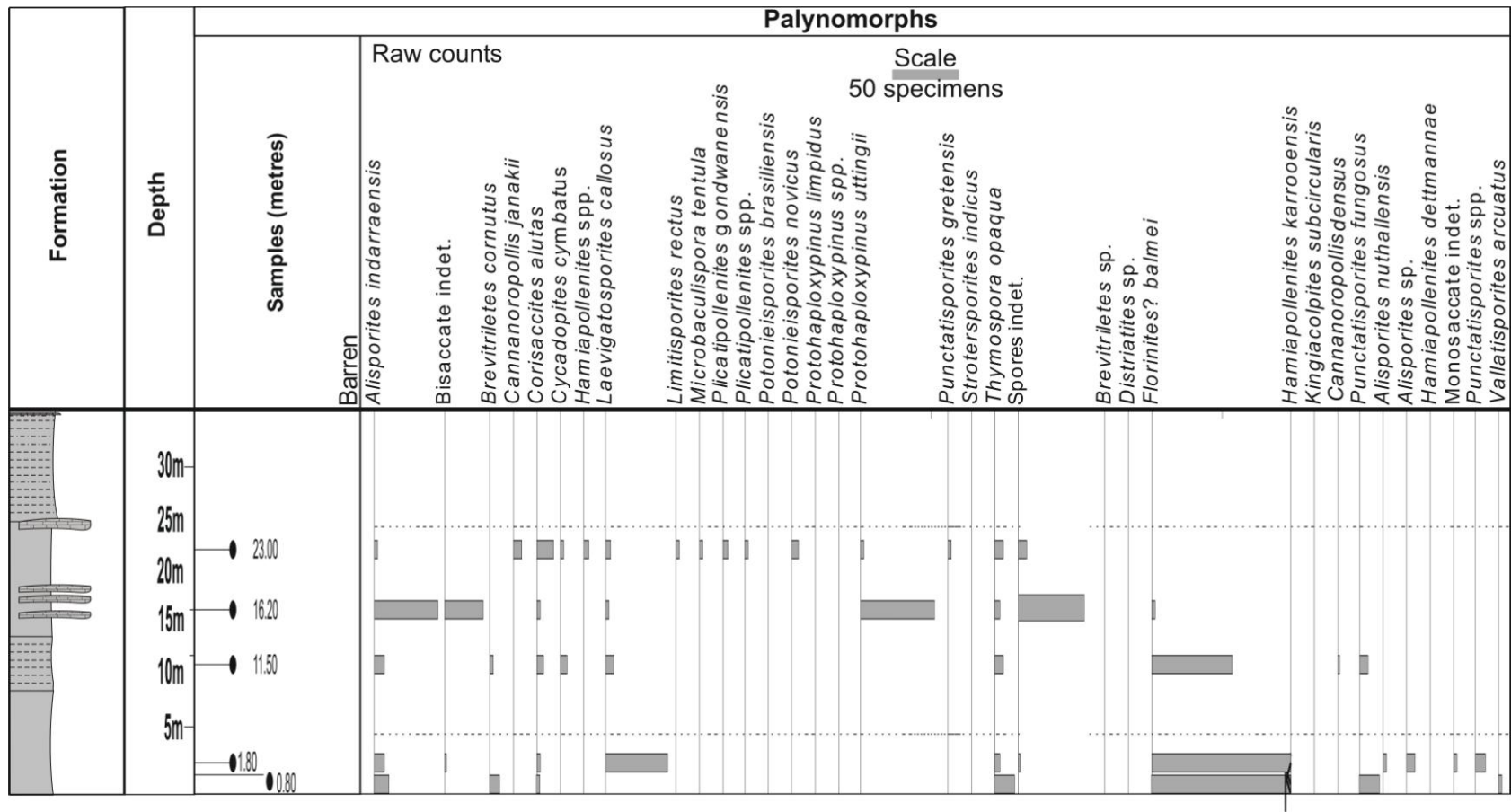


Fig. 6.6 Abundance chart for the Sardhai Formation, at the Saiyiduwali section (Khisor Range). The arrowed bars represent the continuity of the taxa.

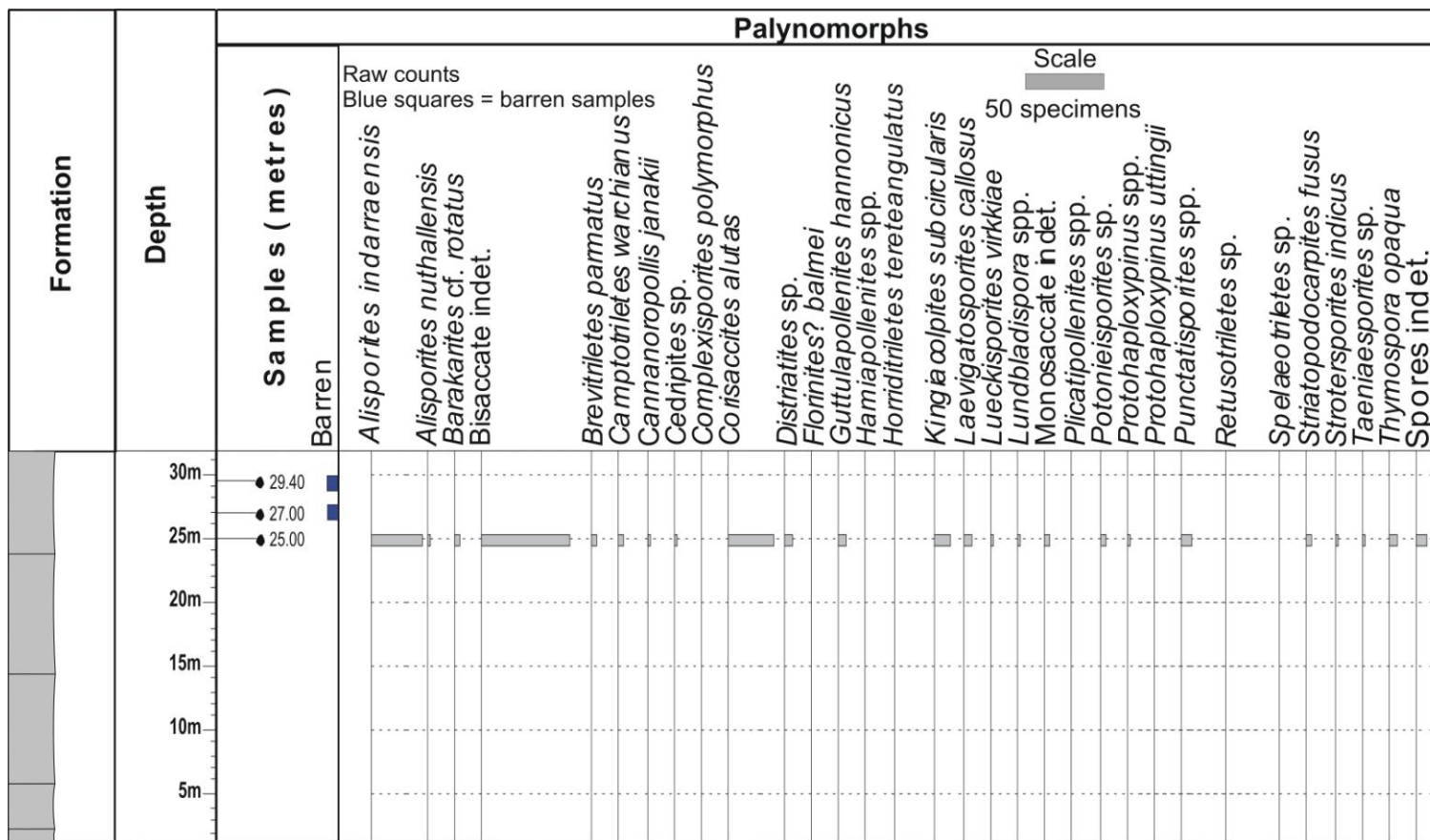


Fig. 6.7 Abundance chart for the Sardhai Formation, Zaluch Nala section (western Salt Range).

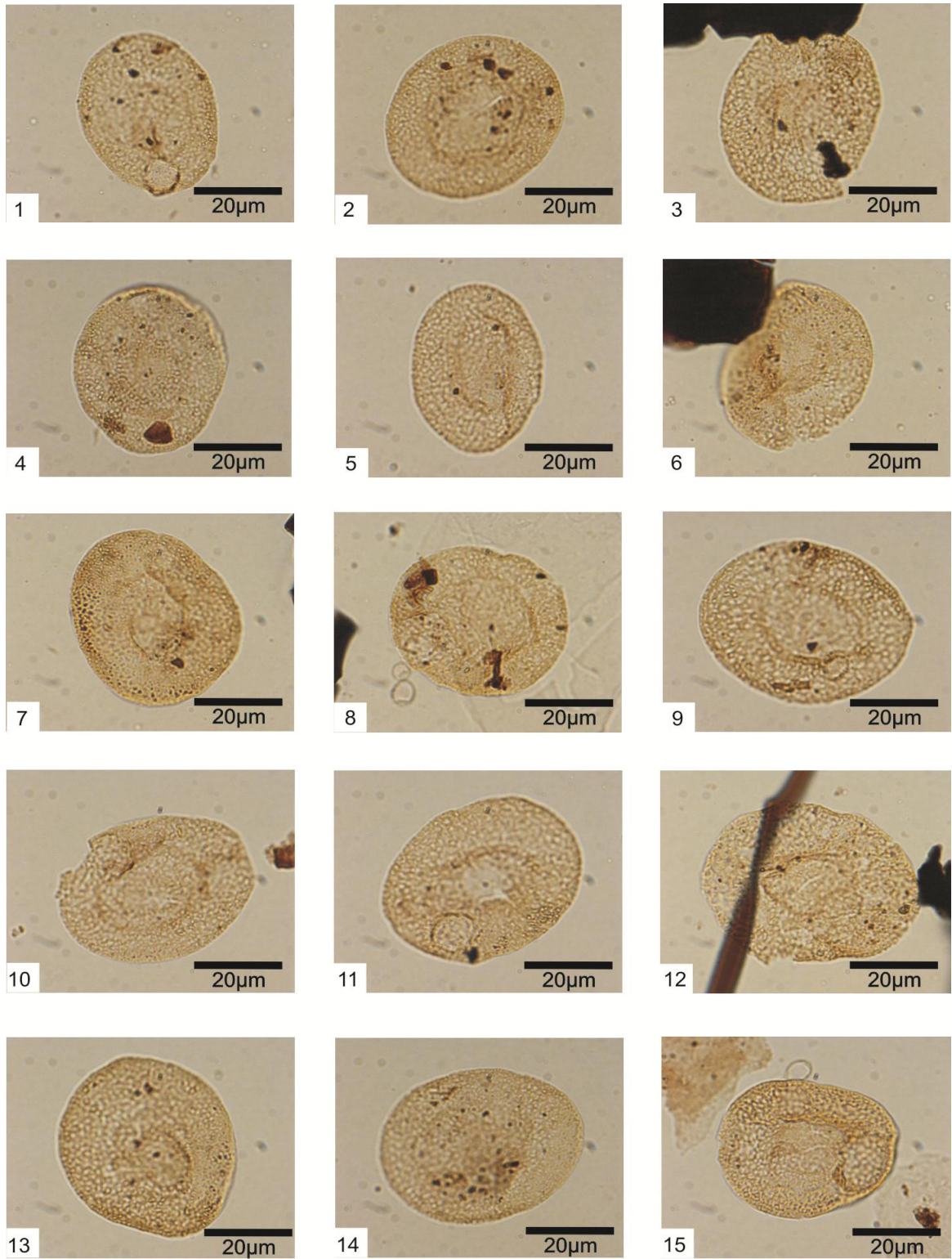


Plate 8

Plate 8 *Florinites? balmei* from the Sardhai Formation at the Saiyiduwali section

(Khisor Range), Pakistan.

The slide number followed by the England Finder coordinates are given as follows,

(1). MPA-57533, W12/3.

(2). MPA-57533, Y11.

(3). MPA-57533, W25.

(4). MPA-57533, S19.

(5). MPA-57533, V8/1.

(6). MPA-57533, V29/1.

(7). MPA-57533, V33/2.

(8). MPA-57533, W20/3.

(9). MPA-57533, T10/3.

(10). MPA-57533, S17/4.

(11). MPA-57533, U3/3.

(12). MPA-57533, W27/4.

(13). MPA-57533, L29/3.

(14). MPA-57533, O12.

(15). MPA-57533, P5.

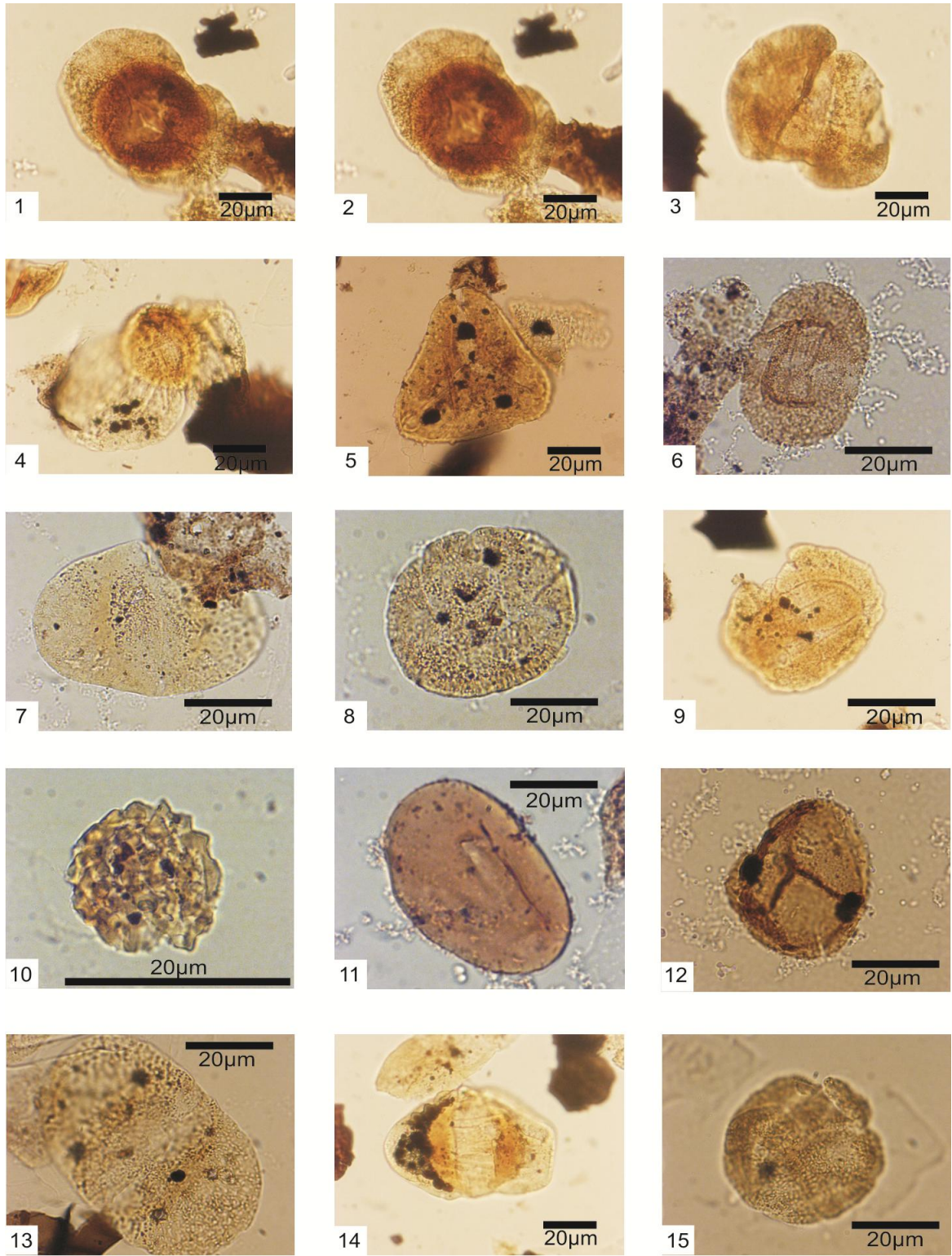


Plate 9

Plate 9 Palynomorphs from the Sardhai Formation, Pakistan. Each with slide number followed by England Finder coordinates is given as follows,

- (1). *Lueckisporites virkkiae*, MPA-57528, T23/3 (proximal focus).
- (2). *Lueckisporites virkkiae*, MPA-57528, T23/3 (distal focus).
- (3). *Corisaccites alutas*, MPA-57528, Q33/3.
- (4). *Striatopodocarpites fusus*, MPA-57528, N24.
- (5). *Camptotriletes warchianus*, MPA-57528, S21.
- (6). *Protohaploxylinus uttingii*, MPA-57528, S35.
- (7). *Alisporites nuthallensis*, MPA-57528, W32/1.
- (8). *Guttulapollenites hannonicus*, MPA-57528, X29/1.
- (9). *Taeniaesporites* sp, MPA-57528, D31/4.
- (10). *Thymospora opaqua*, MPA-57528, S22.
- (11). *Laevigatosporites callosus*, MPA-57528, U4/1.
- (12). *Lundbladispota* sp., MPA-57528, R4/1.
- (13). *Alisporites nuthallensis*, MPA-57528, Q19/2.
- (14). *Protohaploxylinus* sp., MPA-57528, Q19/2.
- (15). *Guttulapollenites hannonicus*, MPA-57528, E17.

The presence in the Sardhai Formation of *Florinites? balmei* in addition to *Alisporites nuthallensis*, *Corisaccites alutas*, *Camptotriletes warchianus*, *Laevigatosporites callosus* and *Thymospora opaqua* suggests a correlation with the OSPZ6 Biozone of Arabia. The Amb Formation above the Sardhai Formation is similar palaeontologically and lithologically to the lower part of the Arabian Khuff Formation and is widely considered to be its temporal and sedimentological equivalent (see Angiolini & Bucher 1999) having been formed by essentially the same marine transgression associated with neo-Tethyan sea floor spreading (Angiolini *et al.* 2003b; Mertmann 2003). The evidence thus suggests that the Sardhai Formation correlates with the immediate pre-carbonate clastic sedimentary rocks of Arabia, including the basal Khuff clastics and the Khuff transition beds. In the light of this correlation, a Wordian age is tentatively suggested for the Sardhai Formation (Fig. 6.8).

6.3.2 Tethyan correlation

Recently Stolle (2007) investigated the Permian Kas and Gomanibrik formations in southeast Turkey. The Kas Formation has been dated as Wordian by foraminifera (Stolle 2007). The assemblages in the Kas Formation are dominated by spores, particularly monolete taxa, including *Punctatisporites* spp., *Spinospores* sp., *Torispora* spp., and *Thymospora opaqua*, but also contain common *Camptotriletes warchianus*, *Distriatites insolitus*, *Florinites? balmei* (up to 23% of assemblages) and *Hamiapollenites dettmannae*. Stolle (2007) correlated the Kas Formation assemblages with OSPZ6, and noted similarities with northern Iraqi subsurface assemblages described by Nader *et al.* (1993) and Singh (1964). As discussed above, OSPZ6 assemblages can be correlated across the Tethyan region, including Turkey, Iraq, Saudi Arabia, Oman and the Salt Range, Pakistan (Fig. 6.8).

Chronostratigraphy		Palynological Biozonation	Lithostratigraphy				
			Southeast Turkey	North Iraq	Central Saudi Arabia	Oman	Pakistan
Middle Permian Guadalupian	Capitanian	OSPZ6	B Gomaniibrik Formation (part)	Chia Zairi Formation (part)	Khuff Formation (part)	Upper part of Khuff Formation missing	Chiddru Formation
			A				Zinner Member
	Wordian	Kas Formation	Clastics	Basal Khuff clastics sensu Stephenson and Filatoff (2000)	Khuff Formation	Amb Formation	
		OSPZ5		Ga'ara Formation (subsurface)		Khuff transition section	Sardhai Formation

Fig. 6.8 Correlation of the OSPZ6 biozone between Southeast Turkey, northern Iraq, central Saudi Arabia, Oman and Pakistan

(From Jan *et al.* 2009).

6.4 Palaeogeographic distribution of *Florinites? balmei*

This correlation shows that the distinctive pollen *Florinites? balmei* is present in approximately coeval rocks in an area of the southern neo-Tethys which is now represented by southeast Turkey and northern Iraq. In addition *Florinites? balmei* has recently been described from the basal Khuff clastics in Kuwait (Tanoli *et al.* 2008) and is known to occur in the same unit in the United Arab Emirates and Qatar (BGS unpublished confidential reports). Its occurrence in the Salt and Khisor ranges and apparent absence from Middle Permian rocks elsewhere in Gondwana, Euramerica and Cathaysia suggests that the plant that produced *Florinites? balmei* had a rather restricted palaeogeographic distribution along the palaeotropical coast of the neo-Tethys Ocean (Fig. 6.9). Its distribution also tends to support the palaeogeographic reconstructions of Ricou in Dercourt *et al.* (1993), Ziegler *et al.* (1998) and Gaetani *et al.* (2000) showing the Salt Range area in contiguity with the southern part of the Arabian Plate.

The complex palaeogeography and palaeotectonics of the Tethyan margin from the Early to Mid Permian has been discussed by amongst others Sengör (1979), Ricou (in Dercourt *et al.* 1993), Ziegler *et al.* (1998), Gaetani *et al.* (2000) and Angiolini (2001). Angiolini's (2001) reconstruction of the palaeogeography of the Wordian Stage shows the Mega Lhasa Block or Cimmerian blocks (comprising Iran, Afghanistan, Karakorum and Sibumasu, Thailand) in contiguity and in relative proximity to the Gondwanan margin, however the form and position of the Mega Lhasa Block is generally considered uncertain (Gaetani 1997; Muttoni *et al.* 2009), thus further work to establish whether *Florinites? balmei* occurs in the Mega Lhasa Block, especially Thailand, might shed more light on such reconstructions.

The well known Oman Gharif palaeoflora (e.g. Broutin *et al.* 1995; Berthelin *et al.* 2003) was described from the uppermost Gharif Formation in the Huqf area in interior

Oman, and is believed to consist of a mixture of Gondwanan, Cathaysian and Euramerican fossil plant taxa. Plant taxa of the Permian Cathaysian paleokingdom present in Oman were considered by Berthelin *et al.* (2003) to indicate a close relationship between the neo-Tethys realm and south China.

6.5 Conclusions

The presence of *Florinites? balmei* together with other stratigraphically important taxa, e.g. *Camptotriletes warchianus*, suggest that the Sardhai Formation correlates with the Khuff transition beds of Oman and the basal Khuff clastics of central Saudi Arabia and can be likewise assigned to the Arabian OSPZ6 biozone, indicating a probable Wordian age. Overall the Salt Range Carboniferous-Permian succession is also similar in lithological character to that of the Arabian Peninsula: both have glacially-influenced successions at the base, overlain by red beds, are followed by distinctive dark shale-sandstone interbeds, and conclude with thick limestones.

This work has also shown that monosaccate pollen grain *Florinites? balmei* had a limited palaeogeographic distribution in the Mid-Permian across most of the southern Tethys and Arabia, whereas it is apparently not reported elsewhere in Gondwana and Euramerica. If this distribution can be more precisely delineated in regions in the wider Middle East and parts of present day southeast Asia, it would help reconstruct this region's complex palaeogeography and tectonics.

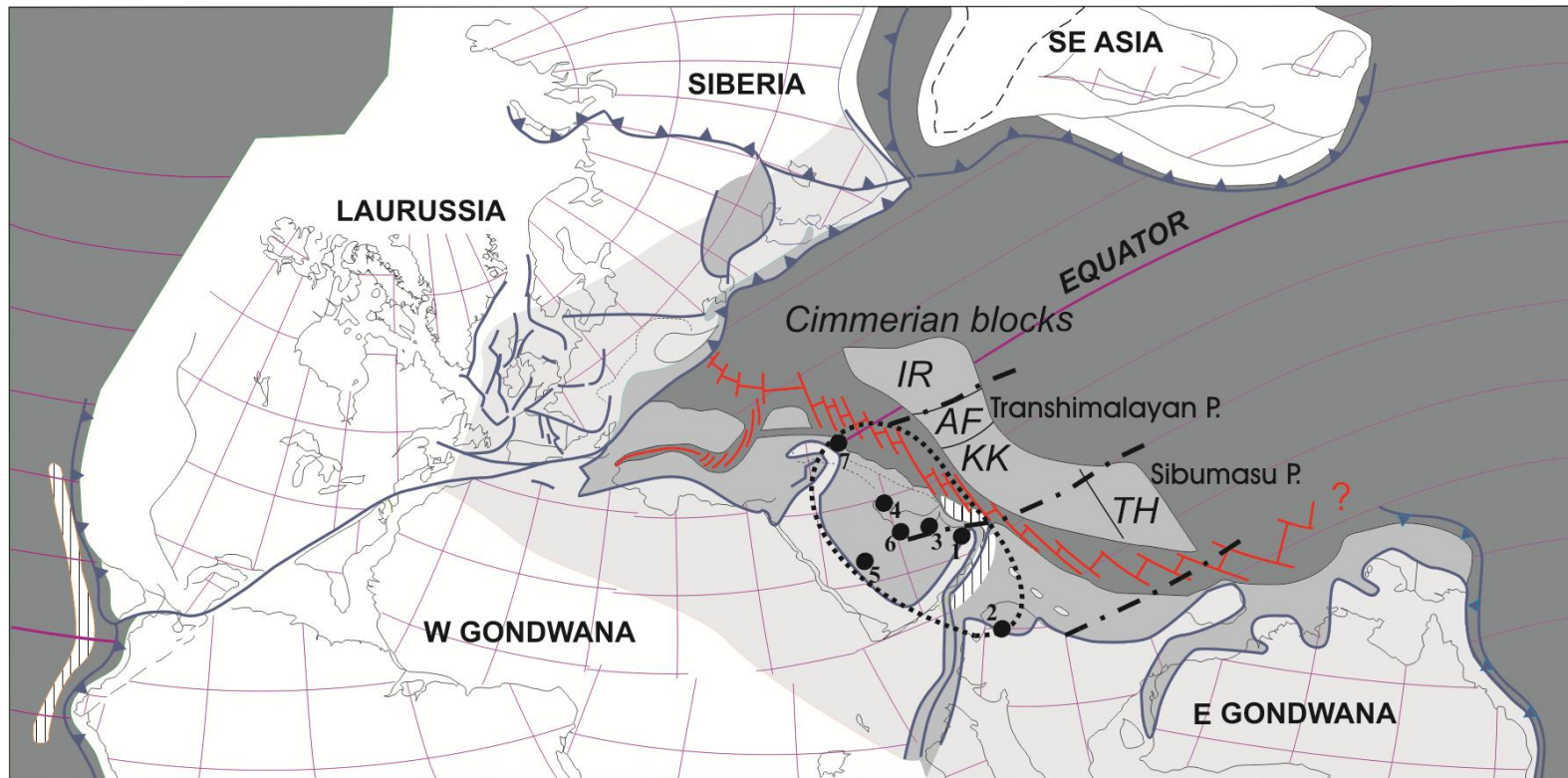


Fig. 6.9 The mid-Permian (Roadian-Wordian) continental configuration. Solid circles indicate the location of *Florinites? balmei* across, 1- Oman, 2- Salt Range, 3- UAE, 4- Kuwait, 5- Saudi Arab, 6- Qatar and 7- southeast Turkey (From Jan *et al.* 2009).

7 Chapter 7: Palynological synthesis

This chapter summarises the results of palynological study across the Nilawahan Group. The palynological assemblages from the Upper Pennsylvanian Tobra, and Middle Permian Sardhai formations have formed an important portion of this research and these are discussed here in details.

7.1 The palynomorphs of the Tobra Formation

The palynomorphs in the Nilawahan Group are concentrated in two stratigraphic intervals i.e. the Upper Pennsylvanian Tobra Formation (Jan & Stephenson 2011) and the Middle Permian (Wordian) Sardhai Formation (Jan *et al.* 2009). The Dandot and overlying Warchha formations have not yielded palynomorphs during the present work (Fig.7.1).

The palynomorphs in the Tobra Formation are represented by 41 species belonging to 20 genera (Fig. 7.1, Appendices 6 & 7). Spores are more diverse than any other group, represented by ten genera and 22 species. *Horriditriletes* show five species, followed by *Brevitriletes*, representing four species and *Punctatisporites* is represented by three species. *Cristatisporites* and *Vallatisporites* are represented by two species each. All other spore genera are represented by only one species. The monosaccate pollen are represented by five genera and nine species; *Plicatipollenites*, and *Potonieisporites* are represented by three species and *Cannanoropollis* is represented by two species.

The bisaccate pollen are represented by the least number in the Tobra Formation, i.e. four genera and eight species. *Protohaploxypinus* is represented by three species whereas *Striatopodocarpites* and *Limitisporites* are each represented by two species. All other bisaccate genera are represented by only one species. The monocolpate pollen are represented by two species.

7.2 The palynomorphs of the Sardhai Formation

In the Sardhai Formation (Fig. 7.1, Appendices 5 and 6), an increase in the diversity of genera, compared to the Tobra Formation is observed. Whilst some species and genera are found to extend from the Tobra Formation, others are observed to terminate in the Sardhai Formation; some new taxa also appear in the Sardhai Formation. Spores still constitute a major proportion of the palynomorph types and are represented by 15 species belonging to 11 genera. The spore species that first occur at the base of the Sardhai Formation belong to genera *Camptotriletes*, *Laevigatosporites* and *Thymospora*, whereas *Cristatisporites*, *Horriditriletes* and *Calamospora* disappear in the Sardhai Formation. The bisaccate pollen represent the second most common category. They are represented by eight genera and 15 species. The bisaccate pollen that originate at this level include *Alisporites*, *Corisaccites*, *Complexisporites* and *Lueckisporites*. The bisaccate pollen genus that is observed to terminate in the Sardhai Formation is *Limitisporites*. Monosaccate pollen are represented by seven genera and 11 species in the Sardhai Formation. The newly introduced species include *Florinites* and *Guttulapollenites*.

8 Chapter 8: Conclusions and recommendations for future work

General palynomorph yields and preservation

- The Tobra and Sardhai formations yielded well-preserved palynomorphs. The data have been used in age determination, palynostratigraphy and correlation of these units with other basins in Gondwana.
- The Dandot and Warchha formations were found to be barren of palynomorphs in the present study and thus could not contribute to the dataset. This posed a problem in determining the continuity of palynomorph ranges between the Tobra Formation and the Sardhai Formation.
- Palynomorphs in the Nilawahān Group units are entirely terrestrial.
- The lithofacies influenced yield of palynomorphs: mudstone lithologies showing greatest yield and siltstone and sandstone lithologies yielding less.
- A biozonation was not developed because of the discontinuous palynomorph yield.

Age of the Salt Range units

- The palynological assemblages of the Tobra Formation are Late Pennsylvanian in age (Jan & Stephenson 2011).
- The present study could not give information about the age of the Warchha and Dandot formations, due to low yield of palynomorphs in these units. However, an Artinskian age was assigned to the Warchha Formation based on the presence of plant megafossils including *Glossopteris*, *Gangamopteris*, *Samaropsis* and *Ottokaria* by Virkki (1939). The Dandot Formation thus might range from Late Pennsylvanian to ?Artinskian in age, based on the stratigraphic position of the unit between the Tobra and Warchha formations.

- The palynological assemblages of the Sardhai Formation are Middle Permian, Wordian in age (Jan *et al.* 2009).

Correlation of the Salt Range units

The palynological assemblages of the Tobra Formation (see Fig. 5.10) correlate with;

- The South Oman 2165B Biozone (Penney *et al.* 2008) and the lower part of the Oman and Saudi Arabia Palynological Zone 2 (i.e. OSPZ2; Stephenson *et al.* 2003). This suggests that the Tobra Formation is equivalent to the middle part of the Al Khlata Formation of Oman (i.e. PDO production unit AK P5), and the Unayzah B member of the Saudi Arabia (Jan & Stephenson 2011).
- Palynological assemblages from the lower part of the Khulan Formation of Yemen (Stephenson & Al-Mashaikie 2010, 2011).
- Western Australian Stage 2 (*sensu* Backhouse 1991), and thus the Tobra Formation is equivalent to the Stockton Formation of the Collie Basin of Western Australia.
- The Eastern Australian *Microbaculispora tentula* Opper-zone (Jones & Truswell 1992) and thus the Tobra Formation is equivalent to the Upper Jochmus Formation of the eastern Australian Galilee Basin.
- The South American Chacoparana Basin, Argentina *Potonieisporites-Lundbladispota* Zone and thus the Tobra Formation is equivalent to the upper part of the Ordóñez Formation (Russo *et al.* 1980; Vergel 1993; Playford & Dino 2002).
- The Central-western Argentina *Raistrickia densa-Convolutispora muriornata* (DM) Assemblage Biozone and *Fusacolpites fusus-Vittatina subsaccata* (FS) Interval Biozone (Césari & Gutiérrez 2000). This shows that the Tobra Formation is equivalent to the El Imperial Formation of the San Rafael, the

Santa Máxima Formation of the Calingasta-Uspallata Basin and the Tupe Formation of the Paganzo Basin of the central-western Argentina.

- The Amazonas Basin, Brazil *Illinites unicus* Zone, which suggests the Tobra Formation is equivalent to the Itaituba Formation of the Brazil (Playford & Dino 2000).
- The *Parasaccites korbaensis* Assemblage-Zone India, suggesting that the Tobra Formation is equivalent to the upper part of the Talchir Formation (Tiwari & Tripathi 1992).

The palynological assemblages of the Sardhai Formation (see Fig. 6.8) correlate with;

- The Oman and Saudi Arabia Palynological Zone 6 (i.e. OSPZ6) and hence with the Khuff transition beds of Oman (Stephenson *et al.* 2003).
- The basal Khuff clastics of central Saudi Arabia (Stephenson *et al.* 2003).
- The Kas Formation of south eastern Turkey (Stolle 2007).

Palaeoenvironments of the Salt Range units

- The Tobra Formation represents alluvial plain and/or glacio-fluvial deposits dominated by debris flow- and stream flow-dominated conglomerates with subordinate overbank fine-grained sandstones and siltstone interbeds.
- The Dandot Formation is a shallow marine deposit of ripple-laminated sandstones. The marine conditions prevailed as the Carboniferous-Permian glaciations waned and northern Gondwana drifted northwards, resulting in sea level rise.
- The overlying Warchha Formation represents deposition in a fluvial system. The deposits are predominantly erosive-based, cross-bedded and lenticular sandstones with interbedded red mudstones, pebbly sandstones, and clay-rich mudstones and silty mudstones.

- The Sardhai Formation is a shallow marine deposit represented of massive mudstone and sandstones with occasional sandy limestones. The deposition of the Sardhai Formation can be related to the development of a shallow marine setting, which occurred as a result of the Wordian transgression associated with the sea floor spreading as neo-Tethys opened.

Recommendations for future work

- Inconsistent yield of palynology samples from the Dandot and Warchha formations meant these formations were not directly dated. It is recommended that a comprehensive study involving of borehole samples from these units should be conducted alongside the outcrop samples, which will help in age determination, correlation and biozonation.
- The Permian successions of the Salt Range, Pakistan contain rich micro- and macrofaunal intervals. Palynological studies of these intervals might help to age calibrate the palynological biozones of the Salt Range and other nearby areas of the Gondwana, e.g. Saudi Arabia and Australia, with the International stages.

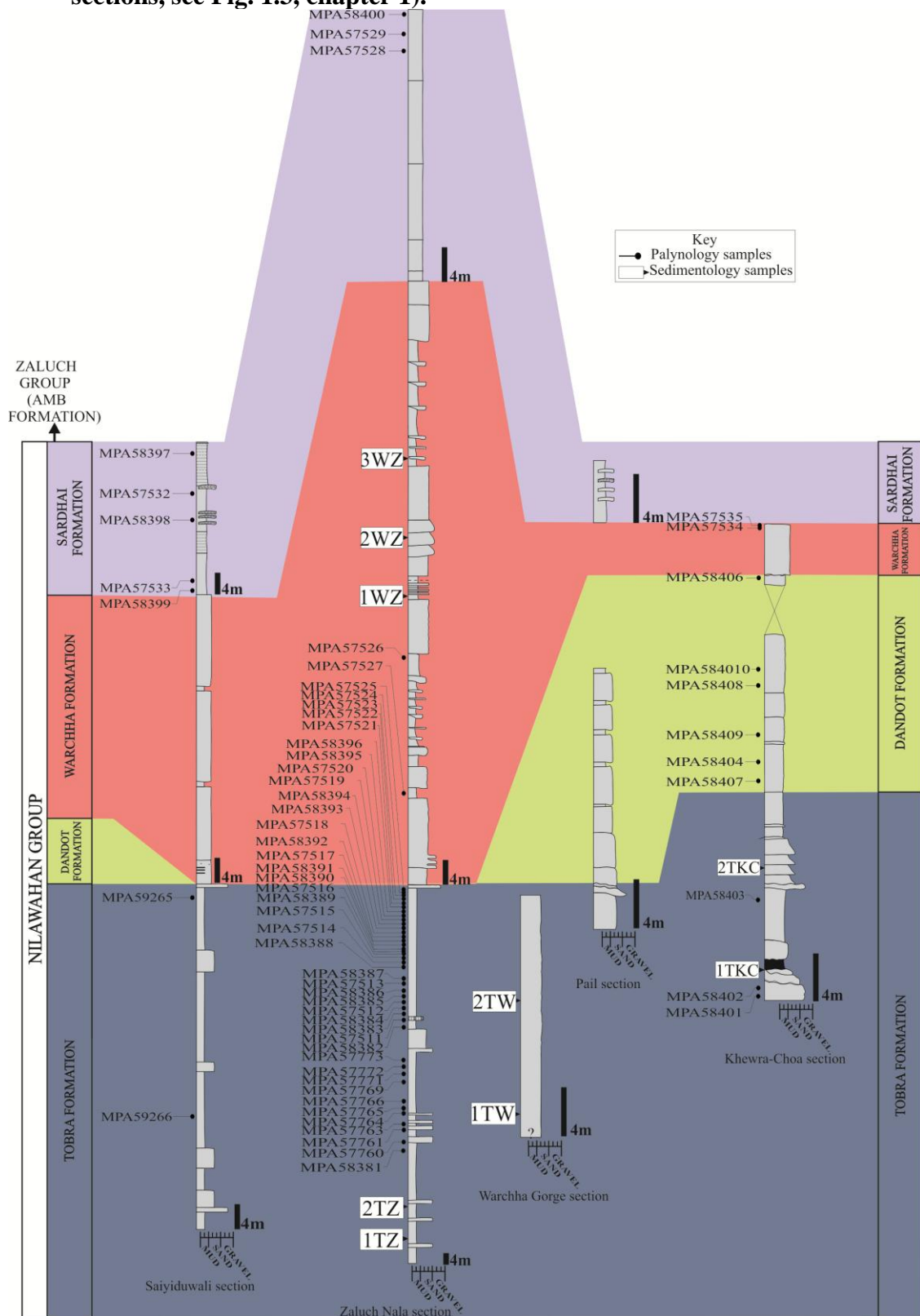
9 Appendices

9.1 Appendix 1 Showing the processed samples for palynology and their population. MPA stands for the BGS in-house palynological laboratory processing code (See Appendix 2 for the exact stratigraphic positions of the palynology samples prefixed with MPA).

LOCATION	SAMPLE DEPTH	BGS CODE
<i>Tobra Formation, Zaluch Nala section western Salt Range</i>	<i>120m below top of member C of Tobra Formation</i>	<i>MPA58381</i>
	<i>84m below top of member C of Tobra Formation</i>	<i>MPA57760</i>
	<i>80m below top of member C of Tobra Formation</i>	<i>MPA57761</i>
	<i>78m below top of member C of Tobra Formation</i>	<i>MPA57763</i>
	<i>74m below top of member C of Tobra Formation</i>	<i>MPA57764</i>
	<i>73m below top of member C of Tobra Formation</i>	<i>MPA57765</i>
	<i>70m below top of member C of Tobra Formation</i>	<i>MPA57766</i>
	<i>64m below top of member C of Tobra Formation</i>	<i>MPA57769</i>
	<i>61m below top of member C of Tobra Formation</i>	<i>MPA57771</i>
	<i>58m below top of member C of Tobra Formation</i>	<i>MPA57772</i>
	<i>57m below top of member C of Tobra Formation</i>	<i>MPA57773</i>
	<i>47m below top of member C of Tobra Formation</i>	<i>MPA58382</i>
	<i>46m below top of member C of Tobra Formation</i>	<i>MPA57511</i>
	<i>42m below top of member C of Tobra Formation</i>	<i>MPA58383</i>
	<i>40m below top of member C of Tobra Formation</i>	<i>MPA58384</i>
	<i>38m below top of member C of Tobra Formation</i>	<i>MPA57512</i>
	<i>36.7m below top of member C of Tobra Formation</i>	<i>MPA58385</i>
	<i>35.7m below top of member C of Tobra Formation</i>	<i>MPA58386</i>
	<i>30.3m below top of member C of Tobra Formation</i>	<i>MPA57513</i>
	<i>29.3m below top of member C of Tobra Formation</i>	<i>MPA58387</i>
	<i>23m below top of member C of Tobra Formation</i>	<i>MPA58388</i>
	<i>22.4m below top of member C of Tobra Formation</i>	<i>MPA57514</i>
	<i>21.7m below top of member C of Tobra Formation</i>	<i>MPA57515</i>
	<i>21.2m below top of member C of Tobra Formation</i>	<i>MPA58389</i>
	<i>19.4m below top of member C of Tobra Formation</i>	<i>MPA57516</i>
	<i>18.2m below top of member C of Tobra Formation</i>	<i>MPA58390</i>
	<i>17.2m below top of member C of Tobra Formation</i>	<i>MPA58391</i>
	<i>15.3m below top of member C of Tobra Formation</i>	<i>MPA57517</i>
	<i>11.8m below top of member C of Tobra Formation</i>	<i>MPA58392</i>
	<i>10.8m below top of member C of Tobra Formation</i>	<i>MPA57518</i>
<i>9.10m below top of member C of Tobra Formation</i>	<i>MPA58393</i>	
<i>6.6m below top of member C of Tobra Formation</i>	<i>MPA58394</i>	
<i>5.6m below top of member C of Tobra Formation</i>	<i>MPA57519</i>	
<i>5m below top of member C of Tobra Formation</i>	<i>MPA57520</i>	
<i>4m below top of member C of Tobra Formation</i>	<i>MPA58395</i>	
<i>1m below top of member C of Tobra Formation</i>	<i>MPA58396</i>	

	80cm below top of member C of Tobra Formation	MPA57521
	60cm below top of member C of Tobra Formation	MPA57522
	40cm below top of member C of Tobra Formation	MPA57523
	20cm below top of member C of Tobra Formation	MPA57524
	0m below (top of) member C of Tobra Formation	MPA57525
Warchha Formation, Zaluch Nala section western Salt Range	42.5m above base of Warchha Formation	MPA57526
	15m above base of Warchha Formation	MPA57527
Sardhai Formation, Zaluch Nala section western Salt Range	25 meters above base of the Sardhai Formation	MPA57528
	27meters above base of the Sardhai Formation	MPA57529
	29.40 meters above base of the Sardhai Formation	MPA58400
Sardhai Formation, Saiyiduwali section Khisor Range	23m above base of the Sardhai Formation	MPA58397
	16.2m above base of the Sardhai Formation	MPA57532
	11.5m above base of the Sardhai Formation	MPA58398
	1.8m above base of the Sardhai Formation	MPA57533
	80cm above base of the Sardhai Formation	MPA58399
Tobra Formation, Saiyiduwali section Khisor Range	54 meters above the base of Tobra Formation	MPA59265
	18m above the base of Tobra Formation	MPA59266
Tobra Formation, Khewra-Choa section, eastern Salt Range	80cm above base (N32 39 57.4 E72 59 09.6)	MPA58401
	1.4m above base of Tobra (Dandot section)	MPA58402
	2m below top of Tobra N32 40 22.9 E72 58 25.3	MPA58403
Dandot Formation, Khewra-Choa section, eastern Salt Range	Dandot Fm N32 40 22.9 E 72 58 25.3 A	MPA58407
	Dandot Fm 1m above A	MPA58404
	Upper Dandot muddy heterolithic (N32 39 59.3 E7259 12.3)	MPA58409
	Lower Dandot near Tobra village N32 39 41.4 E72 59 37.4	MPA58408
	Dandot N32 40 22.9 E 72 58 25.3	MPA58410
	Dandot Basal trace fossils N32 40 22.9 E72 58 25.3	MPA58406
	Upper Dandot N32 40 00.2 E 72 59 13.7	MPA57534
	Upper Dandot plant fragments N32 40 00.2 E 72 59 13.7	MPA57535

9.2 Appendix 2 Stratigraphic positions of palynology and sedimentology samples in the Nilawahan Group, Salt Range, Pakistan. (For locations of these sections, see Fig. 1.3, chapter 1).



9.3 Appendix 3 Paper published in the (journal) “*Palynology*”.

Due to third party copyright restrictions the following published article has been removed from the appendix of the electronic version of this thesis:

Jan, I.U., Stephenson, M.H. 2011. Palynology and correlation of the Upper Pennsylvanian Tobra Formation from Zaluch Nala, Salt Range, Pakistan. *Palynology*, 35 (2), 212-225.

<http://dx.doi.org/10.1080/01916122.2011.573964>

The unabridged version can be consulted, on request, at the University of Leicester’s David Wilson Library.

9.4 Appendix 4 Paper published in the (journal) “*Review of Palaeobotany and Palynology*”.

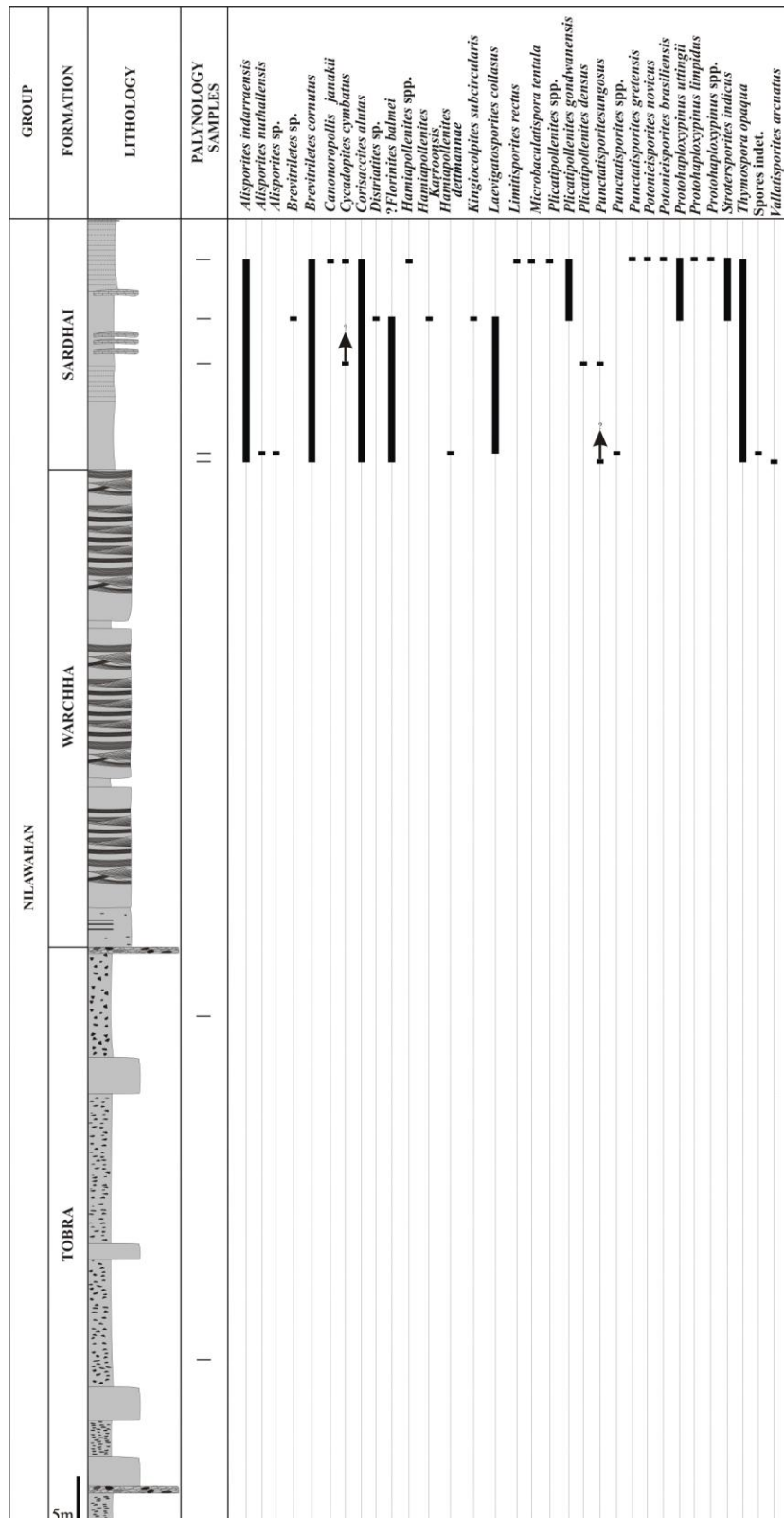
Due to third party copyright restrictions the following published article has been removed from the appendix of the electronic version of this thesis:

Jan, I.U., Stephenson, M.H., Khan, F.R. 2009. Palynostratigraphic correlation of the Sardhai Formation (Permian) of Pakistan. *Review of Palaeobotany and Palynology*, 158 (1-2), 72-82.

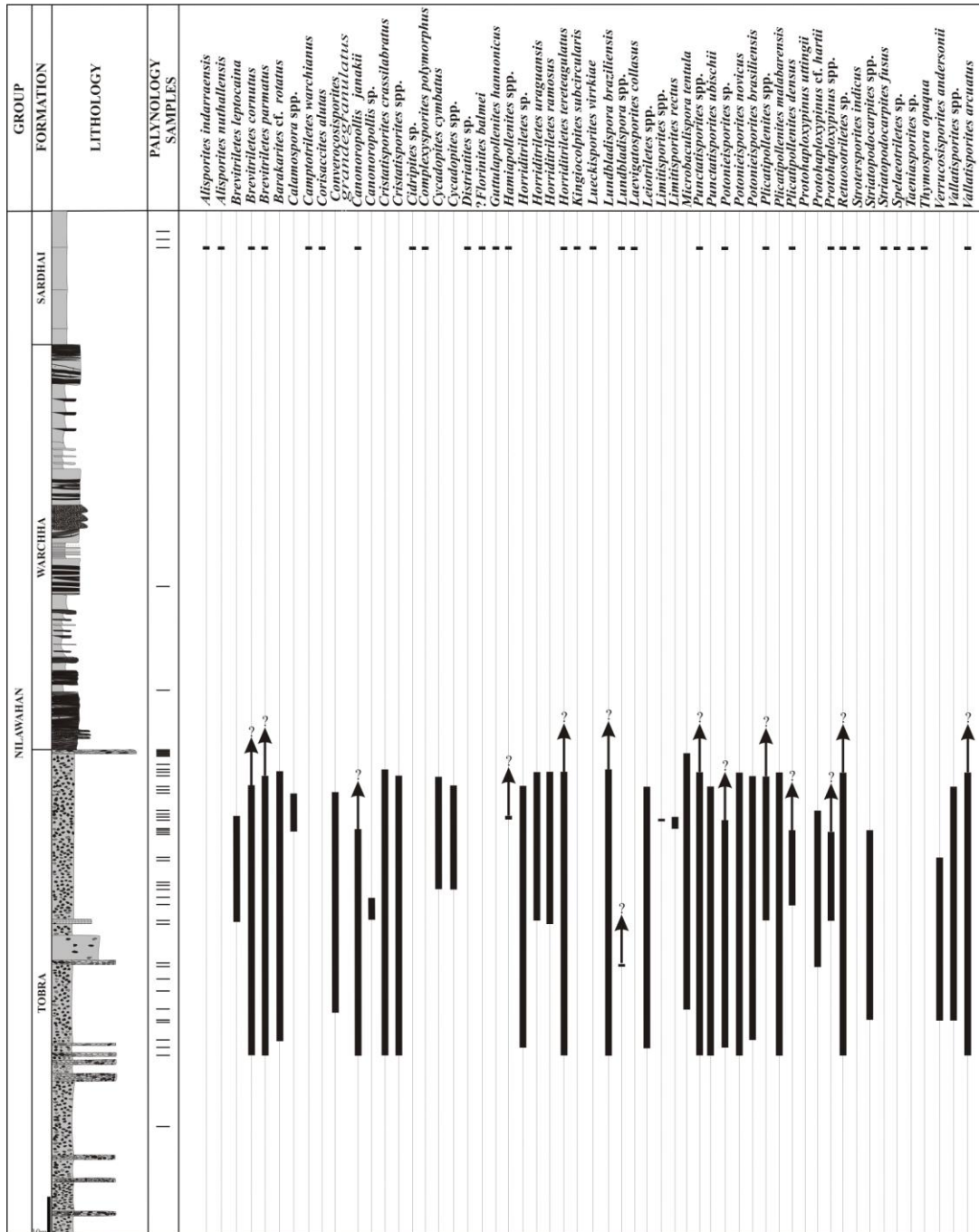
<http://dx.doi.org/10.1016/j.revpalbo.2009.08.002>

The unabridged version can be consulted, on request, at the University of Leicester’s David Wilson Library.

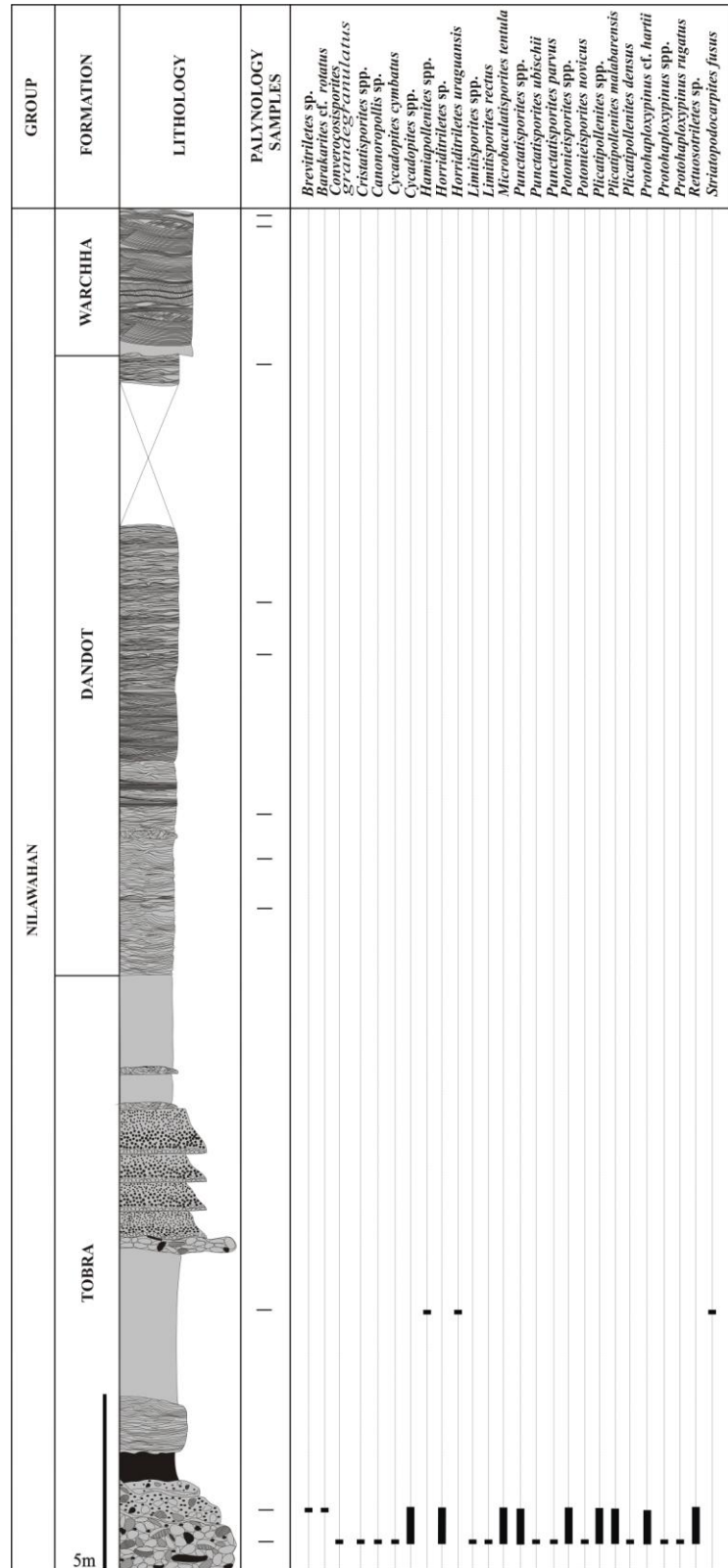
9.5 Appendix 5 Stratigraphic ranges of the palynomorphs in the Nilawahan Group at the Saiyiduwali section (Khisor Range). The arrows represent ?continuity of the taxa up section.



9.6 Appendix 6 Stratigraphic ranges of the palynomorphs in the Nilawahan Group at the Zaluch Nala section (western Salt Range). The arrows represent ?continuity of the taxa up section.



9.7 Appendix 7 Stratigraphic ranges of the palynomorphs in the Nilawahan Group at the Khewra-Choa section (eastern Salt Range). The arrows represent ?continuity of the taxa up section.



References

- ADAMS, A. E., MACKENZIE, W. S. & GUILLFORD, C. 1991. *Atlas of sedimentary rocks under the microscope*. John Wiley & Sons Inc. New York.
- ALAM, I. 2008. *Structural and stratigraphic framework of the Marwat-Khisor Ranges, N.W.F.P., Pakistan*. Unpublished PhD thesis. National Centre of Excellence in Geology, University of Peshawar, Pakistan.
- AMOS, A. J. & LÓPEZ-GAMUNDI, O. R. 1981. Late Palaeozoic Sauce Grande Formation of eastern Argentina. In: HAMBREY, M. J. & HARLAND, W. B. (eds) *Earth's Pre-Pleistocene Glacial Record*. Cambridge University Press, 872-877.
- ANDERSON, J. M. 1977. The biostratigraphy of the Permian and Triassic. Part 3: A review of Gondwana Permian palynology with particular reference to the northern Karoo Basin, South Africa. *Memoir of the Botanical Survey of South Africa*, **41**, 1-133.
- ANGIOLINI, L. 2001. Lower and Middle Permian brachiopods from Oman and Peri-Gondwanan palaeogeographical reconstructions. In: BRUNTON, C. H., COCKS, L. R. M. & LONG, S. L. (eds) *Brachiopods past and present*. Systematic Association Special Volume Series, **63**, 352-362.
- ANGIOLINI, L., BALINI, M., GARZANTI, E., ET AL. 2003a. Gondwana deglaciation and opening of Neotethys: the Al Khlata and Saiwan Formations of Interior Oman. *Palaeogeography, Palaeoclimatology, Palaeoecology*, **196**, 99-123.
- ANGIOLINI, L., BALINI, M., GARZANTI, E., ET AL. 2003b. Permian climatic and palaeogeographic changes in Northern Gondwana: the Khuff Formation of Interior Oman. *Palaeogeography, Palaeoclimatology, Palaeoecology*, **191**, 269-300.
- ANGIOLINI, L. & BUCHER, H. 1999. Taxonomy and quantitative biochronology of Guadalupian brachiopods from the Khuff Formation, Southeastern Oman. *Geobios*, **32**, 665-699.
- ARCHANGELSKY, S., AZCUY, C. L., PINTO, I. D., ET AL. 1980. The Carboniferous and Early Permian of the South American Gondwana area: a summary of the biostratigraphic information. *Actas del II Congreso Argentino de Paleontología y Bioestratigrafía y I Congreso Latinoamericano de Paleontología Buenos Aires abril 1978*, **4**, 257-269.
- ARCHANGELSKY, S. & GAMERRO, J. C. 1979. Palinología del Palaeozoico Superior en el Subsuelo de la Cuenca Chacoparanense, República Argentina 1. Estudio sistemático lospalinomorfos de tres perforaciones de la Provincia de Córdoba. *Revista Española de Micropaleontología*, **11**, 417-478.

- ARCHBOLD, N. W. 1999. Permian Gondwanan correlations: the significance of the Western Australian marine Permian. *Journal of African Earth Sciences*, **29**, 63-75.
- ARCHBOLD, N. W. & DICKINS, J. M. 1997. Comments on subdivisions of the Permian and a standard world scale. *Permophiles*, **30**, 4-5.
- AZCUY, C. L. 1979. A review of the early Gondwana palynology of Argentina and South America. *Proceedings of IV International Palynological Conference, Lucknow, India, Birbal Sahni Institute*, **2**, 175-185.
- AZCUY, C. L. & JELIN, R. 1980. Los palinozonos del límite Carbónico-Pérmico en la Cuenca Paganzo. *Actas II Congreso Argentino de Palaentología y Bioestratigrafía y I Congreso Latinoamericano de Paleontología*, **4**, 52-68.
- AZCUY, C. L., PASQUO, M. D. & ALDIVIA AMPUERO, H. V. 2002. Late Carboniferous miospores from the Tarma Formation, Pongo de Mainique, Perú. *Review of Palaeobotany and Palynology*, **118**, 1-28.
- BACKHOUSE, J. 1991. Permian palynostratigraphy of the Collie Basin, Western Australia. *Review of Palaeobotany and Palynology*, **67**, 237-314.
- BACKHOUSE, J. 1993. Palynology and correlation of Permian sediments in the Perth, Collie and Officer basins. *Geological Survey of Western Australia Report*, **34**, 111-128.
- BAKER, D. M., LILLIE, R. J., YEATS, R. S., *ET AL.* 1988. Development of the Himalayan frontal thrust zone: Salt Range, Pakistan. *Geology*, **16**, 3-7.
- BALME, B. E. 1970. Palynology of Permian and Triassic strata in the Salt Range and Surghar Range, West Pakistan. In: KUMMEL, B. & TEICHERT, C. (eds) *Stratigraphic Boundary Problems: Permian and Triassic of West Pakistan*. University Press of Kansas, Department of Geology Special Publication, **4**, 306-453.
- BALME, B. E. 1980. Palynology and the Carboniferous-Permian boundary in Australia and other Gondwana countries. *Palynology*, **4**, 43-56.
- BALME, B. E. & HENNELLY, J. P. 1955. Bisaccate sporomorphs from Australian Permian coals. *Australian Journal of Botany*, **3**, 89-98.
- BALME, B. E. & HENNELLY, J. P. 1956a. Monolete, monocolpate, and alete sporomorphs from Australian Permian sediments. *Australian Journal of Botany*, **4**, 54-67.
- BALME, B. E. & HENNELLY, J. P. 1956b. Trilete sporomorphs from Australian Permian sediments. *Australian Journal of Botany*, **4**, 240-260.

- BALME, B. E. & PLAYFORD, G. 1967. Late Permian plant microfossils from the Prince Charles Mountains, Antarctica. *Revue de Micropaléontologie*, **10**, 179-192.
- BANERJEE, A. 1959. Carboniferous lithofacies, rhydymwyn to erryrys, North Wales. *Geological Journal*, **6**, 181-184.
- BANGERT, B., STOLLHOFEN, H., LORENZ, V. & ARMSTRONG, R. 1999. The geochronology of ash-fall tuffs in the glaciogenic Carboniferous- Permian Dwyka Group of Namibia and South Africa. *Journal of African Earth Sciences*, **29**, 33-49.
- BERTHELIN, M., BROUTIN, J., KERP, H., *ET AL.* 2003. The Oman Gharif mixed paleoflora: a useful tool for testing Permian Pangea reconstructions. *Palaeogeography, Palaeoclimatology, Palaeoecology*, **196**, 85-98.
- BESEMS, R. E. & SCHURMAN, W. M. L. 1987. Palynostratigraphy of late Paleozoic glacial deposits of the Arabian Peninsula with special reference to Oman. *Palynology*, **11**, 37-53.
- BHARADWAJ, D. C. 1954. Einige neue Sporengattungen des Saarkarbons. *Neues Jahrbuch für Geologie und Paläontologie, Monatshefte*, **11**, 512-525.
- BHARADWAJ, D. & SALUJHA, S. K. 1964. Sporological study of seam VIII in Raniganj Coalfield, Bihar (India). Part 1. Description of spores dispersae. *Palaeobotanist*, **12**, 181-215.
- BHARADWAJ, D. C. & SRIVASTAVA, S. C. 1973. Subsurface palynological successions in Korba Coalfield, Middle Permian, India. *Palaeobotanist*, **20**, 137-151.
- BHARADWAJ, D. C. & TIWARI, R. S. 1964. On two monosaccate genera from Barakar Stage, India. *Palaeobotanist*, **12**, 139-146.
- BLANFORD, W. T. 1886. Notes on the smoothed and striated boulders from a Pre-Tertiary deposit in the Punjab Salt Range. *Geological Magazine*, **3**, 394-395.
- BLATT, H. 1967. Original characteristics of quartz grains. *Journal of Sedimentary Petrology*, **37**, 401-424.
- BOGGS, S. J. 2001. *Principles of sedimentology and stratigraphy: Englewood Cliffs, New Jersey*, Prentice Hall, 3rd edition, 726p.
- BOSE, M. N. & MAHESHWARI, H. K. 1968. Palaeozoic spores dispersae from Congo II- The Epulu River (Ituri). *Annales Musee Royal De L'Afrique Central-Sciences Géologiques, Série in-8°*, **53**, 167-251.

- BROUTIN, J., ROGER, J., PLATEL, J.-P., *ET AL.* 1995. The Permian Pangea. Phytogeographic implications of new paleontological discoveries in Oman (Arabian Peninsula). *C. R. Acad. Sci. Paris, Série IIa* 321, 1069-1086.
- CAPUTO, M. V., MELO, J. H. G., STREEL, M. & ISBELL, J. L. 2008. Late Devonian and Early Carboniferous glacial records of South America. *In: FIELDING, C. R. FRANK, T. D. & ISBELL, J. L. (eds) Resolving the Late Paleozoic Ice Age in Time and Space.* Geological Society of America Special Paper, **441**, 161-173.
- CÉSARI, S. N. 2007. Palynological biozones and radiometric data at the Carboniferous-Permian boundary at western Gondwana. *Gondwana Research*, **11**, 529-536.
- CÉSARI, S. N., ARCHANGELSKY, S. & DE SEOANE, L. 1995. Palinología del Paleozoico Superior de la perforación Las Mochas, Provincia de Santa Fe, Argentina. *Ameghiniana*, **32**, 73-106.
- CÉSARI, S. N. & GUTIÉRREZ, P. R. 2000. Palynostratigraphy of Upper Paleozoic sequences in central-western Argentina. *Palynology*, **24**, 113-146.
- CHAKRABARTI, A. 2005. Sedimentary structures of tidal-flats: A journey from coast to inner estuarine region of eastern India. *Journal of Earth System Science*, 114, 353-368.
- CHERNYKH, V. V. 2002. Zonal scale of the Kasimovian and Gzhelian stages based on conodonts of genus *Streptognathodus*. *In: CHUVASHOV, B. I. & AMON, E. A. (eds) Stratigraphy and Palaeogeography of Carboniferous of Eurasia.* Ekaterinburg. 302-306.
- CHUVASHOV, B. I. CHERNYKH, V. V. & MIZEN, G. A. 1993. Zonal divisions of the boundary deposits of Carboniferous and Permian in sections of different facies in the South Urals. *Permophiles*, **22**, 11-16.
- COLLINSON, J. D. 1996. *Alluvial Sediments.* *In: READING, H.G. (ed) Sedimentary Environments and Facies*, 3rd edition. Blackwell Publishing, Oxford, 37-82.
- CONYBEARE, W. D. & PHILLIPS, W. 1822. *Outlines of the geology of England and Wales, with an introduction compendium of the general principles of that science, and comparative views of the structure of foreign countries, Part 1.* London. William Phillips, p. 470.
- COTTER, E. & GRAHAM, J. R. 1991. Coastal plain sedimentation in the late Devonian of southern Ireland; hummocky cross-stratification in fluvial deposits?. *Sedimentary Geology*, **72**, 201-224.

- DAEMON, R. F. & QUADROS, L. P. 1970. Bioestratigrafia do Neopaleozóico da Bacia do Paraná. *Congresso Brasileiro de Geologia 24, Brasília. Anais*, 359-412.
- DASGUPTA, P. 2006. Facies characteristics of Talchir Formation, Jharia Basin, India: implications for initiation of Gondwana sedimentation. *Sedimentary Geology*, **185**, 59-78.
- DAVYDOV, V. I., ANISIMOV, R. M. & NILSSON, I. 1999. Upper Paleozoic sequence stratigraphy of the Arctic region implied from graphic correlation: Spitsbergen and the Barents Sea Shelf. *Proceedings of the International Conference on Pangea and the Paleozoic-Mesozoic Transition*. China University of Geosciences Press, Wuhan, 94-97.
- DAVYDOV, V. I., GLENISTER, B. F., SPINOSA, C., *ET AL.* 1998. Proposal of Aidaralash as Global Stratotype Section and Point (GSSP) for the base of the Permian System. *Episodes*, **21**, 11-18.
- DERCOURT, J., RICOU, L. E., VRIELINCK, B. 1993. *Atlas Tethys Palaeoenvironmental Maps. Explanatory Notes*. (Paris Ed BEICIP), 1-307.
- DIAZ, M. E. 1993. Palinologia do Grupo Itararé na porção centro-sul do Rio Grande do Sul, Permiano da Bacia do Paraná, Brasil. *Pesquisas*, **20**, 119-131.
- DICKINSON, W. R. 1985. Interpreting provenance relations from detrital modes of sandstones. In: ZUFFA, G.G. (ed) *Provenance of Arenites*. Dordrecht-Boston-Lancaster, D. Reidel Publication Company, 333-361.
- DIENER, C. 1912. The Trias of the Himalayas. *Memoir of the Geological Survey of India*, **36**, 202-360.
- EL-NAKHAL, H. A., STEPHENSON, M. H. & OWENS, B. 2002. New Late Carboniferous-Early Permian palynological data from glacial sediments in the Kooli Formation, Republic of Yemen. *Micropaleontology*, **48**, 222-228.
- ELPHINSTONE, M. 1815. *An Account of the Kingdom of Caubul and Its Dependencies in Persia, Tartary, and India Comprising a View Afghaun Nation and a History of the Dooraunee Monarchy*. Longman, Hurst, Rees, Orm, and Brown, London, 675 p.
- EVANS, P. R. 1969. Upper Carboniferous and Permian palynological stages and their distribution in Eastern Australia. In Gondwana Stratigraphy, IUGS. *1st Gondwana Symposium, Buenos Aires, 1967*. UNESCO, 41-54.
- FATMI, A. N. 1973. Lithostratigraphic units of the Kohat-Potwar Province, Indus Basin, Pakistan. *Geological Survey of Pakistan Memoir*, 1080 pp.

- FIELDING, C. R., FRANK, T. D. & ISBELL, J. L. 2008a. Preface and acknowledgments. *In*: FIELDING, C. R. FRANK, T. D. & ISBELL, J. L. (eds) *Resolving the Late Paleozoic Ice Age in Time and Space*. Geological Society of America Special Paper, **441**, V-VII.
- FIELDING, C. R., FRANK, T. D., BIRGENHEIER, L. P., *ET AL.* 2008b. Stratigraphic record and facies associations of the late Paleozoic ice age in eastern Australia (New South Wales and Queensland). *In*: FIELDING, C. R. FRANK, T. D. & ISBELL, J. L. (eds) *Resolving the Late Paleozoic Ice Age in Time and Space*. Geological Society of America Special Paper, **441**, 41-57.
- FIELDING, C. R., FRANK, T. D. & ISBELL, J. L. 2008c. The late Paleozoic ice age- A review of current understanding and synthesis of global climate patterns. *In*: FIELDING, C. R. FRANK, T. D. & ISBELL, J. L. (eds) *Resolving the Late Paleozoic Ice Age in Time and Space*. Geological Society of America Special Paper, **441**, 343-354.
- FINZEL, E. S. & MCCARTHY, P. J. 2005, *Architectural analysis of fluvial conglomerate in the Nanushuk Formation, Brooks Range Foothills, Alaska*. Alaska Division of Geological & Geophysical Surveys Preliminary Interpretive Report 2005-2, 18 p.
- FLEMING, A. 1848. Report on the Salt Range, and on its coal and other minerals: *Asiatic Society of Bengal Journal*, **17**, 500-526.
- FOSTER, C. B. 1975. Permian plant microfossils from the Blair Athol Coal Measures Central Queensland, Australia. *Palaeontographica Abteilung B*, **154**, 121-171.
- FOSTER, C. B. 1979. Permian plant microfossils of the Blair Athol Coal Measures, Baralaba Coal Measures and Basal Rewan Formation of Queensland. *Geological Survey of Queensland, Publication*, **372**, 1-244.
- FOSTER, C. B. & WATERHOUSE, J. B. 1988. The *Granulatisporites confluens* Opper-zone and Early Permian marine faunas from the Grant Formation on the Barbwire Terrace, Canning Basin, Australia. *Australian Journal of Earth Sciences*, **35**, 135-157.
- FRAKES, L. A., FRANCIS, J. E. & SYKTUS, J. I. 1992. *Climate modes of the Phanerozoic*. Cambridge University Press, 274 p.
- FRAKES, L. A., KEMP, E. M. & CROWELL, J. C. 1975. Late Paleozoic Glaciation: Part VI, Asia. *Bulletin of the Geological Society of America*, **86**, 454-464.
- GAETANI, M. 1997. The Karakoram block in central Asia, from Ordovician to Cretaceous. *Sedimentary Geology*, **109**, 339-359.
- GAETANI, M., ARCHE, A., KIERSNOWSKI, H., *ET AL.* 2000. Wordian palaeogeographic map. *In*: DERCOURT, J., GAETANI, M., VRIELYNCK, B., *ET AL.* (eds) *Peri-Tethys Atlas and Explanatory notes, map 3, CCGM/CGMW*, Paris, 19-25.

- GASTALDO, R. A., DiMICHELE, W. A. & PFEFFERKORN, H. W. 1996. Out of the icehouse into the greenhouse: A late Paleozoic analogue for modern global vegetational change. *GSA Today*, **10**, 1-7.
- GEE, E. R. 1947. Further note on the age of the saline series of the Punjab and of Kohat. *National Academy of Sciences India, section B procedures*, **16**, 95-154.
- GEE, E. R., 1980. *Salt Range Maps. Geological Survey of Pakistan, Lahore.*
- GEE, E. R. 1989. Overview of the geology and structure of the Salt Range, with observation on related areas of northern Pakistan. In: MALINCONICO, L. L. & LILLIE, R. J. (eds) *Tectonics of the Western Himalayas*. Geological Society of America Special Paper, **232**, 95-112.
- GHAURI, A. A. K., ANWAR, M., KAMEL, K. S. & ISSA, I. M. 1977. The study of nature and origin of the Tobra Formation in the eastern part of the Punjab Salt Range. *Geological Bulletin University of Peshawar*, **9**, 67-78.
- GHAVIDEL-SYOOKI, M. 1996. Acritarch biostratigraphy of the Palaeozoic rock units in the Zagros Basin, Southern Iran. In: FATKA, O. & SERVAIS, T. (eds) *Acritarcha in Praha 1996*. Proceedings of international meeting and workshop. Acta Universitatis Carolinae Geologica, **40**, 385-411.
- GHAZI, S. & MOUNTNEY, N. P. 2009. Facies and architectural element analysis of a meandering fluvial succession: The Permian Warchha Sandstone, Salt Range, Pakistan. *Sedimentary Geology*, **221**, 99-126.
- GHAZI, S. & MOUNTNEY, N. P. 2011. Petrography and provenance of the Early Permian fluvial Warchha Sandstone, Salt Range, Pakistan. *Sedimentary Geology*, **233**, 88-110.
- GLENISTER, B. F. & FURNISH, W. M. 1961. The Permian ammonoids of Australia. *Journal of Paleontology*, **35**, 673-736.
- GLENISTER, B. F. & FURNISH, W. M. 1970. Permian Ammonoid *Cyclolobus* from the Salt Range, West Pakistan. In: KUMMEL, B. & TEICHERT, C. (eds) *Stratigraphic Boundary Problems: Permian and Triassic of West Pakistan*. University Press of Kansas, Department of Geology Special Publication, **4**, 153-175.
- GRABAU, A. W. 1931. The Permian of Mongolia. American Museum of Natural History, *Natural History of Central Asia*, **4**, 665.
- GRADSTEIN, F. M., OGG, J. G. & SMITH, A. G. 2004. *A Geologic Time Scale 2004*. Cambridge University press, 589.

- GRANT, R. E. 1970. Brachiopods from Permian-Triassic boundary beds and age of Chhidru Formation, West Pakistan. In: KUMMEL, B. & TEICHERT, C. (eds) *Stratigraphic Boundary Problems: Permian and Triassic of West Pakistan*. University Press of Kansas, Department of Geology Special Publication, **4**, 117-151.
- GUERRA-SOMMER, M., CAZZULO-KLEPZIG, M., FORMOSO, M. L., *ET AL.* 2005, New radiometric data from ash fall rocks in Candiota coal-bearing strata and the palynostratigraphic framework in southern Paraná Basin (Brazil) [abs.], In *Gondwana 12: Mendoza, Argentina*, p. 189.
- HAMMER, Ø., HARPER, D. A. T. & RYAN, P. D. 2001. Paleontological statistics software package for education and data analysis. *Palaeontologia Electronica*, **4**, 9pp.
http://palaeo-electronica.org/2001_1/past/issue1_01.htm
- HART, G. F. 1971. *Statistical evaluation of palynomorph distribution in the Atchafalaya Swamp. Consultant Report*. Texaco Incorporated, Lafayette, 1-80.
- HOWARD, J. P., CUNNINGHAM, W. D., DAVIES, S. J., *ET AL.* 2003. The stratigraphic and structural evolution of the Dzereg Basin, western Mongolia: clastic sedimentation, transpressional faulting and basin destruction in an intraplate, intracontinental setting. *Basin Research*, **15**, 45-72.
- HUANG, T. K. 1932. The Permian formations of Southern China. *Memoirs of the Geological Survey of China Series A*, **10**, 1-40.
- HUSSAIN, B. R. 1967. Saiyiduwali member, a new name for the lower part for the Permian Amb Formation, West Pakistan. *Pakistan Geological Survey Memoir Palaeontologia Pakistanica*, **5**, 88-95.
- ISELL, J. L., GELHAR, G. A. & SEEGER, G. M. 1997. Reconstruction of pre-glacial topography using a post-glacial flooding surface; upper Paleozoic deposits, central Transantarctic Mountains, Antarctica. *Journal of Sedimentary Research*, **67**, 264-272.
- ISELL, J. L., LENAHER, P. A., ASKIN, R. A., *ET AL.* 2003a. Re-evaluation of the timing and extent of late Paleozoic glaciation in Gondwana; role of the Transantarctic Mountains. *Geology*, **31**, 977-980.
- ISELL, J. L., MILLER, M. F., WOLFE, K. L. & LENAHER, P. A. 2003b. Timing of late Paleozoic glaciation in Gondwana: was the glaciation responsible for the development of northern hemisphere Cyclothem?. In: CHAN, M. A. & ARCHER, A. A. (eds) *Extreme Depositional Environments: Mega End Members in Geologic Time*. Geological Society of America Special Paper, **370**, 5-24.

- ISBELL, J. L., KOCH, Z. J., SZABLEWSKI, G. M. & LENAHER, P. A. 2008. Permian glacial deposits in the Transantarctic Mountains, Antarctica. *In: FIELDING, C. R. FRANK, T. D. & ISBELL, J. L. (eds) Resolving the Late Paleozoic Ice Age in Time and Space*. Geological Society of America Special Paper, **441**, 59-70.
- JAN, I. U., STEPHENSON, M. H. & KHAN, F. R. 2009. Palynostratigraphic correlation of the Sardhai Formation (Permian) of Pakistan. *Review of Palaeobotany and Palynology*, **158**, 72-82.
- JAN, I. U. & STEPHENSON, M. H. 2011. Palynology and correlation of the Upper Pennsylvanian Tobra Formation from Zaluch Nala, Salt Range, Pakistan. *Palynology*, **35**, 212-225.
- JIN, Y., WARDLAW, B. R., GLENISTER, B. F., *ET AL.* 1997. Permian chronostratigraphic subdivisions. *Episodes*, **20**, 10-15.
- JOHNSON, H. D. & BALDWIN, C. T. 1996. Shallow clastic seas. *In: READING, H. G. (ed) Sedimentary Environments: Processes, Facies and Stratigraphy*. Blackwell Science, Oxford, 232-280.
- JONES, A. T. & FIELDING, C. R. 2004. Sedimentological record of the late Paleozoic glaciation in Queensland, Australia. *Geology*, **32**, 153-156.
- JONES, M. J. & TRUSWELL, E. M. 1992. Late Carboniferous and Early Permian palynostratigraphy of the Joe Joe Group, southern Galilee Basin, Queensland and implications for Gondwana stratigraphy. *Bureau of Mines and Mineral Resources Journal of Australian Geology and Geophysics*, **13**, 143-185.
- KARPINSKY, A. P. 1874. Geological investigation of the Orenburg area. *Berg-jour., II, Verhandl. Miner. Gesellsch*, **IX**, 13-31.
- KEMP, E. M. 1975. The palynology of Late Palaeozoic glacial deposits of Gondwanaland. *In: CAMPBELL, K. S. W. (ed). Gondwana Geology*. Canberra. Australian National University Press, 397-413.
- KEMP, E. M., BALME, B. E., HELBY, R. J. *ET AL.* 1977. Carboniferous and Permian palynostratigraphy in Australia and Antarctica: a review. *Bureau of Mines and Minerals Resources Journal of Australian Geology and Geophysics*, **2**, 177-208.
- KHAN, Q. M., AHMED, S., MIRZA, K. & KHAN, F. R. 2001. Some monosaccate pollen from the Tobra Formation of the Nilawahan Gorge, Central Salt Range, Pakistan. *Geological Bulletin of the Punjab University*, **36**, 95-102.

- KING, M. R. 2008. *Fluvial Architecture of the interval spanning the Pittsburgh and Fishpot limestones (Late Pennsylvanian), southeastern Ohio*. Unpublished MS thesis, Ohio University.
- KOKEN, E. 1907. Indisches Perm und permische Eiszeit. Neues Jahrbuch für Geologie und Paläontologie, Festband, 446-546.
- KREMP, G., 1965. *Morphologic encyclopedia of palynology*. The University of Arizona Press, Tucson, 263.
- KRUCK, W. & THIELE, J. 1983. Late Palaeozoic glacial deposits in the Yemen Arab Republic. *Geologisches Jahrbuch. Reihe B: Regionale Geologie Ausland*, **46**, 3-29.
- KUMMEL, B. 1970. Ammonoids from the Kathwai Member, Mainsails Formation, Salt Range, West Pakistan. In: KUMMEL, B. & TEICHERT, C. (eds) *Stratigraphic Boundary Problems: Permian and Triassic of West Pakistan*. University Press of Kansas, Department of Geology Special Publication, **4**, 177-192.
- KUMMEL, B. & TEICHERT, C. 1970. Stratigraphy and paleontology of the Permian-Triassic boundary beds, Salt Range and Trans-Indus Ranges, West Pakistan. In: KUMMEL, B. & TEICHERT, C. (eds) *Stratigraphic Boundary Problems: Permian and Triassic of West Pakistan*. University Press of Kansas, Department of Geology Special Publication, **4**, 2-110.
- KYLE, R. A. & SCHOPF, J. M. 1982. Permian and Triassic palynostratigraphy of the Victoria Group, Transantarctic Mountains. In: CRADDOCK, C. (ed) *Antarctic Geosciences*. Madison. University of Wisconsin Press, International Union of Geological Sciences, 649-659.
- LELE, K. M. 1964. Studies in the Talchir flora of India. 2. Resolution of the spore genus *Nuskoisporites* Potonié & Klaus. *Palaeobotanist*, **12**, 147-168.
- LEONOVA, T. B. 1998. Permian ammonoids of Russia and Australia. *Proceedings of the Royal Society of Victoria*, **110**, 157-162.
- LESCHIK, G. 1956. Sporen aus dem Salzton des Zechsteins von Neuhof (Bei Fulda). *Palaeontographica B*, **100**, 122-142.
- LINDSTRÖM, S. 1995. Early Permian palynostratigraphy of the Northern Heimefrontfjella Mountain-Range, Dronning Maud Land, Antarctica. *Review of Palaeobotany and Palynology*, **89**, 359-415.

- LÓPEZ-GAMUNDI, O. R. 1989. Postglacial transgressions in late Palaeozoic basins of western Argentina: a record of glacioeustatic sea level rise. *Palaeogeography, Palaeoclimatology, Palaeoecology*, **71**, 257-270.
- LOTZE, F. 1966. Zur permokarbonischen Eiszeit auf dem indischen Subkontinent. *Neues Jahrbuch für Geologie und Paläontologie, Monatshefte*, 751-752.
- LOVE, C. F. 1994. The palynostratigraphy of the Haushi Group (Westphalian-Artinskian) in Oman. In: SIMMONS, M. D. (ed), *Micropalaeontology and Hydrocarbon Exploration in the Middle East*, Chapman and Hall, London, 23-39.
- MACRAE, C. S. 1978. *Palaeozoic palynology of Botswana*. Unpublished MSc. thesis Witwatersrand University Johannesburg, South Africa,
- MACRAE, C. S. 1988. Palynostratigraphic correlation between the Lower Karoo sequence of the Waterburg and Pafuri coal-bearing basins and Hammanskraal plant macrofossil locality, Republic of South Africa. *Memoirs of the Geological Survey of South Africa*, **75**, 1-217.
- MAEJIMA, W., DAS, R., PANDYA, K. L., HAYASHI, M. 2004. Deglacial control on sedimentation and basin evolution of Permo-Carboniferous Talchir Formation, Talchir Gondwana basin, Orissa, India. *Gondwana Research*, **7**, 339-352.
- MARQUES-TOIGO, M. 1974. Some new species of Spores and pollens of Lower Permian age from the San Gregorio Formation in Uruguay. *Anais da Academia Brasileira de Ciências*, **46**, 601-616.
- MARQUES-TOIGO, M. 1991. Palynobiostratigraphy of the southern Brazilian Neopaleozoic Gondwana sequence. In: International Gondwana Symposium, 7th São Paulo. Proceedings, 503-515.
- MARQUES-TOIGO, M. & KLEPZIG, M. C. 1995. Catálogo de Esporos e Pólen Fósseis do Paleozóico. *Boletim de Geociências da Petrobras*, **1**, 9, 151.
- MARQUES-TOIGO, M. & PICARELLI, A. T. 1984. On the morphology and affinities of *Lundladispora* Balme 1963 in the Permian of the Paraná Basin, Brazil. *Boletim IG-USP, Instituto De Geociências, Universidade De São Paulo*, **15**, 46-52.
- MARTIN, J. R., REDFERN, J. & AITKEN, J., F. 2008. A regional over-view of the late Paleozoic glaciation in Oman. In: FIELDING, C. R. FRANK, T. D. & ISBELL, J. L. (eds) *Resolving the Late Paleozoic Ice Age in Time and Space*. Geological Society of America Special Paper, **441**, 175-186.

- McCLURE, H. A. 1980. Permian-Carboniferous glaciation in the Arabian Peninsula. *Geological Society of America Bulletin*, **91**, 707-712.
- McKERROW, W. S. & SCOTese, C. R. 1990. Palaeozoic paleogeography and biogeography. *Geological Society of London Memoir*, **12**, 435.
- MERTMANN, D. 1999. Das marine Perm in der Salt Range und in den Trans Indus Ranges, Pakistan. *Berliner Geowissenschaftliche Abhandlungen*, **A 204**, 1-94.
- MERTMANN, D. 2003. Evolution of the marine Permian carbonate platform in the Salt Range (Pakistan), *Palaeogeography, Palaeoclimatology, Palaeoecology*, **191**, 373-384.
- MIALl, A. D. 1992. Alluvial deposits. In: WALKER, R.G. & JAMES, N. P. (eds) *Facies Models: Response to Sea Level Change*. Geological Association of Canada, 119-142.
- MIALl, A. D. 1996. *The Geology of Fluvial Deposits: Sedimentary Facies, Basin Analysis, and Petroleum Geology*. Springer-Verlag, New York, 582.
- MILLSTEED, B. D. 1999. Palynology of the Early Permian coal-bearing deposits near Vereeniging, Free State, South Africa. *Bulletin of the Council for Geoscience of South Africa*, **124**, 1-77.
- MODIE, B. N. 2007. *The Palaeozoic palynostratigraphy of the Karoo Supergroup and palynofacies insight into palaeoenvironmental interpretations, Kalahari Karoo Basin, Botswana*. Unpublished PhD thesis, Universite De Bretagne Occidentale, France.
- MODIE, B. N. & HÉRISSE, A. L. 2009. Late Palaeozoic palynomorphs assemblages from the Karoo Supergroup and their potential for biostratigraphic correlation, Kalahari Karoo Basin, Botswana. *Bulletin of Geosciences*, **84**, 337-353.
- MORY, A. J., REDFERN, J. & MARTIN, J. R. 2008. A review of Permian-Carboniferous glacial deposits and Western Australia. In: FIELDING, C. R. FRANK, T. D. & ISBELL, J. L. (eds) *Resolving the Late Paleozoic Ice Age in Time and Space*. Geological Society of America Special Paper, **441**, 29-40.
- MURCHISON, R. I. 1841. First sketch of the principal results of a second geological survey of Russia. *Philosophical Magazine Series*, **319**, 417-422.
- MUTTONI, G., GAETANI, M., KENT, D. V., ETAL. 2009. Opening of the neo-Tethys Ocean and the Pangea B to Pangea A transformation during the Permian. *GeoArabia*, **14**, 17-48.

- NADER, A. D., KHALAF, F.H. & HADID, A. A. 1993. Palynology of the Permo-Triassic boundary in Borehole Mityaha-1, south west Mosul City-Iraq. *Mu'tah Journal for Research and Studies, Mu'tah University, Jordan*, **8**, 223-280.
- NAHUYS, J., ALPERN, B. & YBERT, J. P. 1968. Estudo palinologico de alguns carvões do sul Brazil. *Boletim, Instituto Tecnológico do Rio Grande do Sul*, **46**, 3-61.
- NEMIROVSKAYA, T. I. 1999. Bashkirian conodonts of the Donets Basin. *Scripta Geologica*, **119**, 115p.
- NEVES, R. & OWENS, B. 1966. Some Namurian camerate miospores from the English Pennines. *Pollen spores*, **8**, 337-360.
- NOETLING, F. 1896. Beiträge zur Kenntnis der glaciation Schichten permischen Alters in der Salt Range, Punjab (Indien). *Neues Jahrbuch für Mineralogie Geologie und Palaeontologie*, **2**, 61-86.
- NOETLING, F. 1900a. *Note on the relationship between the Productus limestone and the Ceratite formation of the Salt Range*. General report Geological Survey of India, 176-183.
- NOETLING, F. 1900b. Ueber die Auffindung von *Otoceras* sp. in der Salt Range. *Neues Jahrbuch Mineralogie, Geologie, Palaeontologie*, **1**, 139-141.
- NOETLING, F. 1900c. Die *Otoceras* beds in Indien: *Centralbl. Mineralogie, Geologie, Palaeontologie*, 216-217.
- NOETLING, F. 1901. Beiträge zur Geologie der Salt Range, insbesondere der permischen und triassischen Ablagerungen. *Neues Jahrbuch für Mineralogie, Geologie und Palaeontologie*, **14**, 369-471.
- OLDHAM, R. D. 1887. Note on the faceted pebbles from the Olive Group of the Salt Range, Punjab, India. *Geological Magazine*, **4**, 32-35.
- OPLUŠTIL, S., MARTÍNEK, K. & TASÁRYOVÁ, Z. 2005. Facies and architectural analysis of fluvial deposits of the Nýřany Member and the Týnec Formation (Westphalian D-Barruelian) in the Kladno-Rakovník and Pilsen Basins. *Bulletin of Geosciences*, **80**, 45-66.
- OSTERLOFF, P.L., PENNEY, R., AITKEN, J., ET AL. 2004. Al Khlata Formation, Interior Oman. *GeoArabia Special Publication*, **3**, Gulf PetroLink, Bahrain, p. 61-81.
- PAKISTANI-JAPANESE RESEARCH GROUP. 1985. Permian and Triassic in the Salt Range and Surghar Range, Pakistan. In: NAKAZAWA, K. & DICKINS, J. M. (eds) *The Tethys- Her*

Paleogeography and Paleobiogeography from Paleozoic to Mesozoic. Tokai University Press, 221-312.

PASCOE, E. H. 1959. *A manual of the geology of India and Burma*. India Government Press Calcutta. II 484-1338.

PENNEY, R. A., AL BARRAM, I. & STEPHENSON, M. H. 2008. A high resolution palynozonation for the Al Khlata Formation (Pennsylvanian to Lower Permian), South Oman. *Palynology*, **32**, 213-229.

PETTIJOHN, F. J., POTTER, P. E. & SIEVER, R., 1987. *Sand and sandstone*. 2nd edition. Springer Verlag, p. 533.

PLAYFORD, G. 1990. Proterozoic and Palaeozoic palynology of Antarctica: a review *In*: TAYLOR, T. N. & TAYLOR, E. L. (eds) *Antarctic Paleobiology: Its role in the reconstruction of Gondwana*. Springer Verlag, NY, 51-70.

PLAYFORD, G. & DETTMANN, M. E. 1996. Spores *In*: JANSONIUS, J. & MCGREGOR, D. C. (eds) *Palynology: principles and applications*. American Association of Stratigraphic Palynologists Foundation, **1**, 227-260.

PLAYFORD, G. & DINO, R. 2000. Palynostratigraphy of the upper Palaeozoic strata (Tapajos Group). Amazonas Basin, Brazil: Part One. *Palaeontographica Abt. B*, **255**, 1-46.

PLAYFORD, G. & DINO, R. 2002. Permian palynofloral assemblages of the Chaco-Paraná Basin, Argentina: systematics and stratigraphic significance. *Revista Española de Micropaleontología*, **34**, 235-288.

PLAYFORD, G. & DINO, R. 2005. Carboniferous and Permian palynostratigraphy. *In*: KOUTSOUKOS, E. A. M. (ed). *Applied stratigraphy*, volume 23. Topics in Geobiology, 101-121. Springer, Dordrecht.

PLAYFORD, G. & RIGBY, J. F. 2008. Permian palynoflora of the Ainmin and Aiduna formations, West Papua. *Revista Española de Micropaleontología*, **40**, 1-57.

POTONIÉ, R. 1958. Synopsis der Gattungen der Sporae dispersae II. Teil: Sporites, Saccites, Aletes, Praecolpates, Polylicates, Monocolpates. *Beihefte Geologischen Jahrbuch*, **31**, 1-114.

POTONIÉ, R. 1970. Synopsis der Gattungen der Sporae dispersae Teil V. Nachträge zu allen Gruppen (Turmae). *Beihefte zum Geologischen Jahrbuch*, **87**, 1-222.

- POTONIÉ, R. & KLAUS, W. 1954. Einige Sporengattungen des alpine Salzgebirges. *Geologisches Jahrbuch*, **68**, 517-546.
- POTONIÉ, R. & SAH, S. C. D. 1960. Sporae dispersae of the lignites from Cannanore Beach on the Malabar Coast of India. *Palaeobotanist*, **7**, 121-135.
- POWIS, G. D. 1979. *Palynology of the Late Palaeozoic glacial sequence, Canning Basin, Western Australia*. Unpublished PhD thesis, University of Western Australia.
- POWIS, G. D. 1984. Palynostratigraphy of the Late Carboniferous sequence, Canning Basin, W. A. In: PURCELL, P. G. (ed) *The Canning Basin Western Australia proceedings Geological Society of Australia, Petroleum Exploration Society of Australia Symposium, Perth*, 429-438.
- PUNT, W., BLACKMORE, S., NILSSON, S. & LE THOMAS, A. 1994. Glossary of pollen and spore terminology. *Laboratory of Palaeobotany and Palynology Foundation Utrecht Contributions Series No. 1*, 1-71.
- PUNT, W., HOEN, P. P., BLACKMORE, S., NILSSON, S. & LE THOMAS, A. 2007. Glossary of pollen and spore terminology. *Review of Palaeobotany and Palynology*, **143**, 1-81.
- QURESHI, K. A., GHAZI, S. & BUTT, A. A. 2008. Shallow shelf sedimentation of the Jurassic Samana Suk Limestone, Kala Chitta Range, Lesser Himalayan, Pakistan. *Geological Bulletin of the Punjab University*, **43**, 1-14.
- REED, F. R. C. 1936. Some fossils from the Eurydesma and Conularia beds (Punjabian) of the Salt Range. *India Geological Survey Memoirs Palaeontologia Indica New Series*, **1**, 1-36.
- ROBERTS, J., CLAOUÉ-LONG, J. & FOSTER, C. B. 1996. SHRIMP zircon dating of the Permian System of eastern Australia. *Australian Journal of Earth Sciences*, **43**, 401-421.
- ROCHA-CAMPOS, A. C., BASEI, A. C., NUTMAN, M. A. S. & SANTOS, P. R. 2006, SHRIMP U-Pb zircon geochronological calibration of the late Paleozoic supersequence, Paraná Basin, Brazil, In 5th South American Symposium on Isotope Geology, April 2006, Punta del Este, Uruguay: abstract 322, p. 471-475.
- ROWELL, A. J. 1970. *Lingula* from the Basal Triassic, Kathwai Member, Mianwali Formation, Salt Range and Surghar Range, West Pakistan. In: KUMMEL, B. & TEICHERT, C. (eds) *Stratigraphic Boundary Problems: Permian and Triassic of West Pakistan*. University Press of Kansas, Department of Geology Special Publication, **4**, 111-116.

- RUSSO, A., S., ARCHANGELSKY, S. & GAMERRO, J. C. 1980. Los depósitos supra Palaeozoicos en el subsuelo de la Llanura Chaco-Pampeana, Argentina. *Actas del II Congreso Argentino de Paleontología y Bioestratigrafía y I Congreso Latinoamericano de Paleontología 1978*, **4**, 157-173.
- RUST, B. R. & NANSON, G. C. 1989. Bedload transport of mud as pedogenic aggregates in modern and ancient rivers. *Sedimentology*, **36**, 291-306.
- RUZHENZEV, V. E. 1950. Type section and biostratigraphy of the Sakmarian Stage. *Doklady Akademii Nauk USSR*, **71**, 1101-1104.
- SARJEANT, W. A. S. 1970. Acritarchs and Tasmanitids from the Chhidru Formation, Uppermost Permian of West Pakistan. In: KUMMEL, B. & TEICHERT, C. (eds) *Stratigraphic Boundary Problems: Permian and Triassic of West Pakistan*. University Press of Kansas, Department of Geology Special Publication, **4**, 277-304.
- SCOTESE, C. R., BOUCOT, A. J. & MCKERROW, W. S. 1999. Gondwana palaeogeography and palaeoclimatology. *Journal of African Earth Sciences*, **28**, 99-144.
- SCOTESE, C. R. & MCKERROW, W. S. 1990. Revised world maps and Introduction. *Geological Society London Memoirs*, **12**, 1-21.
- SEGROVES, K. L. 1970. Permian spores and pollen grains from the Perth Basin, Western Australia. *Grana*, **10**, 43-73.
- SENGÖR, A. M. C. 1979. Mid-Mesozoic closure of Permo-Triassic Tethys and its implications. *Nature*, **279**, 590-593.
- SHAH, S. M. I. 1977. Stratigraphy of Pakistan. *Geological Survey of Pakistan Memoir*, **12**, 26.
- SHAH, S. M. I. 1980. Stratigraphy and economic geology of central Salt Range. *Records of the Geological Survey of Pakistan*, **52**, 104 p.
- SINGH, H. P. 1964. A miospore assemblage from the Permian of Iraq. *Palaeontology*, **7**, 240-265.
- SOHN, I. G. 1970. Early Triassic Marine ostracodes from the Salt Range and Surghar Range, West Pakistan. In: KUMMEL, B. & TEICHERT, C. (eds) *Stratigraphic Boundary Problems: Permian and Triassic of West Pakistan*. University Press of Kansas, Department of Geology Special Publication, **4**, 193-206.
- SOUZA, P. A. 2006. Late Carboniferous palynostratigraphy of the Itararé Subgroup, northeastern Paraná Basin, Brazil. *Review of Palaeobotany and Palynology*, **138**, 9-29.

- SOUZA, P. A., AMARAL, P. G. C. & BERNARDES DE OLIVEIRA, M. E. C. 2006. A Late carboniferous palynoflora from the Itararé Subgroup (Paraná Basin) in Campinas, São Paulo State, Brazil. *Revue de micropaléontologie*, **49**, 105-115.
- SOUZA, P. A. & CALLEGARI, L. M. 2004. An Early Permian Palynoflora from the Itararé Subgroup. Paraná Basin, Brazil. *Revista Española de Micropaleontología*, **36**, 439-450.
- SOUZA, P. A. & MARQUES-TOIGO, M. 2003. An Overview on the palynostratigraphy of the Upper Paleozoic strata of the Brazilian Paraná Basin. *Revista del Museo Argentino de Ciencias Naturales, Nueva Serie*, **5**, 205-214.
- SOUZA, P. A. & MARQUES-TOIGO, M. 2005. Progress on the palynostratigraphy of the Permian strata in Rio Grande do Sul State, Paraná Basin, Brazil. *Anais da Academia Brasileira De Ciências*, **77**, 353-365.
- SOUZA, P. A., SAAD, A. R. & LIMA, M. R. 1997. Palinologia dos carvões Paleozóicos do Estado de São Paulo. II- O carvão de Monte Mor. *Revista do Instituto Geológico, São Paulo*, **18**, 7-21.
- STEPHENSON, M. H. 1998a. Preliminary correlation of palynological assemblages from Oman with the *Granulatisporites Confluens* Opper Zone of the Grant Formation (Lower Permian), Canning Basin, Western Australia. *Journal of African Earth Sciences*, **26**, 521-526.
- STEPHENSON, M. H. 1998b. *Stratigraphic and Systematic Palynology of Permian and Permo-Carboniferous Rocks of Oman and Saudi Arabia*. Unpublished PhD thesis, Sheffield University.
- STEPHENSON, M. H. 2004. Early Permian spores from Oman and Saudi Arabia. In: AL-HUSSEINI, M. I. (ed) *Carboniferous, Permian and Early Triassic Arabian Stratigraphy*. GeoArabia Special Publication, **3**, 185-215.
- STEPHENSON, M. H. 2006. Stratigraphic Note: Update of the standard Arabian Permian palynological biozonation; definition and description of the OSPZ5 and 6. *GeoArabia*, **11**, 173-178.
- STEPHENSON, M. H. 2008a. A review of the palynostratigraphy of Gondwanan Late Carboniferous to Early Permian glaciogene succession. In: FIELDING, C. R. FRANK, T. D. & ISBELL, J. L. (eds) *Resolving the Late Paleozoic Ice Age in Time and Space*. Geological Society of America Special Paper, **441**, 317-330.
- STEPHENSON, M. H. 2008b. Spores and Pollen from the Middle and Upper Gharif members (Permian) of Oman. *Palynology*, **32**, 157-182.

STEPHENSON, M. H. 2009. The age of the Carboniferous-Permian Converrucosisporites confluens Opper Biozone: New data from the Ganigobis Shale Member (Dwyka Group) of Namibia. *Palynology*, **33**, 167-177.

STEPHENSON, M. H. & AL-MASHAIKIE, S. Z. A. K. 2010. New age for the lower part of the Kuhlan Formation, northwest Yemen. *GeoArabia*, **15**, 161-170.

STEPHENSON, M. H. & AL-MASHAIKIE, S. Z. A. K. 2011. Stratigraphic Note: Update on the palynology of the Akbarah and Kuhlan formations, northwest Yemen. *GeoArabia*, **16**, 17-24.

STEPHENSON, M. H., AL RAWAHI, A. & CASEY, B. 2008. Correlation of the Al Khlata Formation in the Mukhaizna field, Oman, based on a new downhole, cuttings-based palynostratigraphic biozonation. *GeoArabia*, **13**, 15-34.

STEPHENSON, M. H., ANGIOLINI, L. & LENG, M. J. 2007. The Early Permian fossil record of Gondwana and its relationship to deglaciation: a review. In: WILLIAMS, M., HEYWOOD, A. M., GREGORY, F. J. & SCHMIDT, D. N. (eds) *Deep-Time perspective on Climate Change: Marrying the signal from Computer Models and Biological Proxies*. The Micropalaeontological Society Special Publications. The Geological Society, London, 169-189.

STEPHENSON, M. H. & FILATOFF, J. 2000a. Correlation of Carboniferous-Permian palynological assemblages from Oman and Saudi Arabia. In: AL-HAJRI, S. & OWENS, B. (eds) *Stratigraphic Palynology of the Palaeozoic of Saudi Arabia*. GeoArabia Special Publication, **1**, 168-191.

STEPHENSON, M. H. & FILATOFF, J. 2000b. Description and correlation of Late Permian palynological assemblages from the Khuff Formation, Saudi Arabia and evidence for the duration of the pre-Khuff Hiatus. In: AL-HAJRI, S. & OWENS, B. (eds) *Stratigraphic Palynology of the Palaeozoic of Saudi Arabia*. GeoArabia Special Publication, **1**, 192-215.

STEPHENSON, M. H. & OSTERLOFF, P. L. 2002. Palynology of the deglaciation sequences represented by the Lower Permian Rahab and Lower Gharif members, Oman. *American Association of Stratigraphic Palynologists Contribution Series*, **40**, 1-41.

STEPHENSON, M. H., OSTERLOFF, P. L. & FILATOFF, J. 2003. Palynological biozonation of the Permian of Oman and Saudi Arabia: progress and challenges. *GeoArabia*, **8**, 467-496.

STOLLE, E. 2007. Regional Permian palynological correlations: Southeast Turkey-Northern Iraq. *Comunicacoes Geológicas*, **94**, 125-143.

STOLLE, E. 2010. Recognition of southern Gondwanan palynomorphs at Gondwana's northern margin-and biostratigraphic correlation of Permian strata from SE Turkey and Australia. *Geological Journal*, **45**, 336-349.

STOLLE, E., YALÇIN, M. N. & KAVAK, O. 2011. The Permian Kas Formation of SE Turkey- palynological correlation with strata from Saudi Arabia and Oman. *Geological Journal*, **46**, doi: 10.1002/gj.1296.

STUMP, T. E. & VAN DER EEM, J. G. 1995. The stratigraphy, depositional environments and periods of deformation of the Wajid outcrop belt, southwestern Saudi Arabia. *Journal of African Earth Sciences*, **21**, 421-441.

SWEET, W. C. 1970. Uppermost Permian and Lower Triassic conodonts of the Salt Range and Trans-Indus Range, West Pakistan. In: KUMMEL, B. & TEICHERT, C. (eds) *Stratigraphic Boundary Problems: Permian and Triassic of West Pakistan*. University Press of Kansas, Department of Geology Special Publication, **4**, 207-275.

TANOLI, S. K., HUSSAIN, R. & SAJER, A. A. 2008. Facies in the Unayzah Formation and the Basal Khuff Clastics in subsurface, northern Kuwait. *GeoArabia*, **13**, 15-40.

TEICHERT, C. 1967. Nature of the Permian glacial record, Salt Range and Khisor Range, West Pakistan. *Neues Jahrbuch für Geologie und Paläontologie, Abhandlungen*, **129**, 167-184.

THEOBALD, W. 1854. Notes on the geology of the Punjab Salt Range. *Asiatic Society of Bengal Journal*, **23**, 651-678.

TIWARI, R. S. 1965. Miospore assemblage in some coals of Barakar Stage (Lower Gondwana) of India. *Palaeobotanist*, **13**, 168-214.

TIWARI, R. S. 1996. Palynoevent stratigraphy in Gondwana sequence of India. In: GUHA, P. K. S., AYYASAMI, K., SENGUPTA, S. & GHOSH, R. N. (eds) *Ninth International Gondwana Symposium, January 1994: Hyderabad, India*. Balkema/Rotterdam/Brookfield, p.3-19.

TIWARI, R. S. & TRIPATHI, A. 1988. Palynological zones and their climatic inference in the coal-bearing Gondwana of peninsular India. *Palaeobotanist*, **36**, 87-101.

TIWARI, R. S. & TRIPATHI, A. 1992. Marker Assemblage-Zones of spores and pollen species through Gondwana Palaeozoic and Mesozoic sequence in India. *Palaeobotanist*, **40**, 194-236.

TORSVIK, T. H., SMETHURST, M., BRIDEN, J. C. & STURT, B. A. 1990. A review of Palaeozoic palaeomagnetic data Europe and their palaeogeographical implications. In:

- McKerrow, S. & Scotese, C. (eds) *Palaeogeography and biogeography*. Journal Geological Society London Special Memoir, **12**, 25-41.
- Truswell, E. M. 1980. Permo-Carboniferous palynology of Gondwanaland: progress and problems in the decade of 1980. *BMR Journal of Australian Geology and Geophysics*, **5**, 95-111.
- Tschernyschew, T. 1902. Die obercarbonischen Brachiopoden des Ural und des Timan. *Comité geol. Russie Mémoire*, **316**, 1-116.
- Veevers, J. J. & Tewari, R. C. 1995. Gondwana master basin of Peninsular India between Tethys and the interior of the Gondwanaland Province of Pangea; Boulder, Colorado, Geological Society of America Memoir, **187**, 1-73.
- Venkatachala, B. S. & Kar, R. K. 1966. *Corisaccites* gen. nov., a new saccate pollen genus from the Permian of Salt Range, West Pakistan. *Palaeobotanist*, **15**, 107-109.
- Venkatachala, B. S. & Kar, R. K. 1968. Palynology of the Kathwai Shales, Salt Range, West Pakistan. 1. Shales 25ft above the Talchir Boulder Bed. *Palaeobotanist*, **16**, 156-166.
- Vergel, M. Del. M. 1986. Palinología del Paleozoico Superior en la perforación YPF Sf J1 (Josefina). Provincia de Santa Fe, Argentina I. Anteturma Proximegerminantes. *Ameghiniana*, **23**, 141-153.
- Vergel, M. Del. M. 1987. Consideraciones sobre el contenido microflorístico de la perforación YPF SE AB (Paleozoico superior), Arbol Blanco, Provincia de Santiago del Estero, Argentina. *VII Simposio Argentino de Paleobotánica y Palinología, Actas. Buenos Aires, Abril*, 75-78.
- Vergel, M. Del. M. 1993. Palinoestratigrafía de la secuencia Neopaleozoica en la Cuenca Chacoparanense Argentina. *Douzième Congrès International de la Stratigraphie et de Géologie du Carbonifère et Permien, Compte Rendus*, **1**, 201-212.
- Vijaya. 1994. Advent of Gondwana deposition on Indian Peninsula: a palynological reflection and relationship. *Ninth International Gondwana Symposium January 1994: Hyderabad, India*, 283-298.
- Vijaya, T., A. & Awatar, R. 2001. Vertical distribution of spore and pollen index species in the Permian sequence on Peninsular India. In: Weiss, R.E. (ed) *Contributions to geology and paleontology of Gondwana in honour of Helmut Wopfner: Cologne, Germany*. Geological Institute, University of Cologne, 475-495.

- VILLA, E. 2001. Report of the Working Group to define a GSSP close to the Moscovian/Kasimovian boundary. *Newsletter on Carboniferous Stratigraphy*, **19**, 8-11.
- VIRKKI, C. 1939. On the occurrence of winged spores in a Lower Gondwana glacial tillite from Australia and in Lower Gondwana shales in India. *Indian Academy of Science*, **9**, 7-12.
- VIRKKI, C. 1946. Spores from the Lower Gondwanas of India and Australia. *Proceedings of Indian Academy of Sciences*, **15**, 93-176.
- VISSER, J. N. J. 1997. Deglaciation sequences in the Permo-Carboniferous Karoo and Kalahari basins of southern Africa: a tool in the analysis of cyclic glaciomarine basin fills. *Sedimentology*, **44**, 507-521.
- WAAGEN, W. H. 1882-1885. Salt Range fossils. Part 4: Brachiopoda. *Palaeontologia Indica, Series*, **13**, 329-770.
- WAAGEN, W. H. 1879-1888. Salt Range fossils. Part 4: Brachiopoda. *Palaeontologia Indica, Series*, **13**, 391-546.
- WAHID, S., REHMAN, S. U. & BABAR, S. 2004. *Structural Analysis of Central Khisor Range, North west of Daskki, D.I. Khan NWFP Pakistan*. Unpublished MSc. thesis. Department of Geology, University of Peshawar, Pakistan.
- WALKER, R. G. & CANT, D. J. 1984. Sandy fluvial systems. In: WALKER, R.G. (ed) *Facies Models*. Geoscience Canada Reprint Series 1, 2nd Edition, 71-89.
- WARDLAW, B. R., DAVYDO, V. & GRADSTEIN, F. M. 2004. The Permian Period. In: GRADSTEIN, F. M. OGG, J. O. & SMITH, A. G. (eds) *A Geologic Time Scale 2004*. Cambridge University Press, **16**, 249-270.
- WARDLAW, B. R., LEVEN, E. Y., DAVYDOV, V. I., ET AL. 1999. The base of the Sakmarian Stage: Call for discussion (Possible GSSP in the Kondurovsky Section, Southern Urals, Russia), *Permophiles*, **34**, 19-26.
- WARDLAW, B. R. & POGUE, K. R. 1995. The Permian of Pakistan. In: SCHOLLE, P. A., PERYT, T. M. & ULMER-SCHOLLE, P. M. (eds) *The Permian of Northern Pangea volume 1. Palaeogeography, Palaeoclimates, Stratigraphy*. Springer Verlag, New York, pp. 215-224.
- WATERHOUSE, J. B. 1982. An early Permian cool-water fauna from pebbly mudstones in south Thailand. *Geological Magazine*, **119**, 337-354.

WOOD, G. D., GABRIEL, A. M. & LAWSON, J. C. 1996. Palynological techniques-processing and microscopy. *In: JANSONIUS, J. & MCGREGOR, D. C. (eds) Palynology: Principles and Applications*. American Association of Stratigraphic Palynologists Foundation, **1**, 29-50.

WYNNE, A. B. 1878. On the geology of the Salt Range in Punjab. *Geological Survey of India Memoir*, **14**, 1-313.

WYNNE, A. B. 1886. On a faceted and striated pebbles from the Olive Group conglomerate of Cliel Hill in the Salt Range of the Punjab, India. *Geological Magazine*, **3**, 492-494.

ZIEGLER, A. M., GIBBS, M. T. & HULVER, M. L. 1998. A mini-atlas of oceanic water masses in the Permian period. *Proceedings of the Royal Society of Victoria*, **110**, 323-343.